ASSET MANAGEMENT OF OFFSHORE OIL AND GAS INSTALLATIONS

Serena Karen D'souza

A Doctoral Thesis



Thesis submitted to the University of Nottingham for the degree of Doctor of Philosophy

September 2017

Abstract

The UK sector of the North Sea is a mature oil and gas basin subjected to some of the harshest offshore environments with a majority of the oil and gas installations approaching or having exceeded their original design life, often specified as 25 years. It is likely that the operation of these installations will continue for a substantial period in the foreseeable future. However, the ageing nature of these installations present significant challenges to the delivery of high standards of health and safety required by the UK Health and Safety Executive. The issue of ageing installations has been shown to be an important factor in offshore incidents and accidents, leading to an increased risk of accidental loss of hydrocarbon and failures due to equipment deterioration. Two major hazards resulting from ignition of accidental hydrocarbon release are fires and explosions. Failure to minimise the effects of fires and explosions can bring about significant damage to the structural integrity of offshore installations and pose a risk to personnel safety as evidenced by the 1988 Piper Alpha Disaster and the 2010 Deepwater Horizon Explosion and Oil Spill.

This thesis presents a practical tool that can be used to predict the costs, risks and service reliability of any given asset management policy for an offshore oil and gas installation. The tool is implemented using a standard Petri Net technique with already adopted and newly proposed high level extensions, and fluid flow modelling technique. The tool is further divided into two sub models that work in conjunction with one another: (1) the Petri Net based Offshore Safety System Degradation and Maintenance Model and (2) the Offshore Fire and Explosion Model based on fluid flow modelling techniques.

The aim of the Offshore Safety System Degradation and Maintenance Model is to concurrently simulate the degradation, failure, inspection and maintenance of four safety systems which includes the fire and gas detection system, process isolation, process blowdown, and the deluge system. Simulation of the model generates a variety of statistics such as the estimated operational costs and unavailability associated with implementing any given asset management policy.

The Offshore Fire and Explosion Model is then used to model the occurrence of a hydrocarbon leak from a process vessel located within three enclosed modules; wellhead, separation and compression, of an offshore installation. The aim of this model is to predict the frequencies of fires and explosions in the event that the safety systems previously modelled in the Offshore Safety System Degradation and Maintenance Model fail to function on demand in the presence of an ignition source. The model utilises fluid flow modelling to calculate parameters such as the hydrocarbon discharge rate, gas cloud build-up and dispersion, oil-pool build-up and reduction. These parameters can then be used to predict the magnitude of the fires and explosions in terms of the flame length produced in the event of a fire and the overpressures generated in the event of an explosion.

The results and statistics generated are highly beneficial to offshore asset operations managers as they can be used to predict the number of maintenance interventions necessary to ensure safety systems are in an acceptable condition. From this, associated costs can be determined enabling offshore managers to allocate resources and budget accordingly. Finally, an optimisation study is carried out using Genetic Algorithm to identify the optimum inspection, maintenance and repair strategy for the offshore safety systems with an acceptable risk level.

The methodology presented in this research considers the offshore safety systems and the processes described above in more detail compared to previous literature associated with asset management offshore oil and gas installation. Additionally, the research demonstrates the suitability of Petri Nets for integrating fire and explosion modelling within the asset management framework which is first of its kind. The model can be successfully used to predict costs, risks and service reliability, and to support asset management decisions when the model is implemented in an optimisation framework.

Acknowledgements

First and foremost, I would like express my sincere gratitude to my supervisor, Professor John Andrews, who conceived the overall programme of this research and gave me invaluable guidance throughout my PhD. I would like to thank both my internal examiners, Dr Rasa Remenyte-Prescott and Dr Sean Reed, for guiding me through my research. I would also like to extend my sincerest thanks and appreciation to Dr. Dovile Rama and my dear friend, Hon Xing Wong, for providing me with useful insights and thought-provoking critics during the final year of my research.

To my dear friends, especially, Victoria, Tash, Hakeem, Hadis, Silvia, Osato, Furo and Adonye, thank you for your friendship and support throughout my PhD. I would also like to take this opportunity to thank my colleagues at the University of Nottingham, especially, Marius, Jack I, Jack II, Alex, Omar, Claudia, Raphaelle, Bryant, Paul, Hector and Rattapong, whose company has made this PhD an enjoyable experience.

To my partner, Simon Neale, thank you for your patience and unrelenting support. Without your continuous encouragement, I could not have overcome my anxiety and finished this thesis. I would also like to thank my dear parents, whose lifetime has been devoted to providing me and my sisters with a world-class education. I am grateful for their endless love and prayers. My sisters, Samantha and Sharon, deserve my wholehearted thanks as well.

Lastly, I would like to dedicate my thesis to my dear best friend, Machundi Ando (1991-2016). His outlook at life will always be a reminder for me to stay unruffled and trust in the Lord's timing. I truly hope that by completing this thesis I have made him proud.

Table of Contents

Chapter 1 - Introduction 1

1.1 Introduction 1

1.2 General Description of Offshore Oil and Gas Platforms 1

1.2.1 Offshore Platforms 1

1.2.2 Modular Construction 2

1.2.3 Offshore Drilling and Production 3

1.3 Offshore Hazards 4

1.4 Offshore Safety Systems 6

1.5 Offshore Incidents 8

1.5.1 Piper Alpha Disaster 8

1.5.2 Deepwater Horizon Explosion and Oil Spill 12

1.6 Lessons Learned from Offshore Incidents 14

1.7 Offshore Ageing 15

1.8 Research Aims and Objectives 16

1.8.1 Aims 16

1.8.2 Objectives 16

1.9 Thesis Outline 16

Chapter 2 - Asset Management of Offshore Oil and Gas Installation 19

2.1 Asset Management: A Risk-Based Approach 19

2.2 Definition of Risk 19

2.3 Tolerability of Risk Framework 20

2.4 Risk Assessment 21

2.5 Hazard Identification Techniques 22

2.5.1 Hazard Checklists 23

2.5.2 Hazard and Operability Studies 23

2.6 Risk Analysis Methods 24

2.6.1 Fault Tree Analysis 25

2.6.2 Event Tree Analysis 32

2.6.3 Use of FTA and ETA in Risk Analysis 33

2.6.4 Markov Models 37

2.6.5 Petri Net Analysis 42
2.7 Summary 52
Chapter 3 - Modelling Fires and Explosions 54
3.1 Fires and Explosions on Offshore Installations 54
3.2 Hydrocarbon Releases 54
3.3 Consequence Modelling of Accidental Release of Hydrocarbons 55
3.4 Release Models 56
3.5 Gas Build-Up and Atmospheric Dispersion 57
3.5.1 Factors Affecting Dispersion of Gas Cloud 57
3.5.2 Atmospheric Dispersion Models 58
3.5.3 Passive Dispersion Models 60
3.5.4 Dense Gas Dispersion Models 64
3.5.5 Discussion 64
3.6 Fires on Offshore Installations 64
3.6.1 Ignition 65
3.6.2 Flammability Limits 65
3.6.3 Autoignition Temperature 65
3.6.4 Types of Fires 66
3.6.5 Modelling Jet Fires 66
3.6.6 Modelling Pool Fires 70
3.7 Explosions on Offshore Installations 72
3.7.1 Detonation and Deflagration 72
3.7.2 Explosion Overpressures 73
3.7.3 Modelling Explosions 74
3.8 Mitigating Fires and Explosions 78
3.9 Summary 79
Chapter 4 - Platform Safety Model 82
4.1 Introduction to Model Framework 82
4.2 High Level Extensions to Standard Petri Nets 85
4.2.1 Inhibitor Arc 85
4.2.2 Reset Transition 85
4.2.3 Probabilistic Transition 86
4.2.4 Place Conditional Transition 86
4.3 Description of the Offshore Installation 87

4.3.1 Modules 87
4.3.2 Safety Systems 89
4.4 Offshore Safety System Degradation and Maintenance Model 94
4.4.1 Model Structure 94
4.4.2 Input Data 95
4.4.3 Condition States of Offshore Safety System Components 96
4.4.4 Petri Net Model 100
4.4.5 Building the Petri Net Software 125
4.4.6 Verification of the Petri Net Model 128
4.5 Offshore Fire and Explosion Model 129
4.5.1 Model Structure 129
4.5.2 Outputs of the Fire and Explosion Model 148
4.6 Summary 151
Chapter 5 - Platform Safety Model Application 153
5.1 Simulation of Offshore Safety Systems Degradation and Maintenance Model 153
5.1.1 Simulation Time 153
5.1.2 Monte Carlo Sampling 154
5.1.3 Convergence Analysis 154
5.1.4 Output File 154
5.2 Application of the Offshore Safety System Degradation and Maintenance Model 156
5.2.1 Component Analysis 156
5.2.2 System Analysis 172
5.3 Sensitivity Analysis of Offshore Safety System Degradation and Maintenance Model 175
5.3.1 Effect of Varying Asset Maintenance Strategy 175
5.3.2 Effect of Opportunistic Maintenance 177
5.3.3 Effect of Varying Inspection Interval 177
5.3.4 Effect of Varying Degradation Rates 179
5.4 Simulation of Offshore Fire and Explosion Model 180
5.4.1 Simulation Time 180
5.4.2 Convergence Analysis 180
5.4.3 Output File 181
5.5 Application of the Offshore Fire and Explosion Model 181
5.5.1 Offshore Oil and Gas Platform Results 181
5.5.2 Separation Module 183

5.5.3 Compression Module 191
5.5.4 Wellhead Module 198
5.6 Sensitivity Analysis of Offshore Fire and Explosion Model 204
5.7 Summary 204
Chapter 6 - Optimisation of the Platform Safety Model 206
6.1 Introduction 206
6.2 Overview of Optimisation Techniques 207
6.2.1 Mathematical Programming 207
6.3 Discussion 215
6.4 Offshore Risk Optimisation 216
6.4.1 Objective Function 216
6.4.2 Variables 217
6.4.3 Evaluation 218
6.4.4 Initialisation 219
6.4.5 Evaluating the Fitness Function of Each Individual 219
6.4.6 Selection and Reproduction 219
6.4.7 Crossover 221
6.4.8 Mutation 222
6.4.9 Next Generation and Convergence 222
6.5 Results and Discussion 223
6.6 Summary 230
Chapter 7 - Conclusion 231
7.1 Summary 231
7.2 Conclusions 236
7.3 Key Findings of the Research 238
7.4 Future Work and Recommendations 240
References 241
Appendix A 250
Appendix B 254
Appendix C 266
Appendix D 269
Appendix E 282

List of Figures

Figure 1-1 Typical Fixed Offshore Platform Layout (British Petroleum 2005) 2
Figure 1-2 Schematic of an offshore platform (British Petroleum 2005) 2
Figure 1-3 Arrangement of Equipment on an offshore platform (Arnold and Stewart 2008) 3
Figure 1-4 Piper Alpha Platform (Keane 2013) 9
Figure 1-5 Smoke plume on the Piper Alpha (Keane 2013) 11
Figure 1-6 Deepwater Horizon Rig Explosion (The Guardian 2010) 13
Figure 2-1 Tolerability of Risk Framework (Health & Safety Executive 2001) 20
Figure 2-2 Fault Tree Diagram for Tank Overflow (Tweeddale 2003) 27
Figure 2-3 Reliability bath-tub curve (Andrews and Moss 2002) 31
Figure 2-4 Simplified Event Tree (Andrews and Dunnett 2000) 33
Figure 2-5 Example Isolatable Sections (Lewthwaite 2006) 34
Figure 2-6 Event Tree for Gas Leak (Andrews *et al.* 2005) 35
Figure 2-7 State-Transition Diagram for Repairable two-state component (Andrews and Moss 2002) 38
Figure 2-8 Untimed Petri Net 44
Figure 2-9 Transition T1 enabled 44
Figure 2-10 Enabled Transition T1 fires 44
Figure 2-11 Coloured Petri Net 48
Figure 3-1 Consequence Analysis of an Accidental Release of Hydrocarbons 56
Figure 3-2 Relationship between flammability properties (Perry *et al.* 1997) 65
Figure 3-3 Variation in the sonic and subsonic jet flame lengths (L) against fuel mass flow rate (m), for different orifice outlet diameters (d) (Palacios *et al.* 2009) 67
Figure 3-4 Craven Model (Craven 1972) 68
Figure 3-5 Pool Fire (Mannan 2013) 70
Figure 3-6 Effect of Fuel Concentration on Explosion Overpressures (Lewthwaite 2006) 73
Figure 3-7 Variation in the Overpressure as a function of concentration (Lewthwaite *et al.* 2006) 79
Figure 4-1 Model Framework 84
Figure 4-2 Petri Net with inhibitor arc 85
Figure 4-3 Probabilistic Transition 86
Figure 4-4 Place Conditional Transition 87
Figure 4-5 Illustration of the modelled oil and gas installation 87
Figure 4-6 Process section showing isolation (ISV) and blowdown (BDV) valves 90
Figure 4-7 Section 1 - Atmospheric Separator 91
Figure 4-8 Schematic of Deluge System 92
Figure 4-9 Flow Diagram of a Deluge System 94
Figure 4-10 Constituent elements of the Safety System Degradation and Maintenance Model 95
Figure 4-11 Valve Condition vs Operating Life 99

Figure 4-12 Petri Net Model showing the degradation and failure process for a Submerged Lift Pump 102
Figure 4-13 P-F Diagram 107
Figure 4-14 Petri Net Model showing the Inspection Process 112
Figure 4-15 Petri Net Model showing the inspection and maintenance process for a Submerged Lift Pump 113
Figure 4-16 Petri Net Model showing the failure process for a Submerged Lift Pump 118
Figure 4-17 Petri Net Model showing the failure process for the Firewater Pump Subsystem 119
Figure 4-18 Main Fault Tree 120
Figure 4-19 Petri Net Model showing the failure process for the Deluge System 121
Figure 4-20 Petri Net Model showing the Opportunistic Maintenance Process 123
Figure 4-21 Petri Net Model showing the inspection and maintenance process for a Submerged Lift Pump 125
Figure 4-22 Offshore Safety System Degradation and Maintenance Model Framework 128
Figure 4-23 Platform Safety Model Framework 130
Figure 4-24 Offshore Fire and Explosion Model Framework 132
Figure 4-25 Flow Chart showing the Operational Process of Fire and Explosion Model 132
Figure 4-26 Flow Chart showing the Operational Process of Fire and Explosion Model: Gas Release 133
Figure 4-27 Flow Chart showing the Operational Process of the Fire and Explosion Model: Oil Release 134
Figure 4-28 Separator Vessel 136
Figure 4-29 No Explosive Gas Concentration 145
Figure 4-30 Gas Concentration exceeds the LFL but is below the UFL 146
Figure 4-31 Gas Concentration exceeds the UFL 147
Figure 5-1 Convergence of Mean Time of Residing in the New Condition State for the Submerged Lift Pump 156
Figure 5-2 Convergence of Probability of being in each condition state over 35 years 157
Figure 5-3 Condition distribution for the Submerged Lift Pump 158
Figure 5-4 Negatively Skewed Lognormal Distribution for the duration spent in New Working State by the SLP 160
Figure 5-5 Positively Skewed Lognormal Distribution for the duration spent in Degraded State by the SLP 160
Figure 5-6 Positively Skewed Lognormal Distribution for the duration spent in Severely Degraded State by the SLP 160
Figure 5-7 Positively Skewed Lognormal Distribution for the duration spent in Functional Failure State by the SLP 161
Figure 5-8 Convergence of Average Number of Interventions for the Submerged Lift Pump 162
Figure 5-9 Cumulative Number of Interventions for each component of the Deluge System 164
Figure 5-10 Cumulative Number of Failures for each component of the Deluge System 165
Figure 5-11 Average Yearly Preventive Maintenance Cost for the Submerged Lift Pump 166
Figure 5-12 Average Yearly Corrective Maintenance Cost for the Submerged Lift Pump 167
Figure 5-13 Average Yearly Failure Cost for the Submerged Lift Pump 169
Figure 5-14 Cumulative Preventive Maintenance Cost for all Wear-Out Components of the Deluge System 170

Figure 5-15 Cumulative Failure Cost for each component of the Deluge System 170
Figure 5-16 Average Yearly Life Cycle Cost for the Submerged Lift Pump 171
Figure 5-17 Mean Time of Residing in the Working Condition State against the number of simulations 172
Figure 5-18 Subsystem Failure Contribution 173
Figure 5-19 Average Yearly Operational Cost for the Deluge System 174
Figure 5-20 Average Number of Explosions per year against the Number of Simulations 180
Figure 5-21 Effect of Pressure on the Flammability Limits of a Methane/Air Mixture (Mehta *et al.* 1998) 195
Figure 5-22 Effect of Initial Pressure on the Auto-Ignition Temperature of a Methane/Air Mixture (Caron *et al.* 1999) 195
Figure 6-1 Flowchart showing the Genetic Algorithm Process 213
Figure 6-2 Example of the Crossover Process 214
Figure 6-3 14 bit string is used to code the input variables for a single safety system 218
Figure 6-4 Pareto Ranking 220
Figure 6-5 Fitness of the Population: Generation 1 223
Figure 6-6 Fitness of the Population: Generation 10 224
Figure 6-7 Fitness of the Population: Generation 20 224
Figure 6-8 Fitness of the Population: Generation 30 224
Figure 6-9 Fitness of the Population: Generation 40 225
Figure 6-10 Fitness of the Population: Generation 50 226

List of Tables

Table 2-1 Symbols used to construct Fault Tree (Andrews and Moss 2002) 26
Table 2-2 Symbols used in Untimed Petri Nets 43
Table 2-3 Symbols used in Timed Petri Nets 45
Table 4-1 Hydrocarbon Inventory and Operating Data for the sections of the different modules 89
Table 4-2 Isolation Valve Connections 91
Table 4-3 Blowdown Valve Locations 91
Table 4-4 Degradation Mechanisms Affecting Offshore Safety Systems 97
Table 4-5 Condition states of Blowdown and Deluge System Valves based on Opening Time (Andrews and Fecarotti 2014) 98
Table 4-6 Condition states of Isolation System Valves based on Closing Time (Andrews and Fecarotti 2014) 98
Table 4-7 Condition states of Firewater Pumps based on Vibration Levels (ISO 10816 -1998) 100
Table 4-8 Weibull Distribution Parameters for Different Offshore Safety System Components 103
Table 4-9 Exponential Distribution Parameters for Different Offshore Safety System Components 104
Table 4-10 Definition of the Type of Maintenance Implemented on Offshore Safety Systems 108
Table 4-11 Component Degradation Conditions and Mean Time to Schedule Maintenance for Different Safety System 110
Table 4-12 Average Cost of Performing Inspection and Maintenance 111
Table 4-13 Inspection Interval for the different Safety Systems 112
Table 4-14 Description of the Places in Figure 4-15 114
Table 4-15 Description of the Transitions used in Figure 4-15 115
Table 4-16 Description of the Places used in Figure 4-16 118
Table 4-17 Description of the Places used in Figure 4-17 120
Table 4-18 Description of the Places used in Figure 4-19 122
Table 4-19 Description of the Places used in Figures 4-20 124
Table 4-20 Maintenance Strategies applied to the Offshore Oil and Gas Assets 124
Table 4-21 Additional Inventory Data 129
Table 4-22 Hole Size Frequency Distribution (Lewthwaite 2006) 135
Table 4-23 Hole Size Probability Distribution 135
Table 4-24 Restriction orifice diameter of blowdown system valves 143
Table 4-25 Overpressure Data 149
Table 5-1 Duration (years) spent in each condition state by each of the deluge system components 159
Table 5-2 Statistics on the expected number of maintenance interventions for each component of the Deluge System up to the end of Year 35 163
Table 5-3 Statistics on the duration (years) spent in each condition state by the Deluge System 173
Table 5-4 Four Maintenance Strategies possible for an Offshore Safety System 175
Table 5-5 Effect of Varying Asset Maintenance Strategies 176
Table 5-6 Effect of Opportunistic Maintenance 177
Table 5-7 Five Inspection Intervals possible for an Offshore Safety System 177
Table 5-8 Effect of Varying Inspection Interval on the Fire and Gas Detection System 178

Table 5-9 Effect of Varying Inspection Interval on the Isolation Valves 178
Table 5-10 Effect of Varying Inspection Interval on the Blowdown Valves 178
Table 5-11 Effect of Varying Inspection Interval on the Deluge System 178
Table 5-12 Effect of Varying Mean Time to Degradation 179
Table 5-13 Expected Proportion of Fires and Explosions occurring within each module 181
Table 5-14 Explosion Frequency (per year) from leaks in sections of the separation module 183
Table 5-15 Explosion Frequency (per year) for the different overpressures for the separation module 184
Table 5-16 Explosion Frequency (per year) for the different sections of the separation module 184
Table 5-17 Explosion Frequencies for each concentration range for the Separation Module 185
Table 5-18 Mitigated and Unmitigated Explosion Frequencies for the Separation Module 185
Table 5-19 Unmitigated Explosion Frequencies for the different unmitigated explosion scenarios for the Separation Module 186
Table 5-20 Jet Fire Frequency (per year) following immediate ignition of a leak in sections of the Separation Module 187
Table 5-21 Jet Fire Frequency (per year) following delayed ignition of a leak in sections of the Separation Module 187
Table 5-22 Jet Fire Duration for the Separation Module 187
Table 5-23 Flame Length of the Jet Fire for the Separation Module 188
Table 5-24 Pool Fire Frequency (per year) for a leak in sections of the Separation Module 189
Table 5-25 Pool Fire Duration for the Separation Module 189
Table 5-26 Flame Length of the Pool Fire for the Separation Module 190
Table 5-27 Explosion Frequency (per year) from leaks in sections of the compression module 191
Table 5-28 Explosion Frequency (per year) for the different overpressures for the compression module 192
Table 5-29 Explosion Frequency (per year) for the different sections of the compression module 192
Table 5-30 Explosion Frequencies for each concentration range for the Compression Module 193
Table 5-31 Mitigated and Unmitigated Explosion Frequencies for the Compression Module 193
Table 5-32 Unmitigated Explosion Frequencies for the different unmitigated explosion scenarios for the Compression Module 194
Table 5-33 Jet Fire Frequency (per year) following immediate ignition of a leak in sections of the compression module 194
Table 5-34 Jet Fire Frequency (per year) following delayed ignition of a leak in sections of the compression module 196
Table 5-35 Jet Fire Duration for the Compression Module 197
Table 5-36 Flame Length of the Jet Fire for the Compression Module 197
Table 5-37 Explosion Frequency (per year) from leaks in sections of the wellhead module 198
Table 5-38 Explosion Frequency (per year) for the different overpressures for the wellhead module 198
Table 5-39 Explosion Frequency (per year) for the different sections of the Wellhead Module 199
Table 5-40 Explosion Frequencies for each concentration range for the Wellhead Module 199
Table 5-41 Mitigated and Unmitigated Explosion Frequencies for the wellhead module 200
Table 5-42 Unmitigated Explosion Frequencies for the different unmitigated explosion scenarios for the Wellhead Module 200

Table 5-43 Jet Fire Frequency (per year) following immediate ignition of a leak in sections of the wellhead module 201
Table 5-44 Jet Fire Frequency (per year) following delayed ignition of a leak in sections of the wellhead module 201
Table 5-45 Jet Fire Duration for the Wellhead Module 202
Table 5-46 Flame Length of the Jet Fire for the Wellhead Module 202
Table 5-47 Pool Fire Frequency (per year) for a leak in sections of the Wellhead Module 203
Table 5-48 Pool Fire Duration for the Wellhead Module 203
Table 5-49 Flame Length of the Pool Fire for the Wellhead Module 204
Table 6-1 Input Variables and their value range 218
Table 6-2 13 optimum inspection, maintenance and repair strategies 227

List of Abbreviations

ACPH	Air Changes Per Hour
ALARP	As low as reasonably practicable
BCISC	British Chemical Industry Safety Council
BDV	Blowdown Valve
CAM	Congestion Assessment Method
CBA	Cost-Benefit Analysis
CFD	Computational Fluid Dynamics
CLICHE	Confined LInked CHamber Explosion
CM	Corrective Maintenance
CMR	Christian Michelsen Research Institute
CPN	Coloured Petri Net
DFT	Dynamic Fault Tree
EPA	Environmental Protection Agency
ETA	Event Tree Analysis
EXSIM	EXplosion SIMulator
F&G	Fire and Gas
FLACS	FLame Acceleration Simulator
FTA	Fault Tree Analysis
GA	Genetic Algorithm
GCM	Gas Conservation Module
HAZOP	HAZard and OPerability Study
HOC	Heavy Organics Chemicals
ICI	Imperial Chemical Industries
ISV	Isolation Valve
JT	Joule-Thomson
LCV	Level Control Valve
LEL	Lower Explosive Limit
LFL	Lower Flammable Limit
LIC	Level Controller
LSH	High-level Switch
LT	Level Sensor
MARS	Major Accident Reporting System

MNSL	Mobile North Sea Limited
MTTF	Mean Time to Failure
MTTR	Mean Time To Repair
NRC	Nuclear Regulatory Commission
P&ID	Piping & Instrumentation Diagram
PCT	Place Conditional Transition
PDC	Capacity Distribution
PM	Preventive Maintenance
PN	Petri Net
PNA	Petri Net Analysis
PT	Probabilistic Transition
QRA	Quantitative Risk Assessment
RA	Risk Assessment
RT	Reset Transition
SAROS	Safety and Reliability of Offshore Structures
SCOPE	Shell Code for Overpressure Prediction in Gas-Explosions
SV	Solenoid Valve
TNT	TriNitroToluene
UEL	Upper Explosive Limit
UFL	Upper Flammable Limit
UKCS	UK Continental Shelf

Chapter 1 - Introduction

1.1 Introduction

Fires and explosions are major hazards occurring on offshore oil and gas installations. As such, significant effort in both design and operation of offshore installations is expended in reducing the risks associated with fires and explosions. Safety Systems such as fire and gas detection system, process isolation and blowdown, and deluge, act to reduce the risk of the hazards. Following the fire and explosion on Piper Alpha platform in 1988, it is mandatory for offshore installation managers situated in the UK Continental Shelf (UKCS) to produce a safety case and make evident that the risks due to hazards on offshore oil and gas installations are as low as reasonably practicable (ALARP). However, due to recent changes in economic conditions and an increase in oil and gas recovery possibilities, many offshore firms wish to continue operating installations beyond their 25-years designed lifecycle instead of investing in new installations. Continued operation of deteriorating offshore equipment significantly increases the risks of failure, which is a safety concern, and could potentially increase the costs of replacement/major repair.

1.2 General Description of Offshore Oil and Gas Platforms

1.2.1 Offshore Platforms

A number of structures are employed in the exploration and production of crude petroleum and natural gas deposits located in subsea geological structures, known as “offshore platforms” (United States International Trade Commission 1986). The use of offshore platforms for the exploration and production of offshore petroleum reserves dates back to the 1950s. Initially, drilling began in shallow waters from piers extending out from the shore. As drilling moved into deeper water, a variety of different offshore structures were designed and are now in use across the UKCS including; jack-up platforms, gravity-based platforms, guyed tower platforms, semi-submersible platforms and tension leg. Figure 1-1 shows the layout of a typical fixed offshore platform. In just over 60 years, the offshore oil and gas industry has extended their drilling capability by ranging out to locations that are subject to adverse weather conditions.

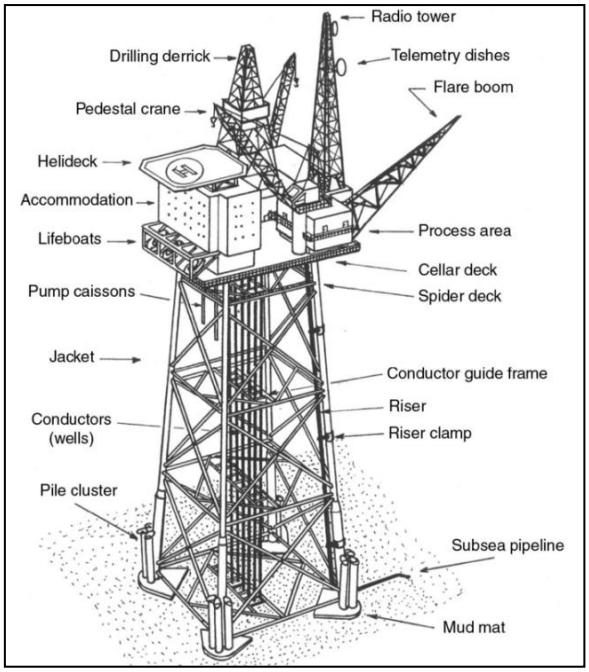


Figure 1-1 Typical Fixed Offshore Platform Layout (British Petroleum 2005)

1.2.2 Modular Construction

After the jacket is completely installed, the platform deck modules and other topside facilities are placed. Deck modules are generally large sized boxes of equipment weighing around 300 to 2000 tons each (Arnold and Stewart 2008).The modules can either be open or closed. Open modules are usually open-sided and naturally aerated compared to closed modules that are fully enclosed and subject to forced aeration. Figure 1-2, illustrates the concept of modularization on an offshore platform.

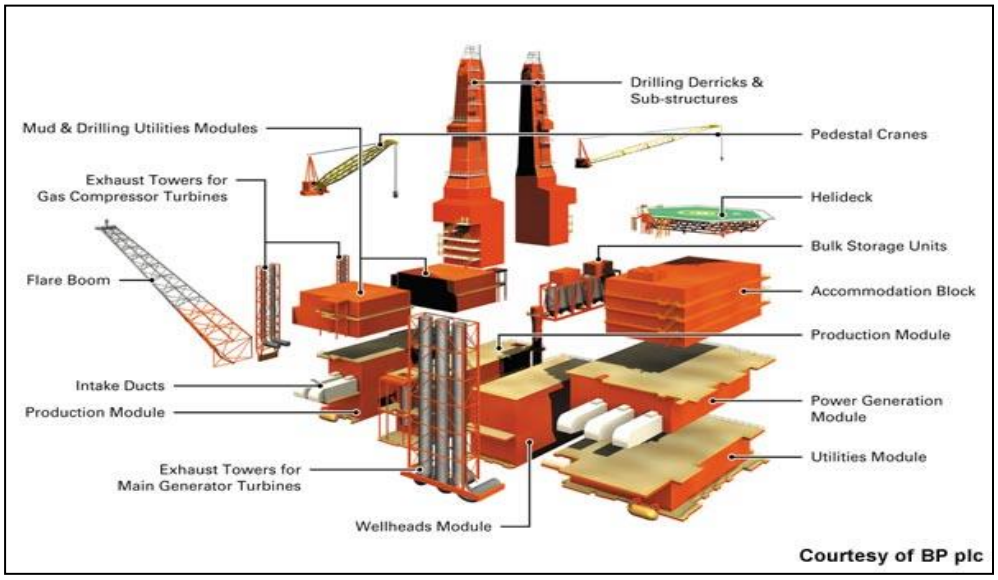


Figure 1-2 Schematic of an offshore platform (British Petroleum 2005)

A typical offshore installation encompasses the following modules: (1) Accommodation/Living Quarters, (2) Utilities, (3) Hydrocarbon Processing (including oil separation and gas compression), (4) Wellhead Module, and (5) Flare Module. Figure 1-3 shows an example arrangement on a typical offshore platform.

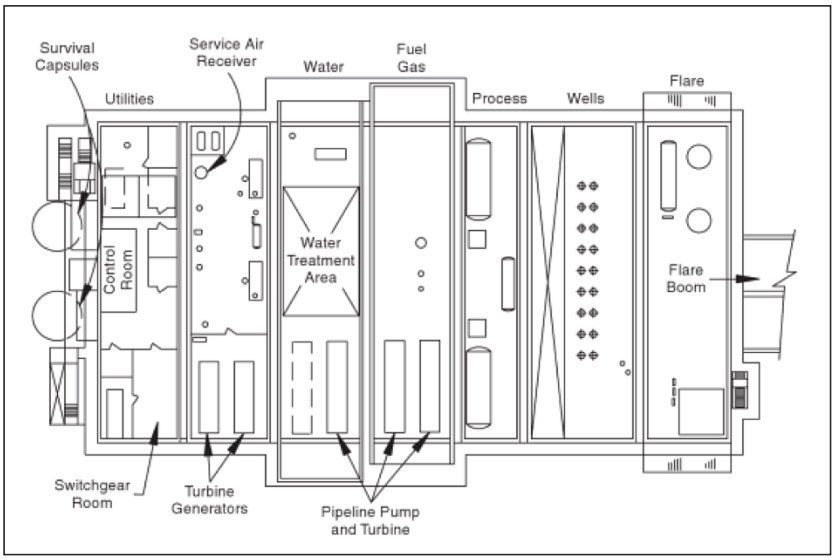


Figure 1-3 Arrangement of Equipment on an offshore platform (Arnold and Stewart 2008)

1.2.3 Offshore Drilling and Production

Over the years, processes such as offshore drilling, well construction and completion have remained fundamentally consistent. Hydrocarbons are produced through wells from the reservoir up to the offshore production facility. A combination of valves is positioned on top of the well to regulate the flow and pressure of the fluids and is commonly referred to as the 'Christmas Tree'. The fluid produced from the reservoir is usually a mixture of gas, oil, water and condensate.

The fluids are then transported from the well to the platform through pipelines and enter a series of separators, which is where the different phases are separated into different streams using gravity separation. In gravity separation, flow from the well is directed into a horizontal vessel, where the gas is allowed to bubble out, the oil is taken out in the middle and pumped to shore for further refining, and the water settles at the bottom of the vessel. The water is then treated before being dumped back into the sea.

The gas mixture from separators is then passed through the first-stage scrubber, where all remaining liquid is separated from the gas before it enters the first-stage compressor. Since compression causes the gas temperature to rise, a cooler is present straight after. As a result of higher pressure, more liquids are likely to separate from the gas, so the gas enters another scrubber before being compressed and cooled again (Arnold and Stewart 2008). The gas is then dehydrated to remove water vapour from the gas, before it can leave the platform through pipelines.

1.3 Offshore Hazards

BS ISO 17776: 2000 defines hazard as "*a situation that has the potential to cause harm, including human injury, damage to property, damage to the environment, or some combination of these*". The oil and gas industry is inherently hazardous (Martin 2011); high pressures and temperatures are involved and the fluid mixture is highly flammable. Add to this the complexity and constraints of constructing an offshore structure suitable for processing and accommodation purposes, the hazards are multiple and can be quite severe. Due to the intricacy of offshore operations, a number of hazards that are likely to be present are described below (Mobile North Sea Limited 2003):

1. Fires

Lees (1996) defines fire as a "*chemical reaction in which a substance combines with oxygen and heat is released*". For a fire to initiate, the three basic conditions which includes fuel, oxygen and heat, are necessary. Fire on an offshore installation is likely to cause death or serious injury or damage to the structure and equipment. In the event of severe escalation, the entire platform could collapse. Two types of fires are likely to occur on offshore installations: (1) Hydrocarbon fires and (2) Non-Hydrocarbon fires. Hydrocarbon fires include: (1) Jet fires (2) Pool fires (3) Fires in running liquids (4) Fireballs and (5) Gas fires. The type of fire is dependent on the state of the release. The effectiveness of the safety systems significantly affects the degree to which a fire will spread. For the purposes of this research, only jet fires and pool fires are considered. Immediate ignition of a high-pressure gas could result in a jet fire while a pool fire occurs when there is immediate ignition of a liquid hydrocarbon release. Non-hydrocarbon fires, on the other hand, may initiate from electrical

equipment. As this research focuses mainly on accidental release of hydrocarbon and hence "hydrocarbon" fires, "nonhydrocarbon" fires are not further studied within this research.

2. Explosions

Mannan and Lees (2005) defines explosions as "a sudden and violent release of energy". Delayed ignition of a flammable gas cloud has the potential to cause an explosion, which may result in partial or complete destruction of an offshore oil and gas installation.

3. Ship Collisions

An offshore installation is exposed to ship collision risk from infield vessels such as tankers and supply ships operating at close proximity to the installation. A collision of this nature would cause significant damage to the installation.

4. Transport Accidents

Helicopters serve an important role in transporting personnel and supplies to offshore installations. However, they are extremely prone to accidents. Some of the leading causes for helicopter accidents include: harsh weather conditions, pilot error, lack of training, mechanical failure and lack of maintenance. A helicopter impact on the normal landing surface of the helideck would potentially have minimal consequences relative to other locations on the platform. For instance, if the helicopter were to crash into the fuel storage area, a fire is more likely to occur on the helipad.

5. Dropped Objects

Dropped objects from various lifting activities represent a potential hazard to personnel and equipment on offshore installations.

6. Structural Failure

Failure of structural components such as the jacket legs may occur as a result of corrosion, fatigue or overloading. This could cause the platform to list or capsize.

7. Severe Environmental Conditions

The North Sea has one of the harshest weather conditions. The winter months are extremely cold; with frequent gales and storms, and waves can get as high as 10 to 15m. Severe environmental conditions have the potential to affect the safe operation of a large range of offshore activities as it could affect communication systems. However, it is unlikely to affect safety systems unless the platform was at the point of collapsing.

8. Seismic Activity

The UKCS is situated in an area of low seismic activity. However, during the occurrence of a high seismic activity, the platform would be shut down with production only resuming after a full inspection has been undertaken.

9. Well Kick and Blowout

Well kick is the entry of formation fluids into the wellbore during drilling. It occurs when the pressure exerted by the formation fluids exceeds the pressure exerted by the drilling mud. The resulting entry of formation fluids leads to the displacement of a measurable amount of drilling mud and kicks it out at the surface, leading to a blowout. This is most dangerous for people and property as the formation fluids can ignite leading to fires and explosions.

Although, a number of different hazards that may occur on an offshore installation have been identified; fires and explosions are the only two hazards whose effects will be considered in this research.

1.4 Offshore Safety Systems

Offshore installations are generally equipped with a number of Safety Systems that are necessary to minimise the damage caused to property and personnel in the event of a fire or explosion. These comprise of the following:

1. Fire and Gas Detection Systems

Fire and Gas detection systems are used to detect fires or gas leaks on platforms and initiate activation of other safety systems such as isolation, blowdown and deluge systems. Depending on the design of the platform, different platforms have different detection systems installed and are located strategically. Fire detectors detect flame using infrared,

ultraviolet or a combination of the two. Gas detectors, on the other hand, measure the level of gas concentration and transmit a signal to the control room. There are three types of gas detectors: sonic, beam and point. Sonic detectors are designed to detect the sound of escaping gases while beam and point detectors are designed to detect the presence of a gas cloud. Point detectors sample the surrounding air whilst beam detectors identify the gas cloud as it passes through an infrared beam (Lewthwaite 2006). Unless manually detected, failure of the gas detectors could result in the release of a large quantity of gas, therefore increasing the risk of an explosion.

2. Isolation and Blowdown Systems

Isolation and Blowdown systems are generally used in conjunction to one another, in order to reduce the quantity of hydrocarbon released into the module. Normally open isolation valves close and segregate segments to prevent escalation of events to adjacent modules. Normally closed blowdown valves open to depressurise the isolated segment and hence reduce the amount of available inventory. In the case of an ignited leak, isolating and blowing down the affected segment seeks to limit the fuel source for fire. There is also a secondary purpose for blowing down and depressurising. In the event of an external fire, the strength of the pipe weakens with internal pressure therefore depressurising minimises the escalation of an external fire on plant hydrocarbon equipment.

3. Deluge Systems

Deluge systems are also located close to major vessels (large inventories) to slow the rate of increase of metal temperatures in the event of a fire to prevent sudden failure of the vessel and leak of large amounts of hydrocarbon. The deluge system can either be water or foam-based depending on the equipment and state of the hydrocarbons present within the module. In gas processing modules, water systems are generally used as the water droplets are able to minimise explosion overpressures. In oil processing modules, foam systems are implemented to extinguish pool fires. The foam is able to cover maximum surface area, thus removing the supply of oxygen to the fire.

4. Heating, Ventilations and Air Conditioning (HVAC) Systems

On detection of a fire or leak, the HVAC systems shutdown to prevent the flow of oxygen into the module. However, a minimal amount of air would continue to leak into the module.

5. Blast and Firewall Systems

The walls of the different modules are designed to be blast and flame resistant so that they are able to withstand an explosion and in the event of a fire, they will be able to sustain it for a certain duration of time until it fails completely.

6. Emergency Power Systems

Emergency power systems are required to keep key systems such as the firewater pumps of the deluge system and the HVAC systems within the temporary refuge, operational. The remaining critical systems have individual back-up power supplies.

While the failure of any of the above mentioned systems could contribute substantially to a major accident, only the failure of the fire and gas detection system, process isolation and blowdown valves and water deluge system are of particular interest to this research.

1.5 Offshore Incidents

The offshore industry has suffered a number of significant accidents that have led to the loss of several lives. Two major incidents that have far more relevance to the current research work, are the Piper Alpha and the Deepwater Horizon disasters. Both incidents are briefly described below:

1.5.1 Piper Alpha Disaster

1.5.1.1 The Platform

The Piper Alpha platform became operational in 1976 and was managed by Occidental Petroleum (Caledonia) Ltd. It was stationed 176 km from the city of Aberdeen, Scotland. The platform produced roughly 10% of the total North Sea oil and gas and was part of a network consisting of three gas pipelines to Claymore, Tartan and MCP-01 and an oil pipeline to the terminal at Flotta. Figure 1-4 shows the Piper Alpha platform before the accident.



Figure 1-4 Piper Alpha Platform (Keane 2013)

The production deck was made up of four modules: A - wellhead, B - separation, C - gas compression and D - power generation. Four accommodation modules were positioned above the production deck level. Two flares, namely the East and West flares, were positioned on the South end of the installation. To provide protection against flare radiation, Module A was protected by a heat shield. The platform was equipped with the following systems: electrical supply, fire and gas detection, deluge, emergency shutdown, communications and evacuation and escape.

1.5.1.2 The Process and the Plant

Fluid extracted from the wells initially passed through the wellhead module. It was then directed into the separation module, here the gas and condensate was separated from the oil and water. Centrifugal compressors contained within the gas compression module were then used to compress the majority of the gas, with the remaining amount fuelling the main generators. The majority gas was then recompressed via second stage of compressors after the condensate had been removed. Finally, the gas was used to lift the well fluids (gas lift), channelled via MCP-01 as export gas, or sent to flare.

However, it must be noted that the method of removing the condensate was dependent on the type of operational mode (Phase 1 or Phase 2) implemented on the platform. In the normal mode (Phase 2), the gas was dried in the Gas Conservation Module (GCM) after the first compression. Pressure across the turbo expander was then reduced to cool the gas, while knocking out the condensate as a result of gas expansion. The condensate from both the GCM and the turbo expander was then passed through the second stage of compressors. In the

alternative mode (Phase 1), the GCM would not be used. Instead, the gas was passed through a Joule-Thomson (JT) valve after first compression. Pressure across the JT valve was then reduced to cool the gas, while knocking out the condensate as a result of the Joule-Thomson effect.

The condensate was then passed through the second stage of compressors, after which a main condensate injection pump is used to pump the condensate into the main oil line. Provisions were made for the failure of the main condensate injection pump by providing a standby pump. The pumps were designed to incorporate single pressure safety valves (PSV) to protect them from overpressure.

1.5.1.3 Events prior to the Explosion

On the 6th of July 1988, major works were scheduled on the platform. The platform was operating on Phase 1 mode, as the GCM was made inoperative to allow changing of the molecular sieve driers. As a result of this mode of operation, the gas was relatively wetter, and was more at risk of forming a hydrate, a risk recognised by onshore management. In line with this mode, the rate of methanol injection increased significantly (twelve times greater) compared to that required by Phase 2. However, between 4:00 and 8:00 p.m., the methanol supply was disrupted.

At the same time, the condensate injection pump B was in operation whilst pump A was down for maintenance and undergoing the following maintenance work:

1. Full 24 month Preventive Maintenance (PM)
2. Repair of the pump coupling
3. Recertification of the PSV 504

Pump A was isolated to carry out a 24 month PM. However, during the repair of its coupling, the maintenance personnel failed to insert slip plates. Moreover, the PSV 504 was removed for testing and it was agreed that it would be replaced prior to the morning shift.

At 9:50 p.m., pump B incurred a spurious fault and could not be restarted. Operating the platform without a condensate injection pump would have caused condensate backup

resulting in a forced shutdown of the platform within 30 minutes. This could lead to a complete loss of electrical power on the platform. Although not dangerous, would stop the rig from producing oil. Hence, to avoid this, pump A was put back into service.

At 9:55 p.m., alarms highlighted the trip of two centrifugal compressors in the gas compression module, shortly followed by a low gas alarm. The third centrifugal compressor then tripped, immediately followed by a series of low and high gas alarms. A loud screeching sound was then heard in Module D for about 30 seconds, before an explosion occurred.

1.5.1.4 The Explosion and the Escalation

The emergency shutdown (ESD) system promptly closed the emergency shut-off valve (ESV) located on the main oil line. The blowdown systems were then initiated and the gas inventories sent to flare. The explosion resulted in a large fireball initiating at the West side of Module B with a large oil pool fire at the west end of that module. This oil pool fire developed into a massive smoke plume, enveloping the platform from the production deck at 84ft level up, making it impossible for the personnel to reach the lifeboats. Figure 1-5 demonstrates the resulting smoke plume.



Figure 1-5 Smoke plume on the Piper Alpha (Keane 2013)

The oil pool from Module B spilled onto the 68ft level, developing the fire at this level. The drums of flammable material stored on this level intensified the fire. As the fire water system failed, the fire continued to intensify. After twenty minutes of the first explosion, this fire caused the rupture of the Tartan riser, hence, producing a large jet flame that consumed majority of the platform.

Around 10:50 p.m., the gas pipeline to MCP-01 ruptured followed by the Claymore line at 11:18 p.m. The pipe deck and the accommodation module then collapsed into the sea. The North end of the platform disappeared by 12:15 a.m. on the 7th of July. This disaster led to the death of 167 personnel, with only 62 escaping the platform.

1.5.1.5 Investigation into the Piper Alpha Disaster

The disaster was investigated immediately by the Department of Energy (DoEn). Two reports were published as a result; an interim report (The Petrie Interim Report) and a final report (The Petri Final Report). Both reports highlighted two main contributions for the hydrocarbon leak, which resulted in the explosion on Piper Alpha; (1) A leak from the site of PSV 504; and (2) A leak due to ingestion of liquid into the reciprocating compressors.

In November 1990, after a 13-month public enquiry driven by Lord Cullen, the Piper Alpha Report was issued (Cullen 1990). The report highlighted the circumstances that led to the accident, together with recommendations to prevent similar accidents in the future. The following causes of the disaster were emphasised in the report; (1) Poor platform design, (2) Poor maintenance management, (3) Inadequate safety training procedures, (4) Poor emergency management and (5) Failure to adhere shift turnover communication protocol.

1.5.2 Deepwater Horizon Explosion and Oil Spill

1.5.2.1 Deepwater Horizon Rig

The Deepwater Horizon was a dynamically positioned, semi-submersible offshore drilling unit owned and operated by Transocean. The rig was contracted to BP and stationed on the Macondo Well in the Mississippi Canyon Block 252 in the Gulf of Mexico. On April 20th 2010, personnel on board the Deepwater Horizon were in the process of completing work on a deep-water exploratory well when a sequences of events lead to the blowout of the well and a huge fire and explosion engulfed the rig. Eleven lives were lost and the event was documented to be one of the largest marine oil spill ever encountered.

1.5.2.2 Chronology of Key Events

On April 19th 2010, the cement job to seal the well bore from the reservoir sand was initiated. While undertaking this job, the crew experienced several complications including those

related to closing check valves on the float collar near the bottom of the cement casing. Nevertheless, the crew assumed that the float collar was holding.

On April 20th 2010, a positive pressure test which is the first integrity test of the well was conducted. The test confirmed the integrity of the cemented production casing. A negative test which is the second integrity test of the well was conducted soon after. Its purpose was to place the well in a controlled under balanced state to test all mechanical barriers of the cement. This was implemented by displacing some of the heavy drilling mud in the well with lighter seawater and checking for flow. The results of the tests were wrongly interpreted by the team who concluded that the spacer fluid that had been used previously was appropriate for discharging overboard.

At 9:40 p.m., there was an overflow of mud onto the rig. A minute later the mud exploded through the derrick. The diverter was closed and the flow was diverted to the mud-gas separator. At that instant, the crew attempted to close the upper annular and upper pipe rams on the blowout preventer (BOP). However, increase in drill pressure over a five minute period, resulted in the uncontrollable release of mud and hydrocarbons onto the rig and overboard. Hence, it was clear that the BOP failed to seal the well.

At 9:47 p.m., gas alarms on the Deepwater Horizon sounded, followed by two explosions at 9:49p.m. With the Deepwater Horizon unable to disconnect from the well, the order to abandon ship was given at 10:00 p.m. After thirty-six hours from the initial explosion, the Deepwater Horizon rig sank, on 22nd April 2010. Approximately five million barrels of oil spilled into the Gulf of Mexico. Figure 1-6 shows the explosion of the Deepwater Horizon rig.



Figure 1-6 Deepwater Horizon Rig Explosion (The Guardian 2010)

1.5.2.3 Investigation into Deepwater Horizon Explosion and Oil Spill

An investigation into the Deepwater Horizon explosion and oil spill revealed eight interrelated causes that led to this event. The first two causes of the incident were associated with the flow of hydrocarbons into the well. Based on the evidence, it is known that both the annular cement barrier and shoe track barrier failed to isolate the flow of hydrocarbons to the wellbore. The following three causes originate from the evidence that the crew failed to identify the influx of hydrocarbons into the riser. A negative pressure test was performed but the results were wrongly accepted. Failure to recognise the influx of hydrocarbons lead to the flow of hydrocarbons to the surface as over time they had already entered the riser. Although well control measures were implemented, the rig crew failed to seal off the well. The next two causes of the incident were associated with the flow of hydrocarbons through the riser, causing it to disperse across the rig, and creating the conditions for them to ignite. Moreover, deviation of the well flow to the mud-gas separator, resulted in gas being vented on the rig. The extent of the disaster could have been minimised if the well flow was diverted overboard. Ignition of the hydrocarbon could not be prevented by the fire and gas system on board the rig. The final cause of the incident was drawn from evidence that the BOP failed to seal the well.

1.6 Lessons Learned from Offshore Incidents

Investigations of past offshore incidents have revealed that the offshore industry has suffered a significant amount of damage to platforms resulting in major loss of human life. Following the Piper Alpha disaster, the Cullen Report made 106 recommendations for changes to North Sea safety procedures. A key recommendation of the report was the obligation to issue the safety case to the Health and Safety Executive for approval. The safety case must prove that the offshore company has adopted acceptable safety management systems, identified hazards within their process, evaluated their risks and that measures were put in place to control those risks to ensure that the relevant statutory provisions were complied with (Health & Safety Executive 2006a). However, despite the offshore industry having adopted a safety code which included changes to platform design and stricter requirements for design review, the Deepwater Horizon Explosion and Oil Spill, still occurred in 2010. This accident was a combination of mechanical failures, human and design errors and lack of communication from the team. It emphasises the need for further improvements to the

offshore safety management system. Furthermore, all of the hazards mentioned in Section 1.3 have the added factor of ageing offshore infrastructure and the impact the ageing equipment can have on the safety and service reliability of offshore oil and gas processing systems. This is described in further detail in Section 1.7. Hence, best practises must therefore be understood and applied through the identification of hazards, proactive risk analysis, risk reduction and hence risk management. A comprehensive examination of the risks inherent in offshore oil and gas production could increase confidence in the asset management of offshore installations.

1.7 Offshore Ageing

A significant number of platforms in the UK sector of the North Sea are approaching or have exceeded their original design life, which was specified as typically 25 years (Stacey *et al.* 2008). It is likely that the operation of these installations will continue for a substantial period in the foreseeable future. The maturing and ageing nature of offshore installations present significant challenges to the delivery of high standards of health and safety. Hence, if not managed properly, ageing can have serious consequences such as the potential loss of an installation and human life.

Health & Safety Executive (2006b) defined ageing as*: "Ageing is not about how old your equipment is; it is about its condition, and how that is changing over time. Ageing is the effect whereby a component suffers some form of material deterioration and damage (usually, but not necessarily, associated with time in service) with an increasing likelihood of failure over the lifetime".*

Research conducted by Health & Safety Executive (2010) shows that approximately 60% of major accidents are related to technical failures of which 50% highlight ageing as the contributing factor. Furthermore, the study highlights that approximately 28% of all reported major accidental loss of containment is a result of ageing. Hence, before life extension of an offshore installation can be considered, detailed understanding of ageing mechanisms and their effect on offshore systems and components is necessary.

1.8 Research Aims and Objectives

1.8.1 Aims

The main aim of this research is to develop a practical and systematic tool to predict the risks, costs and service reliability of any given asset management policy for an offshore oil and gas installation.

1.8.2 Objectives

The principle objectives of this research project are:

- To model the degradation and failure of safety systems such as fire and gas detection system, process isolation, process blowdown and deluge.
- To model the occurrence of a hydrocarbon leak from three enclosed modules, i.e. wellhead, separation and compression module on an offshore installation; generate the discharge rate, allowing for variation of the gas concentration in the module to be calculated over time.
- To estimate the frequencies of jet fires, pool fires and explosions in the event of safety system unavailability and hence predict the overpressures generated as a result of an explosion and the length and duration of the flame generated as a result of a jet or pool fire.
- To derive a set of maintenance and inspection strategies that can be applied to the ageing assets to produce an acceptable risk level.
- To develop an optimisation technique to find the optimum asset management strategies that minimise the operational costs whilst providing an acceptable risk level.

1.9 Thesis Outline

The thesis is organized as follows:

Chapter 1 provide an introduction to the offshore oil and gas industry; describes the main facilities and processes on oil and gas installations focusing on the safety systems that serve to mitigate the main offshore hazards, which are also described. It then reviews two of the industry's most infamous incidents and presents the case for the need to rethink the assessments of the industry's risk assessment process for ageing installations and their asset management policy.

Chapter 2 delivers an extensive literature review of the hazard identification and risk analysis techniques applied in the offshore oil and gas industry. The principles of the different techniques are defined and compared in terms of their strengths and weaknesses. The use of these techniques in offshore asset management has also been critically appraised.

Chapter 3 acknowledges fire and explosions due to hydrocarbon release as a major threat to the integrity of offshore installations. A detailed review of the range of techniques available to model the hydrocarbon release, gas build-up and dispersion, and fires and explosions have been presented and the advantages and disadvantages of the respective models have been critically appraised.

Chapter 4 describes the development of the Platform Safety Model to predict the risks, costs and service reliability of any given asset management policy for an offshore oil and gas installation. The Platform Safety Model is implemented using standard Petri Nets with high level extensions and is sub-divided into the Offshore Safety System Degradation and Maintenance Model and the Offshore Fire and Explosion Model. An overview of the Petri Net modelling technique has been presented before the two sub-models are developed. The Offshore Safety System Degradation and Maintenance Model models the degradation, failure, inspection and maintenance experienced by the different components of the offshore safety systems. The Offshore Fire and Explosion Model is then used to model the occurrence of a hydrocarbon leak from a process vessel located within the three main modules of an offshore installation and predict the frequencies of fires and explosions in the event that the safety systems fail to function on demand in the presence of an ignition source. Using detailed examples, the modelling capability of both models has been presented in this chapter.

Chapter 5 presents the outputs generated from simulations of the Platform Safety model. The results can be used to demonstrate the model's ability to predict costs, risks and availability of any given asset management policy for an offshore oil and gas installation.

Chapter 6 reviews a range of optimisation techniques that can be used to optimise asset management strategies analysed by the Platform Safety Model with the most suitable technique being the Genetic Algorithm (GA). The GA process is applied to the Platform Safety

Model to find the optimum inspection, maintenance and repair strategy that will produce the lowest operational cost whilst minimising the risks to an acceptable level.

Chapter 7 summarises the research, highlights the key findings and contributions to the offshore oil and gas industry, and provides recommendations for future research.

Chapter 2 - Asset Management of Offshore Oil and Gas Installation

2.1 Asset Management: A Risk-Based Approach

Performance of physical assets are critical to the operation of an offshore oil and gas installation. The failure of critical assets pose not only a safety or environmental concern, but in some cases, can lead to the complete shutdown of the installation until the asset can be repaired or replaced. This can have a significant direct commercial effect on the whole business as total production volumes and hence, total revenue will be impacted.

In addition to this, the offshore industry is repeatedly challenged with ageing assets. Furthermore, with the fall in oil prices from $110 per barrel in January 2012 to $50 in August 2017, triggered by the US shale revolution, capital investment in the UKCS is forecast to fall rapidly and there is a need to reduce costs. Hence, offshore asset operations managers are faced with the huge challenge of allocating their limited budget in the most optimal way to their ageing assets.

BS ISO 55000:2014 defines asset management as the "coordinated activity of an organisation to realise value from assets". The standard presents a structured guide to managing critical assets through the adoption of comprehensive inspection, maintenance and repair strategies. For instance, a simple strategy would be to repair as soon as the asset is found to be in a degraded state, however this strategy can prove to be quite expensive, although, its benefits would be that there would be a lower risk of fires and explosions on offshore installations. Thus, a good asset management system supports companies to make improved decisions with regards to choosing the optimal inspection, maintenance and repair strategies to achieve the desired balance of cost, risk and performance.

2.2 Definition of Risk

Andrews and Moss (2002) defines risk, R, as "the product of the consequences, C, of a specific incident and the probability, P, over a time period or frequency of its occurrence". This can be represented using the following equation:

$$R = C \times P \quad (1)$$

To minimise the risk, one may either attempt to reduce the likelihood of occurrence of the undesirable events, or contain, reduce, or mitigate the consequences of these events, or both. For example, in order to reduce the probability of a fire or explosion occurring on an offshore installation, the reliability of safety systems such as the fire and gas detection system, process isolation, process blowdown and deluge would need to be improved to ensure that the risk remains under a tolerable level.

2.3 Tolerability of Risk Framework

The "Tolerability of Risk" framework was developed by the HSE to judge the overall acceptability of risks and is illustrated in Figure 2-1, below.

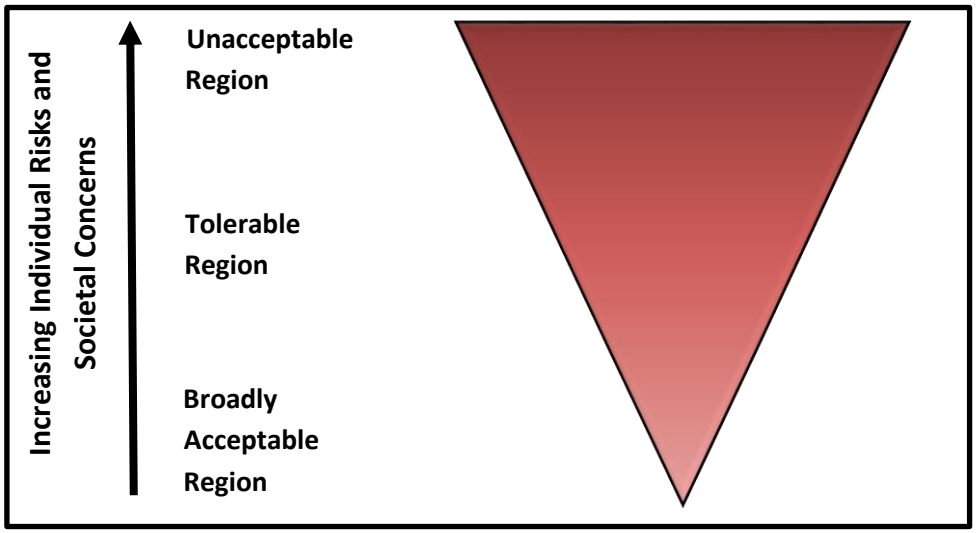


Figure 2-1 Tolerability of Risk Framework (Health & Safety Executive 2001)

The magnitude of the risk involved is represented by the width of the pyramid. The upper region corresponds to all unacceptable risks. For clarity, if a risk falls into this region it is deemed as unacceptable regardless of the benefits associated with the activity. Hence such activities will be ruled out unless it is possible to modify the activity in order to reduce the risk level so that it falls in one of the regions below (Health & Safety Executive 2001).

The lower region, on the other hand, corresponds to all acceptable risks. Again for clarity, if a risk falls into this region it is generally regarded as acceptable provided the risks are controlled adequately. Moreover, it must be ensured that these risks are continuously managed to

remain at this level and reduced if possible.

The region between the unacceptable and broadly acceptable region is known as the tolerable region or as low as is reasonably practicable (ALARP) region. Risks in this region are typical of the risks from activities that people are prepared to tolerate in order to secure benefits. Any risks that fall in this region must be reduced provided that it is reasonably practicable to do so. For instance, consideration would be given to the associated costs of reducing a risk versus the benefits gained.

Health & Safety Executive (1988) defined the maximum tolerable risk to workers and public to be 1 fatality per year per 1000 workers and 1 fatality per year per 10,000 population, respectively. It should be noted that the broadly acceptable risk to workers and public was set to 1 fatality per year per 1,000,000 workers and 1 fatality per year 1,000,000 population, respectively.

2.4 Risk Assessment

Hope & Bjordal (1984) define risk assessment as "*the systematic examination of an actual or proposed industrial installation, to identify, and form an opinion on potentially hazardous occurrences and their possible consequences*". The key aim of a risk assessment is to make informed decisions on risk avoidance or reduction by the appropriate use of qualitative and quantitative methods.

Risk assessment techniques were originally developed by the nuclear engineering community as a "probabilistic risk assessment". In 1983, the risk assessment framework was formalised by the Nuclear Regulatory Commission (NRC) to assist federal agencies, such as the Environmental Protection Agency (EPA), to make informed decisions about chemical substances, in terms of their exposure and adverse health effects to public. Over the years, risk assessment has evolved substantially. In the chemical industry, risk assessment are known as "quantitative risk assessment (QRA)" and are used to manage the risks associated with chemical processing and transportation. In recent years, the use of QRA has been extended to the marine and offshore industry.

System Description is the first step of a risk assessment process. In this step, a description of the following is presented; (1) system's structure and operation, (2) dependencies between components of a system, and (3) system constraints. An assessment of the system's capability to tolerate failures and its susceptibility to accidental effects are also provided.

Hazard Identification is the second step of the risk assessment process. Hazards are documented in a hazard register which outlines the development of the hazard into an accident along with its potential consequences, and the precautions implemented to provide protection from the hazard. The hazards are analysed for all reasonably foreseeable detrimental impact on asset reliability.

A **Frequency Analysis** is then carried out which estimates how likely it is for accidents to occur (Chandrasekaran 2016). In many cases, frequencies may be estimated from historical data or engineering judgement. However, in a majority of risk assessments, the frequencies are found to be very low and hence some form of theoretical modelling must be carried out.

Consequence Analysis, in conjunction with the frequency analysis, assesses the subsequent effects of an accident, and their overall impact on staff, property, plant, equipment, the environment and business. The estimated frequencies and consequences of each modelled event are then combined to form measures of overall **Risk**; also known as, **Risk Analysis**.

The result of the risk analysis process can be used to generate a risk matrix which gives each of the identified risks a significance rating, thereby providing a tool for prioritising risk treatment efforts. This step is known as **Risk Evaluation**. **Risk Reduction Measures** may then be necessary to reduce the risks to ALARP level. As a result, inspection, maintenance and repair activities are planned and implemented accordingly. The condition of equipment following inspection or maintenance is documented, analysed and is used to update the risk-based action plan (DNV 2010). A **Cost-Benefit Analysis (CBA)** would then be used to compare the associated costs of the risk reduction measures against their benefits.

2.5 Hazard Identification Techniques

Hazards can be identified using Hazard Checklists or Hazard and Operability Studies (HAZOP).

2.5.1 Hazard Checklists

A hazard checklist is a written list of questions intended to prompt consideration of a full range of safety issues (Health & Safety Executive 2001). They are an effective and simple way of ensuring that basic types of events have been considered. Many industrial organisations have their own checklists for specific areas of design and operation. Checklists make use of experience of previous risk assessments, which avoids past accidents from recurring. Checklists are carried out by individuals or groups who are trained to understand the questions listed on the checklist. They are designed to provoke thought and enquiry by phrasing the questions as 'open' rather than in a form which requires 'yes/no' answers. As experience reveals problems, more questions have to be added to the list (Hope and Bjordal 1984). Hence, checklists can be an exhaustive technique to use in industry; however, checklists are general thus insufficient on their own, since, they may not cover all types of hazards such as facility-specific hazards. Additionally, checklists may suppress lateral thinking.

2.5.2 Hazard and Operability Studies

HAZOP was first developed in the Heavy Organics Chemicals (HOC) Division of Imperial Chemical Industries (ICI) in the 1960s, following some major problems with new process plants (Kletz 1997). The method was helpful in determining the potential hazards these plants present to the personnel and general public.

The British Chemical Industry Safety Council (BCISC) defines HAZOP as: "*the application of a formal systematic critical examination of the process and engineering intentions of the new facilities to assess the hazard potential of maloperation or malfunction of individual items of equipment and the consequential effects on the facility as a whole*" (Andrews and Moss 2002).

The technique is now widely acknowledged as the most comprehensive qualitative method by the BCISC and is in a widespread use in chemical manufacturing plants throughout the world. A team comprising of multidisciplinary expertise conducts the HAZOP analysis. The team generally have expertise in, process plant design, operation and maintenance, and are directed by an experienced safety analyst through the careful examination of possible

consequences of the disturbances in the plant originated by equipment failure or human error.

The HAZOP approach involves considering each section of the plant, also known as a node, on the Piping & Instrumentation Diagram (P&ID), to determine deviations from the design intent as well as the causes and consequences of these deviations, through the appropriate use of guidewords and parameters. In order to identify potentially hazardous deviations, the study team applies a specific set of guidewords, such as 'NO or NOT', 'LESS', 'MORE', 'PART OF', 'AS WELL AS', 'REVERSE' and 'OTHER THAN' to a pre-defined set of process parameters, for example, 'Flow', 'Pressure', 'Temperature' and 'Level', for each node. Hence, by combining guidewords with process parameters, potential hazards and the possible causes for, and consequences of, the deviation from design intent can be identified and recommendations made to prevent occurrence of deviations and reduce the risk to an acceptable level.

Although HAZOP is broadly used in the chemical industries for hazard analysis related to design, operation and maintenance of the systems, there are some limitations associated with this technique. The method assumes that the design is in line with the appropriate code, i.e. the requirements of normal operating conditions. Hence, it only identifies deviations from these supposedly ideal situations.

Moreover, the method does not account for the decomposition of the plant into subsystems. Another limitation of HAZOP is its dependence on the availability and reliability of engineering information. The method can be time consuming and it must also be highlighted that the experience of the team members can affect the accuracy of the HAZOP study.

2.6 Risk Analysis Methods

The Offshore Installations (Safety Case) Regulations defines QRA as "*the identification of hazards and evaluation of the extent of the risk arising therefrom, incorporating calculation based upon the frequency and magnitude of hazardous events*" (Ramsay *et al.* 1994). Quantitative methods can be divided into tree-based techniques, which include Fault Tree and Event Tree Analysis and techniques for dynamic systems such as Markov Models and Petri Net Models.

2.6.1 Fault Tree Analysis

Fault Tree Analysis (FTA) was first developed in 1961 in Bell Telephone Laboratories and was used to eliminate several weak points in the Minuteman missile launch control program. The technique was improved by the Boeing Company and computer programs were introduced for both qualitative and quantitative fault tree analysis. It was later adopted by the nuclear and chemical industries (Lees 1996a).

A fault tree graphically shows the interrelationships between a potential failure event and the causes of this event. The graphical representation assists engineers by providing an improved understanding of how their systems fail as well as allowing them to carry out either a quantitative or qualitative analysis. The logic and rigor of the analysis simulates the thought process of the experts, allowing them to add their knowledge in a structured way (Sutton 2014). FTA is a deductive, top-down method, capable of modelling potentially large number of events and event combinations that can result in system failure.

The logic of the analysis is represented using gates and events. An event is defined as a "graphical and mathematical representation of a fault or other unwanted occurrence." Each event has an associated probability of occurrence. Gates are logic symbols that are used to link contributory events and conditions. Table 2-1 illustrates the symbols that are commonly used to construct a fault tree, along with a brief description for each of the symbols.

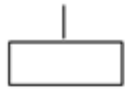
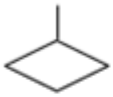
Symbol	Name	Fundamental Relation
	Top Event and Intermediate Events	The top event is the undesired event (accident) that is being analysed. The intermediate events are system states or occurrences that somehow contribute to the accident.
	Basic Events	Basic events represent a component failure and are the lowest levels of resolution in the fault tree. They are characterised by failure frequency data.
	Undeveloped Events	An event which is not further developed either because it is of limited consequence or relevant information is not available.
	AND gate	The output event associated with this gate exists only if all of the input events occur.
	OR gates	The output event associated with this gate exists if at least one of the input events occur.
	Exclusive OR gate	Output event occurs if one, but not both, of the two input event occurs.
	Voting gate	Output event occurs if at least *k* out of the *n* input events occur (For instance, 2-out-of-3)
	Priority AND gate	Output event occurs if all input events occur in the right order from left to right.
	Transfer symbols	Indicates a transfer continuation to a subtree.

Table 2-1 Symbols used to construct Fault Tree (Andrews and Moss 2002)

The structure and applicability of FTA is illustrated using an example based on a storage tank (Tweeddale 2003). The first step in constructing the fault tree is to clearly define the system. In this example, there are two systems – the control system and the safety protection system. The control system is made up of the level sensor (LS), level controller (LC) and level control valve (LCV) and the safety protection system is made up of the high-level switch (LSH), solenoid valve (SV) and level control valve (LCV).

The second step of the analysis is to define the top event, which in this case, is “Tank Overflow”. From the top event, the possible immediate causes of the top event are

established. Based on the example, two intermediate events, “Control System Fails” and “Safety Protection System Fails” are realised. The basic events that most directly lead to each intermediate event are then determined. Each of these elements are represented using single letters to simplify the Boolean algebra. The process is repeated at each successive level of the tree until a basic event is encountered. A basic event is a component failure event for which probability data is available. Hence, at each stage of development, one must question what causes the upper level events. Figure 2-2 shows the fault tree analysing the hazard “Tank Overflow”.

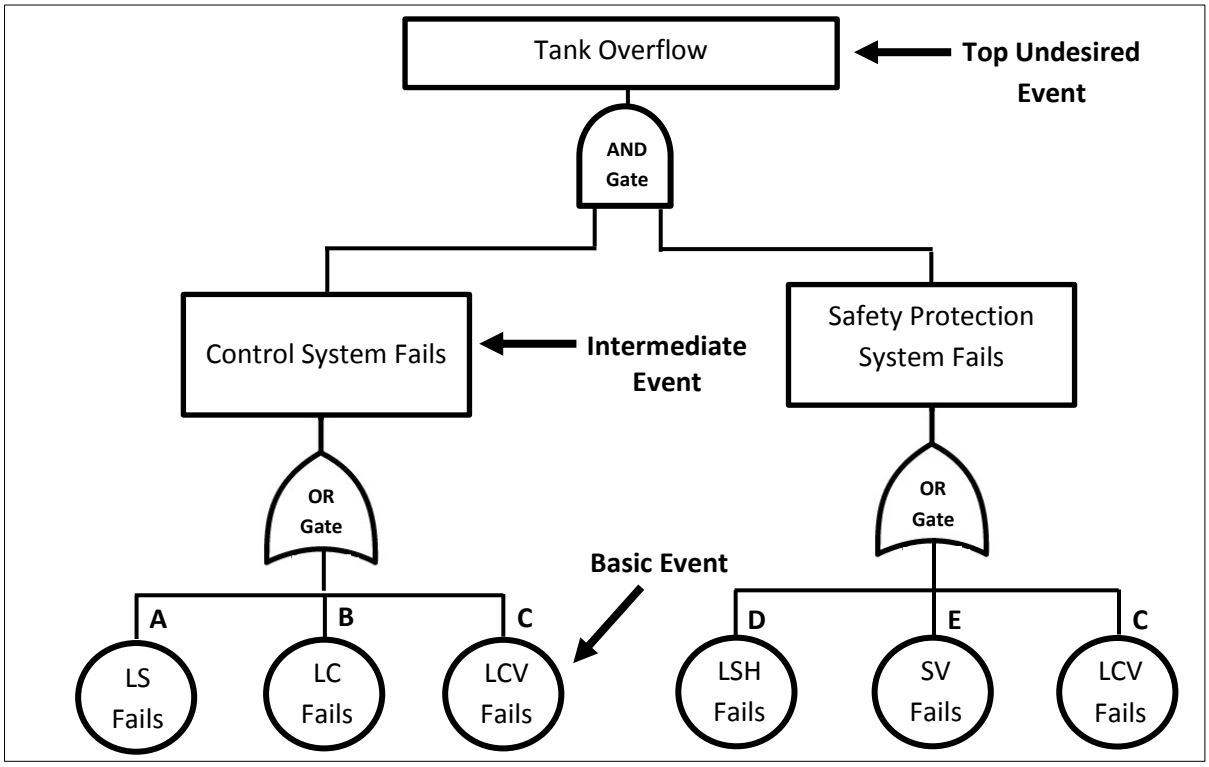


Figure 2-2 Fault Tree Diagram for Tank Overflow (Tweeddale 2003)

Qualitative Evaluation

Skelton (1997) defines a cut set as a “combination of basic events” that are necessary to cause the top event. For industrial engineering systems there are generally a very large number of cuts sets each of which can consist of many component failure events. However, we are more concerned in the list of component failure modes that are necessary and sufficient to cause the system failure mode (top event). This introduces the notion of minimal cut set. Dawkins and Hale (2004) defines minimal cut set as “a cut set such that if any basic event is removed

from the set, the top event will not occur, i.e. it is the smallest combination of component failures, which if they all occur will cause the top event to occur."

The cut sets can be determined by using Boolean expression. For Figure 2-2, the control system fails if A or B or C fail, which in Boolean form is A + B + C, where "+" represents logical OR. The protection system fails if D or E or C fail, which, in Boolean form is D + E + C. Hence, the tank overflows if the control system and safety protection system fails, which, in Boolean form would be as follows:

$$\boldsymbol{T = (A + B + C).(D + E + C)} \quad \textbf{(2)}$$

where, "." represents logical AND.

The Boolean expressions are used in conjunction with the following Boolean identities to obtain the minimal cut sets:

1. Distributive: (A+B) . (C+D) = A.C + A.D + B.C + B.D
2. Idempotent: A + A = A and A.A = A
3. Absorption: A + A.C = A

Thus, the top event, T, can be written as:

$$\boldsymbol{T = (AD) + (AE) + (AC) + (BD) + (BE) + (BC) + (CD) + (CE) + (CC)} \quad \textbf{(3)}$$

where, AD, AE, AC, BD, BE, BC, CD, CE and CC are cut sets.

Using the Boolean identities, the top event, T, can be simplified and written in terms of the minimal cut sets as:

$$\boldsymbol{T = AD + AE + BD + BE + C} \quad \textbf{(4)}$$

where, AD, AE, BD, BE and C are the minimal cut sets.

Qualitatively, the minimal cut sets provide asset operations managers with a clear understanding about which component failures contribute most towards risk. Consequently, they can determine where to allocate capital in order to achieve greatest reduction to that risk. Once the minimal cut sets are identified, the fault tree can be quantified.

For components with a constant failure and repair rate and where the failure event is revealed and repair is performed immediately; the unavailability of the basic event is calculated using the following equation:

$$\boldsymbol{Q}\,(\boldsymbol{t}) = \frac{\boldsymbol{\lambda}}{\boldsymbol{\lambda}+\boldsymbol{\mu}}\left(\mathbf{1} - \boldsymbol{e}^{-(\lambda+\mu)t}\right) \quad \textbf{(5)}$$

where, λ is the constant failure rate and μ is the constant repair rate. In this research, components such as deluge nozzles are modelled using equation (5).

For non-repairable components with a constant failure rate, the unavailability of the basic event is calculated as:

$$\boldsymbol{Q}\,(\boldsymbol{t}) = \mathbf{1} - \boldsymbol{e}^{-\lambda t} \quad \textbf{(6)}$$

In this research, components such as fire and gas detectors are modelled using equation (6).

For dormant components whose failure remains unrevealed until periodic inspection is performed, the average unavailability of the basic event is calculated as:

$$\boldsymbol{Q_{AV}} = \boldsymbol{\lambda}\left(\boldsymbol{\tau} + \frac{\boldsymbol{\theta}}{\mathbf{2}}\right) \quad \textbf{(7)}$$

where, Θ is the inspection interval and τ is the Mean Time To Repair (MTTR). For instance, components such as deluge valves, solenoid valves and air release valves are modelled using equation (7).

Quantitative Evaluation

Quantitative analysis of the fault tree can be used to assess system performance by computing the system failure probability. The analysis is based on a probabilistic method known as Kinetic Tree Theory (Vesely 1969) which assumes that all basic events are independent. Quantitative analysis of a fault tree requires values to be assigned to the frequency or probability of the basic events. The top event probability is then evaluated using the probabilities of the minimal cut sets. If a fault tree has N_c minimal cut sets C_i, i = 1,⋯, N_c then the top event exists if at least one minimal cut set exists:

$$\boldsymbol{T} = \boldsymbol{C_1} + \boldsymbol{C_2} + \cdots + \mathbf{C}_{\mathbf{N}_c} \quad \textbf{(8)}$$

$$= \cup_{i=1}^{N_c} \boldsymbol{C_i}$$

Hence, as the exact probability of the top event, P[T] = P $\left(\cup_{i=1}^{N_c} \boldsymbol{C_i}\right)$, by using the inclusion-exclusion expansion principle, the following equation is derived:

$$\mathbf{P}[\mathbf{T}] = \sum_{\mathbf{i=1}}^{N_c} \mathbf{P}\,(\mathbf{C_i}) \;-\; \sum_{\mathbf{i=2}}^{N_c} \sum_{\mathbf{j=1}}^{\mathbf{i-1}} \mathbf{P}\,(\mathbf{C_i} \cap \mathbf{C_j}) \ldots + (-\mathbf{1})^{N_C+1} \boldsymbol{P}(\mathbf{C_1} \cap \mathbf{C_2} \ldots \cap \mathbf{C_{N_c}}) \qquad \textbf{(9)}$$

However, for large engineering systems, there may be a large number of minimal cut sets. In this case, application of the inclusion-expansion principle would be computationally intensive and expensive. As a result, the top event probability is computed using the rare-event approximation, $\mathrm{P_{RE}[T]}$:

$$\boldsymbol{P_{RE}[T]} = \sum_{\mathbf{i=1}}^{N_c} \mathbf{P}\,(\mathbf{C_i}) \qquad \textbf{(10)}$$

A more accurate approximation called the Minimal Cut Set Upper Bound, $\mathrm{P_{MCSUB}[T]}$, can be used:

$$\boldsymbol{P_{MCSUB}[T]} = \mathbf{1} - \prod_{\boldsymbol{i=1}}^{N_c} \left(\mathbf{1} - \mathbf{P}\,(\boldsymbol{C_i})\right) \qquad \textbf{(11)}$$

Once the probability of the top event occurring has been calculated, asset operations managers may have the desire to reduce the likelihood of this top event. Deterministic or probabilistic importance measures can be used to determine which component contribute the most to the overall unavailability of the system (Andrews and Moss 2002). These include; (1) Birnbaum's measure, (2) Criticality Importance and, (3) Fussell-Vesely's measure.

Advantages and Disadvantages of FTA

While FTA provides an efficient tool for investigating potential causes of system failure; there are several limitations associated with this technique. In the case of large engineering systems, the fault tree becomes enormous and requires a large amount of time to be completed. Furthermore, when quantifying these large fault trees, it may be difficult to obtain an exact solution, hence approximations are used. However, these approximations can be inaccurate.

Binary Decision Diagram (BDD) (Pecht 1995), on the other hand, can be used to solve large fault trees. It analytically encodes Boolean expressions to deduce the failure probability of the top event without approximation or truncation. While it uses less memory to represent large Boolean expressions compared with other methods, it only considers two states per variable. For complex systems with more than one failure state, multiple nodes are required to represent the variable. Hence, the size of the resulting BDD increases, which nullifies the advantages of the BDD technique.

Furthermore, the kinetic tree theory applied in FTA requires the statistical independence of the basic events (Andrews and Moss 2002). This assumption is violated in the case of sequentially operating systems and standby systems. While FTA can be applied to these systems, the resulting outcome is an overestimate as it ignores all dependencies.

Moreover, commercial FTA software assumes a constant failure rate for the basic events. A component's failure rate depends on multiple factors such as its age and the environmental and operational conditions it has been exposed to within its lifetime. Maintenance can also affect an equipment's age and hence their failure rate. The reliability characteristics of most component families can be described using the 'reliability bath-tub' curve shown in Figure 2-3.

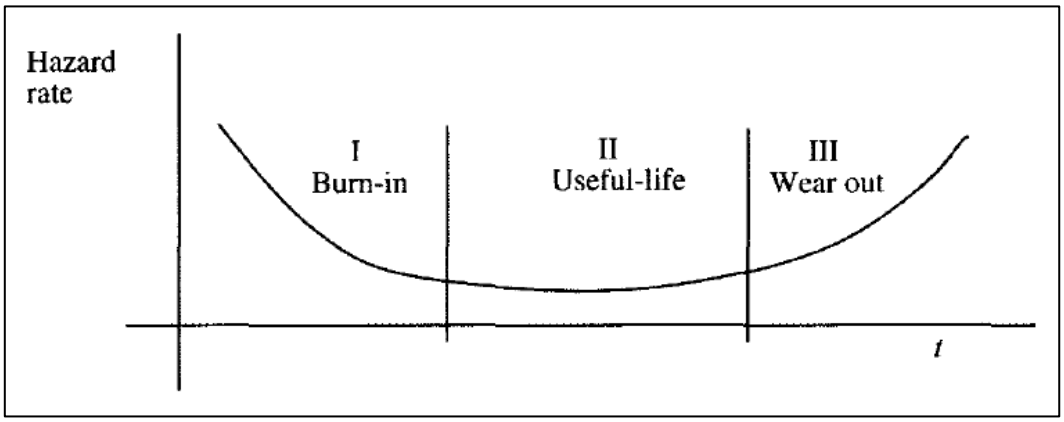


Figure 2-3 Reliability bath-tub curve (Andrews and Moss 2002)

In phase I, the hazard rate (failure rate) will reduce as weak components are eliminated; in phase II (the useful-life phase), it will remain approximately constant; and in phase III

components will start to wear out and the hazard rate will increase. As FTA assumes a constant failure rate, it is unsuitable for ageing assets such as offshore oil and gas processing systems whose study is focused on the wear-out region of the bathtub curve. Hence, non-constant failure rate methods for estimation of reliability parameters may be required.

Furthermore, FTA is incapable of treating time explicitly during the progression of an accident. In the case of dynamic systems such as offshore oil and gas processing systems, certain events trigger other events sequentially or there may be a time delay between the occurrences of two events. These types of scenarios can be quite challenging to incorporate in a fault tree. To overcome the limitation of conventional fault trees, Dynamic Fault Trees (DFT) have been developed. They enable the top event probability to be calculated as a function of time (Cepin & Mavko 2002). However, in order to analyse a DFT, they must be converted into a Markov Chain, which have limitations of their own, as explained in Section 2.6.4.3 of the thesis.

2.6.2 Event Tree Analysis

Event Tree Analysis (ETA) is an inductive reasoning technique used for demonstrating a series of outcomes that may arise following the occurrence of a potentially hazardous event (Stapelberg 2009). Event Trees were first used in combination with fault tree analysis to conduct probabilistic risk analyses of nuclear reactor safety (U.S. Nuclear Regulatory Commission 1975). Its use has now been extended to other industries including the offshore oil and gas industry.

An event tree begins with an initiating event on the left-hand side of the diagram. The consequences of this initiating event can be followed through a sequence of possible paths to the right-hand side of the diagram. The branch points on the tree structure represent the success or failure of different systems which can respond to the initiating event (Andrews and Dunnett 2000). Each event branch can be used as the top event for a fault tree. Hence, the probability of the top event calculated would represent the conditional probability of the occurrence of the event, given that the events, which proceed on that sequence, have occurred.

An example event tree is shown in Figure 2-4. The initiating event is a gas leak. The branch

points on the tree structure represent the success (W) and failure (F) of the safety systems which can respond to the initiating event. The outcomes determined by the end point of each event tree branch identifies a different consequence following the initiating event (Andrews and Dunnett, 2000).

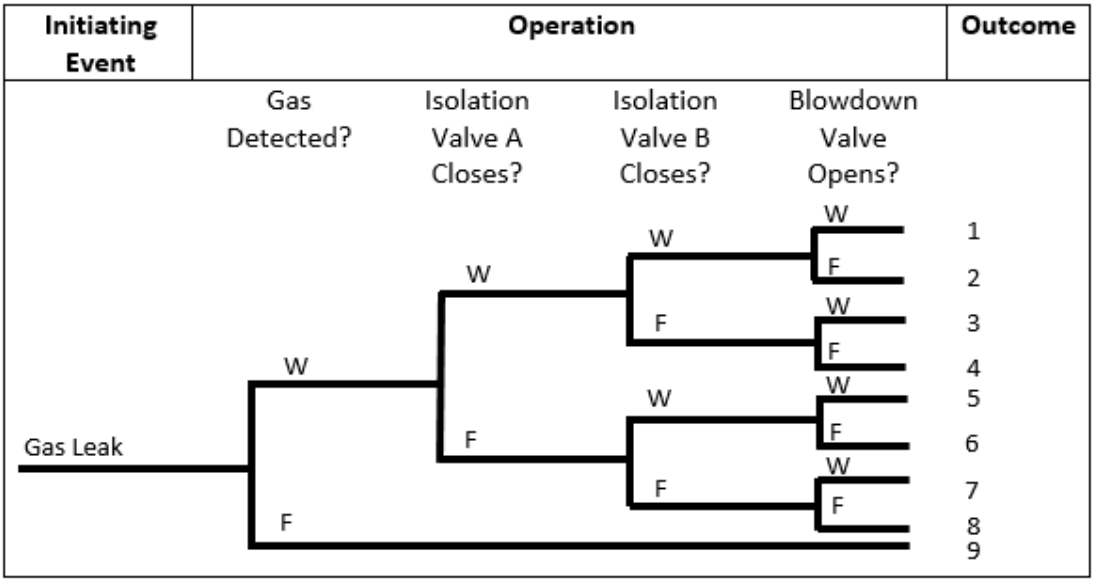


Figure 2-4 Simplified Event Tree (Andrews and Dunnett 2000)

Each branch of the event tree diagram is assigned a probability of occurrence and when multiplied by the starting frequency, the frequencies for all the different outcomes can be generated. The probability for all of the branches at any given level of the tree should add up to 1.

Advantages and Disadvantages of ETA

Event trees are relatively simple and easy to understand. They can be used to recognise critical events that have the greatest impact upon system failure. Unlike FTA, ETA can identify multiple consequences and deal with both dependent and independent failures. However, an event tree only takes into consideration one initiating event at a time. Moreover, as the system increases in complexity, the analysis becomes more complicated.

2.6.3 Use of FTA and ETA in Risk Analysis

In the offshore industry, ETA and FTA have been used extensively to qualitatively or

quantitatively analyse risks such as offshore fire and explosions. ETA and FTA are so closely linked that fault trees are often used to quantify events that are parts of event tree sequences. Fault trees can be constructed to develop causes of each subsystem failure identified and constructed in the ETA (Andrews and Dunnett 2000).

Lewthwaite et al. (2006) developed SAROS (Safety and Reliability of Offshore Structures) to predict the frequency of explosions occurring from the accidental release of gas on an offshore installation. The methodology combines Event Tree Analysis (ETA) and Fault Tree Analysis (FTA), with fluid flow modelling.

FTA and ETA was used to determine the frequencies of occurrence of all possible scenarios resulting from a gas leak. The scenarios evolve from a gas leak on an isolatable process section shown in Figure 2-5. The branch points of the Event Tree determine whether the gas detection system, process isolation and blowdown valves and deluge system are working. Lewthwaite (2006) developed SAROS based on an event tree developed by Andrews *et al.* (2005) (Figure 2-6).

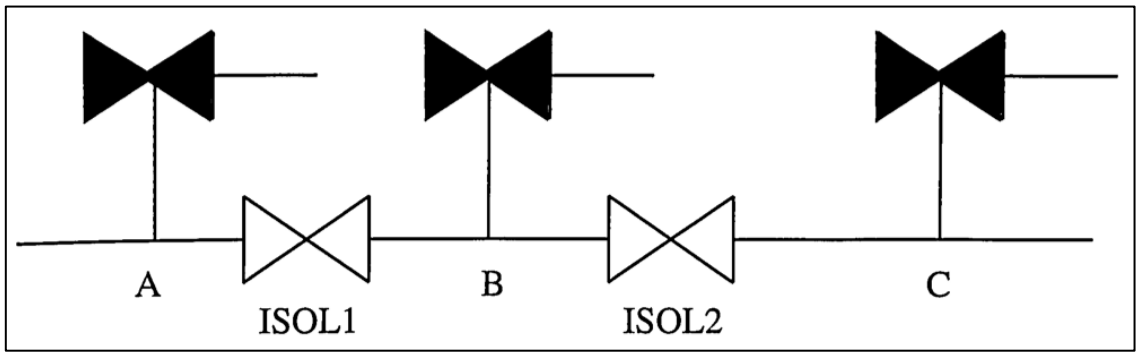


Figure 2-5 Example Isolatable Sections (Lewthwaite 2006)

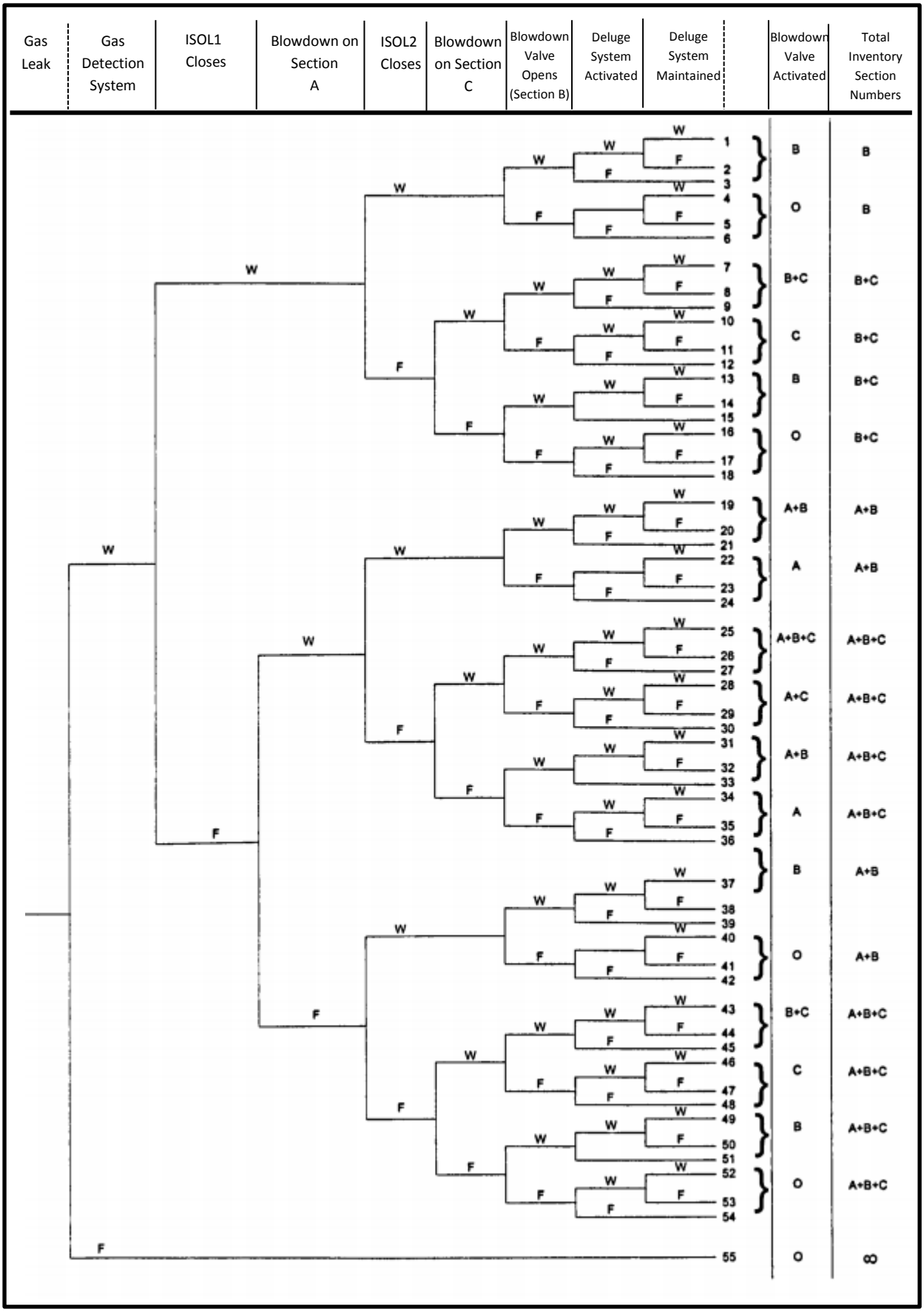


Figure 2-6 Event Tree for Gas Leak (Andrews *et al.* 2005)

The Event Tree shows 55 scenarios that may occur as a result of a gas leak from Section B in Figure 2-5. Initially, the detection of the gas leak is considered. Failure to detect the leak would mean that none of the other safety systems are activated. This would result in an infinite release of gas into the module, i.e. scenario number 55. However, if the gas leak is successfully detected, the second consideration is to check if the isolation valve ISOL1 closes. Subsequently if ISOL1 closes, then Section A would not be able to add to the leak. Hence, the blowdown on Section A is not considered any further. It then considers if isolation valve ISOL2 closes. Subsequently, if ISOL2 closes, then Section C would not be able to add to the leak. Hence, the blowdown on Section C is not considered any further. However, as the leak occurs on Section B the blowdown of Section B must be taken into account. Following this, the activation of the deluge system must also be considered as it can affect the severity of the overpressures produced in an explosion. For instance, if the water spray fails to function on demand in the presence of an ignition source, an unmitigated explosion can occur. An unmitigated explosion can also occur if the water spray activates, however, it is not maintained for the entire duration of the leak.

Therefore, the events are either a success or a failure, with each event having an associated probability of occurring. The frequency of occurrence of each outcome can be calculated by multiplying the frequency of the initiating event with the probabilities of each branch leading to that outcome. FTA is used to determine the probabilities of failure for each safety system prior to the construction of an Event Tree. The analyses performed by means of these tree-based techniques were well structured and well suited for identifying logically correct, or at least, conservative relationships between top event successes and failures (Swaminathan 1999). However, the kinetic tree theory applied in FTA requires the statistical independence of the basic events (Andrews and Moss 2002). Hence, these techniques cannot be used for further analysis of sequential operating systems or standby systems.

2.6.4 Markov Models

Markov models can be used to analyse systems with dependencies. They were developed by the Russian mathematician, A. A. Markov (1856-1922) to investigate alternation of vowels and consonants. His work contributed to the development of the modern theory of stochastic processes. Tijms (2012) defines a stochastic process as "a collection of random variables, indexed by an ordered time variable". Markov chains and stochastic process now form the basis for model-based system evaluation in a vast number of fields, including science and engineering.

Markov models are made up of two main elements: States and Transitions. States are used to represent the possible states of a component while transitions represent the occurrence of events that result in the component changing state. A stochastic process is called a Markov process when it has the memoryless property:

$$\mathbf{P}(X_{t+dt} = k \mid X_t = \mathrm{j}, X_{t-dt} = \mathrm{i}, X_{t-2dt} = \mathrm{h}, \dots, X_0 = \mathrm{a}) = \mathbf{P}(X_{t+dt} = k \mid X_t = j) \qquad (12)$$

This means that, the future state of a Markov process is independent of all past states except the immediately preceding one. So the future behaviour depends only on its current state, not the history of what has happened in the past (Andrews and Moss 2002).

There are two types of Markov models: Discrete Markov chains and Continuous Markov processes. Both models are classified according to time and state space. A Markov chain is discrete in time and hence state changes only occur at discrete points in time. A Markov process, on the other hand, is continuous in time. As a result, state changes are expressed as happening at constant rates, meaning that state residence times are exponentially distributed. Moreover, as the system is continuous, the probability of being in each state can be expressed as a continuous function of time. This is an advantage over Markov chain models, where the state of the system is only known at discrete times.

In this research, the safety systems studied are considered to be repairable systems that operate in a random environment and the systems are subjected to degradation, modes of failure and various types of maintenance activities. Hence, to describe the system dynamics of such continuously-monitored, multi-state repairable systems, Markov processes seem to be more appropriate than Markov chain models and are thus further explained below.

2.6.4.1 Markov Processes

A Markov process model is characterised by a finite set of states, S. Consider the example of a repairable two-state component model shown in Figure 2-7.

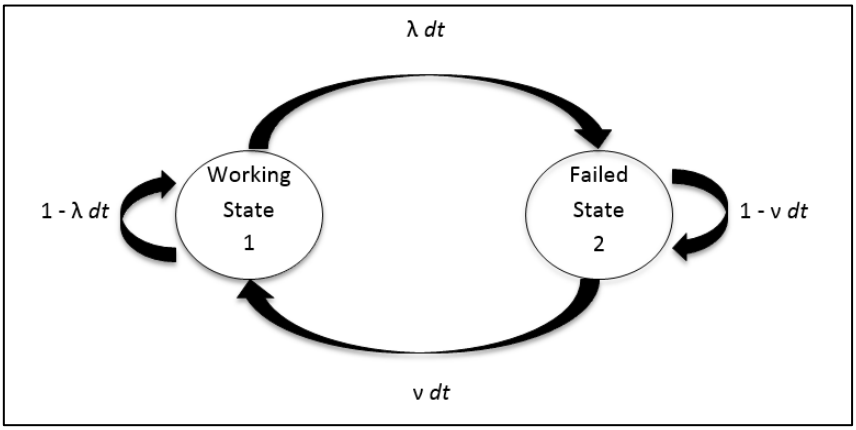


Figure 2-7 State-Transition Diagram for Repairable two-state component (Andrews and Moss 2002)

The component resides in two states: working and failed. Transition from state 1 to state 2 is denoted by a constant failure rate, λ. Hence, the probability of failure at $t+dt$ given that the component is working at t, is $\lambda\, dt$. As the failure is revealed immediately, the transition back to state 1 from state 2 is denoted by a constant repair rate, ν.

Using the state transition diagram, the state equations are found using the following differential equation:

$$\frac{dP_{state}}{dt} = (\boldsymbol{rate\ of\ entering\ state}) - (\boldsymbol{rate\ of\ leaving\ state}) \quad \textbf{(13)}$$

As a result of the Markov property, the probability of residing in state *i* will always be a first-order differential equation.

Similarly, a first-order differential equation can be developed to represent the probability of residing in the working state and failed state, at time *t*, as shown below:

$$\frac{dP_W(t)}{dt} = -\lambda P_W(t) + \nu P_F(t) \quad \textbf{(14)}$$

$$\frac{dP_F(t)}{dt} = \lambda P_W(t) - \nu P_F(t) \quad \textbf{(15)}$$

where, $P_W(t)$ is the probability of the component being in the working state at time, *t*; and $P_F(t)$ is the probability of the component being in the failed state at time, *t*.

Hence, a Markov diagram showing *n* states can be characterized at time *t* by a system of *n* simultaneous first-order differential equations.

In matrix form, equation (14) and (15) would be as follows:

$$\left[\dot{\boldsymbol{P}}_{\boldsymbol{w}}(\boldsymbol{t}), \dot{\boldsymbol{P}}_{\boldsymbol{F}}(\boldsymbol{t})\right] = \left[\boldsymbol{P}_{\boldsymbol{w}}(\boldsymbol{t}), \boldsymbol{P}_{\boldsymbol{F}}(\boldsymbol{t})\right] \begin{bmatrix} -\boldsymbol{\lambda} & \boldsymbol{\lambda} \\ \boldsymbol{\nu} & -\boldsymbol{\nu} \end{bmatrix} \quad \textbf{(16)}$$

From which we have recursively,

$$\left[\dot{\boldsymbol{P}}\right] = \boldsymbol{P} \cdot [\boldsymbol{A}] \quad \textbf{(17)}$$

where,

[A] is the *n*x*n* transition rate matrix or generator matrix = $\begin{cases} a_{ij} & \text{Transition rate from } i \rightarrow j \\ a_{ii} & -\sum_{\substack{j=1 \\ j \neq i}}^{p} a_{ij} \end{cases}$

The transition rate matrix can be formulated using the following key pointers:

- The number of states in the model is equal to the number of rows and columns in the matrix.
- The row sums are equal to 0.
- A non-diagonal element in row *i* and column *j* indicates the transition rate from state *i* to state *j*
- A diagonal element in row *i* and column *i* is the transition rate out of state *i* (this is always negative).

Solving $\left[\dot{\boldsymbol{P}}\right] = [\boldsymbol{P}] \cdot [\boldsymbol{A}]$ returns a vector of state probabilities at the specified time, t. Solution of the differential equations would depend on whether a steady-state solution or transient solution is required. However, it must be noted that the example shown in this section was for a two-state component and it is relatively simple to solve two differential equations to find the steady-state probabilities. This would not be the case for large engineering systems with a large number of states and hence a large number of differential equations. As a result, a numerical method is required to solve the differential equations.

2.6.4.2 Use of Markov Models in Asset Management

Markov methods have proved a popular method in asset management in a wide range of

industries. For instance, Kawauchi & Rausand (2002) applied the Markov modelling approach to assess the production regularity of oil and gas production systems by generating its probability distribution of throughput capacity (PDC). In order to model the system, the system was split into three levels: components, basic subsystems and merged subsystems. Markov analysis was then used to calculate the steady state probability, i.e. the average proportion of time the basic subsystem spends in a particular state. Each state was assigned a unique throughput capacity and therefore the PDC for each basic subsystem was determined. By applying a set of merging rules, the PDC for the merged subsystems were then determined, following by the PDC of the entire system.

Cowing et al. (2004) used a Markov model to track the evolution of a nuclear reactor and its components through different performance phases. The parameters of the model were then linked to different operational strategies to study the effect of each strategy on the system's performance over its specified lifetime. As a result, the model generated long-term system performance measures that were beneficial in decision-making such as set planned and unplanned outage policies for a nuclear power plant.

Fleming (2004) used a Markov model to track the condition of the piping system of the nuclear power plant. The model was subjected to alternative in-service inspection strategy to determine the effect on the frequency of pipe ruptures. The results generated showed that the model was capable of predicting the piping system reliability. Moreover, the model successfully predicts changes in risk due to changes in leak detection as a result of direct changes to in-service inspection strategies.

Le & Andrews (2012) applied the Markov modelling approach to predict the condition of individual railway bridge elements over a 60-year period along with the effects that different maintenance, inspection and repair strategies will have on the bridge elements. In an attempt to incorporate degradation of the individual bridge elements within the Markov model, the degradation rates of each element were determined through thorough examination of maintenance records obtained for UK rail network. The model was successful in producing results such as the probability of the individual bridge elements being in different states at any given time in the future, the expected costs of maintenance over a 60-year period for

each type of strategy applied to the bridge elements and, hence, the cumulative maintenance cost for the whole bridge.

Prescott & Andrews (2013) used a Markov model to investigate the asset management strategy applied to a railway track. The model tracked the condition of the track section over a 30-year period. Similar to Le & Andrews (2012), Prescott & Andrews (2013) analysed degradation data obtained for the UK rail network to determine the rates of degradation for the track section. In order to conduct a more realistic analysis, the authors accounted for the change in degradation rate as a result of maintenance. Hence, due to "memoryless" property of the Markov method, after every maintenance activity, the model is returned to a new state which represents the number of maintenance activities performed previously. Once 7 maintenance activities have been carried out on the track section, the number of maintenance activities carried out on the section is no longer affected by the degradation rate, hence, the system will degrade at the same rate. After a 30-year period, the whole section of the track is renewed, and the system is returned to its initial state. A Runge-Kutta algorithm was used to solve the equations and obtain results such as the proportion of time the track spent in certain conditions and the probability of performing maintenance interventions on the track throughout its lifetime.

2.6.4.3 Advantages and Disadvantages of Markov Models

A review of current literature shows that Markov models are a good tool for understanding system operation and predicting the future condition of the assets by calculating the probability of being in each of the potential states. The approach can be used to model the degradation and failure process and hence predict the future condition of the component (Zio 2012). Moreover, the model is capable of identifying safety issues early in the design. Unlike tree-based techniques, Markov models can be used to analyse a system of components, which have strong dependencies between each other (Chew 2010). However, Markov models have several limitations. The model can only deal with constant failure and repair rates, which is inapplicable to ageing offshore assets whose study is focussed on the wear-out region of the bathtub curve. Although Markov models can be used to capture the dynamic behaviour and dependencies among components, state-space explosion due to their memoryless property, limits their usage. When modelling component failure, the key factor of applying a

Markov process to system failure modelling is to identify the system states and transition probabilities. The number of possible system states is equal to the total number of possible combination of component states. For instance, a system containing n components may require up to 2^n states in a Markov chain representation (Melnick and Everitt 2008). This means that the number of system states increases exponentially as the number of components in a system increases. This can result in the Markov models becoming excessively large, hence, making it difficult to solve analytically.

2.6.5 Petri Net Analysis

Petri Net Analysis (PNA) relies upon the use of Petri Nets (PN) as a modelling formalism. They were first introduced by Carl Adam Petri as part of his thesis dissertation titled "Kommunikation mit Automaten" in 1962 (Petri 1962). Since their introduction, PN have been used to model dynamic systems in a variety of speciality disciplines such as computer science and engineering. PN combine a well-defined mathematical theory with graphical representation of the dynamic behaviour of systems (Mohammed and Ali 2015). The theoretical feature of PN allows detailed modelling and investigation of system behaviour, while their graphical representation supports the visualisation of state changes of the modelled system. PN are capable of simulating large engineering systems whose computational time becomes too significant to ignore. Like Markov models, PN models are a state-based method. However, unlike Markov chains, the probability distributions for the rates of transitions for the PN are not restricted. PN are capable of simulating any distribution for event times and hence simulation of complex system behaviour.

2.6.5.1 Untimed Low-Level Petri Nets

PN is a bipartite, directed graph, where P and T are the disjoint sets of nodes, namely places and transitions that are linked by directed arcs. Mathematically, a PN is defined as a five-tuple (18):

$$\boldsymbol{N} = (\boldsymbol{P}, \boldsymbol{T}, \boldsymbol{A}, \boldsymbol{W}, \boldsymbol{M_0}) \quad \textbf{(18)}$$

where,

N is the set of integers;

P = (P_i), i = 1 , 2 , ..., n, is a finite set of places;

T = (T_j), j = 1 , 2 , ..., m, is a finite set of transitions, $P \cup T \neq \emptyset \; and \; T \cap P = \emptyset$;

$A \subseteq P \times T \cup T \times P$ is a set of directed arcs connecting places to transitions and transitions to places;

$W : A \rightarrow N$ is a function defining the weight of each arc of the net;

$M_0: P \rightarrow N$ is a function defining the initial marking, i.e. the initial number of tokens in each place of the net.

PN can be constructed using the following components:

- **Places** are used to represent a particular state or condition of the system. The system is evolving when it goes from one state to another. Places can store a number of tokens.
- **Tokens** reside in the places to indicate the state of the system at any time. Presence or absence of a token in a place can indicate whether a condition associated with this place is true or false. The number and position of tokens may change during the execution of a PN.
- **Transitions** enable the movement of tokens from input places to output places and thereby represents the dynamics of the system as it changes state. Each transition is associated and labelled with a time delay, t. In the case of untimed Petri Nets, the transitions are immediate, i.e. t=0, and are represented using a solid black transition box.
- **Arcs** link input places to transitions and transitions to output places using directed edges to represent the movement of the token. Each arc on the PN has an associated multiplicity or weight, *k*. Arc multiplicity is used when more than one token is to be transferred to or from a place. By default, if no number is assigned then its multiplicity is 1.

Graphical representation of the different components used in untimed PNs is shown in Table 2-2, below.

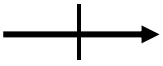
Component	Graphical Representation
Tokens	
Places	
Transitions	
Normal Arcs	*k* 

Table 2-2 Symbols used in Untimed Petri Nets

An example of an untimed low-level PNs is given in Figure 2-8. This net consists of 4 places, P_1, P_2, P_3 and P_4; 3 transitions, T_1, T_2 and T_3 and 3 arcs connecting places to transitions and 4 arcs connecting transitions to places.

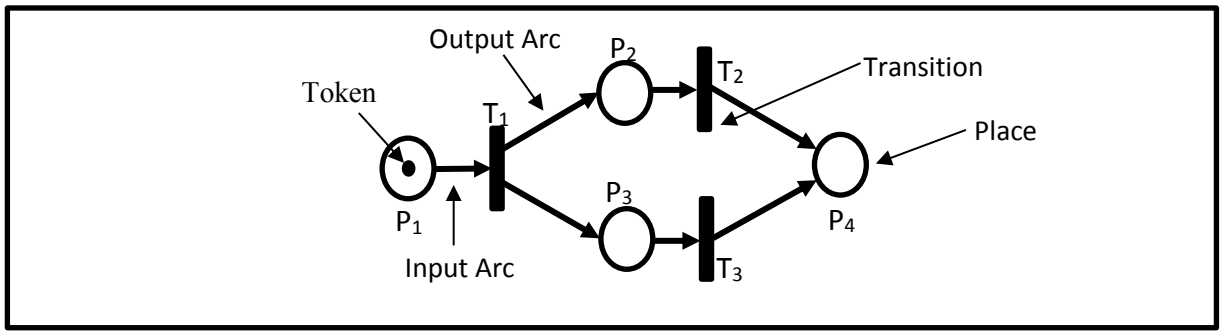


Figure 2-8 Untimed Petri Net

The execution of a PN is controlled by the number and distribution of tokens in the PN (Wang, 2007). A PN executes by firing transitions which adhere to the following rules:

1. A transition, T, is enabled when the input places contain at least a number of tokens equal to their multiplicity. The transition, T_1, shown in Figure 2-9 is said to be enabled as the input place, P_1, contains two tokens which matches the associated arc multiplicity.
2. After $t \geq 0$, has elapsed, the enabled transition switches or fires.
3. On firing, the multiplicity of tokens is removed from each input place and a multiplicity of tokens is added to the output places. The status of the net following the firing process is shown in Figure 2-10.

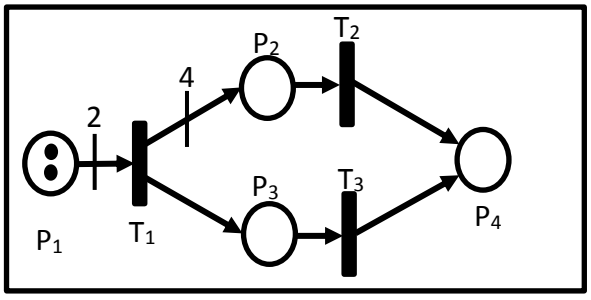


Figure 2-9 Transition T1 enabled

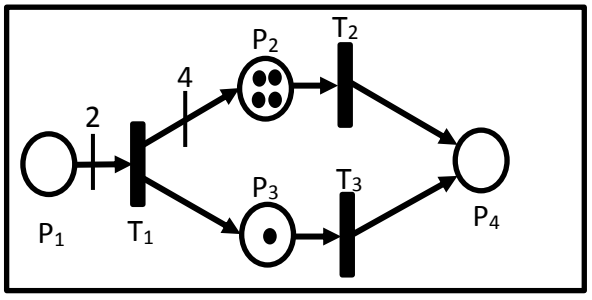


Figure 2-10 Enabled Transition T1 fires

2.6.5.2 Timed Low-Level Petri Nets

In timed PN, both untimed as well as timed transitions may be used. In order to fire, a timed transition shall be enabled after a specific time duration, called delay. This duration can either be stochastic or deterministic. For deterministic transitions, the duration is generally a fixed time assigned to it. After this duration has elapsed, the transition is allowed to fire. For

stochastic transitions, the duration is sampled from a probabilistic distribution. Graphical representation of the transitions used in timed PN are shown in Table 2-3, below.

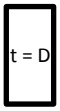
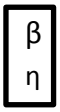
	Type of Transition			
	Deterministic		Stochastic	
	Delay is Zero	Delay is Fixed Time	Exponential Distribution	Weibull Distribution
Symbol				

Table 2-3 Symbols used in Timed Petri Nets

However, there is a possibility that a conflicting situation such as the following may arise; (1) more than one transition is enabled from the same place at different times and (2) more than one transition is enabled from the same place at the same time. In the first situation, the transition whose time delay ends the soonest will fire and switch a determinate number of tokens from the input place. If the input place is now unmarked, the other transition is disabled. Otherwise, it will also fire after its time delay has passed. In the second situation, when there are one or more enabled transitions for a given marking, it means that every one of these transitions can be fired. It is possible that each of the enabled transitions performs its operations on a different state of input values. As a result, an execution policy must be imposed such that transitions fire in the correct order. Two policies are available to resolve this situation (Begain *et al.* 2012); (1) 'Preselection policy' – transitions are given a certain level of preference as to which fires first. The preference could be based on the number of tokens in the input place for the transitions and (2) 'Race policy' – one transition automatically overrides the other.

2.6.5.3 Solving Petri Nets using Monte Carlo Simulation

Monte Carlo simulation can be used to solve the PN model for the system being studied. For each Monte Carlo simulation, the firing times of stochastically timed transitions are randomly sampled from the appropriate statistical distributions as described in Section 2.6.5.4, and the tokens are moved around the net accordingly until the predefined lifetime of the system is reached. A number of simulations are performed and data is collected after each simulation run. The system is assessed once the data obtained has converged. The data generated as a

result of simulating the model may include the number of times a particular place is occupied or the amount of time a token resides in a particular state. This provides information such as offshore safety system availability, number of maintenance activities performed and the associated costs for the different maintenance activities, which is highly beneficial to offshore asset operations managers.

2.6.5.4 Distribution for generating transition firing times

Two main distributions are used in this research:

1. Exponential Distribution

Exponential Distribution uses the following density function:

$$\boldsymbol{f(t) = \frac{1}{\mu}\, e^{-t/\mu}} \quad \textbf{(19)}$$

where, μ is the mean or mean time to failure (MTTF). In this research, when the failures are all due to random processes, i.e. degradation is not the primary cause of component failure (because components are maintained before their condition influences failure rates), then the probability of a certain component's failure, is described by an exponential distribution. A lambda parameter is then equal to the derived failure rate for that component type; where $\lambda = 1 / \mu$.

For calculation of firing times, the following steps are performed:

1. The density function is integrated to obtain the cumulative failure distribution, F(t):

$$\boldsymbol{F(t) = \int_0^t f(u)\, du = 1 - e^{-t/\mu}} \quad \textbf{(20)}$$

2. A random number, X, uniformly distribution in the range [0,1], is generated and equated to the cumulative failure distribution:

$$\boldsymbol{X = 1 - e^{-t/\mu}} \quad \textbf{(21)}$$

3. To find the firing time, Equation (21) is rearranged as follows:

$$\boldsymbol{t = -\mu \ln(1 - X)} \quad \textbf{(22)}$$

where, X is assumed to be a random uniform number over (0, 1), as such it also applies to (1-X). Hence, Equation (22) can be simplified to the following:

$$\boldsymbol{t = -\mu \ln X} \quad \textbf{(23)}$$

2. Weibull Distribution

The Weibull Distribution uses the following density function:

$$f(t) = \beta \frac{t^{\beta-1}}{\eta^{\beta}} e^{-(t/\eta)^{\beta}} \quad \textbf{(24)}$$

where, η is the Weibull scale parameter or characteristic life; and β is the Weibull shape parameter; where, $\beta < 1$ indicates a reducing hazard rate, $\beta = 1$ indicates a constant hazard rate and $\beta > 1$ indicates an increasing hazard rate. Due to its flexibility to model all phases of the reliability bath-tub curve, Weibull distribution is extensively used to analyse component lifetime data. In this research, Phase III – wear out of a component is described using Weibull distribution.

For calculation of firing times, the following steps are considered:

1. The density function is integrated to obtain the cumulative failure distribution, F(t):

$$F(t) = 1 - e^{-(t/\eta)^{\beta}} \quad \textbf{(25)}$$

2. A random number X, uniformly distribution in the range [0,1], is generated and equated to the cumulative failure distribution:

$$X = 1 - e^{-(t/\eta)^{\beta}} \quad \textbf{(26)}$$

3. To find the firing time, Equation (26) is rearranged as follows:

$$t = \eta [-\ln(X)]^{1/\beta} \quad \textbf{(27)}$$

2.6.5.5 Coloured Petri Nets

Coloured Petri Nets (CPNs) were developed by Jensen & Kristensen (2009) and its use has been demonstrated by several authors in risk and reliability assessment (Volovoi 2004). Unlike, standard PNs, which uses only one kind of anonymous token, CPNs use tokens that contain a data value. Each data value has a specified property and can belong to a set of values, for instance, a data value could be an integer in the set {0, 1, 2, 3}. The data values are referred to as colours and the set of data values is referred to as a colour set. The different tokens can be distinguished according to their data values, which represent different instances of each component being modelled. Transitions would fire depending on the token colours of the available input tokens. The structure and applicability of CPN is further explained using the example shown in Figure 2-11.

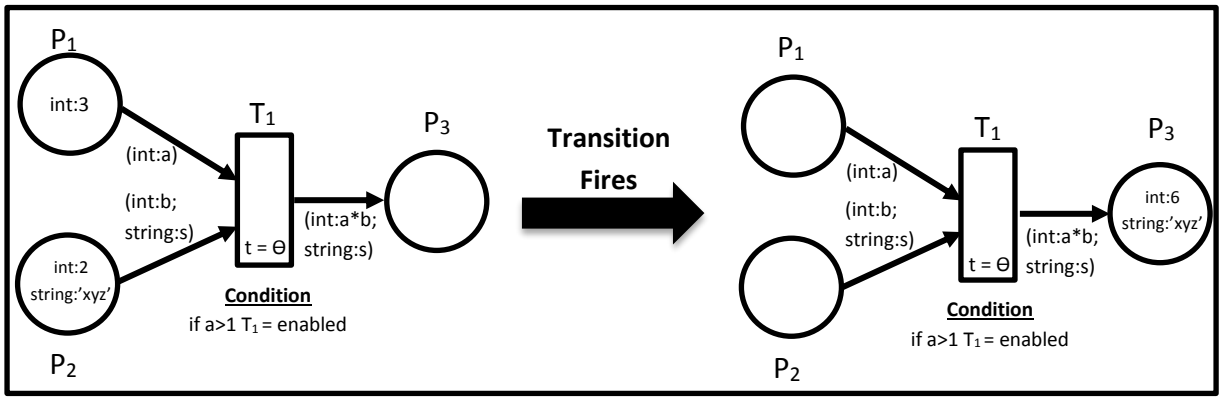


Figure 2-11 Coloured Petri Net

P_1 and P_2 both contain a token. However, the tokens are of different types. While P_1 contains a token with an integer value of 3, P_2 contains a token with an integer value of 2 and a string 'xyz'. The transition, T_1, is a function and contains a condition which states that in order for it to be enabled, the token in place P_1 must have an integer value > 1. Once T_1 is enabled, it fires after a time, $t = \Theta$. The input arcs of the transition provides the inputs for the function while the output arc generates the output from that function. When the transition fires, the tokens are removed from P_1 and P_2 and a token is added to P_3. P_3 now contains a token with integer value of 6 and a string 'xyz'.

CPNs are advantageous over standard PNs as they can be used to model complex systems without the limitations of the net becoming infinitely large. Tokens used in CPNs are distinguishable and can contain particular characteristics (e.g. age of the component, number of previous maintenance interventions conducted on the component, etc.) unlike anonymous tokens used in standard PNs. Hence, instead of creating several nets with lots of places and transitions to represent the degradation of the different components, one net can be used containing different coloured tokens for each component. In addition to this, the transitions used in CPN contain a function that can change the characteristics of the token once fired. CPNs can also be constructed and simulated using a readily available graphical software, called CPN tools.

However, it must be noted that the application of CPN tools is limited and cannot be used to obtain certain desired results, as it is not specific to the problem being investigated. Hence, it may be necessary to code a CPN to make it problem-specific. This process would complicate interfaces making it difficult to understand. Moreover, in theory, the computational power

required to simulate standard and coloured PNs is the same, as the number of processes modelled is the same, i.e. same number of transitions and places are used. Hence, although the graphical representation of CPNs are intuitively very appealing; they offer the same modelling capabilities as standard Petri Nets. Thus, there is no gain in applying CPN to the system being studied in this research.

2.6.5.6 Use of Petri Nets in Asset Management

The use of PN in risk and reliability assessment and in asset management models in quotient is relatively new. However, its use has been explored in a variety of industries such as the chemical, nuclear and railway industries. For instance, Balasubramanian et al. (2002) developed a hierarchical approach to construct a PN model to describe the sequential operation of loading liquid ammonia into storage facilities. PN models were developed for all the components used in the loading operation, taking into consideration their individual failure modes. The PN model for the individual components were then connected to create the system model. By introducing predefined hazards to the system model, the model was simulated to identify critical fault propagation scenarios. The results generated as a result of the simulation were quite useful to analyse the risks associated with loading liquid ammonia into storage facilities and hence lower it to an ALARP level.

Dejean et al. (2007) developed a global model of a representative deep offshore production system, based on hybrid stochastic PN into which the Response Surface Models (RSMs) were directly integrated. The aim of their research was to obtain realistic estimates of the performance of deep offshore production systems through coupling simulation of Flow Assurance phenomena (wax deposition and hydrate plugs formation) with reliability phenomena. Stochastic PNs were created to simulate the behaviour of elementary equipment, for instance, well completion. The final model for the whole system consisted of about 50 PNs. Reliability data for the model were obtained from a database. The simulations were run for a 16-year period and results such as average production and production availability of the system for a given flow assurance risk over its lifecycle were obtained.

Thangamani (2012) used a Generalised Stochastic PN to model the availability of a lube oil system used in a combined cycle power plant. Nets were created for the different subsystem,

which were then combined to form the system model. The firing times for the transitions used in their PN were either instantaneous or randomly sampled from an exponential distribution. The proposed net was simulated for a 30-year period and results such as system downtime, failure criticality index and components causing unavailability of the lube oil system were obtained. Hence, it can be seen that PNs are an effective tool for obtaining a variety of statistics that can be useful in risk and reliability assessment of a wide range of assets.

Li et al. (2012) described a Stochastic PN to model the stress corrosion cracking of a metal weld in a primary coolant system of a nuclear power plant. The different states of the crack growth process in the metal weld were represented via the PN and simulated for an 80-year period to obtain the probabilities of being in the different states at any given time. The effects of external influencing factors such as uncertainty in temperature were also modelled. The output data as a result of simulating the net can be useful in understanding the dynamics of a degradation process for any given asset and hence prove useful to asset operations managers who are trying to improve their asset management strategy.

Andrews (2012) used a Stochastic PN with extended features to model the degradation process of a railway track along with the effects of inspection, maintenance and renewal on the condition of the track. The firing times for the transitions used in the net was sampled from both Exponential and Weibull distribution. The net was simulated using Monte Carlo simulation for a 180-year period and generated a wide range of statistics such as the number of interventions carried out on the track section, the number of times line closure was imposed, the number of times speed restrictions were imposed and the duration of the speed restriction imposed. This data provides asset operations managers with useful insight about the future condition of the track for any asset management policy they may choose to implement. By determining the costs of performing the different interventions on the track section along with the penalty costs of implementing speed restriction and line closures, the life cycle costs of the different asset management policies can be evaluated and the most effective policy can be chosen. In conclusion, Andrews (2013) provides a detailed methodology that uses the PN modelling approach to model the asset management of any asset over their lifetime.

Briš (2013) described the application of PNs to evaluate the availability of a multi-state, multi-output offshore installation with operational loops. A stochastic model of the plant evolution was developed taking into account the component's reliability parameters, process capacities and operational dependencies as well as taking into consideration several complex processes like the degradation of components, corrective and preventive maintenance strategy, resource allocation and the different failures of the system. PN models were developed for the individual components and combined to build the system model. Their model assumes that the transition times of the degradation and failure events are exponentially distributed. The PN model was successful in studying the effects of preventive maintenance on the availability of each production level by simulating four different scenarios; Case A – system without preventive maintenance, Case B – system with preventive maintenance, Case C – system without preventive maintenance and with standby and D – system with preventive maintenance and with standby and Case E – the components are preventively maintained with predefined policy.

Le & Andrews (2015) used a Stochastic PN with extended features to model the degradation of an offshore wind turbine along with the effects of a specified maintenance strategy on the condition of the wind turbine over a 40-year period. PN models were created for the different processes of a subsystem and its components which were linked to form the wind turbine system model. The transition times for the component degradation and failure were sampled from a Weibull distribution. The net was simulated using Monte Carlo Simulation method to generate a selection of results such as probability of the wind turbine being in different condition states, the expected number of component failures over the system lifetime and the number of maintenance interventions. As a result of these statistics, the costs for performing maintenance on the different components of the wind turbine were then calculated.

A review of current literature shows the potential of PN for risk and reliability assessment of a wide range of assets. PNs can be used to model the degradation and failure of an asset as well as investigate the effects of different maintenance policies on the condition of the asset over its lifetime. By using Monte-Carlo Simulation, the net can be solved to produce a variety

of statistics which can be used by asset operations managers to choose the optimal intervention for a particular asset to reduce their risk close to an ALARP level.

2.7 Summary

Operating an offshore production facility demands a high level of safety and reliability, hence, the implementation of a strict set of regulatory procedures is required to ensure that risks are at an acceptable level. However, failure to comply with these regulations can lead to catastrophic consequences for the offshore installation, its personnel and the environment. Thus, a robust risk assessment tool which quantifies the likelihood and consequences of an undesirable event is necessary. Asset risks can be evaluated using qualitative and quantitative techniques. Qualitative techniques such as HAZOP and Hazard Checklists can be categorised as the most important in identifying hazards on offshore oil and gas installations. However, these methods are only capable of identifying hazards in a process. They fail to provide an extensive analysis of the occurrence, frequency, overall effects, and hence a definite solution to the hazard.

Quantitative techniques such as FTA and ETA address some of the deficiencies of qualitative techniques. With the availability of operational data, they can be used to quantify the probability of occurrence of an undesired event. However, tree-based techniques lack the ability to model the dynamic aspects of an offshore installation. The techniques are incapable of representing events that have a certain time duration (Nivolianitou *et al.* 2004). Furthermore, basic events are assigned constant failure rates which is inapplicable to ageing offshore components whose study is focused on the wear-out region of the bathtub curve. In addition, the kinetic tree theory applied in FTA requires the statistical independence of the basic events (Andrews and Moss 2002). This assumption is violated in the case of sequentially operating systems and standby systems. It can be difficult to quantify large fault trees, hence, approximations are used. However, the results generated can be highly inaccurate.

Unlike tree-based techniques, Markov Analysis based models are able to capture the dynamic behaviour and dependencies among components (Thangamani 2011). By using appropriate states and transitions between these states, Markov models can be used to represent the different functionality of a component and hence used to analyse systems containing

dependences. Markov analysis is highly effective when applied to small engineering systems containing dependencies. However, when applied to large engineering systems, Markov models can become excessively large, making it difficult to construct and solve analytically. A numerical solution may be necessary that would require large amounts of computational power and time. A further disadvantage of Markov models is that like tree-based techniques, Markov models are also limited to constant failure rates for each component.

PNs provide a modelling formalism that is a combination of tree-based techniques and Markov modelling. PNs, like tree-based techniques, are capable of providing a graphical representation of the system. However, unlike FTA and ETA, PNs can be used to represent the dynamic aspects of a system to a detailed level. They provide a better representation of time sequence of the events including duration between the events. Like Markov models, statistical dependencies among components in PN are represented via states and transitions between these states. However, unlike Markov models, PNs are not limited to constant failure and repair rates for each component. In addition to exponential distributions for generating event firing times, Weibull distributions can also be used. Hence, according to Le (2014), in terms of computational time, PN models are much more efficient for modelling large engineering systems.

Furthermore, literature reviewed in Section 2.6.5.6, shows that PNs are an efficient tool for modelling asset management. To meet the specific needs of different applications, different varieties of PN models are available that are all related by the basic net formalism which they build upon. Hence, based on the advantages outlined, the PN modelling approach has been chosen to model the degradation and failure of offshore safety systems, dependencies among the different systems and components, along with the effects of inspection and maintenance on the condition of the safety systems. In particular, standard PN with high level extensions will be used to model these processes. The model will be solved via Monte Carlo Simulation to generate a variety of results that can be used by offshore asset operations managers to make well-informed decision with regards to asset management without compromising the safety of the assets.

Chapter 3 - Modelling Fires and Explosions

3.1 Fires and Explosions on Offshore Installations

Most offshore fire and explosion incidents occur due to the sudden release of highly flammable hydrocarbon (Simpson, 1997). Release of hydrocarbon can occur due to flange failures on pipe work or occurrence of a hole on a process vessel. This can be highly damaging to the structure of the installation and its personnel. Hence, it is essential to carry out a fire and explosion study to determine the characteristics and severity of the subsequent fire and/or explosion and hence reduce the frequencies of their occurrence. The characteristics and severity of the subsequent explosion and/or fire are a function of: (1) fuel mass; (2) type of release; (3) dispersion and mixing of the fuel with the surrounding air; (4) ignition time; (5) ventilation and confinement and (6) location of ignition source.

3.2 Hydrocarbon Releases

Hydrocarbon releases can be defined as major, significant or minor (Health & Safety Executive, 2015):

Major - "*Potential for a quick and significant impact on the local area e. g. affecting the Temporary Refuge, blocking escape routes, escalating to other areas of the installation, and causing serious injuries or fatalities.*" The following criteria are considered for three types of major releases:

- Gas Releases: either a leak amount > 300 kg or a leak rate > 1 kg/s and a leak duration > 5 minutes. This could result in a jet fire with a flame length of 10m or an explosion.
- Liquid Releases: either a leak amount > 9000 kg or a leak rate > 10 kg/s and leak duration > 15 minutes. This could result in a pool fire with a diameter of over 10m which could fill the module and obstruct escape routes. If the fire lasts longer than 15 minutes, it could result in the death of more than one person.
- Two-Phase Releases: either an amount of released liquids > 300 kg or liquid release rate > 1 kg/s and release duration > 5 minutes.

Significant - "*Potential to cause serious injury or fatality among personnel within the local area and to escalate within that local area e. g. by causing structural damage, secondary leaks*

or damage to safety systems." The criteria for significant releases fall between those for major and minor releases:

- Gas Releases: This could result in a jet fire with a flame length between 5 and 10m and duration between 2 and 5 minutes or a release rate between 0.1 to 1.0 kg/s lasting 2 to 5 minutes and producing flammable clouds of between 10 and 3000m^3 in size.
- Liquid Releases: capable of producing a pool fire with a diameter between 2 and 10m and a duration between 5 and 15 minutes.
- Two-Phase Releases: possible combinations of gas and liquids.

Minor - "*Potential to cause serious injury to personnel in the immediate vicinity but no potential to escalate or cause multiple fatalities*." A minor leak, even if ignited, is not expected to result in a multiple fatality event, however, it could cause serious injuries or a fatalities to those nearby or within the module in which it occurs. The following criteria are considered for three types of major releases:

- Gas Releases: either a leak amount > 1 kg or a leak rate > 0.1 kg/s and a leak duration < 2 minutes.
- Liquid Releases: either a leak amount < 60 kg or a leak rate < 0.2 kg/s and leak duration < 5 minutes.
- Two-Phase Releases: either an amount of released liquids < 1 kg or liquid release rate < 0.1 kg/s and release duration < 2 minutes.

3.3 Consequence Modelling of Accidental Release of Hydrocarbons

In offshore risk assessment, the standard methodology (Bain *et al.* 2014) for dealing with an accidental release of hydrocarbon is to evaluate a number of different release scenarios. The number of scenarios would depend on the number of isolatable sections, the number of areas on the installation and the phase of the material released. The material released can either be gaseous, liquid or two-phase liquid-gas release. The consequence of the release would depend on a variety of factors such as size of the leak hole, duration of release, wind speed, wind direction, weather stability, geometrical layout (confinement and obstructing objects), ignition probability, ignition sources/location, ignition strength, and availability of safety systems such as detection system, isolation and blowdown system and deluge system.

Factors such as the hole size would have an effect on the hydrocarbon release rate, which in turn would have an effect on the size of the gas cloud produced and its concentration. If ignition were to occur, it would have an effect on the size of the flames produced. Furthermore, the size of the gas clouds would influence the ignition probability and overpressure of an explosion. Eventually, all these factors would have an effect on the number of fatalities on the offshore oil and gas installation. For this research, the general logic diagram for consequence analysis of an accidental release of hydrocarbons is shown in Figure 3-1.

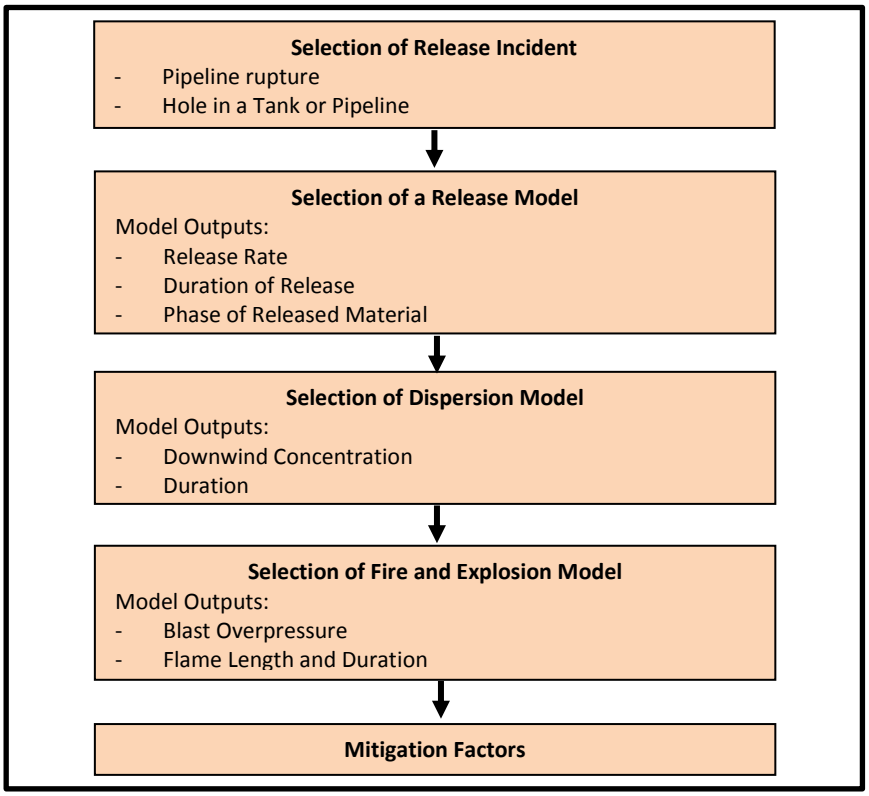


Figure 3-1 Consequence Analysis of an Accidental Release of Hydrocarbons

3.4 Release Models

Release models are used to calculate the amount of hydrocarbon released, or the release rate. The model is based on well-developed theories of chemical engineering and thermodynamics. The initial hydrocarbon release rate would depend mainly on the pressure within the vessel, size of the hole and the type of discharge, e.g. gas, oil or two-phase. A two-phase release can occur if the inventory is a liquid at the pressure and temperature at which it is contained, but a gas at normal atmospheric pressure and temperature. Key literature presenting methodology for evaluating the release rate of gas, liquid or two-phase release

though holes, or through pipework, include Crowl & Louvar (1990), Fisher et al. (1992), Fthenakis (1993), CCPS (1996), Lees (1996) and Perry et al. (1997). The equations used for calculating the discharge rates of oil, gas and condensate are presented in Section 4.5.1.2.1, 4.5.1.2.2 and 4.5.1.2.3, respectively. Release models are critical in risk assessment as the release rate and the mass of hydrocarbon released would determine the size of the gas cloud generated or the area of the oil-pool and hence the ignition probability.

3.5 Gas Build-Up and Atmospheric Dispersion

If the release is gaseous, a vapour cloud is produced. The size of the gas cloud is dependent on the release rate and the volume within which it accumulates. As the gas mixes with the existing air, its concentration would decrease due to atmospheric structure and turbulence. This process is referred to as atmospheric dispersion. Atmospheric dispersion models are used to predict the dilution of the gaseous release in the atmosphere.

3.5.1 Factors Affecting Dispersion of Gas Cloud

Factors that have a profound effect on gas cloud dispersion would be as follows (Lees 1996a):

1. Momentum

Material released with low kinetic energy would form a plume, while material released with high kinetic energy would form a jet that entrains large quantities of air into the gas cloud. The level of air entrainment would have an effect on the density of the cloud.

2. Buoyancy Effects

Gases can be categorised as either having a positive, negative or neutral buoyancy. Gases with low molecular weights are positively buoyant and are mostly hot gases that tend to rise and disperse more readily. Negatively buoyant gases, on the other hand, are mostly heavy gases, which tend to settle closer to the surface. Buoyancy effects would importantly determine the dispersion of such gases. The Richardson number can be used to quantify this degree of importance:

$$\boldsymbol{R_i = \frac{rg(\rho_a - \rho_g)}{u_0^2 \rho_a}} \qquad \textbf{(28)}$$

where, ρ_a is the density of air; ρ_g is the density of gas; g is the gravitational acceleration; r is the radius of the leak hole; and u_0 is the initial velocity of the jet. The higher the Richardson

number, the more significant the effect of buoyancy (Perry *et al.* 1997). Negatively buoyant gases are capable of displacing the atmospheric flow field. Gases are neutrally buoyant when there is no density difference between the gas and air. Dispersion of neutrally buoyant gases is referred to as passive dispersion as they do not displace the atmospheric flow field and simply follow the airflow.

3. Source Terms

Release from a pipe would be characterised as a point source. Alternatively, vaporisation from an oil pool would be characterised as an area source. The leak may occur either instantaneously or continuously. If the release is instantaneous, it will only last for a couple of seconds and form a puff. However, if the release is continuous, it would form a plume as the gas disperses.

4. Source Elevation

Source elevation can be categorised as either ground level or elevated level. An elevated source of positively buoyant gas is likely to disperse to atmosphere quickly while a ground level source of negatively buoyant gas can be quite hazardous as it follows the contour of the surface as it disperses.

5. Meteorology and Topography

Meteorological factors such as wind direction, speed and atmospheric stability can affect the dispersion of gas. The greatest amount of dispersion would occur during instable atmospheric conditions while the least amount of dispersion would occur during stable atmospheric conditions.

6. Obstacles

Presence of obstacles in the path of the gas cloud would have an effect on its dispersion and flow rate, causing velocity variations and flow alterations.

3.5.2 Atmospheric Dispersion Models

The fundamental equation that forms the basis of most dispersion models is the gas diffusion equation (Baukal 2001):

$$\boldsymbol{u}\frac{\partial \overline{\boldsymbol{c_g}}}{\partial \boldsymbol{x}} = \frac{\partial}{\partial \boldsymbol{x}}\left(\boldsymbol{K_x}\frac{\partial \overline{\boldsymbol{c_g}}}{\partial \boldsymbol{x}}\right) + \frac{\partial}{\partial \boldsymbol{y}}\left(\boldsymbol{K_y}\frac{\partial \overline{\boldsymbol{c_g}}}{\partial \boldsymbol{y}}\right) + \frac{\partial}{\partial \boldsymbol{z}}\left(\boldsymbol{K_z}\frac{\partial \overline{\boldsymbol{c_g}}}{\partial \boldsymbol{z}}\right) \quad \textbf{(29)}$$

where, c_g is the average gas concentration (kg/m^3), u is the mean wind speed in x direction (m/s) and $\mathrm{K_x}$, $\mathrm{K_y}$ and $\mathrm{K_z}$ are the diffusion coefficients in the x, y and z directions (m^2/s).

3.5.2.1 Gradient-Transfer Models

Gradient-Transfer or K-Theory model are solutions of the gas diffusivity equation (29). In early literature, constant diffusion coefficient was assumed and has since been identified as an oversimplification generating inadequate results. Hence, a fresh approach was proposed which involved solving the gas diffusivity equation using relationships for the variation of the individual diffusion coefficients, $\mathrm{K_x}$, $\mathrm{K_y}$ and $\mathrm{K_z}$ and for the mean wind speed, u, and thus obtaining an analytical or numerical solution.

3.5.2.2 Statistical Models

Statistical models provide an analytical solution of the diffusivity equation (29) by representing the individual diffusion coefficients with a constant diffusion coefficient, K. For releases such as puffs and plumes, the concentration profiles produced are in Gaussian form and may therefore be characterised by standard deviations or dispersion coefficients; σ_x, σ_y and σ_z. Moreover, statistical properties of turbulence can be described using the autocorrelation function and Lagrangian time scale.

3.5.2.3 Similarity Models

Similarity models use an equation derived from the dimensional analysis, for the rate of growth of some characteristic dimension of the cloud (Mannan and Lees 2005). However, the model is unable to provide data with respect to the variation of concentration within the gas cloud. As a result, there is a requirement for additional relations with an empirical basis. These models are mainly used to study buoyant plumes and momentum jets.

3.5.2.4 Top Hat, Box and Slab Models

The Top Hat model has an essentially flat top, implying that the cloud has a well-defined height. In a Box model, the cloud is treated as a vertical cylinder. A further assumption of the box model is that the gas particles are dispersed homogenously within the box and uses this

assumption to evaluate the average gas concentration anywhere within the box area. The simplicity of this assumption, limits the use of this model to accurately predict gas concentration in situations where the wind field may influence the gas concentration. In a Slab model, the concentration of the gas cloud is a function of the distance from the source. Box and Slab models are mainly used to model the dispersion of dense gases.

3.5.3 Passive Dispersion Models

Passive dispersion can be modelled using the following models; (1) Roberts model, (2) Sutton model, (3) Pasquill model and (4) Pasquill-Gifford model. The models are based on the Gaussian distribution, which is a standard bell curve and is specifically appropriate for gaseous release into confined spaces. Random nature of turbulence can be incorporated into these models. The equations are easy to solve and require less computational time to perform the various calculations.

3.5.3.1 Roberts Model

The Roberts model was developed by Roberts (1923) when studying the behaviour of smoke from various types of release. For a continuous point source when the dispersion is anisotropic, Roberts's model evaluates the concentration of the gas cloud as follows:

$$c_g(x,y,z) = \frac{Q}{4\pi x (K_x K_y)^{\frac{1}{2}}} e^{\left[\frac{-u}{4x}\left(\frac{y^2}{K_y}+\frac{z^2}{K_z}\right)\right]} \quad \textbf{(30)}$$

where, Q is the continuous mass rate of release (kg/s); K_x, K_y and K_z are the diffusion coefficients in the x, y and z directions (m^2/s); c_g is the average gas concentration at point (x,y,z) (kg/m^3) and u is the mean speed (m/s) in the x-direction.

However, the above equation is only applicable to an elevated source dispersion. For ground source dispersion, the concentration would be double. Hence, for a continuous point source at ground level, Roberts's model evaluates the concentration of the gas cloud as follows:

$$c_g(x,z) = \frac{2Q'}{(2\pi x K_z x)^{\frac{1}{2}}} e^{\left(-\frac{uz^2}{4K_z x}\right)} \quad \textbf{(31)}$$

where, Q' is the continuous mass rate of release per unit length (kg/ms). The greatest concentrations occur along the centreline of the plume. It must be noted that equations for

continuous sources are steady-state and hence can only be applied to fully established plumes. Furthermore, for the above equations to be valid, the duration of the release must be equal to or greater than the ratio of the distance at the location of interest to the wind speed (i.e. t ≥ x/u). Moreover, Roberts's model assumes that the concentration on the centre line of a continuous point source, c_g is proportional to x^{-1} while experiments on passive dispersion assume that c_g is proportional to $x^{-1.76}$(Lees 1996a). Hence, the two set of results do not correlate. Thus, Robert's model is considered inappropriate for modelling passive dispersion.

3.5.3.2 Sutton Model

The Sutton model was developed by Sutton (1953) to overcome the limitations of Roberts's model. For a continuous point source at elevated level, Sutton's model evaluates the concentration of the gas cloud as follows:

$$c_g(x,y,z) = \frac{Q}{\pi C_y C_z u x^{2-n}} e^{\left(-x^{n-2}\frac{y^2}{C_y^2}\right)} \times \left\{ e^{\left[-x^{n-2}\frac{(z-H)^2}{C_z^2}\right]} + e^{\left[-x^{n-2}\frac{(z+H)^{1/2}}{C_z^2}\right]} \right\} \quad \textbf{(32)}$$

where, C_x, C_y and C_z are the diffusion parameters in the downwind, crosswind and vertical (x, y, z) directions ($m^{1/2n}$), n is the diffusion index, the coordinates x, y and z are measured from an origin moving with the cloud at the mean wind speed u and H is the height of the source (m).

For a continuous point source at ground level, Sutton's model evaluates the concentration of the gas cloud as follows:

$$c_g(x,y,z) = \frac{2Q}{\pi C_y C_z u x^{2-n}} e^{\left[-x^{n-2}\left(\frac{y^2}{C_y^2}+\frac{Z^2}{C_z^2}\right)\right]} \quad \textbf{(33)}$$

Like Roberts model, for the above equations to be valid, *t* should be ≥ x/u. It is common for the above equations to be written assuming isotropic conditions, hence the diffusion parameters are $C_x = C_y = C_z = C$. The diffusion index, n, and the generalised diffusion parameter, C, are meteorological constants. n is a function of stability conditions with limiting values of 0 for high turbulence conditions and 1 for low turbulence conditions. In average conditions, n is approximately 0.25. The generalised diffusion parameter, C, is a function of the height above ground level and of the stability conditions.

3.5.3.3 Pasquill Model

Pasquill (1961) proposed another system of dispersion equations also known as the Pasquill model. The Pasquill model is based upon the equations of the Sutton Model. For a continuous point source at ground level, Pasquill model evaluates the concentration of the gas cloud as follows:

$$C_o = \frac{2.8 \times 10^{-3} Q}{udh\theta} \quad \textbf{(34)}$$

where, C_0 is the ground level concentration on the axis of the plume (units/m^3); d is the distance in the downwind direction (km); u is the mean wind speed (m/s); h is the vertical spread (m); and θ is the lateral spread (degrees).

For a continuous point source at elevated level, Pasquill model evaluates the concentration of the gas cloud as follows:

$$C_c = \frac{2.8 \times 10^{-3} Q F_1}{udh\theta} \quad \textbf{(35)}$$

where, F_1 is the stack correction factor = $e^{\left[-2.303\left(\frac{H}{h}\right)^2\right]}$; C_c is the ground level concentration on the axis of the plume for the elevated source (units/m^3); and H is the height of the stack (m).

For both equations to be valid, t must be equal to or greater than the ratio of the distance to the wind speed u (i.e. t ≥ d x 10^3/u). The equations are able to support slow changes in wind direction.

3.5.3.4 Pasquill-Gifford Model

Pasquill-Gifford model modifies the equations of the Sutton model by taking into account dispersion coefficients obtained by Gifford (1961). For a continuous point source at ground level, Pasquill-Gifford model evaluates the concentration of the gas cloud as follows:

$$c_g(x, y, z) = \frac{Q}{\pi \sigma_y \sigma_z u} e^{\left[-\frac{1}{2}\left(\frac{y^2}{\sigma_y^2}+\frac{z^2}{\sigma_z^2}\right)\right]} \quad \textbf{(36)}$$

where, σ_x, σ_y and σ_z are the standard deviations or dispersion coefficients in the downwind, crosswind, and vertical (x, y, z) direction (m).

For a continuous point source at elevated level, Pasquill-Gifford model evaluates the concentration of the gas cloud as follows:

$$c_g(x,y,z) = \frac{Q}{2\pi\sigma_y\sigma_z u}\, e^{\left(-\frac{y^2}{2\sigma_y^2}\right)} \times \left\{ e^{\left[-\frac{(z-h)^2}{2\sigma_z^2}\right]} + e^{\left[-\frac{(z+h)^2}{2\sigma_z^2}\right]} \right\} \quad \textbf{(37)}$$

The dispersion coefficients, σ_x, σ_y and σ_z, are meteorological constants.

3.5.3.4.1 Pasquill-Gifford Plume Model Characteristics

At a given downwind direction x, Pasquill-Gifford model evaluates the concentration for a continuous passive plume from a point source at ground level as follows:

$$c_g(x,0,0) = \frac{2Q}{\pi C^2 u x^{2-n}} \quad \textbf{(38)}$$

For n = 0.25 and C = 0.14

$$c_g = \frac{32Q}{u x^{1.75}} \quad \textbf{(39)}$$

At a given downwind direction x, Pasquill-Gifford model evaluates the concentration for a continuous passive plume from a point source at elevated level as follows:

$$c_g(x,y,0) = \frac{Q}{\pi\sigma_y\sigma_z u} \quad \textbf{(40)}$$

It must be noted that the predicted vales of σ_y and σ_z are sensitive to the specification of atmospheric stability.

3.5.3.4.2 Pasquill-Gifford Puff Model Characteristics

At a given downwind direction x, Pasquill-Gifford model evaluates the concentration for an instantaneous passive puff from a point source at ground level as follows:

$$c_g(0,0,0,t) = \frac{2Q}{\sqrt[3]{\pi^2 C^3 (ut)^{3/2(2-n)}}} \quad \textbf{(41)}$$

For n = 0.25 and C = 0.14

$$c_g = \frac{131Q}{(ut)^{2.62}} \quad \textbf{(42)}$$

where, t is the sampling period which yields the concentration c_g

At a given downwind direction x, Pasquill-Gifford model evaluates the concentration for a continuous passive plume from a point source at ground level as follows:

$$c_g(x, y, 0, t) = \frac{2Q}{(2\pi)^{3/2}\sigma_x\sigma_y\sigma_z} \quad (43)$$

It must be noted that the predicted vales of σ_y and σ_z are sensitive to the specification of atmospheric stability.

3.5.4 Dense Gas Dispersion Models

A method for calculating the dispersion of dense gas was proposed by Britter & McQuaid (1988). The method uses an empirical diagram to evaluate the gas concentration during a continuous or instantaneous dispersion, as a function of downwind dispersion. The method is simple and can be solved analytically. However, it must be noted that models such as Pasquill-Gifford and Britter-McQuaid are dependent on the correlation of atmospheric dispersion data for characteristic release scenarios. Hence, they cannot be applied to a scenario which is not considered in the correlation.

3.5.5 Discussion

On offshore oil and gas installations, the gaseous release is mainly methane. Methane is a positively buoyant gas. Hence, dense gas models and passive dispersion models cannot be used to model the release. Instead, a gaseous release into an unconfined, obstacle free region of an offshore oil and gas module can be effectively modelled using atmospheric dispersion techniques. From this, a Bi-Gaussian distribution is produced which is skewed according to wind strength and direction.

3.6 Fires on Offshore Installations

As mentioned earlier, for a fire to occur, three basic conditions are required: (1) fuel, (2) oxygen and (3) source of ignition. In reality, the concentration of the fuel and oxygen must be within certain limits (flammability limits), and the source of ignition must be vigorous enough to initiate a fire.

3.6.1 Ignition

Ignition of a flammable gas mixture can occur by either heating the mixture to its auto-ignition temperature, or by an ignition source (e.g. hot surfaces, electrical appliances, static electricity, combustion sparks and open flames).

3.6.2 Flammability Limits

A flammable vapour burns in air only over a limited range of fuel-to-air composition. There are two factors that define the flammable range, these are: the Lower Flammable Limit (LFL) or Lower Explosive Limits (LEL) and the Upper Flammable Limit (UFL) or Upper Explosive Limits (UEL). The LFL/LEL is the minimum concentration of fuel in air that can support combustion while the UFL/UEL is the maximum concentration of fuel in air that can support combustion. For clarity, if a flammable mixture is below the LFL/LEL, it is too 'lean' to burn or explode whilst a mixture above the UFL/UEL is too 'rich' to burn or explode.

3.6.3 Autoignition Temperature

If a flammable mixture is to burn, its temperature must be at or above its flashpoint. However, the source of ignition must also be of sufficiently high temperature and contain sufficient energy to ignite the mixture. If the mixture is heated to a high enough temperature, it will ignite spontaneously. This temperature is called an 'autoignition temperature'. On the other hand, if the temperature of the flammable mixture is below its flashpoint, it will not burn, regardless of the existence of an ignition source. Figure 3-2 shows the relationship between the flammability properties.

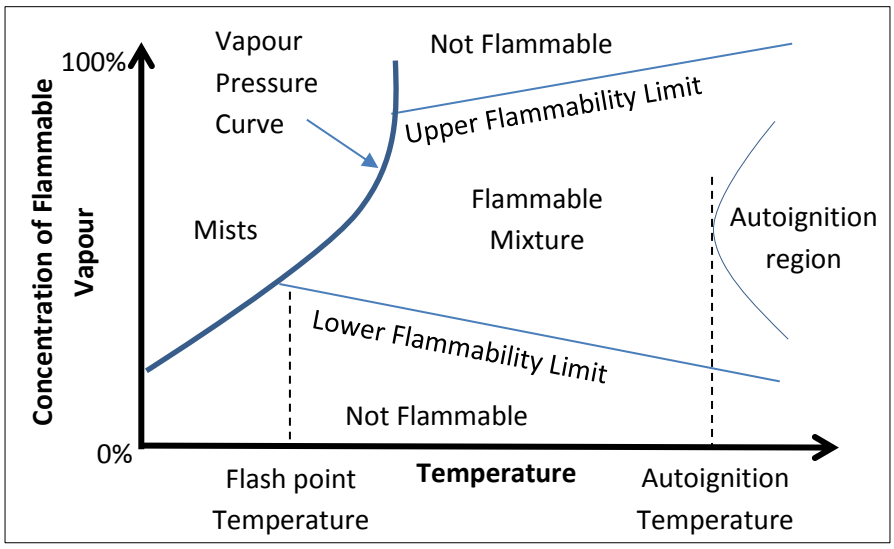


Figure 3-2 Relationship between flammability properties (Perry *et al.* 1997)

3.6.4 Types of Fires

Fires on offshore installations may be classed as follows:

3.6.4.1 Pool Fire

Simpson (1997) defined pool fire as a "*turbulent diffusion fire burning above a horizontal pool of vaporising hydrocarbon liquid under conditions where the fuel has zero or very low initial momentum*". The transfer of heat from the fire to the fuel pool can have a significant effect on the evaporation rate and hence influence the size of the fire. The fuel pool is not stagnant and may be spreading with additional fuel coming from a leak.

3.6.4.2 Jet Fire

Simpson (1997) defined jet fire as a "*turbulent diffusion flame resulting from the combustion of a fuel continuously released with some significant momentum in a particular direction*". Source momentum, and hence directionality distinguishes a jet fire from a pool fire. A second distinction is the absence of heat transfer from the fire to the source. This means that the evolution of their behaviour is different from that of pool fires. It also means that jet fire hazards can be treated more deterministically, because the mass flow rate and its behaviour with time is determined to a first order by the leak characteristics, the inventory and blowdown characteristics. Unlike pool fires, jet fires reach full intensity almost immediately. In principle, the fire can also be extinguished very quickly.

3.6.5 Modelling Jet Fires

To predict the effects of jet fires, a profound understanding of geometrical features such as jet flame orientation, flame shape and flame length is required. The orientation of a jet flame can either be vertical, inclined or horizontal in calm or windy conditions. These circumstances will have a strong influence on the shape of the flame.

Sonju & Hustad (1984) and Bagster & Schubacht (1996) assumed the shape of the jet flame as a cylinder based on experimental and theoretical studies on subsonic jet fires, while Craven (1972) assumed the jet to be cone-shaped. Furthermore, Kalghatgi (1983) and Chamberlain (1987) assumed the shape of the jet to be the frustum of a cone under the influence of cross-wind. Based on the literature reviewed, different shapes of the flame have been assumed and a model has been developed for each flame shape.

The most important step in jet fire modelling is determining the length of the flame. Palacios et al. (2009) plotted the length of a jet flame against the mass flow rate for different outlet diameters, for both subsonic and sonic regimes, as shown in Figure 3-3. The figure shows that the length of the jet flame increases as the mass flow rate and outlet orifice diameter increases.

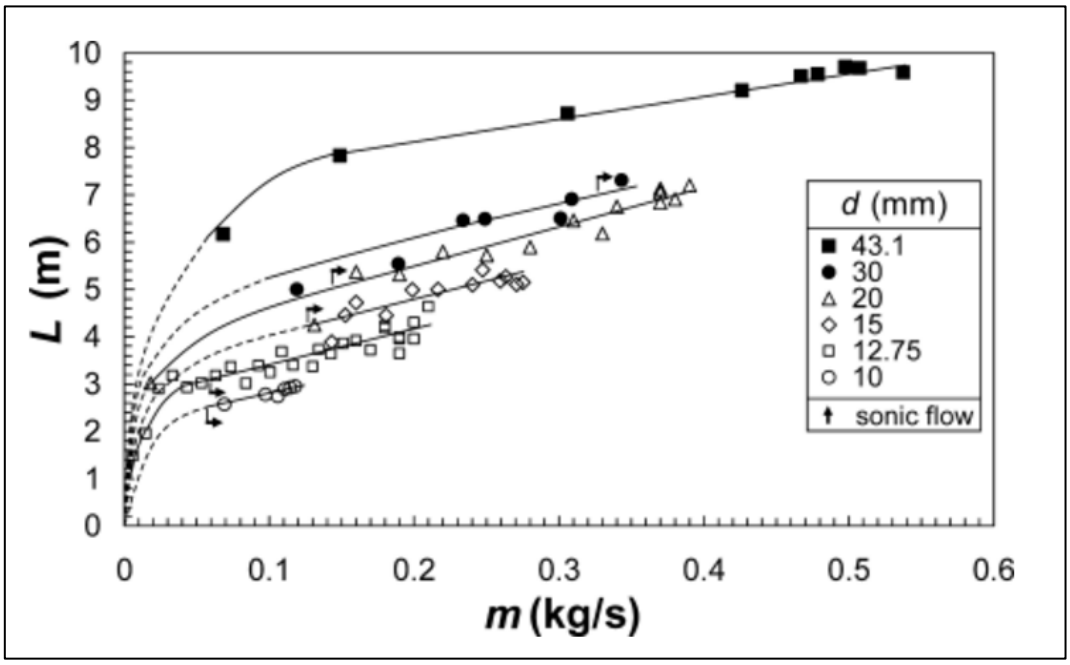


Figure 3-3 Variation in the sonic and subsonic jet flame lengths (L) against fuel mass flow rate (m), for different orifice outlet diameters (d) (Palacios *et al.* 2009)

3.6.5.1 Jet Fire Models

In literature, several fire models are available that can be used to estimate the different parameters of a jet fire. Hottel & Hawthorne (1949) developed the first jet flame model. The flame was modelled as an inverted cone with the apex on the orifice. The length of the flame, L, and the diameter of the top of the cone, W, were evaluated using the following equations:

$$L = \frac{5.3D}{C_t}\left\{\frac{T_f}{\alpha_t T_n}\left[C_t + (1 - C_t)\frac{M_s}{M_n}\right]\right\}^{1/2} \quad (44)$$

$$\frac{L}{D} = 5.3\frac{W}{D} \quad (45)$$

where, C_t is the concentration of fuel in the stoichiometric mixture; D is the pipe diameter (m); M_n is the molecular weight of the fuel; M_s is the molecular weight of air; T_f is the absolute adiabatic flame temperature (K); T_n is the absolute temperature of the fuel in the pipe (K);

α_t is the ratio of the number of moles of unreacted and reacted gas in the stoichiometric mixture; and W is the diameter at the top of the flame (m).

Craven (1972) developed a model of a jet flame to calculate the heat flux on a target near the flame. The flame dimensions used for the model is shown in Figure 3-4.

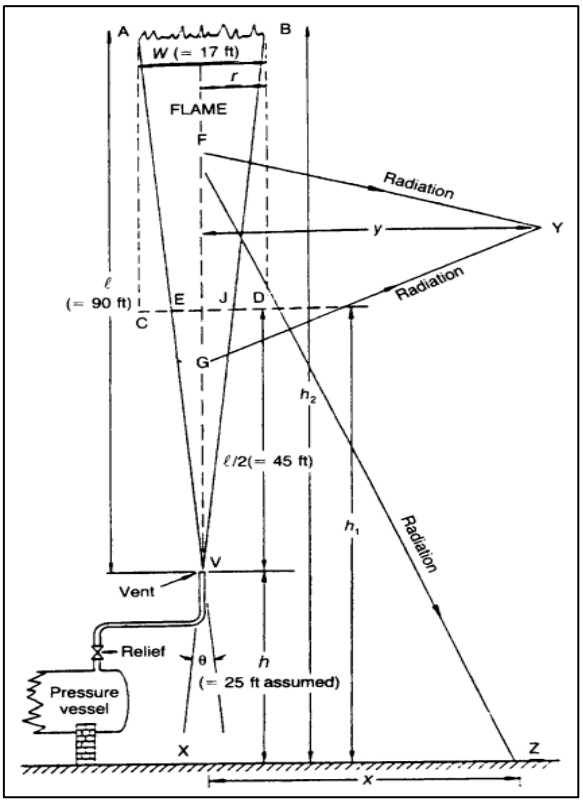


Figure 3-4 Craven Model (Craven 1972)

The flame dimensions were evaluated based on the correlation provided by Hottel & Hawthorne (1949). The heat flux radiated from the fire, E, was then evaluated for targets at point X, Y and Z, as shown in Figure 3-6, using the following equation:

$$\boldsymbol{E = \varepsilon \sigma T^4} \qquad \textbf{(46)}$$

where, T is the absolute temperature of the flame (K); ε is the emissivity of the flame; and σ is the Stefan-Boltzmann constant.

Craven (1972) also evaluated the view factor, F, which is the fraction of the emitted radiation that reaches the receptor (human or material) per unit area, for targets at point X,Y and Z, using the following equations:

$$\boldsymbol{F_X = \frac{r^2}{(L+h)^2 + r^2}} \qquad \textbf{(47)}$$

$$F_Y \approx \frac{rL}{\pi y^2} \quad (48)$$

$$F_Z = \frac{xy}{\pi}\left[\frac{1}{(h_1^2 + x^2)} - \frac{1}{(h_2^2 + x^2)}\right] \quad (49)$$

where, r is the radius of the flame at its (m); h is the height of the vent orifice (m); h_1 is the distance from the ground to the bottom of the radiator ABCD (m); h_2 is the distance from the ground to the top of the radiator (m); x is the distance between points X and Z (m); L is the length of the flame (m); and y is the horizontal distance to the axis of the flame (m) $\approx 10\mathrm{D}_{\max}$ (D_{max} is the maximum cone diameter (m)). However, the model developed by Craven (1972) is only applicable to turbulent flames and its use was intended for design instead of hazard assessment.

MITI (1976) proposed a jet flame model for jet flames formed as a result of ignition of flashing liquids. The model uses the following equation to calculate the flame length, L:

$$q = 0.0006785L^{2.5} \quad (50)$$

where, q is the fuel flow (kg/s).

Sonju & Hustad (1984) proposed a jet flame model. The flame dimensions were presented in terms of the Froude number, Fr, and the following equations were employed:

$$\frac{H}{d} = AFr^m \quad (51)$$

$$\frac{D}{d} = BFr^m \quad (52)$$

$$Fr = \frac{u^2}{gd} \quad (53)$$

where, d is the diameter of the orifice (m); D is the diameter of the flame (m); g is the acceleration due to gravity (m/s^2); H is the height of the flame (m); u is the gas velocity at the nozzle exit (m/s); A and B are constants; and m is an index. The fraction of heat radiated, F_r, was evaluated using the following equation:

$$F_r = 4.7\dot{Q}^{-0.2} + 11.6\dot{Q}^{0.4} \quad (54)$$

where, $\dot{Q}$ is the heat release rate (MW).

Furthermore, Considine & Grint (1985) proposed a model based on the work presented by MITI (1976). The shape of the flame was assumed to be conical. The length of the flame, L, and the half-width of the flame tip, W, were calculated as follows:

$$\boldsymbol{L = 9.1Q^{0.5}} \quad \textbf{(55)}$$

$$\boldsymbol{W = 0.25L} \quad \textbf{(56)}$$

where, Q is the mass flow (kg/s).

3.6.6 Modelling Pool Fires

Modelling pool fires covers parameters such as flame geometry, liquid burning rate, flame characteristics, heat radiated and view factor. The flame of the pool fire is assumed to be an upright cylinder with the length, L, twice the diameter, D, as shown in Figure 3-5.

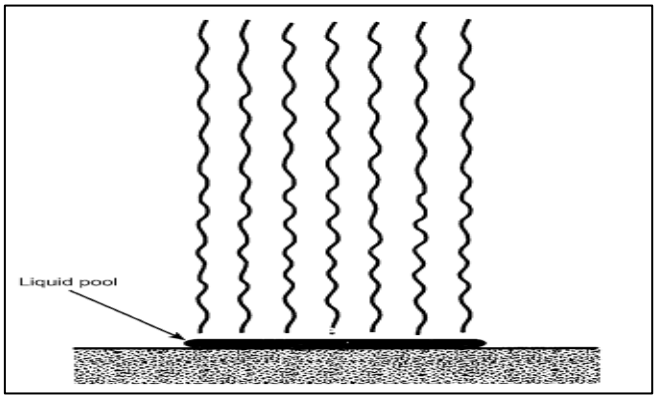


Figure 3-5 Pool Fire (Mannan 2013)

Thomas (1963) developed an equation to calculate the mean flame length of the pool fire based on experimental measurements of fire on wood. The equation used was as follows:

$$\frac{\boldsymbol{L}}{\boldsymbol{D}} = \boldsymbol{42}\left[\frac{\boldsymbol{m'}}{\boldsymbol{\rho_{air}\sqrt{gD}}}\right]^{\boldsymbol{0.61}} \quad \textbf{(61)}$$

where, m' is the specific mass burning rate (kg/m^2/s) and ρ_{air} is the density of air at ambient conditions (kg/m^3). However, the above equation is limited to cases where the wind influence is small and there is no soot.

Thus, in an event of the presence of a strong wind, Thomas (1963) proposed the following equation for a tilted flame:

$$\frac{\boldsymbol{L}}{\boldsymbol{D}} = \mathbf{55}\left[\frac{\boldsymbol{m'}}{\boldsymbol{\rho_{air}}\sqrt{\boldsymbol{gD}}}\right]^{\mathbf{0.67}} (\boldsymbol{u}^*)^{\mathbf{-0.21}} \quad \textbf{(62)}$$

where, u* is dimensionless wind velocity = $\frac{u}{u_c}$; u is the wind velocity (m/s); and u_c is the characteristic velocity = $\left[\frac{gm'D}{\rho_{air}}\right]^{1/3}$. However, the above equation underestimates the length of the flame.

Hence, to overcome the limitations of this equation, Pritchard & Binding (1993) modified the above equation to the following:

$$\frac{\boldsymbol{L}}{\boldsymbol{D}} = \mathbf{55}\left[\frac{\boldsymbol{m'}}{\boldsymbol{\rho_{air}}\sqrt{\boldsymbol{gD}}}\right]^{\mathbf{0.305}} (\boldsymbol{u}^*)^{\mathbf{-0.03}} \quad \textbf{(63)}$$

The burning rate, m', which is the rate at which the flammable material that forms the pool burns can be calculated using the method developed by Zabetakis & Burgess (1961).

$$\boldsymbol{m'} = \frac{\boldsymbol{\sigma T_f^4}(\mathbf{1} - \boldsymbol{e}^{\boldsymbol{-k\beta D}})}{[\Delta \boldsymbol{H_V} + \boldsymbol{C_p}(\boldsymbol{T_b} - \boldsymbol{T_a})]} \quad \textbf{(64)}$$

where, T_f is the temperature of the flame (K); T_b is the boiling temperature of the fuel (K); T_a is the ambient temperature; $-\Delta H_v$ is the heat of vaporisation (J/kg); C_p is the specific heat capacity of the fuel (J/kg K); β is the mean-beam-length corrector (1/m); k is the absorption extinction coefficient of the flame (1/m); D is the diameter of the pool (m).

Consequently, the equation is modified to produce the burning rate a function of the pool diameter and the equivalent burning rate of an infinite diameter pool. The modified equation is given as follows:

$$\boldsymbol{m'} = \boldsymbol{m}_\infty (\mathbf{1} - \boldsymbol{e}^{\boldsymbol{-k\beta D}}) \quad \textbf{(65)}$$

where, m_∞ is the equivalent burning rate (kg/m^{2}s) = $\frac{\sigma T_f^4}{\Delta H_G}$; and ΔH_G is the total heat of gasification (kJ/kg) = $\Delta H_V + C_p(T_b - T_a)$. The burning rate increases with increasing pool diameter. However, for very large diameters, the burning rate reaches a fixed value.

Burgess et al. (1961) examined correlations of the burning rate against the ratio of$\Delta H_C/\Delta H_G$, where, ΔH_G =$\Delta H_V + C_p(T_b - T_a)$. The burning rate, m', was then calculated as follows:

$$m' = p_L c_1 \frac{\Delta H_c}{\Delta H_V + C_p(T_b - T_a)} \quad (66)$$

where, c_1 = 1.27 x 10-6 m/s. The method was successful in calculating the burning rate of hydrocarbons and liquid fuels in general.

3.7 Explosions on Offshore Installations

An explosion is a result of energy being released into the gas phase in a very short time span, typically milliseconds or less. The energy causes the gases to expand rapidly, forcing back the surrounding gas and initiating a pressure wave that moves rapidly outward from the blast origin (Perry *et al.* 1997). Offshore oil and gas installations are prone to a wide variety of explosions such as confined and unconfined explosions, internal and external explosions, physical explosions, solid phase explosions and mist explosions. Explosion severity is influenced by a number of factors such as temperature, pressure, gas turbulence, mixing, location of the ignition source, time before ignition, gas concentration, the degree of confinement and congestion. As a result, explosions can be challenging to predict and characterise.

3.7.1 Detonation and Deflagration

There are two types of explosions; (1) deflagration and (2) detonation. In a deflagration, the pressure wave moves at a speed less than the speed of sound in the ambient gas. For hydrocarbon – air mixtures, the deflagration velocity is typically 300m/s. In a detonation, the pressure wave moves at a speed greater than the speed of sound in the ambient gas. For hydrocarbon-air mixtures, the detonation velocity is typically of the order of 2000-3000 m/s (Lees 1996a). Deflagration occurs when the concentration of the flammable mixture is between a set of flammable limits and a source of ignition is present. On the other hand, detonation occurs when the concentration of the flammable mixture is between a set of detonability limits and a strong source of ignition is present. Detonation is a more severe form of explosion than a deflagration, resulting in overpressures of 20 bar, compared to only 8 bar for deflagration. However, the damage caused during a detonation, is usually localised, whereas in the case of a deflagration, the damage is more widespread.

3.7.2 Explosion Overpressures

An explosion results in a blast wave that tends to compress the air in front of it, causing a rapid rise in ambient atmospheric pressure. The rise in pressure over the normal ambient atmospheric pressure is called an overpressure. The rise in atmospheric pressure is propagated in all directions, which can cause damage to humans and structure. The overpressures generated as a result of a gas explosion can vary depending on the fuel concentration, location and energy of ignition source, degree of confinement of the vapour cloud and congestion in the path of the flame front.

British Gas and Mobile North Sea Ltd. conducted a series of experiments to investigate the effect of these different parameters on explosion overpressures. Initially, the fuel concentration in the air was varied and the overpressures generated in the event of an explosion were determined. The normalised overpressures were plotted against the equivalence ratio as shown in Figure 3-6, below. Stern (2014) defines equivalence ratio as the "ratio of the actual fuel/air ratio to the stoichiometric fuel/air ratio". The figure shows that overpressure is reduced when the fuel concentration is above or below the stoichiometric concentration. This is due to the burning velocity of the flame being lower than that at stoichiometric.

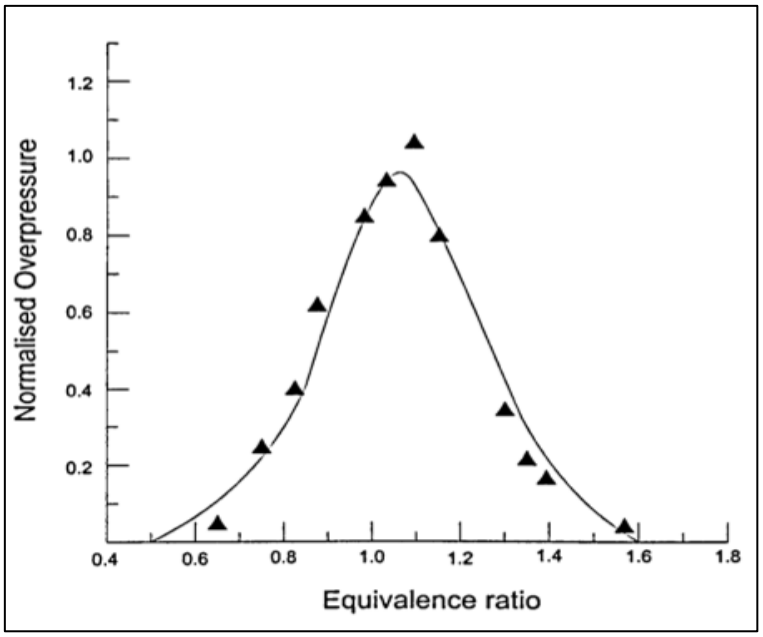


Figure 3-6 Effect of Fuel Concentration on Explosion Overpressures (Lewthwaite 2006)

British Gas also studied the effect of ignition source location on explosion overpressures within a three-sided module. Based on their experiment, if the source of ignition was located in the centre of the module, the overpressures generated were four times less than the overpressure generated if the source of ignition source was located at the rear wall of the module. This is because, for a central ignition, the distance over which the flame can accelerate is shorter compared to the distance the flame needs to accelerate for rear wall ignition, before venting can occur.

Furthermore, by reducing the level of confinement, the magnitude of the overpressures generated reduced significantly. However, by increasing the level of congestion, the magnitude of the overpressures generated increased significantly. This is because increasing the level of congestion, increases the turbulence and acceleration in the flow in front of the flame.

3.7.3 Modelling Explosions

There are three main approaches to modelling offshore explosions: (1) Empirical Models, (2) Phenomenological Models, and (3) Computational Fluid Dynamics (CFD). The Health and Safety Laboratory (HSL) Fire and Explosion group published a detailed document entitled "A Review of State-of-the-Art in Gas Explosion Modelling" (Lea and Ledin 2002), which reviews these different models and their accuracy.

3.7.3.1 Empirical Models

Empirical models are based on correlations obtained from analysis of experimental data (Lea and Ledin 2002). However, as the correlations are experiment specific, in order to model something different, new set of experiments are required.

3.7.3.1.1 TriNitroToluene (TNT) Equivalence Model

The model was first introduced by Brasie & Simpson (1968) and is based on the assumption that a gas explosion resembles an explosion involving a high charge explosion of TriNitroToluene (TNT). While the model can be used to estimate explosion overpressures, authors such as Van den Berg *et al.* (1984) have expressed concerns over the applicability of the TNT equivalency model to model gas explosions. The following differences can be noted between the two explosions; (1) the local pressure for gas explosions is much less compared

to TNT explosions, (2) the TNT explosion exhibits a pressure decay that is more rapid than the acoustic wave from a gas explosion, and (3) the TNT equivalency model does not take into consideration the effect of confinement and congestion (Bjerketvedt et al., 1997). Hence, due to the various reasons outlined, the TNT Equivalency Model is not considered a suitable choice for modelling gas explosions.

3.7.3.1.2 TNO Method

The TNO method (Lees 1996a) makes the assumption that the entire vapour cloud contributes to the overpressure rather than just a proportion occurring within a confined and/or congested area. The Multi-Energy method described below has superseded the TNO method; hence the TNO method will not be discussed any further.

3.7.3.1.3 Multi-Energy Method

The multi-energy method (Van den Berg, 1985) was developed to estimate the overpressures from gas explosions with variable strength. The method assumes that only the part of the gas cloud which is confined or obstructed contributes to the overpressure. Hence, the overpressure increases with increasing confinement. Although this method allows a conservative estimate, it is difficult to set a sensible value for the ignition size and strength, leading to an overestimation of the overpressure caused by the blast.

3.7.3.1.4 Baker-Strehlow Method

The Baker-Strehlow method (Baker et al.,1996) was developed to estimate overpressures generated from vapour cloud explosions in congested or partially confined areas. In this method, the strength of the blast wave is proportional to the maximum flame speed, which is presented in the form of a Mach number. Although this method is relatively simple and takes into consideration geometrical details, it has been found to be overly conservative.

3.7.3.1.5 Congestion Assessment Method (CAM)

CAM was first developed at Shell Thornton Research Centre by Cates & Samuels (1991). A simple computer-based algorithm was developed to estimate the overpressures of a vapour cloud explosion in a vented box containing obstacles. An estimation was made for the overpressure at varying distances from the location of the ignition. The model assumes a

simple decay law inversely proportional to the distance and is designed to generate conservative pressures. CAM was later enhanced by Puttock (1995) to include the estimation of the pulse shape and duration. This version was later known as Shell CAM2 and is the most advanced empirical model reviewed. However, a disadvantage of the Shell CAM2 is the uncertainty of the model's performance when simulated for a scenario that has not been calibrated for.

3.7.3.2 Phenomenological Models

Phenomenological models simplify the essential physics and geometry of explosions by reasonably approximating geometric systems to allow the extrapolation of data beyond the original experimental validation. For example, with offshore oil and gas installations, no attempt is made to model the actual scenario details but an idealised system is used instead. This then places phenomenological models between empirical correlations and CFD models on the complexity scale; providing a balance between accuracy and precision, with faster computation times, and allowing for a large number of scenarios to be modelled with a greater degree of confidence.

3.7.3.2.1 Shell Code for Overpressure Prediction in Gas-Explosions (SCOPE)

The SCOPE model was developed for modelling explosions in offshore modules and is continually being developed by the Shell Thornton Research Centre. The model is based on work carried out by Cates & Samuels (1991). In order to model gas explosions, the SCOPE algorithm solves a series of differential equations. The method is based on the idealised geometry of a vented vessel containing obstacles. On the other hand, SCOPE 2 is capable of modelling vent openings. The vented gas forms a mushroom-shaped jet. The highest overpressure is generated when the flame burns in the vortex at the mushroom head. SCOPE 3 is capable of handling mixed scale objects and allows rear venting. Venting behind the ignition point can influence the overpressures generated. SCOPE 3 was further extended to include the modelling of unconfined, congested plant, with central ignition as well as the effect of water deluge on explosion overpressures. In general, the SCOPE model has been validated using over 300 experiments involving different gases and various degrees of congestion. However, the code can only deal with single enclosures and is unable to provide sufficient information with regards to the flow field.

3.7.3.2.2 Confined LInked CHamber Explosion (CLICHE)

The CLICHE code (Catlin 1990) was initially developed to study confined explosions in buildings. The model is an adaption of earlier work carried out by Fairweather & Vasey (1982) and Chippett (1984) on confined explosions occurring in single empty vessels. Its use has now been extended to the offshore oil and gas industry. In CLICHE simulations, the offshore oil and gas module is idealised as a series of interlinked explosion chambers. The model assumes that the parameters such as pressure and density within each chamber are uniform. It also assumes that any changes in momentum only occur at the perimeter of these volumes, thus, it is incapable of predicting flame distortions directly. Instead, the flame shape is described empirically as a function of the geometry and volume of burnt gas it encloses. While these approximations are sensible when applied to a volume with a single vent and no significant spatial pressure gradient, the model is deemed unsuitable for offshore oil and gas installations with several vents.

3.7.3.3 Computational Fluid Dynamics

CFD models the physical processes by providing numerical solutions to partial differential equations that govern the explosion process. The equations concern the conservation of mass, energy and momentum of the gas. A vast amount of information regarding the flow field such as velocities, pressure, density and species concentrations, can be obtained using CFD codes. However, although the equations are theoretically simple, they can be difficult to solve. Numerical methods are required to solve these equations which require the calculation 'domain' to be split into a number of small volumes with boundary conditions and smaller time steps. However, iteratively solving these volumes and time steps can be computationally demanding and expensive, hence, approximations are used.

3.7.3.3.1 Explosion SIMulator (EXSIM)

The EXSIM code is continually being developed by the Telemark Technological R&D Centre (Tel-Tek) in Norway (Høiset et al. (2000). It uses a finite volume code based on a structured Cartesian grid to solve fluid flow conservation equations. The Semi-Implicit Method for Pressure Linked Equations (SIMPLE) algorithm is used to solve the pressure/velocity/density coupling of the momentum equations and the mass balance. The model allows the code to specify the location and features of obstacles and can be applied to congested geometries.

However, the model requires further development and validations against large-scale experiments in a variety of geometries, degree of confinement and congestion.

3.7.3.3.2 FLame ACceleration Simulator (FLACS)

The FLACS code was developed at the Christian Michelsen Research (CMR) Institute in Norway, now known as CMR-GEXCON. FLACS uses a finite volume code based on a structured Cartesian grid. The model assumes that the flame propagates at a constant burning velocity and has a specified constant flame thickness (Arntzen 1998). The model can be applied to congested geometries as well as for external explosion and also, incorporates a water deluge model. The model has been validated against more than 2000 experiments. Although, the model tended to under or over predict the overpressures generated, the results are generally within 30-40% of the experimental data.

3.7.3.3.3 AutoReaGas

AutoReaGas code was jointly developed by Century Dynamics and TNO in 1993. The code integrates the features of a gas explosion simulator – REAGAS, and a blast wave propagation simulation - BLAST. AutoReaGas uses a finite volume code based on a structured Cartesian grid. The SIMPLE algorithm is implemented for pressure correction. Scenario geometry is supplied to the code by defining a combination of simplified objects such as boxes and cylinders. Moreover, the code is capable of incorporating a water deluge model.

3.8 Mitigating Fires and Explosions

In the last few decades, deluge systems have shown to effectively control, mitigate and extinguish fires (Liang *et al.* 2015). Research has shown that for optimum extinguishment of a fire the deluge must initiate from above the fire. Deluge injection through sidewalls, front and rear walls proved less effective (Prasad *et al.* 2002). However, in the case of enclosed modules, it must also be considered that the fire would extinguish as soon as the oxygen is consumed by the fire or diluted by water vapour (Bill *et al.* (1997) and Back III *et al.* (2000)).

Blast walls are commonly used to protect against explosions. They are generally designed by simulating accidental scenarios and the resultant overpressure. This therefore determines whether the blast wall is capable of fulfilling its protective function even if slight deformation

occurs. A series of experiments have been performed by British Gas to investigate the ability of deluge water sprays to reduce overpressures generated from gas explosions within partially confined modules. Figure 3-7 illustrates the explosion overpressure against the concentration curves for a number of deluge pressures. The figure shows that highest overpressure is generated when the explosion occurs in the absence of the deluge system.

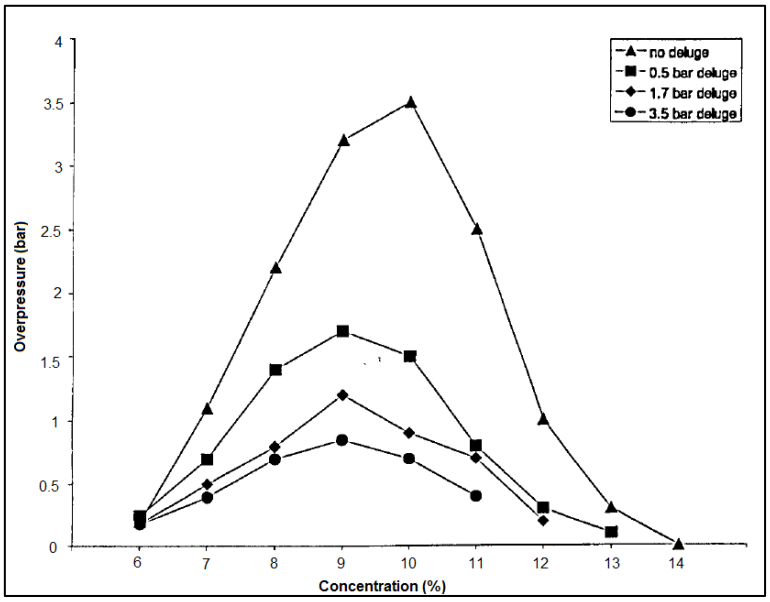


Figure 3-7 Variation in the Overpressure as a function of concentration (Lewthwaite *et al.* 2006)

However, it must be noted that, deluge systems are not an effective means of mitigating explosions in very confined modules. Studies conducted by Acton *et al.* (1990) revealed that that in order for deluge systems to effectively mitigate explosions in very confined modules, the water droplets must be broken down into smaller droplets. Smaller droplets create a much larger surface area which allows heat to be extracted from the fire. However, in very confined modules, flame speeds are relatively lower and the water droplets cannot be broken down into smaller ones as the acceleration of these water droplets are low. Hence, the explosion potential cannot be mitigated.

3.9 Summary

Accidental release of hydrocarbon from pipes and processing equipment can result in the dispersion of flammable gases into the atmosphere, which in the presence of an ignition source could result in a jet fire or an explosion. Hydrocarbon liquid releases also have the

potential to ignite to form pool fires. Release models can be used to calculate the hydrocarbon release rate. The equations are based on well-developed theories of chemical engineering and thermodynamics. Release models are critical in risk assessment as the release rate and the mass of hydrocarbon released would determine the size of the gas cloud generated or the area of the oil-pool formed.

If the release is gaseous, it would form a vapour cloud that will change in size and gas concentration. On an offshore oil and gas installation, there may be several factors that influence the dispersion of a gas cloud such as gas buoyancy, momentum, source terms and elevation, meteorological conditions such as wind speed and direction, obstacles and level of confinement. Hence, in order to effectively model the gas build-up and dispersion, different atmospheric dispersion models are utilised.

On offshore oil and gas installations, the gaseous release is mainly methane. Methane is a buoyant gas which tends to rise to the atmosphere. Hence, an accidental release into an unconfined and obstacle free region can be effectively modelled via atmospheric dispersion techniques. This results in a Bi-Gaussian distribution skewed according to wind strength and direction.

The type of atmospheric dispersion model used may also vary according to the effect of the wind and the momentum of the release. If there is no effect from the wind and the momentum of the release is low, models that use diffusion equations are used to model the diffusion of gas in the atmosphere. In this research, since the modules modelled are enclosed and there is no effect from the wind, diffusion equations are sufficient to model the dispersion of the gas cloud.

Additionally, if an ignition source was present in the event of a leak, immediate ignition of a gas or oil release would result in an explosion or pool fire, respectively, while delayed ignition of a gas release would result in a jet fire. Different types of models were used to predict the magnitude of jet and pool fires, in terms of the flame length generated. For any fire model, to effectively predict the flame length, profound knowledge of geometrical features such as jet flame orientation and flame shape are required.

Moreover, a variety of explosion models which includes empirical, phenomenological and CFD models have been developed over the years to predict the overpressures generated in the event of an explosion. In many cases, the models have been validated against experimental data from large scale explosion experiments, providing a predictive capability for explosion overpressure. Empirical models require substantial judgement by the analyst to idealise equipment layouts into obstacle grid arrangements, hence, are deemed inappropriate. Compared to empirical and phenomenological models, CFD models seem to be the most promising techniques for modelling explosions as realistically as possible. However, CFD models can be complex and may require a specialised user, large computational power and an extremely long run time to obtain a prediction for a single scenario. Moreover, CFD requires a mesh and necessitates incorporation of many engineering approximation (e.g. turbulence model), modelling shortcuts (e.g. unconverged meshes) and real-world variabilities. These all introduce limitations that pollute the solution and force the analyst to determine degree of pollution that is acceptable enough to be useful. Phenomenological models, on the other hand, are a cost-effective alternative to empirical and CFD models. They allow for a large number of scenarios to be modelled with a great degree of confidence. Hence, if a simple estimate of the overpressure generated is required, then phenomenological models would be appropriate and are used in this research study.

In conclusion, modelling of an accidental release of hydrocarbons and its consequences allows offshore asset operations managers to assess the reliability of offshore safety systems and hence, it is a critical design step in ensuring the integrity of an offshore oil and gas installation. Moreover, this step improves the basis for identification of corrective measures required to reduce the risks in both the design and operational phases of the offshore oil and gas installation.

Chapter 4 - Platform Safety Model

4.1 Introduction to Model Framework

In this research, software known as the Platform Safety Model, has been developed to predict the costs, risks and service reliability of any given asset management policy for an offshore oil and gas installation. The Platform Safety Model is implemented using standard PNs with high level extensions. The model is further divided into two sub models that work in conjunction with one another: (1) Offshore Safety System Degradation and Maintenance Model and (2) Offshore Fire and Explosion Model.

The primary aim of the Offshore Safety System Degradation and Maintenance Model is to model dynamic processes such as degradation, inspection and maintenance experienced by the components of the offshore safety systems i.e. fire and gas detection system, process isolation, process blowdown and deluge. However, for an assessment of the effectiveness of any given asset management policy, it is necessary to determine the effect of possible single or multiple component failures on the system under study. Fault trees are used to establish the relationship between component failure and system failure. The fault trees were also used to design the safety system PN. As a result the model can then be used to investigate the effects of different asset management strategies on the offshore oil and gas installation in terms of; costs, risks and service reliability.

The Safety System Degradation and Maintenance PN model is implemented using a C++ code which is then solved using a Monte-Carlo simulation method. For the simulation of the PN model, input data such as failure and repair time distributions are used. A number of simulations are performed and information, such as the number of times a place of interest is marked with a token and the duration that the token resides in this particular place, are extracted. After each simulation run, the data is saved to a results file.

Once the predictions are considered to have converged, the result files are analysed using MATLAB software to produce statistics, such as the probability of the system being in any of the condition states, the total number of component replacements over the system lifetime,

the total number of maintenance interventions performed on each component and the system availability. By assigning unit costs for the different types of maintenance activities, the costs of performing inspection and maintenance on offshore safety systems can also be estimated.

The Offshore Fire and Explosion Model is then used to model the occurrence of a hydrocarbon leak from a process vessel located within the three main modules; wellhead, separation and compression, of an offshore installation. The aim of this model is to predict the frequencies of fires and explosions in the event that the safety systems, previously modelled in Model 1, fail to function on demand in the presence of an ignition source. The model utilises fluid flow modelling to calculate parameters such as the hydrocarbon discharge rate, gas cloud build-up and dispersion, oil-pool build-up and reduction. These parameters can then be used to predict the intensity of the fires and explosions in terms of the flame length produced in the event of a fire and the overpressures generated in the event of an explosion. This step holds the key to developing the most effective strategy for offshore accident prevention and management. Once the frequencies of fires and explosions are determined for a given maintenance process, different asset management strategies can be applied to predict their effect on the safety systems and hence, produce the optimal interventions for the offshore assets with an acceptable risk level.

Improving service reliability often contrasts with the necessity of controlling costs. However, it is crucial that the safety of the installation is not compromised. Therefore, the trade-off between conflicting objectives must be considered in a decision support process. Hence, an Offshore Optimisation Model is developed in Chapter 6 so that an optimum asset management policy with minimal life cycle costs can be determined which produces acceptable risks. In conclusion, the Platform Safety Model in conjunction with the Offshore Optimisation Model can be used to support asset operations managers to make informed decisions with regards to asset management policies without compromising the safety of the offshore oil and gas installation. Figure 4-1 summarises the main aspects of the Platform Safety Model framework.

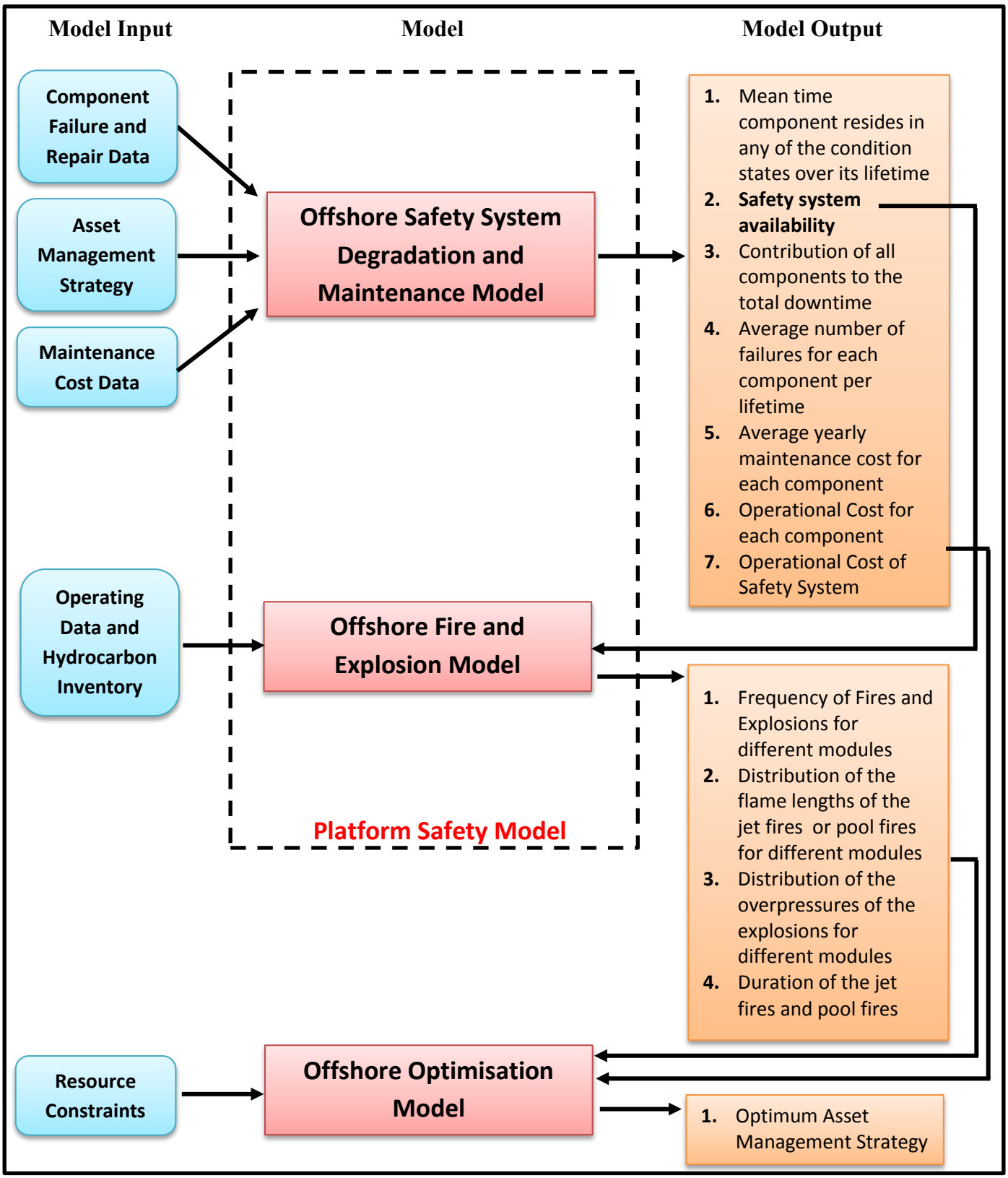


Figure 4-1 Model Framework

4.2 High Level Extensions to Standard Petri Nets

A detailed outline of the PN technique and its application has been described in Chapter 2 – Section 2.6.5. Current literature shows that although the method has been widely used to model dynamic systems in a range of industries, its use in offshore oil and gas has been quite limited. Due to the complexity associated with offshore oil and gas assets, standard PN models can be inadequate to model such complex processes. Hence, high level extensions are added to standard PNs to increase its ability to model complex component/system behaviour as well as a variety of different maintenance options.

The different high level features used are described below:

4.2.1 Inhibitor Arc

Inhibitor arcs (Reisig and Rozenberg 1998) connect a place to a transition and are graphically represented with a small circle on the end of the line instead of an arrowhead. If the input place contains a token, the inhibitor arc prevents a transition from firing as long as the token remains within the input place. The inhibitor arc can be assigned with an arc multiplicity. In this case, a transition is disabled, whenever a place contains at least as many tokens as the multiplicity of the inhibitor arc. Figure 4-2 shows a PN with arc multiplicity and an inhibitor arc. The presence of a token in P_2 inhibits T_1 from firing.

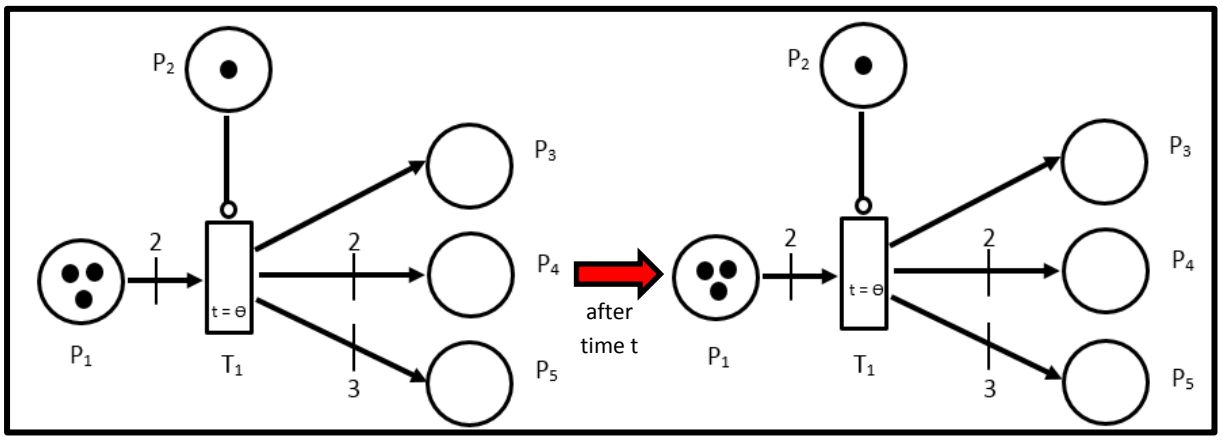


Figure 4-2 Petri Net with inhibitor arc

4.2.2 Reset Transition

The reset transition (R.T.) was defined by Andrews (2012). When a reset transition fires, the marking of the subscribed places are reset to a required state. The reset transition contains

an associated list of places and tokens these places will contain once the reset transition has fired. The reset transition is implemented when the net needs to be returned to its original state. The main advantage of reset transitions is the reduction of places and transitions that would normally be implemented to carry out a reset action in a standard PN.

4.2.3 Probabilistic Transition

Probabilistic transitions (P.T.) have been created for the purpose of this research. P.T. have multiple output arcs but only one of them is chosen to fire. These output arcs are assigned probabilities (that must add to 1) that are used to choose which arc fires. Figure 4-3 shows an example of a firing process of a transition with probabilistic arcs. The presence of a token in P_1 enables T_1 which randomly samples from a uniform distribution [0, 1]. If the random number is between 0 and 0.8, P_2 is marked and if the random number is between 0.8 and 1, P3 is marked.

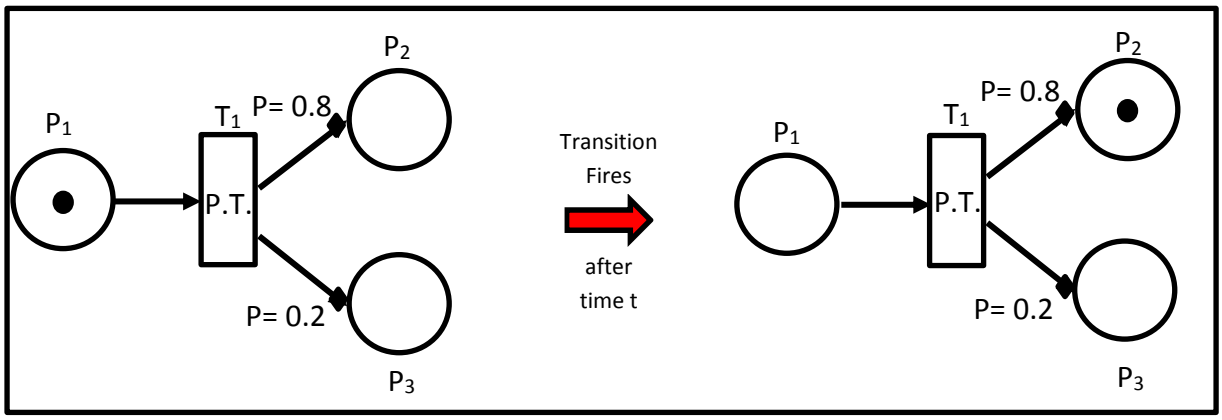


Figure 4-3 Probabilistic Transition

4.2.4 Place Conditional Transition

The Place Conditional Transition (PC.T) (Andrews 2012) enables the transition time distribution to be dependent on the number of tokens in another place on the net to which it is linked via a green arrow. Figure 4-4 shows an example of a firing process of a PC.T. The number of tokens in place P_3 would identify the distribution to sample to get the time at which T_1 fires. Each time T_1 fires, the transition time changes as the number of tokens in P_3 changes.

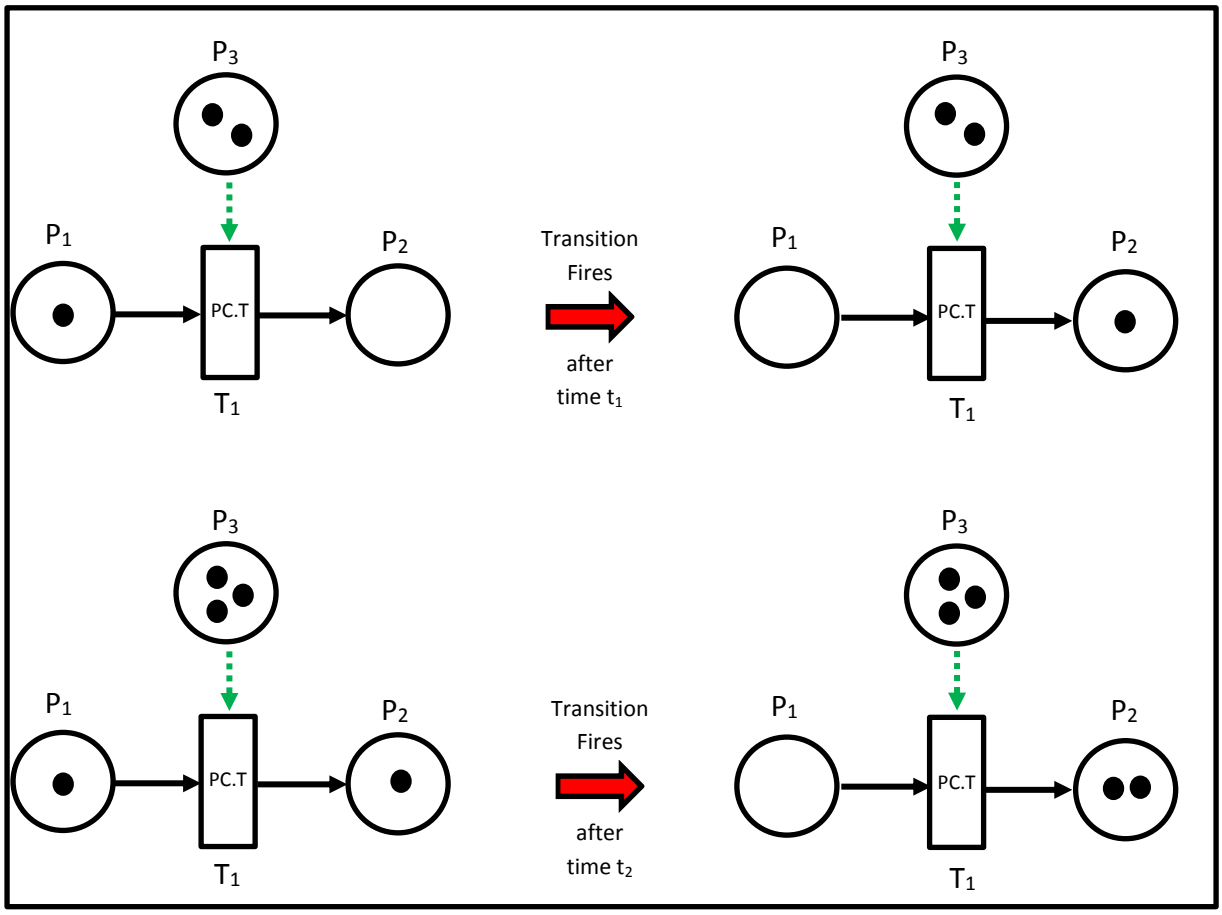


Figure 4-4 Place Conditional Transition

4.3 Description of the Offshore Installation

4.3.1 Modules

In this study, the oil and gas installation modelled is a fixed platform sited in the United Kingdom Continental Shelf (UKCS). Figure 4-5 shows a schematic diagram of the modelled oil and gas installation.

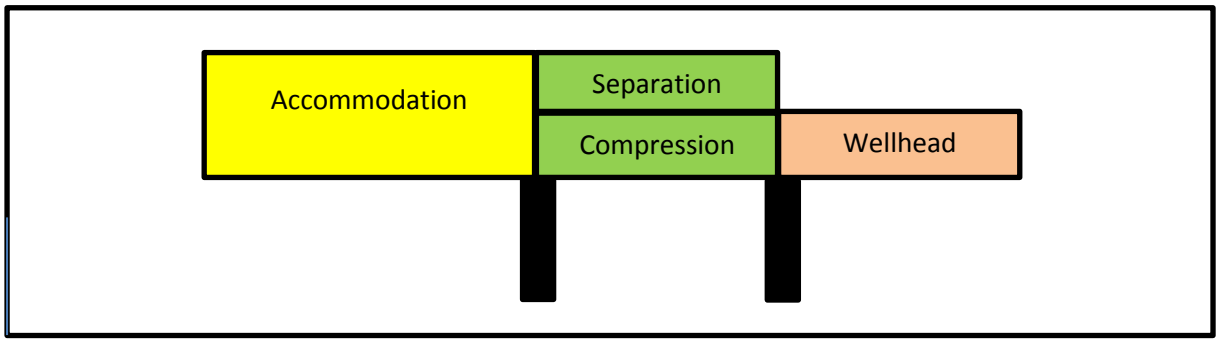


Figure 4-5 Illustration of the modelled oil and gas installation

Although a typical offshore installation comprises of a variety of different modules, the modules that are of particular interest to this research are those in which the release of hydrocarbon oil or gas is most likely. Since processing modules such as separation, compression and wellhead contain the highest amount of hydrocarbon inventory, they are considered to be three of the most susceptible modules. Hence, the study focuses on these three modules. For this platform, the modules are assumed to be enclosed.

Each module is subdivided into sections. Each section contains a set of process vessels and pipework that are isolatable. The separation module comprises of two sections – 1 and 2. Section 1 is the atmospheric separator and section 2 is the inlet separator. The actual volume of the separation module is 8000m^3 while the effective volume of the module is 2000m^3.

The compression module comprises of four sections – 3, 4, 5 and 7. Section 3 consists of the low pressure compressors and scrubbers, section 4 consists of the medium pressure compressors, section 5 consists of the medium pressure scrubbers and section 7 consists of the injection compressors. The actual volume of the compression module is 8000m^3 while the effective volume of the module is 2000m^3.

The wellhead module comprises of three sections - 8, 9 and 10. Section 8 is the wellhead and production header line which is linked to 19 production heads, section 9 is the gas injection line which is linked to 2 gas injected wells and section 10 is the gas lift line which is linked to 5 gas lift wells. The actual volume of the wellhead module is 3630m^3 while the effective volume is 907.5m^3. The effective volume represents the volume in which the gas and air are assumed to mix, taking into consideration the volume occupied by the process vessel.

Schematic diagrams of the different sections of the modules are shown in Figure 4-7 and Appendix A. Table 4-1 describes the different isolatable process sections that make up each module and their operating data, i.e. pressure, temperature and volume, including their hydrocarbon inventory. Note that section 6 is not located within the compression module, however, it is connected to sections 3, 4, 5 and 7 in the compression module via isolation valves. Likewise, sections 11 to 15 are not located within the wellhead module, however, they

are connected to sections 8, 9 and 10 in the wellhead module via isolation valves. The sections the isolation valves connect are shown in Section 4.3.2.2 - Table 4-2.

Module Name	Section Number	Section Name	Pressure (bar g)	Temperature (°C)	Volume (m^3)		
					Gas	Oil	Condensate
Separation	1	Atmospheric Separator	1.60	61.00	51.49	57.03	-
Separation	2	Inlet Separator	19.69	71.00	78.02	88.27	-
Compression	3	Low Pressure Scrubbers and Compressors	1.20	61.00	14.44	-	-
			5.60	145.00	1.54	-	-
			4.65	30.00	6.94	-	2.78
			2.10	147.00	0.28	-	-
			1.40	61.00	0.28	-	-
Compression	4	Medium Pressure Scrubbers, Coolers and Compressors – Stage 1	19.40	76.00	1.75	-	-
			18.30	30.00	26.15	-	11.34
Compression	5	Medium Pressure Scrubbers, Coolers and Compressors – Stage 2	46.10	105.00	2.75	-	
			45.30	30.00	13.88	-	4.46
			44.80	30.00	10.76	-	-
			169.50	150.00	2.63	-	-
	6	Glycol Contactor	46.60	30.00	21.34	-	-
Compression	7	Injection Scrubbers, Coolers and Compressor	173.50	146.00	3.11	-	-
			169.90	38.00	5.81	-	-
			380.00	111.00	1.52	-	-
Wellhead	8	Wellhead and Production Header Lines	19.67	71.00	1.73	15.00	-
	9	Gas Injection Line	380.00	107.00	3.00	-	-
	10	Gas Lift Line	178.00	51.00	10.90	-	-
	11	Fuel Gas Scrubber	41.00	27.00	5.16	-	1.84
	12	Gas Sales	179.00	51.00	3.00	-	-
	13	Wells connected to Wellhead and Production Header Lines	122.45	22.00	1.47	1.14	-
	14	Injection Wells connected to Gas Injection Line	258.50	22.00	3.55	-	-
	15	Wells connected to Gas Lift Line	191.63	25.00	1.67	-	-

Table 4-1 Hydrocarbon Inventory and Operating Data for the sections of the different modules

4.3.2 Safety Systems

Each module also contains safety systems to protect against the occurrence of a fire or explosion. The safety systems include fire and gas detection, process isolation and blowdown and deluge. A brief description of these systems and their components is given next:

4.3.2.1 Fire and Gas Detection System

These systems feature three different fire and gas detectors. The fire detectors include infrared, ultraviolet and a combination infrared/ultraviolet while the gas detectors include sonic, beam and point.

4.3.2.2 Isolation and Blowdown System

An example diagram of a simple isolation and blowdown system in a process is shown in Figure 4-6. Contiguous sections labelled 1, 2 and 3, contain process equipment and have different hydrocarbon inventories as shown in Table 4-1. If a gas leak were to occur on Section 2, the fire and gas detection system would need to detect the release and hence activate the other safety systems, i.e. (1) close the isolation valves, ISV-1 and ISV-2, to limit the hydrocarbon inventory; (2) open the blowdown valve, BDV-2, to depressurise the section; and (3) activate the deluge system and maintain it until the effects of the leak have been minimised. Failure of the safety systems has the potential to increase the consequences of the incident.

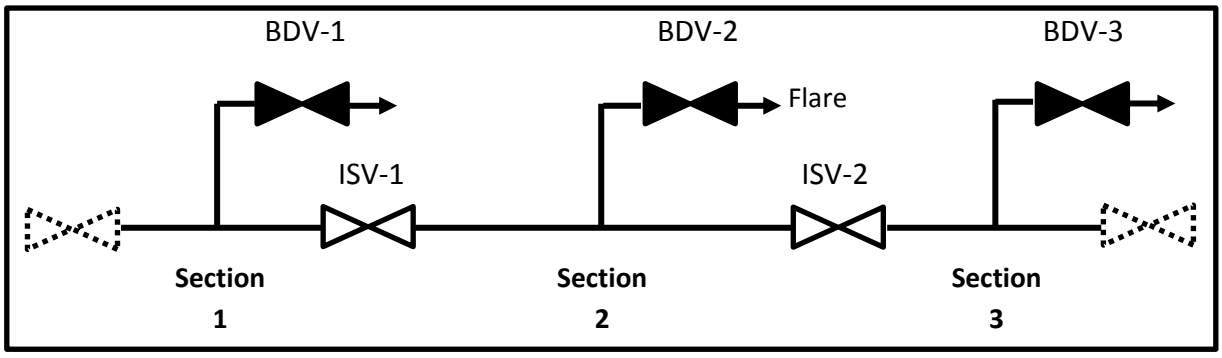


Figure 4-6 Process section showing isolation (ISV) and blowdown (BDV) valves

In this analysis, 21 isolation valves and 12 blowdown valves are modelled. Diagrammatic representation of Section 1 and the sections it connects to via different isolation valves have been shown in Figure 4-7, below. Schematic diagrams of the other isolatable sections have been presented in Appendix A. All isolation valves and the sections they connect have been listed in Table 4-2; and the locations of the blowdown valves have been listed in Table 4-3.

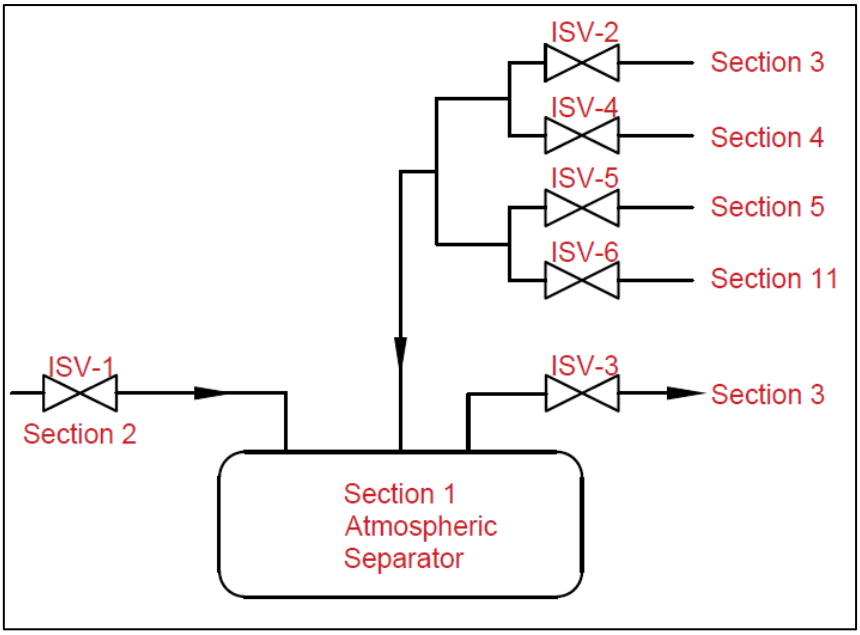


Figure 4-7 Section 1 - Atmospheric Separator

Connecting Sections		Isolation Valve
1	2	ISV-1
1	3	ISV-2/ISV-3
1	4	ISV-4
1	5	ISV-5
1	11	ISV-6
2	4	ISV-7/ISV-8
2	8	ISV-9
3	4	ISV-10
4	5	ISV-11
5	6	ISV-12
5	7	ISV-13
5	11	ISV-14
7	9	ISV-15
7	10	ISV-16
7	12	ISV-17/ISV-18
8	13	ISV-19
9	14	ISV-20
10	15	ISV-21

Table 4-2 Isolation Valve Connections

Section	Blowdown Valve
2	BDV-1
3	BDV-2/BDV-3
4	BDV-4/BDV-5
5	BDV-6/BDV-7
6	BDV-8
7	BDV-9/BDV-10
11	BDV-11
12	BDV-12

Table 4-3 Blowdown Valve Locations

4.3.2.3 Deluge System

Deluge systems are used both to minimise the consequence of a fire and reduce the blast overpressures following an explosion. When a leak is detected, the deluge system is activated to prevent ignition. The performance of the deluge system is dependent on the following: (1) time taken to detect the leak; (2) type of fire; (3) coverage area; (4) pressure of the water spray; and (5) response time. A schematic of the deluge system is shown in Figure 4-8.

The ring main covers the entire facility with an aim to distribute fire water to water deluge systems in the modules. The pressure in the ring main is sustained by a jockey pump pumping water from the sea. In the event of a fire in any of the modules, the Main Fire and Gas Panel receives a signal that causes the solenoid valves to de-energise and open. As the valves open, water passes into the dry pipework and the pressure in the ring main drops. This drop in pressure is detected by the fire and gas logic unit sensors whose function is to activate the firewater pumps.

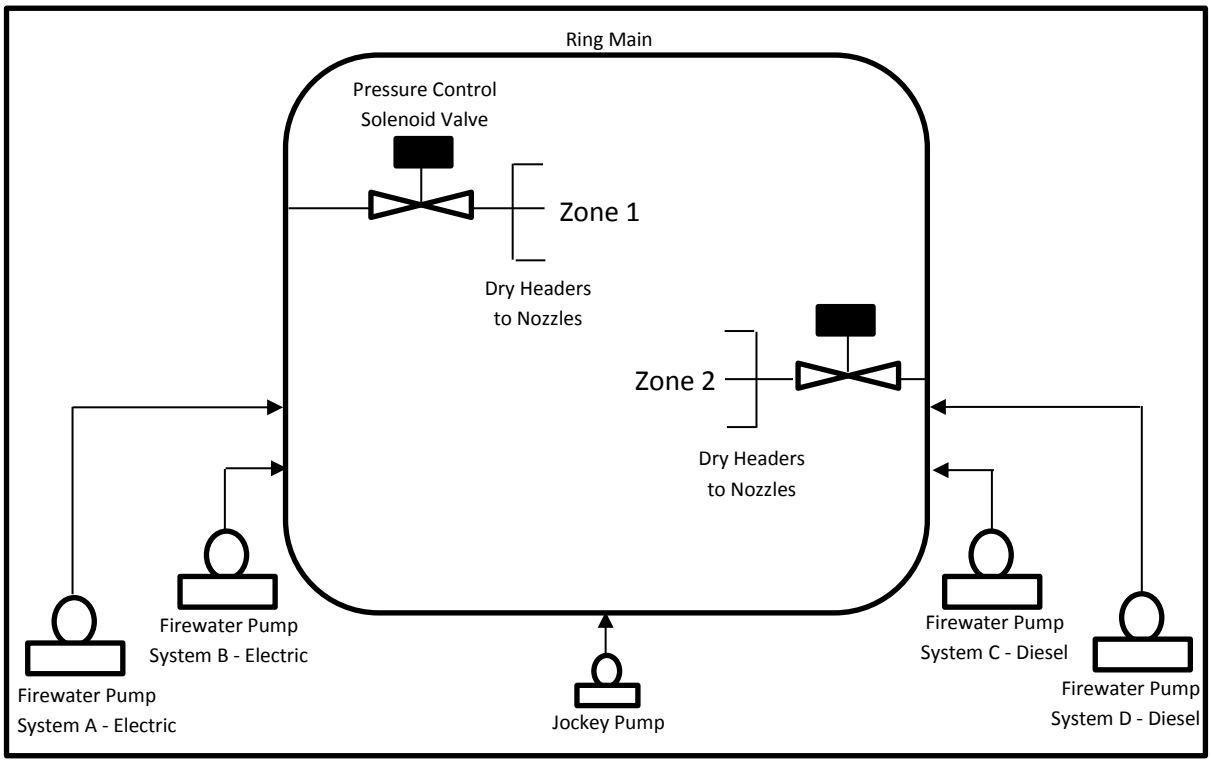


Figure 4-8 Schematic of Deluge System

Several redundant firewater pump systems are in standby mode and provide water to the ring main on demand. The pump subsystem consists of four fire water pumps running at 50%

capacity; where two pumps are electrically powered while the other two are powered via their own dedicated diesel engines. Hence, in the event that two fire water pumps were to fail, the remaining two would still be able to meet the deluge requirements. However, if three fire water pumps were to fail, it would be impossible to meet this demand.

The fire water pump subsystem is made up of the following components: (1) submerged lift pump; (2) booster pump and; (3) air release valve. The submerged lift pump is located below the sea level and pumps water up to the booster pump located on the rig. However, before the pumps are started, the caisson between the sea level and the booster pump is filled with air. Hence, the air release valve are opened for about 10 seconds to bleed out the air. Failure of the air release valve to close after 10 seconds, would result in the flow of water out of the valve and hence failure of that particular valve on the deluge system to fulfil its requirements.

The deluge valves are designed to supply the nozzles with fire water. Each valve is located within a heated protected cabinet also known as a deluge skid. On demand, the normally closed deluge valves open. However, they can fail to open on demand. Failure of the deluge valve are usually related to the solenoid valves, i.e. they fail to open on demand. Figure 4-9 shows a flow diagram of the deluge system. The fault trees for the different subsystems of the deluge system are shown in Appendix C (Mobile North Sea Limited 2003). The main fault tree that was used to design the deluge system Petri Net is described in further detail in Section 4.4.4.4.

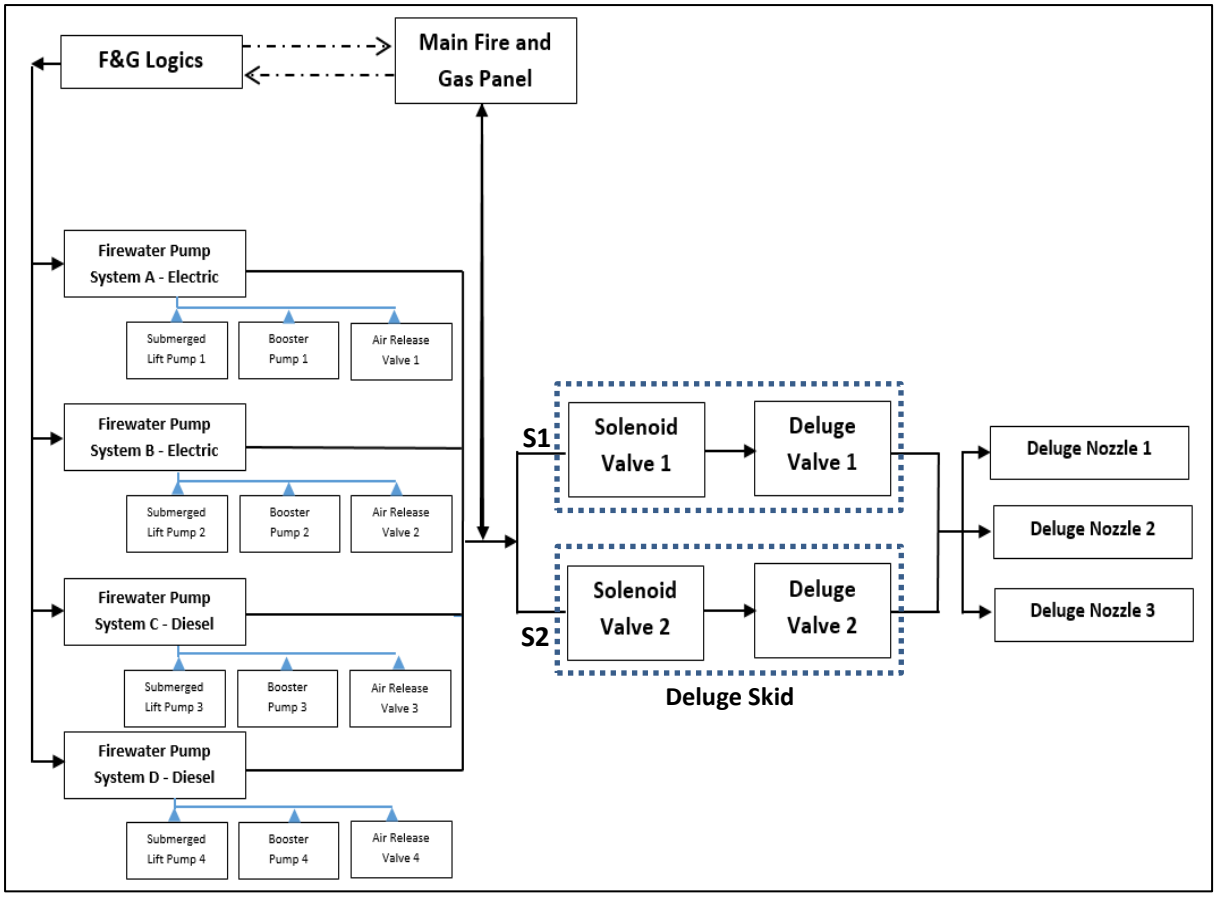


Figure 4-9 Flow Diagram of a Deluge System

4.4 Offshore Safety System Degradation and Maintenance Model

4.4.1 Model Structure

The Offshore Safety System Degradation and Maintenance PN Model is divided into three component sub nets:

1. **Component Degradation and Failure**: models the state change of the Offshore Safety System components.
2. **Component Inspection**: models the inspection process of the Offshore Safety System components.
3. **Component Maintenance**: models the different maintenance strategies experienced by the Offshore Safety System components.

Once set up, the **component** nets are combined to form the **subsystem** net. Combinations of subsystem failure can lead to system failure. Hence, the **subsystem** nets are used to define the **main Safety System net**. The main constituent elements of the Offshore Safety System

Degradation and Maintenance model are outlined in Figure 4-10 and is further described in Section 4.4.4 and 4.4.4.2.5 of the thesis.

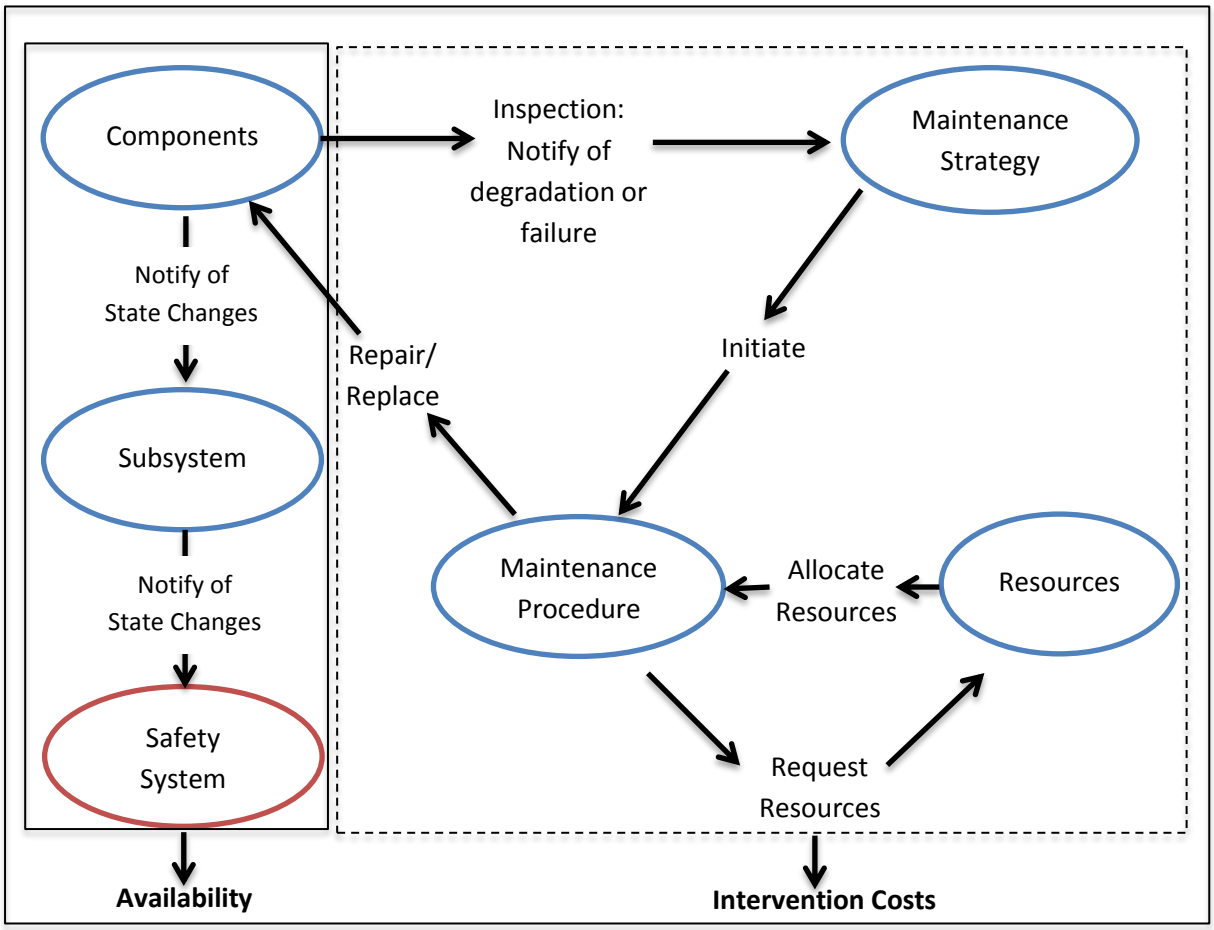


Figure 4-10 Constituent elements of the Safety System Degradation and Maintenance Model

4.4.2 Input Data

In order to use the model, input data such as component failure and repair rates are required. The most common sources of failure rate data are historical data, published data and reliability testing data. The validity of the data used in the model is of paramount importance as it aids decision-making necessary to improve safety and life cycle costs. Therefore, the failure rates derived should, where possible, be based on real life data. Gaining a better understanding of the component degradation and failure rates, through real data, is imperative for improving asset management capabilities. Hence, the following sources were used in descending order of preference to obtain failure and repair data:

1. Failure and repair data provided by Mobile North Sea Limited (MNSL) Beryl Bravo. The MNSL Beryl Bravo Availability study contains reliability data for critical equipment derived

from their maintenance information system, 'MIMICS'. The study gives a true, unbiased picture of equipment performance under the actual operating and environmental stresses experienced. Failure rates could increase if an old machine is called upon to work at a sustained higher output. These changes will have to be taken into account before the historic site data can be used to assess the availability of the plant in the future.

2. The next most satisfactory data is that obtained from the OREDA database, which has considerable failure and repair data for safety systems on offshore installations. The inventory contains information such as component description, its operational mode, internal and external environment and boundary specification. The failure and repair data includes the number of failures, failure rate and repair time.
3. In cases where data was not readily available, engineering judgement was used to estimate the failure rate and repair time of the component.

4.4.3 Condition States of Offshore Safety System Components

In order to study the degradation and failure process of components in the safety systems, the condition states in which the components reside in throughout their lifecycle should be clearly defined. According to Hokstad and Johnsen (2010), the degradation mechanisms that affect offshore safety systems and their components are shown in Table 4-4. The rate at which the degradation occurs is dependent upon the combination of the following factors: (1) Material of Construction; (2) Environmental Conditions; (3) Operating Conditions and (4) Maintenance strategies.

Mechanism	Description
Corrosion	Offshore systems are constantly exposed to highly corrosive seawater as a result of their location and splash zone.
Erosion	The relative motion of fluids can result in the mechanical removal of material from the surface especially in the presence of solids.
Corrosion Fatigue	Horrocks *et al.* (2010) defined corrosion fatigue as "*the enhancement of the rate of crack growth in a corrosive environment above that which would be expected in a purely mechanical fatigue dry environment*". Sources of corrosion fatigue include vibration and also the expansion and contraction associated with thermal cycling of equipment.
Cracking	Cracks often originate from weld defects. Impact from a dropped object or accidental overload may also potentially lead to initiation of cracks. If such initial cracking is left undetected and / or not repaired immediately, it can grow into a crack that continues to propagate under repeated loads.

Manufacturing Defect	Weld defects can occur during manufacture resulting in the physical damage of the component.
Wear	Material properties can deteriorate as a result of friction between moving parts.
Extreme Temperature or Pressure	Extreme temperatures or pressures beyond the design limits can damage or rupture the system.
Blockage	Offshore equipment such as process vessels, pipe work, valves, and nozzles of the deluge system can be blocked (partially or completely) because of scaling, fouling or build-up of corrosion products.
Creep	Creep is the continuous deformation of a metal at a load increasingly experienced at high temperatures.

Table 4-4 Degradation Mechanisms Affecting Offshore Safety Systems

In this work, components such as the Fire and Gas detectors and deluge system nozzles are simply considered to be either in a working or failed state. Both components start in the normal working condition. However, a build-up of salt and grime on the sensitive part of the detector may result in an increased number of nuisance alarms. This is also referred to as a spurious failure. Such failures are considered undesirable as they can result in unwanted shut down of the platform or in this case divert the attention of the offshore operator unnecessarily. Moreover, the detector can also fail to detect a fire or gas leak because of a lack of power to the detector or due to its position within the module. Therefore, to avoid the spurious initiation of the other safety systems, a Koo3 voting system is applied to most Fire and Gas detectors. This means that for an alarm to activate, 2oo3 detectors are required to emit a signal.

The pipework of the deluge system is commonly made from galvanised steel. Due to regular contact with seawater, the zinc corrodes, leaving behind mild steel. Over time, the corrosion product accumulates and in the event that the deluge system is required or routine inspection is conducted, the corrosion product is expelled under the force of the water. However, in most cases, due to the size of the dislodged product, the deluge nozzles can get blocked, resulting in their failure.

On the other hand, the valves of the deluge system, isolation system and blowdown system would show signs of gradual degradation. In this work, the condition of the valve is assessed based on the time it takes to close or open from their normal, fully open or fully closed, position. There are four condition states that the valves of the blowdown and deluge system

are assumed to be in: normal, degraded opening time, slow opening time and functional failure. Moreover, the valve can experience two types of functional failure modes: 'fail close' or 'fail open'. The condition states of the blowdown and deluge valves are defined in Table 4-5 below.

Condition States	Opening Time (s)	State Description
Normal Opening Time	10	Valve is in a good working order. No repair action is recommended.
Degraded Opening Time	11 - 20	Movement times of the valve are showing signs of degradation. Minor repair required to avoid unexpected valve failure.
Slow Opening Time	21 - 30	Valve opening time is extremely slow. Major repair required to avoid valve failure.
Functional Failure	> 30	Sufficient severity to cause damage to the platform or loss of hydrocarbon inventory. Immediate replacement of the valve is required.

Table 4-5 Condition states of Blowdown and Deluge System Valves based on Opening Time (Andrews and Fecarotti 2014)

Alternatively, the valves of the isolation system are presumed to be in the following condition states: normal, degraded closing time, slow closing time and functional failure. The condition states of the isolation valves are defined in Table 4-6.

Condition States	Closing Time (s)	State Description
Normal Closing Time	10	Valve is in a good working order. No repair action is recommended.
Degraded Closing Time	11 - 20	Movement times of the valve are showing signs of degradation. Minor repair required to avoid unexpected valve failure.
Slow Closing Time	21 - 30	Valve closing time is extremely slow. Major repair required to avoid valve failure.
Functional Failure	>30	Sufficient severity to cause damage to the machine or platform. Immediate replacement of the valve is required.

Table 4-6 Condition states of Isolation System Valves based on Closing Time (Andrews and Fecarotti 2014)

Figure 4-11 shows the relationship between the closing time of an isolation valve and its operational life.

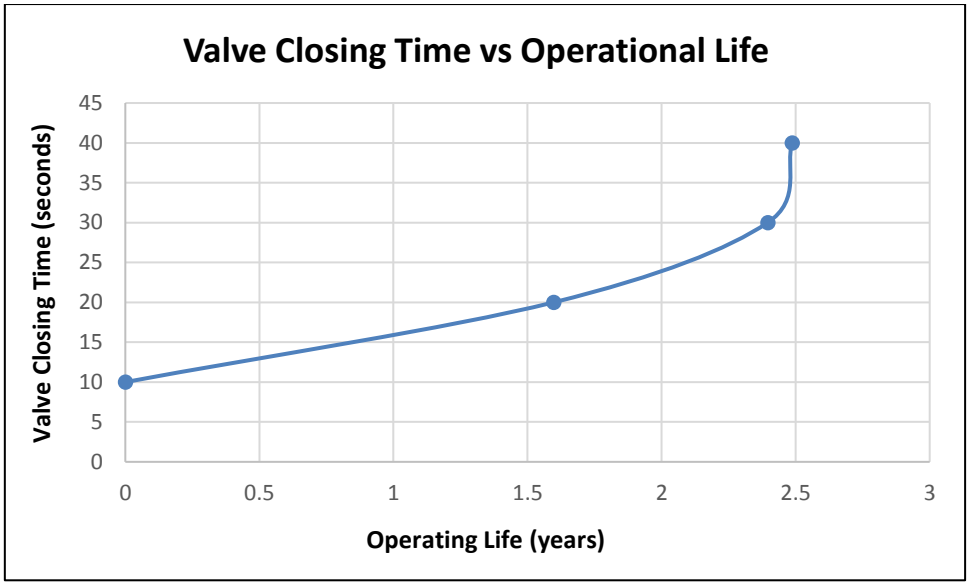


Figure 4-11 Valve Condition vs Operating Life

As shown in Figure 4-11, in the normal condition, the valve has a closing time of 10 seconds. However, after 1 year in operation, the closing time will increase to more than 10 seconds and hence the valve will be in a degraded state with a closing time between 11 to 20 seconds.

Likewise, the deluge system firewater pumps also show signs of degradation. The pumps are observed for excess vibration levels. Many vibration problems involve the wear and tear of the internal components of the pump. Key vibration-related problems for pumps in all types of services include: (1) pressure variations; (2) manufacturing defect; (3) improper installation; (4) corrosion; (5) improper lubrication; (6) improper alignment between pump and its driver; (7) improper bearing selection or fitting; (8) unbalanced rotating components; and (9) internal recirculation and cavitation. When the vibration is excessive, pump performance deteriorates steadily in the absence of routine maintenance. It tends to generate less flow and head, requiring more power to achieve the desired output.

In this study, the firewater pumps are assumed to be in four condition states: new, degraded, severely degraded and functional failure. The key difference between degraded and severely degraded states is the time taken to schedule maintenance where the mean time to schedule maintenance for a severely degraded component is less than that for a degraded component. The condition states of firewater pumps are defined in Table 4-7 and is assessed based on the

vibration velocity range defined in ISO 10816 vibration severity chart for medium size (15kW to 75kW) machines.

Condition States	Root-Mean- Square (RMS) Vibration Velocity Range (mm/s)	State Description
New	0.28-1.12	Newly commissioned machines would normally fall within this zone. No repair action is recommended.
Degraded	1.12-2.80	Normally considered acceptable for unrestricted, long-term operation, however, minor repair is required to avoid unexpected pump failure.
Severely Degraded	2.80-7.10	Normally considered unsatisfactory for long-term, continuous operation. Generally, the pump may be operated for a limited period in this condition until a suitable opportunity arises to conduct major repair work and prevent pump failure.
Functional Failure	> 7.10	Normally considered to be of sufficient severity to cause damage to the machine.

Table 4-7 Condition states of Firewater Pumps based on Vibration Levels (ISO 10816 -1998)

It must also be noted that occasionally, pumps and valves can fail spuriously due to a site power failure or a spurious signal from the fire and gas logic unit sensors. Failure of the firewater pump system can have serious consequences, hence, the deluge system contains two redundant firewater pump systems.

4.4.4 Petri Net Model

Each safety system net contains component nets for the different components it comprises of. The component net is made up of three subnets: (1) Degradation and Failure Subnet, (2) Inspection Subnet and (3) Maintenance Subnet. The component life cycle generally begins in the new/normal condition. The degradation process of a component is assumed to be independent, i.e. it is not affected by the state of another component in the same system. Hence, the degradation nets for the other components are similar, however, they are not linked. After a certain period of time, the component degrades and the level of degradation is revealed via an inspection. The individual component models of a safety system are linked together via the inspection subnet. All defects are identified following inspection. If the component is revealed to be in a degraded state, it is maintained to restore its condition back to new/normal state. If the component is revealed to be in a functional failure state, the component is replaced and it is restored back to new state. Each component subnet records

statistics such as the amount of time the component resides in different condition states, the number of times the component has been subjected to minor or major repair, the total number of replacements, and the cost of preventive or corrective maintenance. Opportunistic maintenance can also be considered, such that when maintenance is being performed on one component, the other components that are part of the same system are maintained at the same time. In the case of the deluge system, the component nets are integrated to form the subsystem net. Failure of a single or combination of components can result in the failure of its respective subsystem. The subsystem net is then integrated to form the main safety system net. Failure of a single or combination of subsystems can result in the failure of the whole safety system. Simulation of these nets can be used to determine the unavailability of the various safety systems such as fire and gas detection system, isolation and blowdown valves and deluge system. Sections 4.4.4.1 to 4.4.4.6 demonstrate the Petri Net development for the deluge system while providing details about similarities and dissimilarities to the other safety system nets.

4.4.4.1 Modelling Component Degradation and Failure

A section of the PN developed to model the degradation and failure processes of the deluge system submerged lift pump is shown in Figure 4-12. Please note that the numbering represents the arrangement of the components within the system and is not indicative of the order presented in the text. Places from, P_{126} to P_{129}, represent the different states of the pump. Transitions from, T_{90} to T_{92}, enable the pump to move from one state to another, hence incorporating the dynamic behaviour. The pump lifetime begins in the new state (P_{126}). This is indicated by marking P_{126} with a token. Transitions direct the movement of the tokens from one place to another. Over time, due to corrosion or wear mechanisms, the pump condition deteriorates reaching a degraded state (P_{127}), needing minor preventive maintenance. At this state the vibration velocity of the pump exceeds the critical threshold set for the pump, i.e. >1.12 mm/s (see Table 4-7). In this research, the pumps are only observed for excess vibration levels due to misalignment. However, hydraulic factors such as cavitation and pulsations can also lead to degraded state. Failure to perform maintenance at this point would cause the pump to degrade further reaching a severely degraded state (P_{128}), needing major preventive maintenance. If the pump degrades beyond P_{128}, it reaches functional failure state, P_{129}. At this point, the pump requires corrective maintenance to return it back to 'new' state. P_{142}

represents the number of repairs performed on the submerged lift pump and is explained in further detail in Section 4.4.4.2.5.

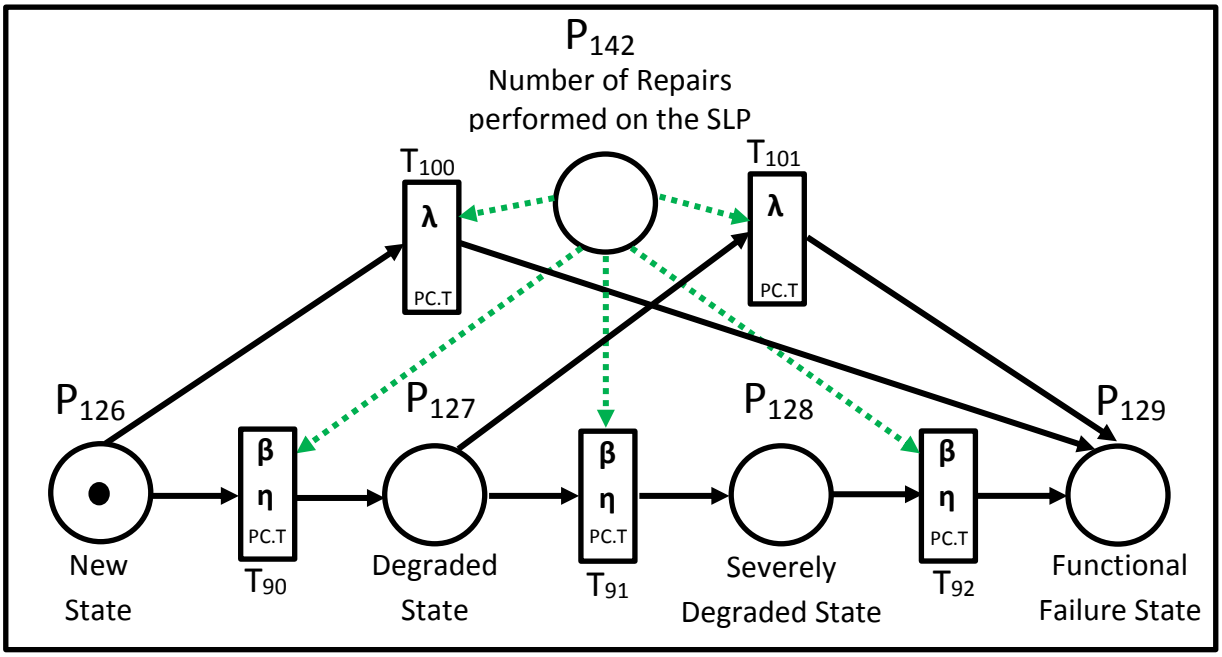


Figure 4-12 Petri Net Model showing the degradation and failure process for a Submerged Lift Pump

The transition times between the degradation states are governed by the Weibull distribution due to its flexibility to model all phases of the reliability bath-tub curve. The equations used to obtain the transition firing times have been described previously in Chapter 2 – Section 2.6.5.4. Due to the lack of data, the distributions of the times to reach certain degradation levels are indicative and were estimated using failure rate data obtained from several published studies (Lees (1996b) and Mobile North Sea Limited (2003)). In the event of real application, data would be collected to provide the times to achieve different levels of degradation. This data would then be used to determine the parameters of the appropriate Weibull parameters. The Weibull distribution parameters that were assumed for all wear-out type components in this research are shown in Table 4-8. The shape parameters (β) are larger than 1 to capture the increasing degradation rates of mechanical components in line with the Bathtub curve.

Safety System	Components	Condition	Intervention	Shape Parameter β	Scale Parameter η (hours)
Deluge System	Submerged Lift Pumps	Degraded	Minor Repair	1.50	35040
		Severely Degraded	Major Repair	1.50	17500
		Functional Failure	Replacement	2.50	1500

	Booster Pumps	Degraded	Minor Repair	1.50	35040
		Severely Degraded	Major Repair	1.50	17500
		Functional Failure	Replacement	2.50	1500
	Air Release Valves	Degraded Opening Time	Minor Repair	1.50	17500
		Slow Opening Time	Major Repair	1.85	8000
		Functional Failure	Replacement	2.50	800
	Deluge Valves	Degraded Opening Time	Minor Repair	1.50	14000
		Slow Opening Time	Major Repair	1.80	7000
		Functional Failure	Replacement	2.50	800
	Solenoid Valves	Degraded Opening Time	Minor Repair	1.50	14000
		Slow Opening Time	Major Repair	1.80	7000
		Functional Failure	Replacement	2.50	800
Isolation System	Isolation Valves	Degraded Closing Time	Minor Repair	1.50	14000
		Slow Closing Time	Major Repair	1.80	7000
		Functional Failure	Replacement	2.50	800
Blowdown System	Blowdown Valves	Degraded Opening Time	Minor Repair	1.50	14000
		Slow Opening Time	Major Repair	1.80	7000
		Functional Failure	Replacement	2.50	800

Table 4-8 Weibull Distribution Parameters for Different Offshore Safety System Components

Moreover, the submerged lift pump is also likely to fail spuriously. When the failures are all due to random processes, then the probability of the component's failure, is described via an exponential distribution. This means that the submerged lift pump can go from new or degraded state to functional failure state via two exponential distributions, T_{100} and T_{101}, respectively. The exponential distribution parameters (Mannan and Lees 2005) used for components that fail spuriously are shown in Table 4-9, below.

Safety System	Components	Condition	λ(t)/hour
Fire and Gas Detection System	Gas Detector	Working → Fail to Detect Gas	3.80×10^{-5}
		Working → Spuriously Detect Gas	1.90×10^{-5}
	Fire Detector	Working → Fail to Detect Fire	3.80×10^{-5}
		Working → Spuriously Detect Fire	1.90×10^{-5}
Deluge System	Submerged Lift Pumps	New → Functional Failure	2.30×10^{-5}
		Degraded → Functional Failure	2.40×10^{-5}
	Booster Pumps	New → Functional Failure	2.00×10^{-5}
		Degraded → Functional Failure	3.00×10^{-5}
	Air Release Valves	Normal Opening Time → Functional Failure	2.50×10^{-5}
		Degraded Opening Time → Functional Failure	2.70×10^{-5}
	Deluge Valves	Normal Opening Time → Functional Failure	1.67×10^{-5}
		Degraded Opening Time → Functional Failure	1.80×10^{-5}
	Solenoid Valves	Normal Opening Time → Functional Failure	1.67×10^{-5}
		Degraded Opening Time → Functional Failure	1.80×10^{-5}
	Deluge Nozzles	Working → Failed	2.30×10^{-4}
Isolation System	Isolation Valves	Normal Closing Time → Functional Failure	4.00×10^{-5}

		Degraded Closing Time → Functional Failure	6.00 x 10^{-5}
Blowdown System	Blowdown Valves	Normal Opening Time → Functional Failure	4.00 x 10^{-5}
		Degraded Opening Time → Functional Failure	6.00 x 10^{-5}

Table 4-9 Exponential Distribution Parameters for Different Offshore Safety System Components

Furthermore, the PN accounts for the pump maintenance history by implementing Probabilistic Condition Transitions for transitions T_{90}, T_{91}, T_{92}, T_{100} and T_{101} shown in Figure 4-12. This means that the time taken for the pump to degrade depends on the number of repairs performed previously. Dashed lines (shown in green) are used to represent these dependencies.

Similar nets have been constructed for all wear-out components of the deluge system and are shown in Appendix B of the thesis. Note that the isolation and blowdown valves and the deluge system valves experience two types of functional failure modes: 'fail open' or 'fail close'. Hence, the net used to model their degradation and failure is slightly different from that of the submerged lift pump. When the functional failure state of the valve is marked with a token, it enables a probabilistic transition which fires immediately and selects 'fail open' or 'fail closed' state based on probability.

4.4.4.2 Offshore Safety System Inspection and Maintenance

4.4.4.2.1 Safety System Inspection

The two most common inspection regimes implemented on offshore safety systems include:

1. **Visual Inspection** – Maintenance personnel visually inspect systems and components that are easily accessible in the different offshore modules. For instance, the firewater pumps positioned in the pump room can be visually inspected to check for leaks.
2. **Periodic Inspection** – Many of the components are subject to hidden or unrevealed failures. Hence, they are subject to periodic inspection to establish their condition and highlight any failure. For instance, the firewater pumps of the deluge system, are periodically inspected to check for bearing, coupling or impeller wear, misalignment, cavitation and lack of lubrication.

4.4.4.2.2 Safety System Maintenance

BS 3811:1984 defines maintenance as "*the combination of all technical and associated administrative actions, including supervision actions intended to retain an item in, or restore*

*it to, a state in which it can perform its required functi*on". A maintenance management system should deliver an effective inspection and maintenance policy that examines the condition of plant, detects degradation and failure and remedies the identified shortcomings. On offshore oil and gas installations, three major types of maintenance policies are generally implemented: Corrective Maintenance (CM), Preventive Maintenance (PM) and Shutdown Maintenance (Health & Safety Executive 2014). These maintenance policies will be included in the model.

When an asset reaches functional failure state, CM is performed to restore it to a working state. Under CM, it is necessary to ensure that spares and personnel are readily available at all times to restore the component and to keep availability above organisational requirements. Since maintenance does not need to be scheduled in advance, planning requirements are very low. CM makes sense when the total cost of repairing the component after functional failure is less than the cost of performing other types of maintenance on the component. However, due to the unpredictable nature of the asset failures, it is difficult to anticipate when personnel and spares are required for the repairs. The intermittent nature of failures means the efficient planning of personnel and spares can be difficult. As a result, the unexpected failure of a critical asset translates into huge cost overruns in either lost production or the cost of labour and spare parts. Thus, making CM as an expensive maintenance policy. Moreover, CM is unsuitable for applications where equipment failure poses a safety risk. CM is often referred to as breakdown or run-to-failure maintenance.

PM, on the other hand, is regularly performed on a component while it is in a working state, to lessen the likelihood of functional failure. In the case of offshore installations, this decreases the amount of downtime experienced. Since maintenance is planned, the resource requirements are known and can be made available in advance. Assets that are suitable for PM include those that have a critical operational function, have failure modes that can be prevented with regular maintenance and have a likelihood of failure that increases with time or use. Unsuitable assets include those that have random failures that are unrelated to maintenance and do not have a critical function. Planning is the biggest advantage of PM. Hence, the cost of PM is much lower than that of CM, though the active repair time is almost the same. However, maintenance may occur too often with a PM strategy. Unless

maintenance frequencies have been optimised, too much or too little PM will occur. For instance, submerged lift pumps are installed completely underwater, making it more susceptible to corrosion and seaweed build up. As a result, the pump may need to be cleaned two or three times instead of just once. Hence, a threshold limit is set to ensure that enough PM is performed.

PM can be further subdivided into three categories: time-based, age-based and condition-based maintenance. Under time-based maintenance, PM is carried out at predefined times set out by offshore operators, whereas under age-based maintenance, PM is carried out at a specified age of the component. The aim of condition-based preventive maintenance is two-fold. Firstly, to predict when component functional failure might occur, and secondly, to prevent the occurrence of the failure by performing maintenance. The task of monitoring for future failures allows maintenance to be planned before the failure occurs. Condition-based maintenance dictates that maintenance should only be performed when certain indicators show signs of performance degradation or upcoming failure (e.g. vibration monitoring in pumps). Hence, condition-based maintenance relies on regular inspection. The inspection frequency is predetermined and is usually dependent on experience of the asset's behaviour. Based on the inspection, maintenance is scheduled. The completion time for repairs is dependent on the severity of the defect found.

A graph that illustrates the behaviour of equipment as it approaches failure is the P-F curve shown in Figure 4-13. The graph shows that as a failure starts manifesting, the equipment deteriorates to the point at which it can possibly be detected (P). If the failure is not detected, it continues until functional failure occurs (F). The time range between P and F, also referred to as the P-F interval, is the window of opportunity during which an inspection can possibly detect the imminent failure and address it. For instance, if the P-F Interval is 200 days and the item will fail at 1000 days, the approaching failure begins to be detectable at 800 days.

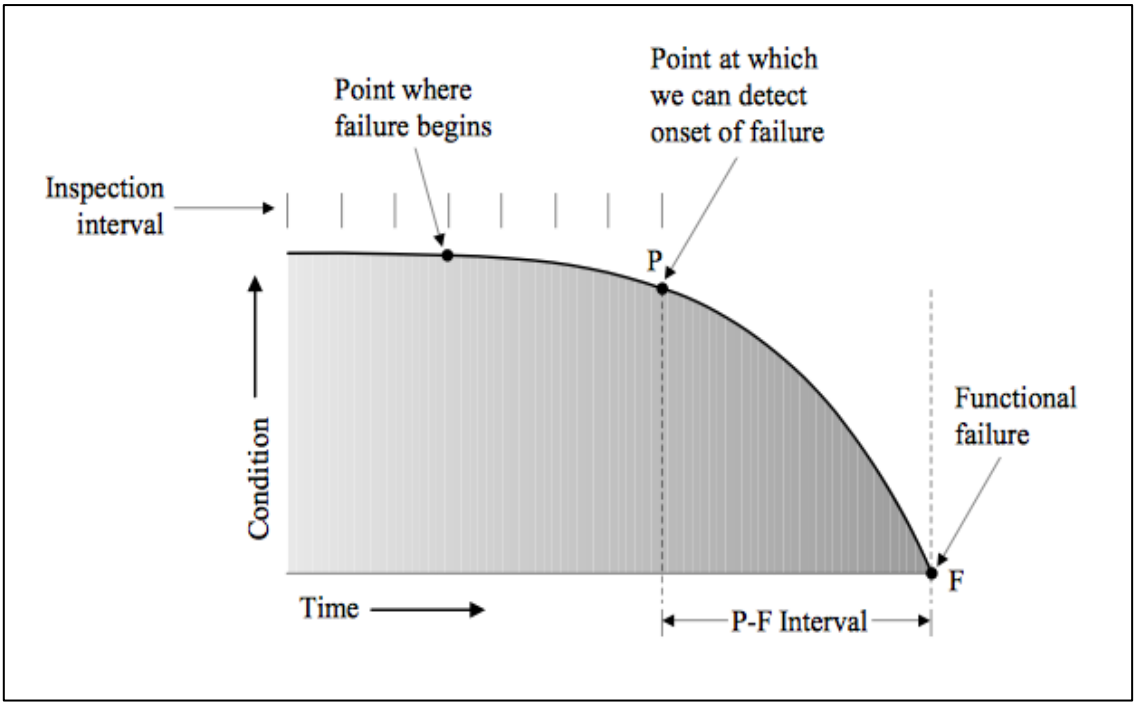


Figure 4-13 P-F Diagram

However, it must be noted that the cost of the equipment necessary for condition monitoring can be expensive. Moreover, the skill level and experience required to accurately interpret condition monitoring data is also high. Wrong interpretation of the data can lead to the unwanted shutdown of a system or the entire platform.

Shutdown maintenance is a major overhaul performed on systems that are usually inaccessible when the platform is fully operational. It is assumed that all safety systems, i.e. fire and gas detection system, isolation and blowdown valves, and deluge system, undergo shutdown maintenance every 5 years.

4.4.4.2.3 Summary of Maintenance Policies Implemented

Four types of maintenance interventions are performed on the safety systems, which have been defined in Table 4-10.

Maintenance Type	Type of Work	Definition
1. Condition-based PM	Minor	Minor repair work to restore the component from degraded condition back to new condition.
	Major	Major repair work to restore the component from severely degraded condition back to new condition.

2. CM	Replacement	Complete replacement of a failed component.
3. Opportunistic Maintenance		Opportunistic maintenance is performed on multi-component systems where maintenance tasks on other components provides an opportunity to carry out maintenance on components that were not the cause of the opportunity. For instance, when a downtime opportunity is created due to functional failure of the deluge valve, opportunistic maintenance is carried out immediately on all the other components of the deluge system.
4. Shutdown Maintenance		Complete replacement of all components of the safety systems every 5 years.

Table 4-10 Definition of the Type of Maintenance Implemented on Offshore Safety Systems

It is assumed that any maintenance intervention performed on a component will restore the state of the component back to the 'new' state in the case of a pump or 'normal' state in the case of a valve. Table 4-11 outlines the maintenance interventions implemented to rectify component degradation and restore it back to the 'new' or 'normal' condition, along with the mean time to schedule maintenance and the active repair time. The time taken to schedule maintenance depends on how fast the maintenance team can get to the site as well as the urgency to repair the component. Thus, depending on the seriousness of the component condition, appropriate times are assigned to each type of maintenance intervention. The mean time to schedule maintenance and active repair times have been assumed based on engineering judgement.

System	Component	Condition						Active Repair Time (hours)
		Degraded		Severely Degraded		Functional Failure		
		Description of Maintenance Intervention	Mean Time to Schedule Maintenance (hours)	Description of Maintenance Intervention	Mean Time to Schedule Maintenance (hours)	Description of Maintenance Intervention	Mean Time to Schedule Maintenance (hours)	
Fire and Gas Detection System	Detector	N/A	N/A	N/A	N/A	Replace	1	4.5
Deluge System	Submerged Lift Pump	Check alignment and adjust Lubricate all moving parts Tighten connections	24	Repair or replace motor Replace wear ring	8	Replace	2	40
	Booster Pump	Check alignment and adjust Lubricate all moving parts Tighten connections	24	Repair or replace motor Replace wear ring	8	Replace	2	40
	Air Release Valve	Clean out extraneous matter Lubricate	336	Replace torn diaphragm Replace rubber parts and springs Replace flange 0-ring	168	Replace	2	4

	Deluge Valve	Clean out extraneous matter Lubricate	336	Replace torn diaphragm Replace rubber parts and springs Replace flange 0-ring	168	Replace	2	4
	Solenoid Valve	Clean out extraneous matter Lubricate	336	Replace torn diaphragm Replace rubber parts and springs Replace flange 0-ring	168	Replace	2	4
	Deluge Nozzle	N/A	N/A	N/A	N/A	Replace	5	12
Isolation System	Isolation Valve	Clean out extraneous matter Lubricate	336	Replace torn diaphragm Replace rubber parts and springs Replace flange 0-ring	168	Replace	2	6
Blowdown System	Blowdown Valve	Clean out extraneous matter Lubricate	336	Replace torn diaphragm Replace rubber parts and springs Replace flange 0-ring	168	Replace	2	6

Table 4-11 Component Degradation Conditions and Mean Time to Schedule Maintenance for Different Safety System

4.4.4.2.4 Costs of Performing Inspection and Maintenance

The cost units of performing inspection and maintenance on the different components of the offshore safety systems are shown in Table 4-12. Each time a component is replaced, the system incurs a high fixed cost. The corrective maintenance cost is much higher when compared to the preventive maintenance cost.

System	Components	Inspection Cost (Units)	Minor PM Cost (Unit)	Major PM Cost (Unit)	CM Cost (Units)
Fire and Gas Detection System	Detector	25	N/A	N/A	350
Deluge System	Submerged Lift Pump	110	300	550	2800
	Booster Pump	110	300	550	2800
	Air Release Valve	75	150	350	500
	Deluge Valve	75	150	350	500
	Solenoid Valve	75	150	350	500
	Deluge Nozzle	30	N/A	N/A	200
Isolation System	Isolation Valve	85	185	385	550
Blowdown System	Blowdown Valve	85	185	385	550

Table 4-12 Average Cost of Performing Inspection and Maintenance

System or component downtime as defined by Rausand and Hoyland (2004) is "*the time in a specified mission period where the component or system is not able to perform one or more of its intended functions*." Unexpected component failures can quickly lead to platform shutdowns costing millions of pounds in lost production. Hence, assessing downtime costs is key in determining the operational costs of a system. In this study, the downtime cost is assumed to be 2000 units/hour.

4.4.4.2.5 Modelling Component Inspection and Maintenance

The section of the PN developed to model the inspection process of safety system components' is shown in Figure 4-14. Inspection takes place at fixed-time intervals, during which the true condition of the components are revealed and appropriate maintenance work with the appropriate priority is assigned.

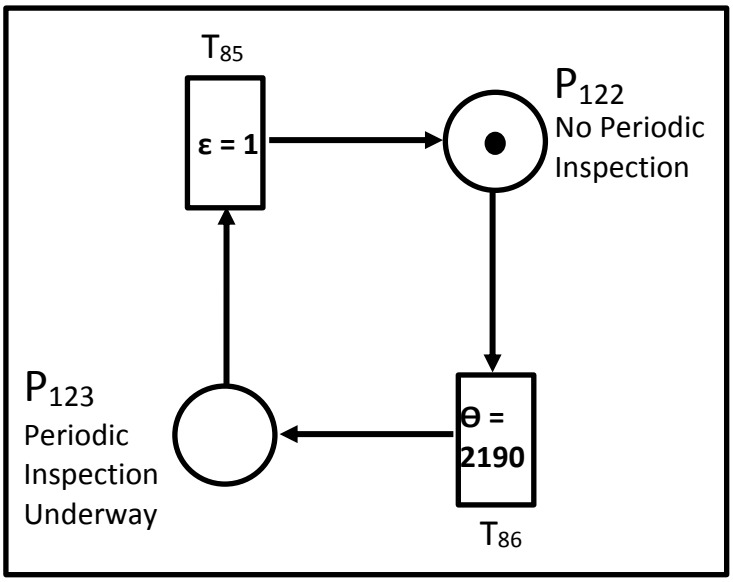


Figure 4-14 Petri Net Model showing the Inspection Process

Table 4-13 outlines the inspection intervals that were assumed based on common offshore practices for the different safety systems.

Safety System	Inspection Interval, Θ_i	Source
Fire and Gas Detection System	3 months (≈ 2190 hours)	United States Code of Federal Regulations (2011)
Isolation System	6 months (≈ 4380 hours)	Petrofac (2010)
Blowdown System	6 months (≈ 4380 hours)	Petrofac (2010)
Deluge System	3 months (≈ 2190 hours)	Grannes *et al.* (1990)

Table 4-13 Inspection Interval for the different Safety Systems

Consider the example where the submerged lift pump of the deluge system has reached a degraded state that requires minor PM (P_{127} in Figure 4-12). This place is replicated in Figure 4-15 with a token marking P_{127}. The component is not known to be in a degraded state until an inspection is performed. The inspection process is modelled via the loop: **P_{123} –>T_{85} –>P_{122} –> T_{86}**. Description of the places and transitions are provided in Table 4-14 and 4-15, respectively.

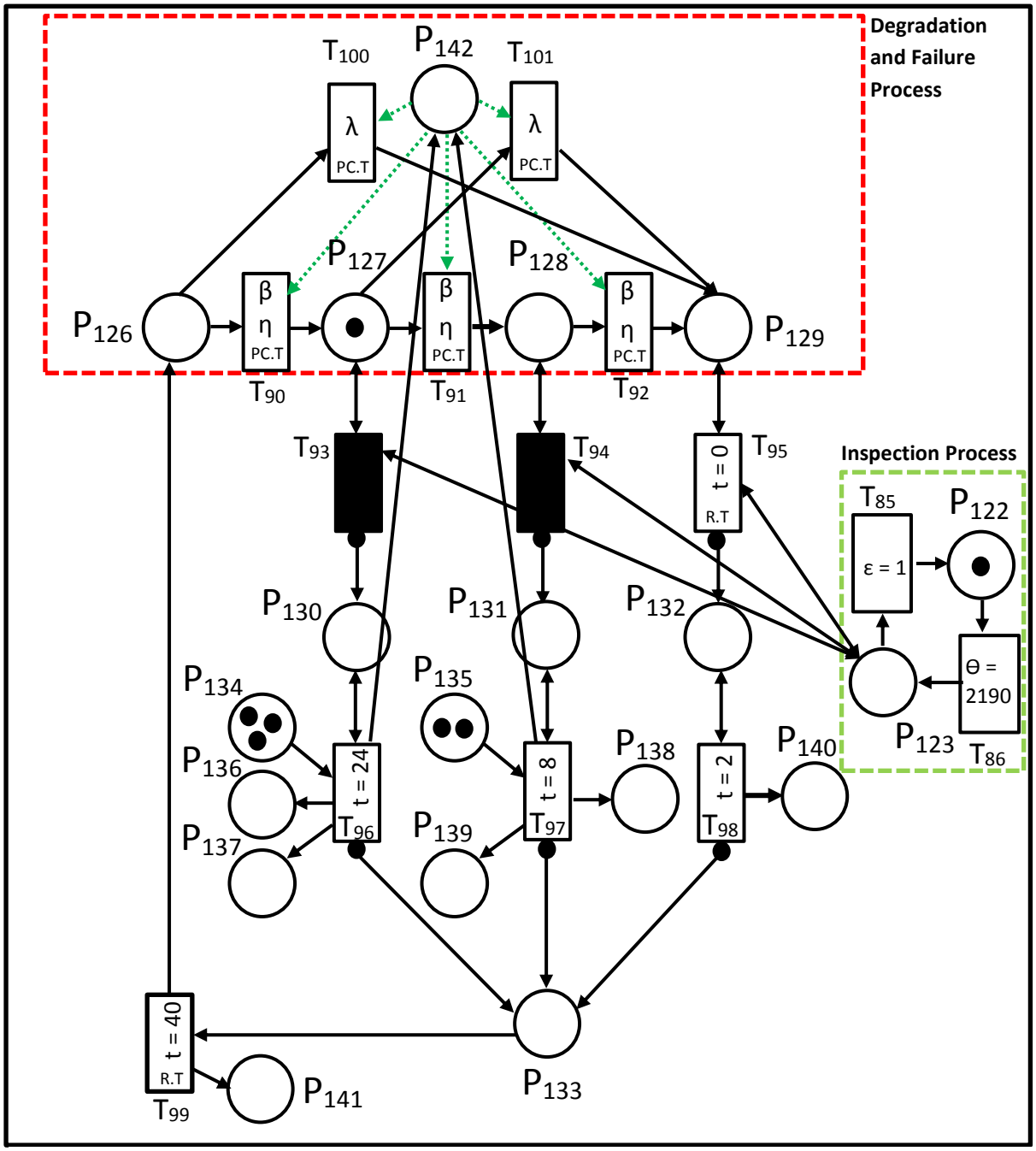


Figure 4-15 Petri Net Model showing the inspection and maintenance process for a Submerged Lift Pump

Place	Description
P122	No Periodic Inspection
P123	Periodic Inspection Underway
P126	New State
P127	Degraded State
P128	Severely Degraded State
P129	Functional Failure State
P130	Degraded State Revealed needing minor PM
P131	Severely Degraded State Revealed needing major PM
P132	Functional Failure State Revealed needing CM
P133	Maintenance Scheduled
P134	Maximum Number of Minor Repairs

P135	Maximum Number of Major Repairs
P136	Current Number of Minor Repairs
P137	Records statistics associated with the number of minor repairs and the corresponding costs incurred.
P138	Current Number of Major Repairs
P139	Records statistics associated with the number of major repairs and the corresponding costs incurred.
P140	Records statistics associated with the number of failures and the corresponding costs incurred.
P141	Total Number of Interventions
P142	Total Number of Repairs performed on the component

Table 4-14 Description of the Places in Figure 4-15

Transition	Function	Description
T85	Firing Time	=1
T86	Firing Time	=2160

T90	Firing Time	If P142 = 0 then
		Sampled from Weibull Distribution A: β = 1.50 and η = 35040
		Else If P142 = 1 then
		Sampled from Weibull Distribution B: β = 1.50 and η = 33288
		Else If P142 = 2 then
		Sampled from Weibull Distribution C: β = 1.50 and η = 31624
		Else If P142 = 3 then
		Sampled from Weibull Distribution D: β = 1.50 and η = 30043
		Else If P142 = 4 then
		Sampled from Weibull Distribution E: β = 1.50 and η = 28541
		Else
		Sampled from Weibull Distribution F: β = 1.50 and η = 27114

T91	Firing Time	If P142 = 0 then
		Sampled from Weibull Distribution A: β = 1.50 and η = 17500
		Else If P142 = 1 then
		Sampled from Weibull Distribution B: β = 1.50 and η = 16625
		Else If P142 = 2 then
		Sampled from Weibull Distribution C: β = 1.50 and η = 15794
		Else If P142 = 3 then
		Sampled from Weibull Distribution D: β = 1.50 and η = 15004
		Else If P142 = 4 then
		Sampled from Weibull Distribution E: β = 1.50 and η = 14254
		Else
		Sampled from Weibull Distribution F: β = 1.50 and η = 13541

T92	Firing Time	If P142 = 0 then
		Sampled from Weibull Distribution A: β = 2.50 and η = 1500
		Else If P142 = 1 then
		Sampled from Weibull Distribution B: β = 2.50 and η = 1425
		Else If P142 = 2 then
		Sampled from Weibull Distribution C: β = 2.50 and η = 1354
		Else If P142 = 3 then
		Sampled from Weibull Distribution D: β = 2.50 and η = 1286
		Else If P142 = 4 then
		Sampled from Weibull Distribution E: β = 2.50 and η = 1222
		Else
		Sampled from Weibull Distribution F: β = 2.50 and η = 1161

T93	Firing Time	=0
T94	Firing Time	=0
T95	Reset Transition	=0 and Reset Marking of Places: P142, P130, P131, P134, P135, P136 and P138

T96	Firing Time	=24
T97	Firing Time	=8
T98	Firing Time	=2
T99	Firing Time	=40 and Reset Marking of Places: P126, P127, P128, P130, P131. P132, P133, P262, P1, P2 and P367.
T100	Firing Time	Sampled from Exponential Distribution: $\lambda = 2.30 \times 10^{-5}$/hour
T101	Firing Time	Sampled from Exponential Distribution: $\lambda = 2.40 \times 10^{-5}$/hour

Table 4-15 Description of the Transitions used in Figure 4-15

P_{122} is the place which is marked when the submerged lift pump is not undergoing inspection. Presence of a token in P_{122} enables T_{86} which fires every $\Theta = 2190$ hours, hence removing the token from P_{122} and placing it in P_{123}. P_{123} indicates that the component is undergoing inspection to reveal its current state. Presence of a token in P_{127} and P_{123} would enable T_{93} which fires immediately, hence removing the token from P_{127} and P_{123} and placing it in P_{123}, P_{127} and P_{130}. The token is fired back into P_{127} to ensure that all other transitions that are dependent on the token being in P_{127} (e.g. P_{128}) are enabled. Hence, while the component is awaiting inspection, the pump condition can change from degraded to severely degraded state.

Moreover, the token back in P_{123} enables T_{85}, which fires after $\varepsilon = 1$ hour (the time period over which the inspection takes place), and removes the token from P_{123} and places it in P_{122}. P_{122} indicates that the component is awaiting its next inspection. P_{130} represents the state that the degraded pump condition has now been revealed. Presence of a token in P_{130} would inhibit T_{93} from becoming enabled again (in the same state), as degraded state is now revealed. When the condition of a component is revealed, a certain type of maintenance is performed on the component to restore its condition back to 'new'. In the case of the pump, when the degraded state is revealed, maintenance such as minor PM is performed.

A token in P_{130} enables T_{96} which represents the time required to schedule minor PM. This is because maintenance does not occur immediately, resources and personnel need to be allocated and often has an associated time delay. T_{96} fires after $\theta = 24$ hours and marks P_{133} with a token. P_{133} indicates that maintenance has been scheduled and the component is waiting to undergo repair or replacement depending on its condition. P_{133} enables T_{99}, which fires after $\theta = 40$ hours indicating that the pump has been repaired/replaced and its condition is returned back to 'new' state. Transition T_{99} is a reset transition that resets places P_{126}, P_{127},

P_{128}, P_{130}, P_{131}, P_{132}, P_{133}, P_{262}, P_1, P_2 and P_{367} upon firing. The reset transition updates the status of both the component and system PN and clears any duplicate tokens that may exist within the net. A similar maintenance route to that of a degraded pump state is followed when a severely degraded or functional failure state is revealed.

Moreover, the number of minor or major repairs that can be performed on any particular component is limited. This is because, every time an intervention is performed on a component, its effectiveness decreases. For instance, improper pump packing can cause several problems such as loss of prime or suction due to an air leak, shaft damage and water contamination of bearings. The maximum number of minor and major repairs is modelled by introducing places P_{134} and P_{135} where P_{134} contains three tokens and P_{135} contains two tokens. This means that a maximum number of three minor repairs and two major repairs can be performed on the pump. For instance, if the pump is in a degraded state (P_{127}) when it is inspected, T_{93} fires and marks P_{127} and P_{130}. P_{130} enables T_{96} which fires after θ = 24 hours. A token is removed from both P_{130} and P_{134} and placed in P_{133}, P_{136}, P_{137} and P_{142}. P_{133} indicates that maintenance has been scheduled, P_{136} records the number of times minor repair has been performed on the component, P_{137} records statistics associated with the number of minor repairs and the corresponding costs incurred and P_{142} records the total number of repairs performed on the component.

As explained earlier in Section 4.4.4, the PN accounts for the pump maintenance history by implementing PC.Ts for transitions T_{90}, T_{91}, T_{92}, T_{100} and T_{101}. Hence, to model this change in degradation behaviour after maintenance, the firing time of T_{90}, T_{91}, T_{92}, T_{100} and T_{101} is dependent on the total number of repairs previously performed on the component. Thus, if the number of tokens in P_{142} is equal to zero, it means the component has not undergone maintenance as yet and distribution A is used to sample the firing time. However, once the component undergoes maintenance, the degradation increases by 5%, i.e. the η value decreases by 5%, hence, a different distribution is used as shown in Table 4-15. As the number of tokens in P_{142} increases, the distribution used to sample the firing time changes from A to B, B to C, and so on. When the number of tokens in P_{142} is equal to five and no more tokens are present in P_{134} or P_{135}, minor or major PM is not possible anymore.

Moreover, following functional failure of a component (P_{129}), the total number of repairs in P_{142} is cleared as it does not relate to the newly replaced component. Likewise, places P_{134}, P_{135}, P_{136}, P_{138}, P_{130} and P_{131} should also be cleared. This is implemented by using a reset transition for T_{95}. When T_{95} fires, the tokens in P_{130}, P_{131}, P_{134}, P_{135}, P_{136}, P_{138} and P_{142} are reset. Similar nets have been constructed for isolation and blowdown valves and an example net is shown in Appendix B of the thesis.

4.4.4.3 Integration of Component and Subsystem Model

Once, PN models have been developed for the individual components, subsystem PNs showing critical fault propagation scenarios can then be developed with the help of Fault Trees. However, it must be noted that only the deluge system consists of subsystems while the fire and gas detectors, isolation and blowdown valves are modelled only at component level. Hence, in this section, only a detailed example of integration of component and subsystem model for the deluge system has been presented.

As described in Section 4.3.2.3, the deluge system consists of four main subsystems: (1) Fire and Gas Logic Unit; (2) Deluge Skid; (3) Deluge Nozzles and; (4) Firewater Pumps. The fault trees for the different subsystems are shown in Appendix C (Mobile North Sea Limited 2003). The top event of the fault tree for the Fire and Gas Logics is defined as “Failure of Logics” which refers to the failure of processing a demand signal from the fire and gas detectors. The top event of the Deluge Skid fault tree is defined as “Failure of Deluge Skid”. The deluge skid comprises of two deluge and solenoid valve combinations located in S1 and S2, respectively. Failure of solenoid valve 1 or deluge valve 1 can lead to the failure of S1. However, for the deluge skid to fail, both S1 and S2 need to be in a failed state. The top event of the Deluge Nozzle fault tree is defined as “Deluge Nozzle blockage leads to reduced or fail flow” which refers to the failure or blockage of 2 or more deluge nozzles. The top event of the Firewater Pump fault tree is defined as “Failure of Firewater Pumps” which refers to the failure of 3 or more firewater pump subsystems.

To demonstrate the integration of the component and subsystem model, the formation of the firewater pump subsystems is further discussed as an example. The firewater pump subsystem is made up of four fire water pumps running at 50% capacity; where two pumps

are electrically powered and the other two are powered via their own dedicated diesel engines. It is assumed that a failure of a firewater pump occurs if any of the following events occur: (1) Failure of the Submerged Lift Pump; (2) Failure of the Booster Pump and (3) Failure of the Air Release Valve. Hence, consider the example where the submerged lift pump reaches functional failure state as a result of a spurious failure or failure due to degradation. In the event that either of the three transitions - T_{92}, T_{100} or T_{101} shown in Figure 4-16 were to fire, places P_{129} and P_{262} would be marked with a token. Description of the places shown in Figure 4-16 is provided in Table 4-16.

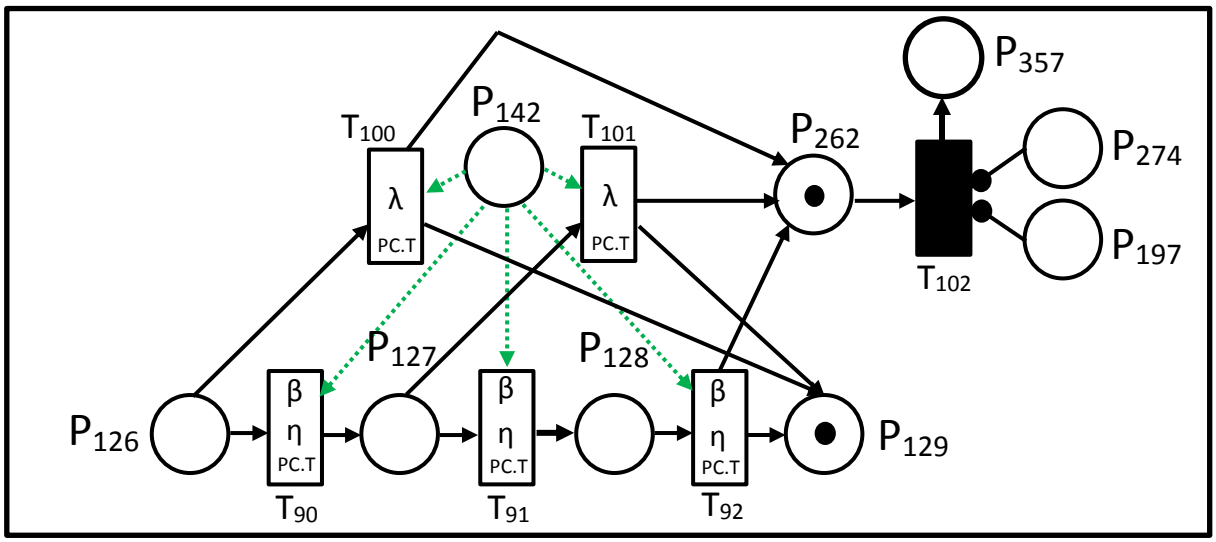


Figure 4-16 Petri Net Model showing the failure process for a Submerged Lift Pump

Place	Description
P126	New State
P127	Degraded State
P128	Severely Degraded State
P129	Functional Failure State
P142	Total Number of Repairs performed on the Component
P197	Air Release Valve Failed
P262	Submerged Lift Pump Failed
P274	Booster Pump Failed
P357	Submerged Lift Pump of Pump System 1 in Failed State

Table 4-16 Description of the Places used in Figure 4-16

Presence of a token in P_{129} indicates that the submerged lift pump is in a functional failure state while a token in P_{262} indicates that the submerged lift pump is in a failed state which enables transition T_{102}. T_{102} fires immediately and marks P_{357}. P_{357} indicates that the submerged lift pump of pump system 1 is in a failed state. The PN structure for both the booster pump and air release valve are similar to the submerged lift pump. If both the booster

pump and air release valve of pump system 1 were to reach functional failure state (P_{274} and P_{197}) at the same time as the submerged lift pump, presence of a token in P_{197} and P_{274} would inhibit T_{102} from firing again. This prevents multiple tokens accumulating in P_{367} due to the subsequent firing of P_{355}, P_{356} and P_{357} (shown in Figure 4-17 below) as failure of one component is sufficient to cause failure of a single pump system (indicated by marking P_{367} with a token). Description of the places shown in Figure 4-17 is provided in Table 4-17.

Moreover, in the event that two firewater pumps were to fail (P_{367} and P_{368} or P_{368} and P_{370} or P_{367} and P_{369} or P_{368} and P_{370}), the remaining two would still be able to meet the deluge requirements. However, if three or more firewater pumps were to fail, it would be impossible to meet this demand. Thus, leading to the overall failure of the firewater pump subsystem (P_{13} marked in Figure 4-17).

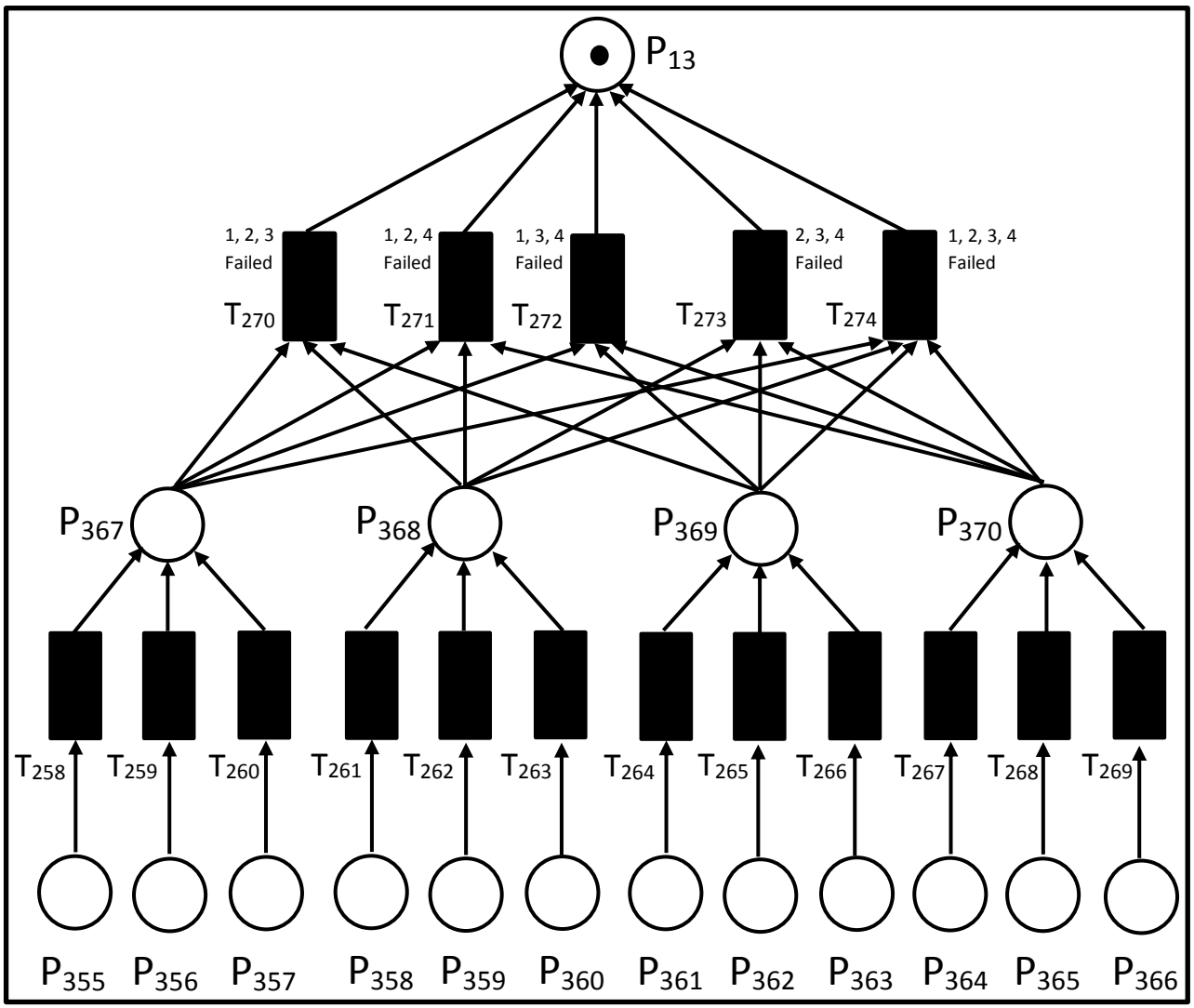


Figure 4-17 Petri Net Model showing the failure process for the Firewater Pump Subsystem

Place	Description
P13	Complete Failure of Firewater Pump Subsystem
P355	Air Release Valve of Pump System 1 in Failed State
P356	Booster Pump of Pump System 1 in Failed State
P357	Submerged Lift Pump of Pump System 1 in Failed State
P358	Air Release Valve of Pump System 2 in Failed State
P359	Booster Pump of Pump System 2 in Failed State
P360	Submerged Lift Pump of Pump System 2 in Failed State
P361	Air Release Valve of Pump System 3 in Failed State
P362	Booster Pump of Pump System 3 in Failed State
P363	Submerged Lift Pump of Pump System 3 in Failed State
P364	Air Release Valve of Pump System 4 in Failed State
P365	Booster Pump of Pump System 4 in Failed State
P366	Submerged Lift Pump of Pump System 4 in Failed State
P367	Failure of Pump System 1
P368	Failure of Pump System 2
P369	Failure of Pump System 3
P370	Failure of Pump System 4

Table 4-17 Description of the Places used in Figure 4-17

4.4.4.4 Integration of Subsystem and System Model

The subsystem nets are integrated to form the main deluge system system net. The main fault tree that was used to define the deluge system Petri Net is shown in Figure 4-18. The top event in the fault tree analysis of the deluge system is defined as a "failure to deliver firewater according to OREDA requirements". This means that water is not distributed with sufficient pressure to the most distant nozzles within 30 seconds after a confirmed signal from the fire and gas detectors to the fire and gas logic unit. Hence, as seen in the fault tree, failure of the deluge system occurs if any of the following events occur: (1) Failure of atleast 2 or more fire and gas logics; (2) Failure of the deluge skid; (3) Failure of atleast 3 or more firewater pumps or (4) Failure or blockage of atleast 2 or more deluge nozzles.

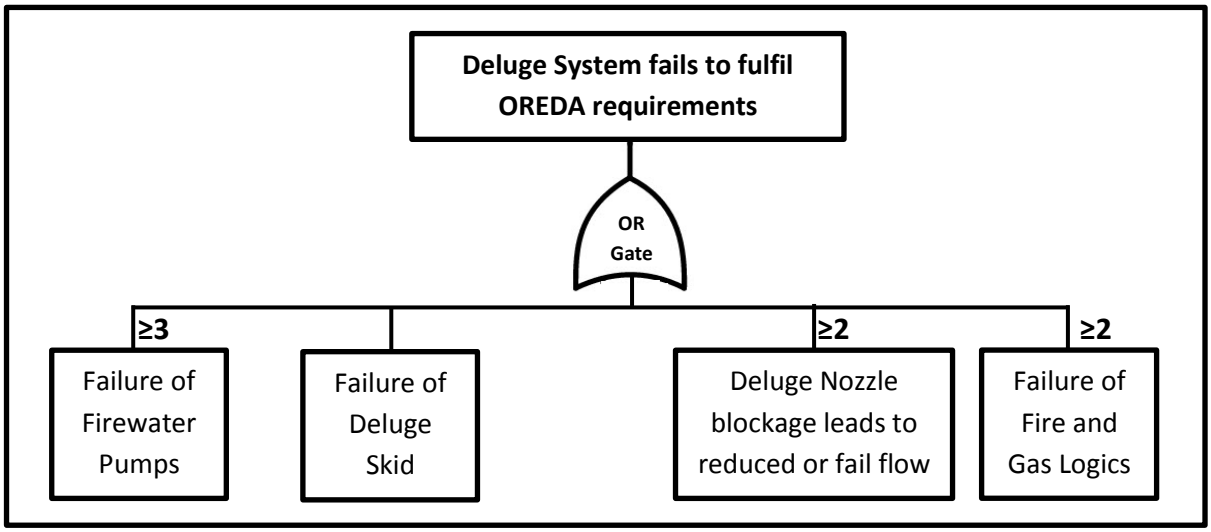


Figure 4-18 Main Fault Tree

The following demonstrates the conversion of the above fault tree to the main system Petri net. The deluge system lifetime begins in a working state (indicated by marking P1 in Figure 4-19 below), however, over time, due to random processes or component degradation, the subsystems, i.e. firewater pumps, deluge skid, deluge nozzles or fire and gas logics, can fail to function on demand. Consider the example where firewater pump subsystem fails. This would be indicated by marking P_{13} with a token (see Figure 4-19 below).

P_{13} would enable T_3 which would fire immediately and move the token from P_1 and P_{13} to P_2 and P_6. P_2 indicates that the deluge system is now in a failed state and is unable to function on demand. P_6 records the number of times the firewater pump subsystem fails. The deluge system is restored back to working state once the failed components of the subsystem have been been replaced. Description of the places shown in Figures 4-19 is provided in Table 4-18.

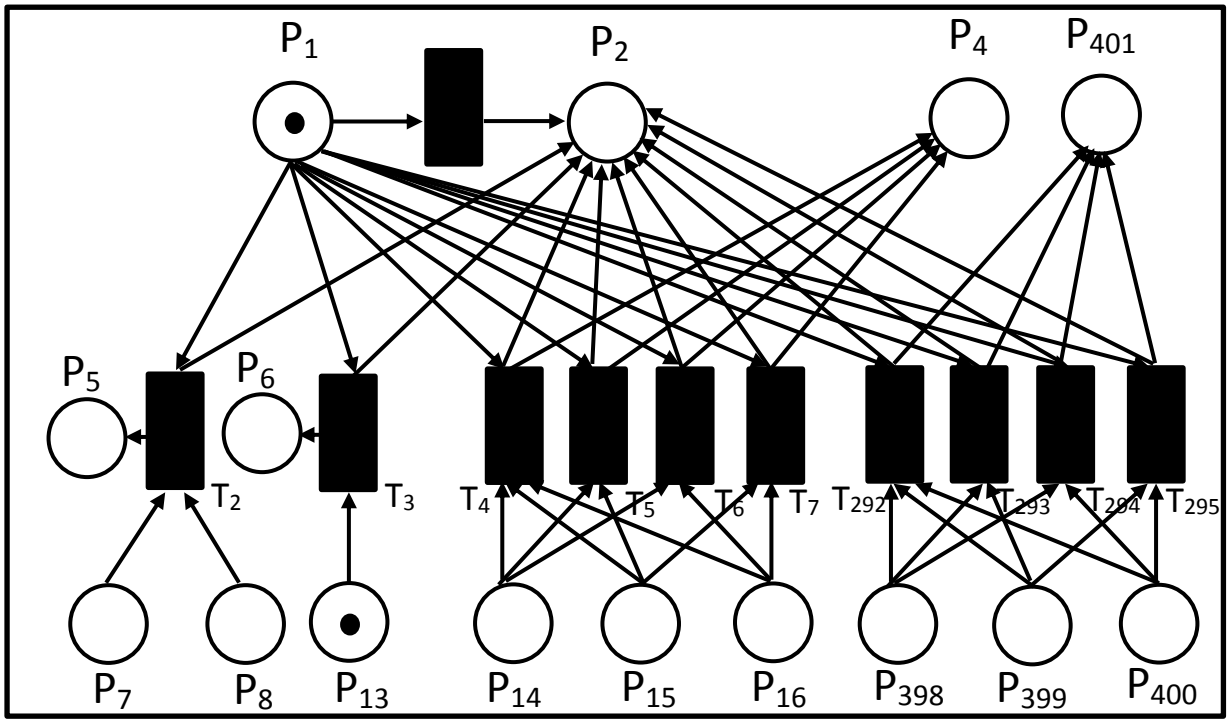


Figure 4-19 Petri Net Model showing the failure process for the Deluge System

Place	Description
P1	Deluge System Working
P2	Deluge System Failed
P4	Total Number of Deluge Nozzle Subsystem Failures
P5	Total Number of Deluge Skid Subsystem Failures
P6	Total Number of Firewater Pump Subsystem Failures
P7	Complete Failure of Deluge Skid 1

P8	Complete Failure of Deluge Skid 2
P13	Complete Failure of Firewater Pump Subsystem
P14	Complete Failure of Deluge Nozzle 1
P15	Complete Failure of Deluge Nozzle 2
P16	Complete Failure of Deluge Nozzle 3
P398	Complete Failure of Pressure Sensor 1
P399	Complete Failure of Pressure Sensor 2
P400	Complete Failure of Pressure Sensor 3
P401	Total Number of Fire and Gas Logic Subsystem Failures

Table 4-18 Description of the Places used in Figure 4-19

4.4.4.5 Modelling Opportunistic Maintenance

Dependencies between various components of the deluge system have been modelled via opportunistic maintenance. Opportunistic maintenance is a form of preventive maintenance that is undertaken on a component when another component of the same system is undergoing corrective maintenance and is experiencing downtime.

For instance, in this research, only when a downtime opportunity is created due to functional failure of the deluge valve, opportunistic inspection is carried out immediately on all the other components of the deluge system. This is because the deluge valve has the shortest active repair time (≈ 4 hours) compared to the other components of the deluge system. Hence, downtime costs incurred are low. If the components are revealed to be in a 'degraded' or 'severely degraded' state in the case of the pumps or 'degraded closing time' or 'slow closing time' in the case of valves, preventive maintenance is performed to restore the condition of the components back to 'new'. Figure 4-20 shows an example of opportunistic maintenance. Description of the places shown in Figures 4-20 is provided in Table 4-19.

The main aim of opportunistic maintenance is to improve system availability and reduce downtime and subsequent production loss. Hence, all component nets are connected to global places - P_{125} and P_{371}. P_{125} indicates opportunistic maintenance for the deluge system is underway while P_{371} indicates no opportunistic maintenance. Presence of a token in P_{371} inhibits opportunistic maintenance from being performed on any components of the deluge system.

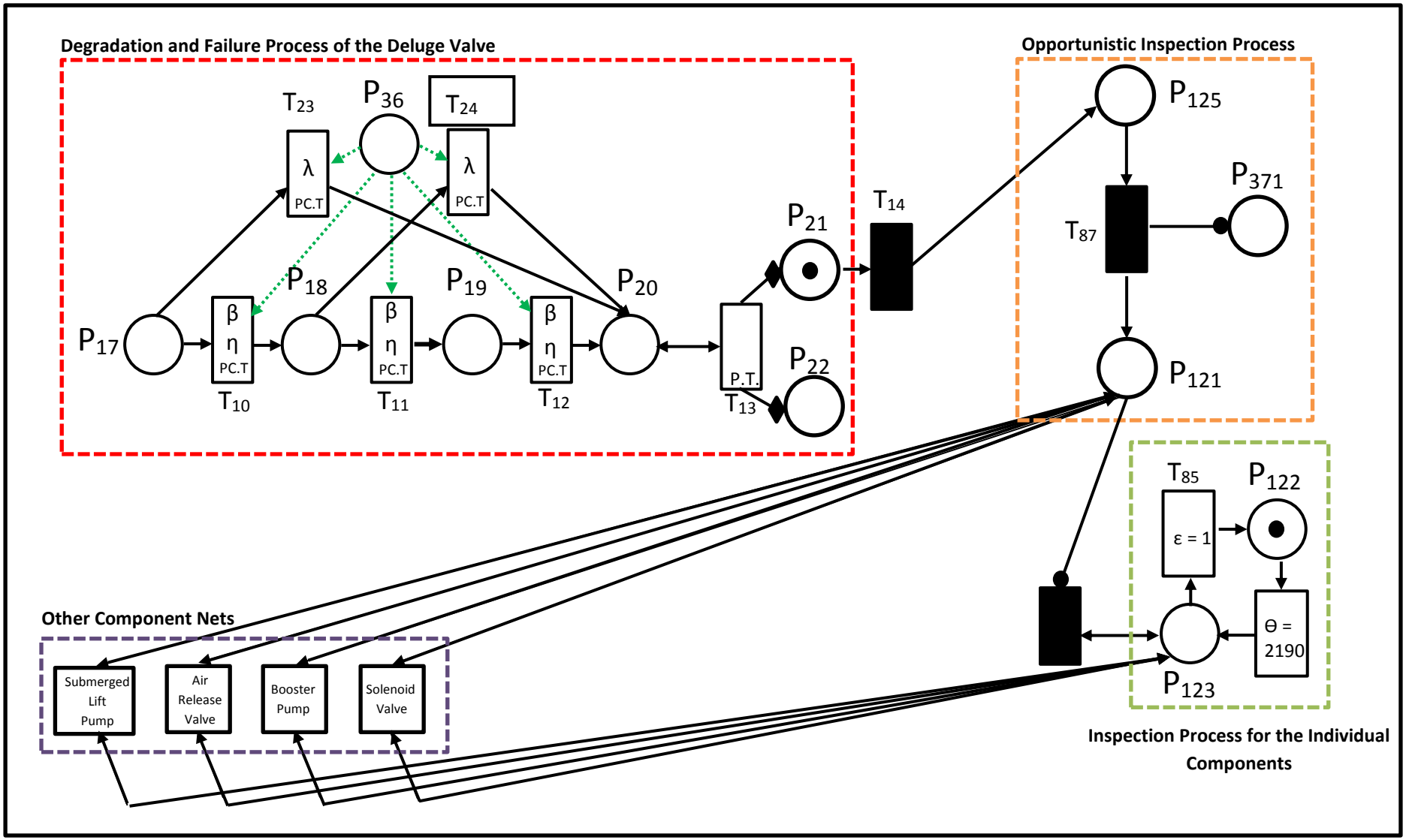


Figure 4-20 Petri Net Model showing the Opportunistic Maintenance Process

Place	Description
P17	Normal Opening Time
P18	Degraded Opening Time
P19	Slow Opening Time
P20	Functional Failure State
P21	Fails Closed
P22	Fails to Open
P36	Total Number of Repairs performed on the component
P125	Prepare Opportunistic Maintenance for Deluge System
P121	Opportunistic Inspection Underway
P371	No Opportunistic Maintenance
P122	No Periodic Inspection
P123	Periodic Inspection Underway

Table 4-19 Description of the Places used in Figures 4-20

4.4.4.6 Modelling Different Maintenance Strategies

The maintenance strategy can be varied by placing a token in either global place, P_{372} or P_{373}, as shown in Figure 4-21. These places inhibit a certain type of intervention on the components of a system. A token in P_{373} indicates that minor repair on the component is disabled, i.e. the component is allowed to deteriorate to a 'Severely Degraded' state and maintenance only happens at major level. A token in P_{372} indicates that major repair on the component is disabled, i.e. the component is allowed to deteriorate to a 'Functional Failure' state after which the component is replaced. Token in both P_{372} and P_{373} would indicate that both major and minor repair on the component is disabled. No tokens in Place P_{372} or P_{373} indicates that all components are repaired as soon as they are in a state where repair is possible. Thus, the PN model allows us to model the effect of different maintenance strategies on the operational costs of the system. In this research, the effect of four maintenance strategies are modelled as shown in Table 4-20.

Strategy	Description	Petri Net Representation
1	Repair as soon as component is revealed to be in a state where repair is required.	P_{372} and P_{373} are unmarked.
2	Minor Repair is disabled, only major repair and replacement is considered.	P_{373} is marked with a token.
3	Major Repair is disabled, only minor repair and replacement is considered.	P_{372} is marked with a token.
4	Both Minor and Major Repair are disabled, only replacement is considered.	P_{373} and P_{372} are marked with a token.

Table 4-20 Maintenance Strategies applied to the Offshore Oil and Gas Assets

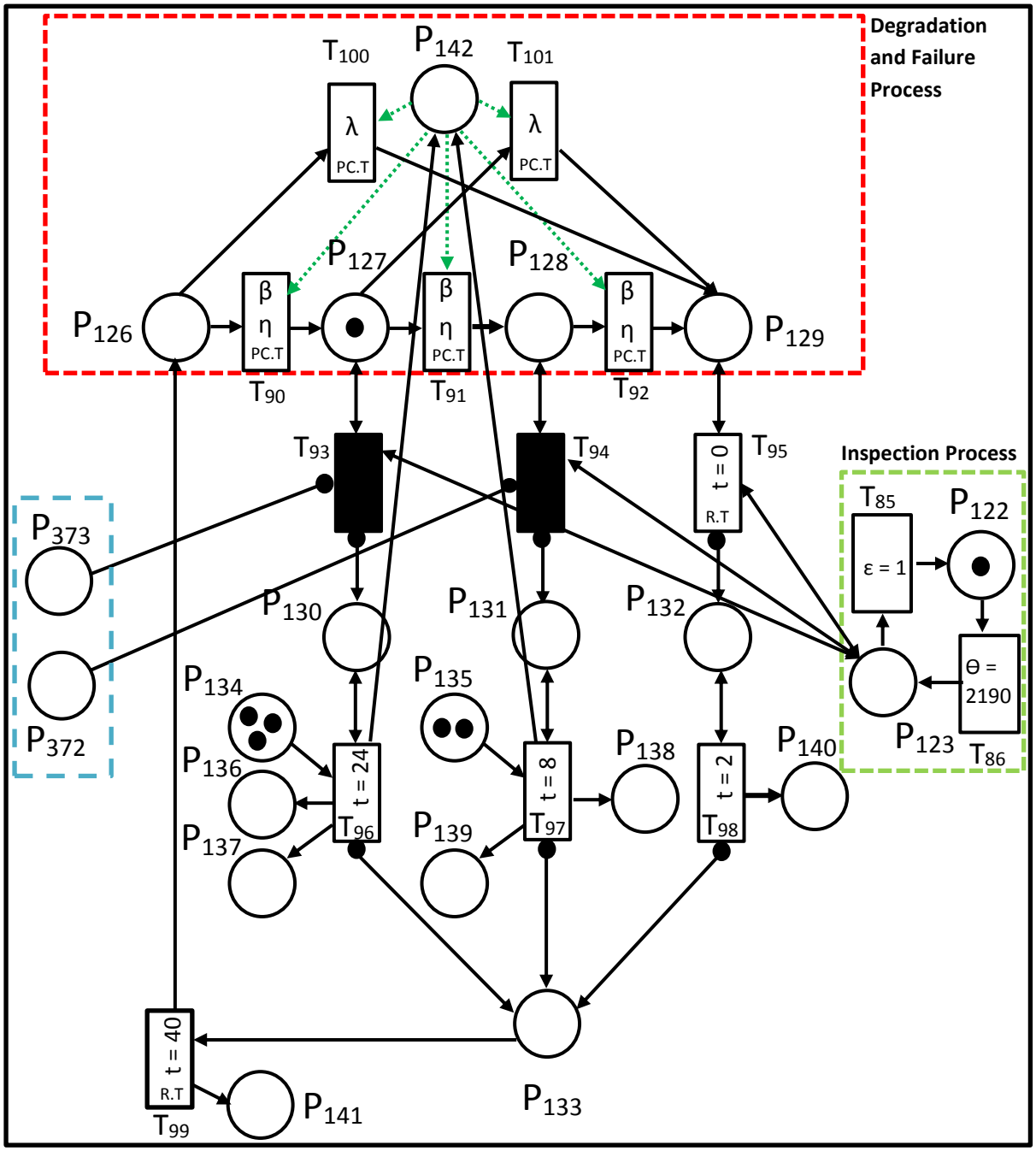


Figure 4-21 Petri Net Model showing the inspection and maintenance process for a Submerged Lift Pump

4.4.5 Building the Petri Net Software

The software used for creating and solving the Petri Nets via Monte Carlo Simulation was developed using the C++ programming language. C++ was selected due to its object-oriented features such as objects, classes, data abstraction and encapsulation, inheritance and polymorphism. Objects and classes are important features of C++ programming language. Classes are user-defined objects whose data can be protected, initialised and accessed via a

set of functions. In this research, multiple interrelated classes are used. For instance, class Place which describes the basic data structure of a place, hence allowing it to store tokens; and class Transition which contains the code to determine if the transition is fireable and to fire it.

Classes use data abstraction to represent essential features of the object while encapsulation allows data and functions to be stored in a single class. This protects the data from outside interference and misuse. Data encapsulation is implemented via keywords such as public, protected and private which are placed in the declaration of the class. Inheritance, on the other hand, allows objects to acquire properties of objects of another class. This means that a new class is derived (also known as inherited class) containing characteristics of the parent class. For instance, a transition with a special action (e.g. a Probabilistic Transition) is an inherited class from the parent class Transition. Moreover, polymorphism allows one class to inherit from multiple classes. For instance, the execution of the different functions, e.g. Weibull or Exponential distribution, by a transition. In this research, the source code developed by De Rozieres *et al.* (2014), was used and necessary enhancements, for instance, Probabilistic Transitions were added to adapt the code to this research requirements. The several enhancements made to De Rozieres' code has been shown and explained in Appendix D. Once the C++ code is prepared, it is compiled using Qt creator 5.7.1 and hence create an executable software. The compilation process involves linking libraries to the source code. A screenshot of the modelling tool is shown in Appendix E.

The structure of the software can be split in two sections: Graphical User Interface (GUI) and Simulation. The aim of the GUI is to allow the user to draw the Petri Nets and input data such as number of tokens in a particular place, the firing times of the transitions which includes degradation rates, inspection interval, maintenance scheduling time and the active repair time. This data is saved as a binary file within the software. Operations such as cut, copy, paste, zoom-in and zoom-out are added to enhance the software's drawing capability as shown in Appendix D. The simulation function, on the other hand, performs a step-by-step execution of the Petri Net by firing transitions and generating new markings. The user is able to visualise the movement of tokens through the net. Hence, this graphical representation acts as a debugging tool as it enables the user to spot design flaws more easily. The animation

can be paused, stopped or accelerated at any time and the current simulation time is displayed at each step. Before starting the simulation, the user must define the desired number of simulation runs and the simulation period. In the event that insufficient simulations are performed, the results may fail to converge. In this research, 10,000 simulations were carried out. The model was able to undertake 10,000 simulations in approximately 5 minutes, using a computer with a dual core Intel i3 processor.

Moreover, the simulation function allows the user to obtain important information such as number of times a place of interest is marked with a token and the duration that the token resides in this particular place for each simulation. This information is written to a .mat file which is then analysed on MATLAB to generate statistics such as the probability of the system being in any of the condition states, the total number of component replacements over the system lifetime, the total number of maintenance interventions carried out on each component and the system availability. By assigning unit costs for the inspection and maintenance activities, the costs of performing inspection and maintenance on offshore safety systems can also be estimated.

In summary, by simulating the Offshore Safety System Degradation and Maintenance Model, the following results are aggregated: (1) Mean time a component resides in any of the condition states over its lifetime, (2) Number of Component Failures per lifetime, (3) Number of Component Maintenance Interventions per lifetime, (4) Mean time a system resides in each condition state, (5) Subsystem Contribution to the Total System Downtime, (6) System Availability and (7) System and Component Operational Cost. Figure 4-22 shows the overall framework, i.e. main inputs and outputs, of the Offshore Safety System Degradation and Maintenance Model.

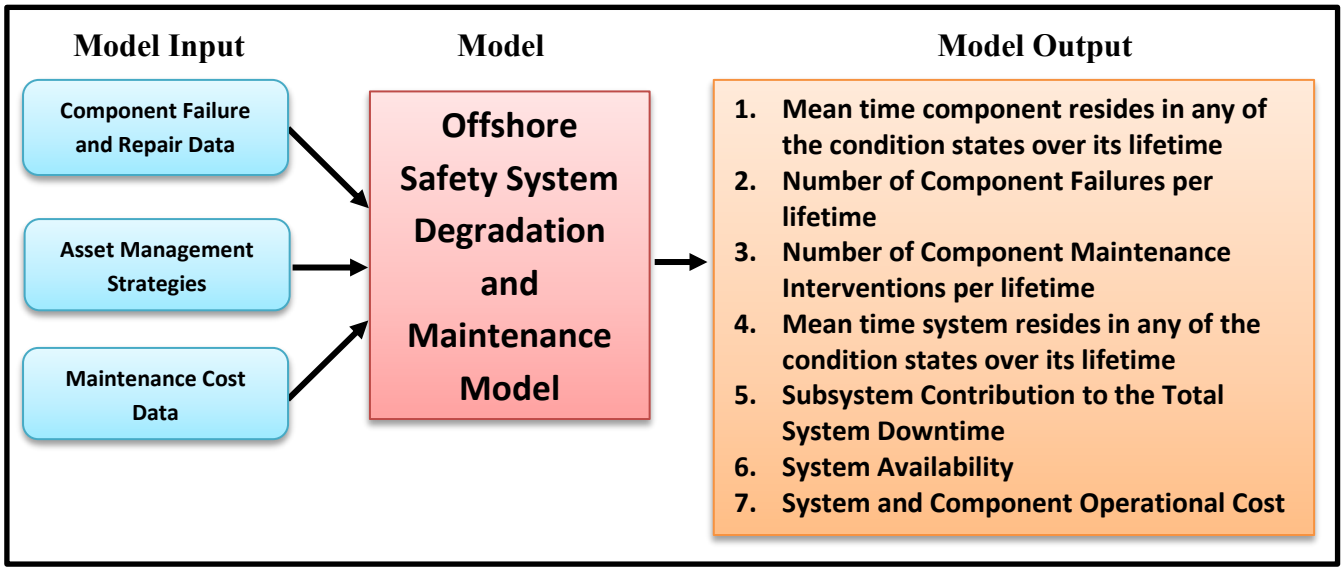


Figure 4-22 Offshore Safety System Degradation and Maintenance Model Framework

4.4.6 Verification of the Petri Net Model

The graphical interface of the Petri Net Software allows us to visually verify the firing process of the Petri Net model. Smaller Petri Nets are created that contain all the high level features used in the different component, subsystem and system nets. A test is then conducted whereby the simulation clock is started and at each time step, the net is checked to see if the enabled transitions would fire tokens as intended. If the transition fails to fire as intended, a subsequent debugging process rectifies the found defects. The firing process is tested on smaller Petri Net models as testing on the main system Petri Net model can be too complicated due to the large number of transitions and places it contains. Instead, the credibility of the main system Petri Net model is checked by validating the results generated via simulating the main system Petri Net model. This is further discussed in Chapter 5 of the thesis.

4.5 Offshore Fire and Explosion Model

4.5.1 Model Structure

The Offshore Fire and Explosion Model is used to model the occurrence of a hydrocarbon leak from a process vessel located within the three main modules; wellhead, separation and compression, of an offshore installation. The aim of this model is to predict the frequencies of fires and explosions in the event that the safety systems previously modelled in Offshore Safety System Degradation and Maintenance Model, fail to function on demand in the presence of an ignition source.

The Fire and Explosion Model is implemented in MATLAB. Before starting the simulation, the user must define the simulation period (usually the same simulation time period adopted for the Offshore Safety System Degradation and Maintenance Petri Net Model, i.e. 35 years). Once initiated, the MATLAB function reads an input file containing inventory data for each module and their isolatable sections. This includes hydrocarbon inventory and section operating data (i.e. volume, temperature and pressure) previously outlined in Table 4-1. In addition to this, data such as densities of oil, gas and condensate, latent heat of vaporisation, specific heat capacity at constant volume and pressure and ambient conditions of the modules as shown in Table 4-21 is also read.

Parameter		Units
Gas Density	2.350	Kg/m^3
Oil Density	987.00	Kg/m^3
Condensate Density	970.00	Kg/m^3
Air Density	1.22	Kg/m^3
Atmospheric Pressure	101.325	KPa
Specific heat capacity at constant volume	1675.55	J/Kg ^oC
Specific heat capacity at constant pressure	2200.00	J/Kg ^oC
Latent heat of vaporisation	511000.00	J/Kg

Table 4-21 Additional Inventory Data

The Offshore Fire and Explosion Model follows the event tree structure outlined by Andrews *et al.* (2005) (Figure 2-5 in Chapter 2). Each scenario begins with a hydrocarbon leak on an isolatable process section. Each scenario varies depending on the following factors: (1) module the leak has occurred in, (2) process section that is leaking, (3) size of the hole from which the leak occurs and (4) type of leak. Once these parameters are determined, the input

data is used to calculate the hydrocarbon discharge rate using fluid flow modelling equations shown in Section 4.5.1.2.

The code then models the activation of the safety systems, i.e. the fire and gas detection system, isolation and blowdown valves and the deluge system. The results files generated from simulating the Offshore Safety System Degradation and Maintenance Model is linked to the Fire and Explosion Model. This means that the MATLAB function reads the result files generated by the C++ code. Hence, when a hydrocarbon leak occurs during the simulation of the Fire and Explosion Model, the status of these safety systems (i.e. working, degraded, severely degraded or failed) are extracted for the current time from the results files generated by the Offshore Safety System Degradation and Maintenance Model. Figure 4-23 shows the integration of the two sub-models to make up the Platform Safety Model.

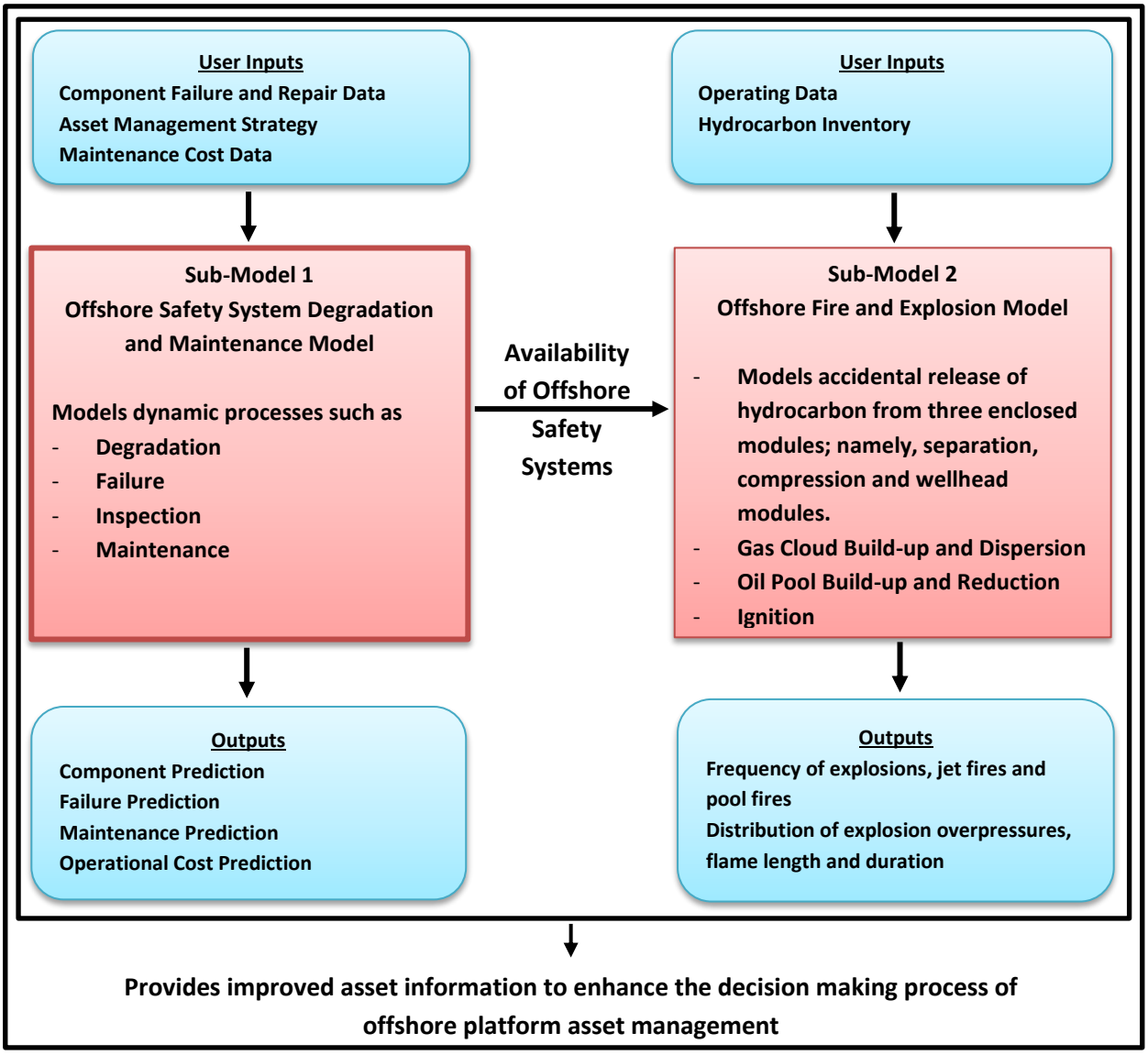


Figure 4-23 Platform Safety Model Framework

Sub-model 1 is the asset management model and when it is combined with Sub-model 2, which is the fluid flow model, it can be used to evaluate the frequencies of fires and explosions generated in the event of an accidental hydrocarbon release. In conclusion, the Platform Safety Model provides improved asset information to enhance the decision making process of offshore platform asset management.

Furthermore, for each leaking section, the ways that the sections combine due to isolation valve failure are considered in turn and for each combination all possible blowdown situations are also taken into consideration. The MATLAB code then calculates the new hydrocarbon discharge rate following isolation and blowdown.

In the event of a gas leak, the code models the variation of gas concentration in the module over time or the build-up of the oil in the event of an oil leak. The code then models the type of ignition (immediate or delayed) and the probability of occurrence of an ignition source (pre or post isolation) (Lewthwaite 2006). The latter also depends on the availability of the deluge system. Delayed ignition of a gas leak would result in an explosion if the gas concentration was between the explosive range while immediate ignition of a gas and oil leak would result in a jet and pool fire, respectively. Moreover, depending on the status of the deluge system during the course of the leak, explosions can be further subdivided into mitigated and unmitigated explosions (See Section 4.5.2.2).

In summary, by simulating the Fire and Explosion Model, the following results are aggregated: (1) Frequency of Fires and Explosions, (2) Frequency of Mitigated and Unmitigated Explosions, (3) Magnitude of the Explosion in terms of Explosion Overpressures and (4) Magnitude of the Fires (both jet and pool) in terms of the Flame Lengths generated and the duration of these fires. This step holds the key to developing the most effective strategy for offshore accident prevention and management. Once the frequencies of fires and explosions are determined for a given maintenance process, different asset management strategies can be applied to predict their effect on the safety systems and hence, produce the optimal interventions for the offshore assets with an acceptable risk level. Figure 4-24 shows the overall framework, i.e. main inputs and outputs, of the Fire and Explosion Model while Figures 4-25, 4-26 and 4-27 demonstrates the operational process of the Fire and Explosion code.

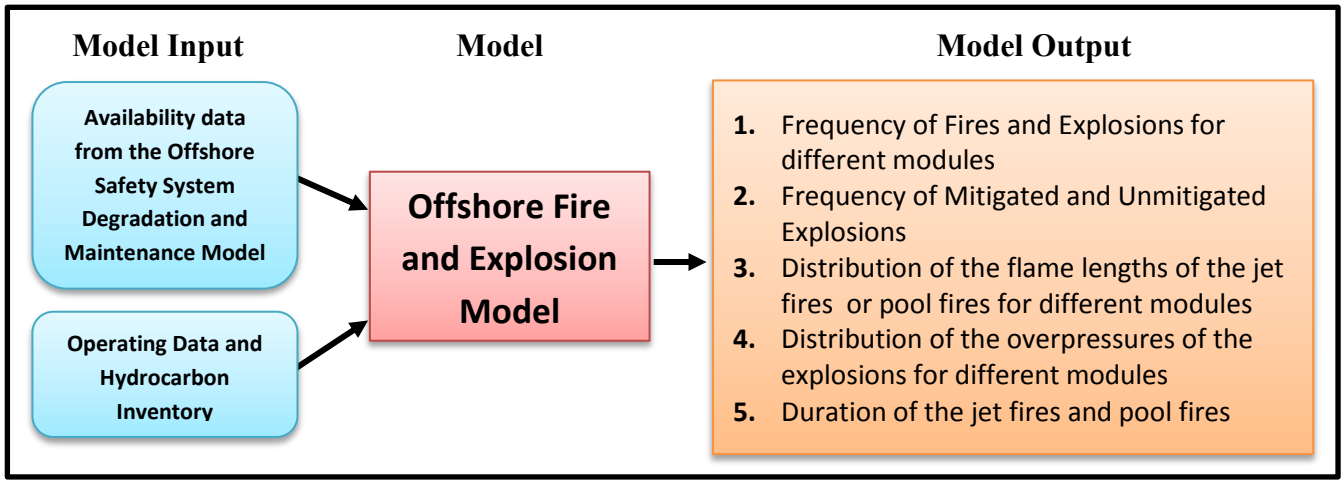


Figure 4-24 Offshore Fire and Explosion Model Framework

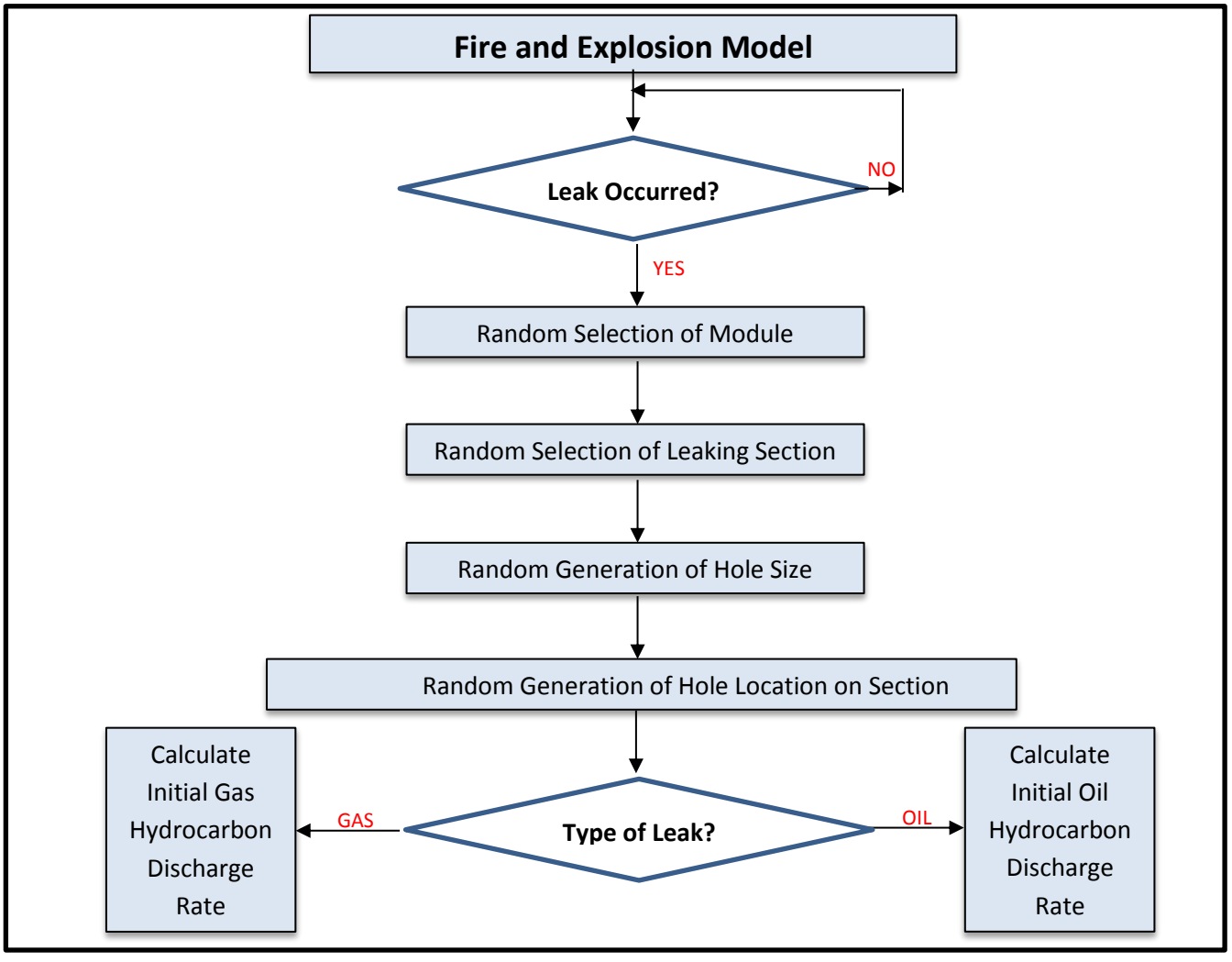


Figure 4-25 Flow Chart showing the Operational Process of Fire and Explosion Model

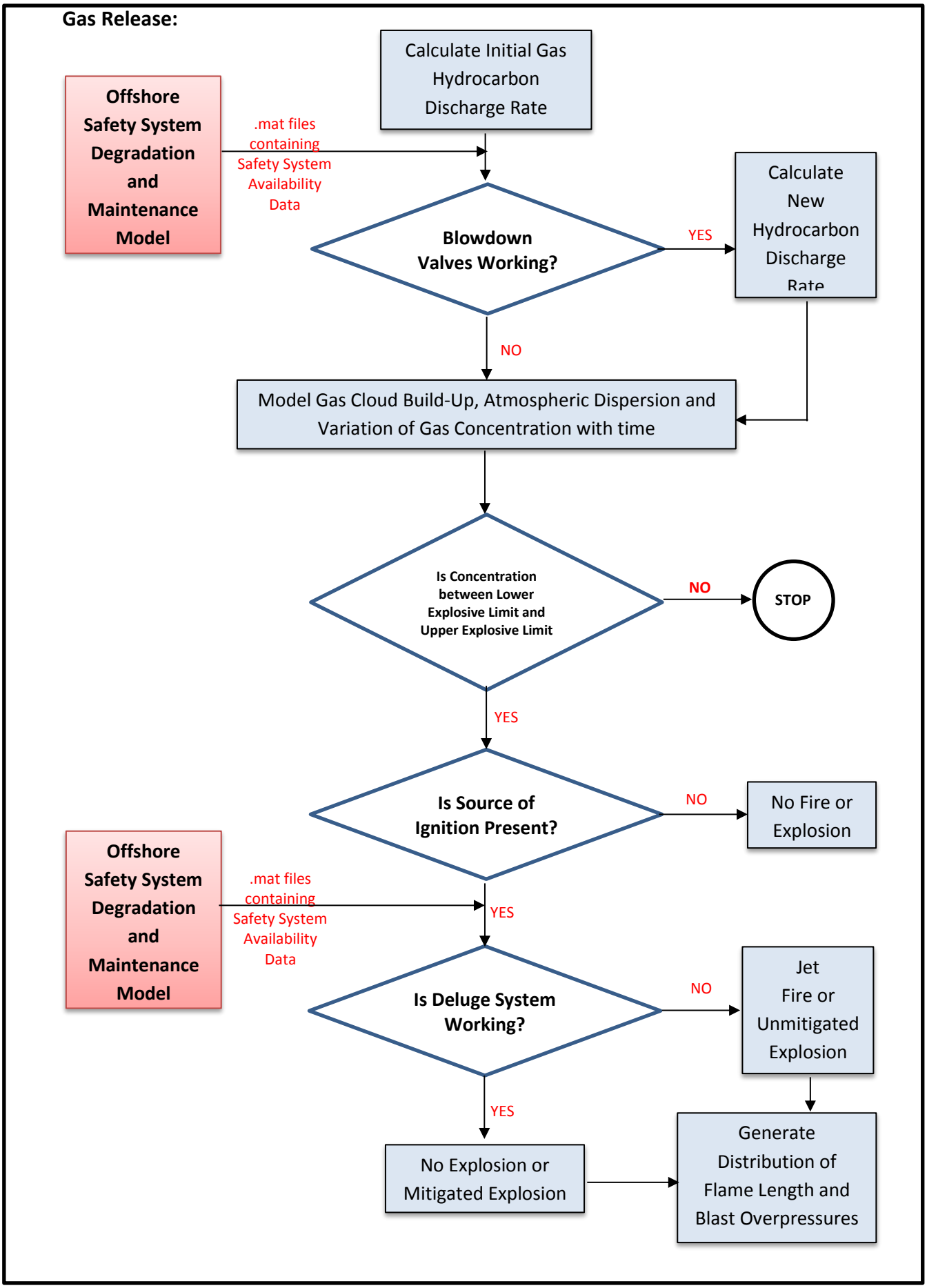


Figure 4-26 Flow Chart showing the Operational Process of Fire and Explosion Model: Gas Release

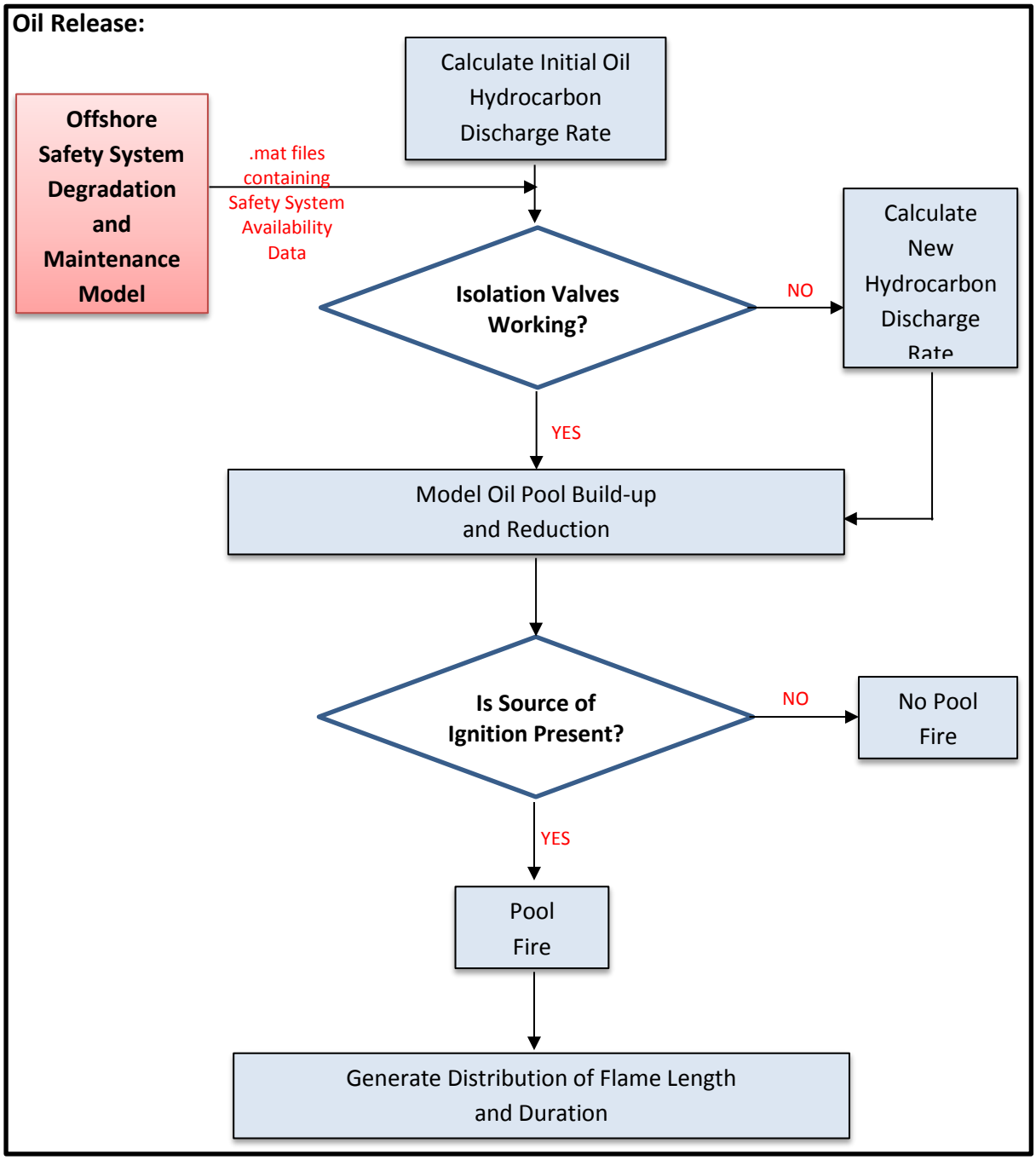


Figure 4-27 Flow Chart showing the Operational Process of the Fire and Explosion Model: Oil Release

4.5.1.1 Modelling the Hydrocarbon Leak

A hydrocarbon leak is expected to develop from a hole on the isolatable process sections located in any of the three modules. During the simulation of the Fire and Explosion Model, the leaking section is selected according to the Frequency of Occurrence (per year) as shown in Table 4-22.

Module	Section Number	Frequency of Occurrence (per year)			
		0-3mm	3-18mm	18-50mm	>50mm
Separation	1	4.42E-02	1.38E-01	2.80E-02	1.08E-02
Separation	2	3.10E-02	9.63E-02	1.95E-02	8.24E-03
Compression	3	4.39E-02	1.35E-01	3.38E-02	7.11E-03
Compression	4	2.82E-02	8.69E-02	2.07E-02	5.16E-03
Compression	5	4.10E-02	1.28E-01	2.82E-02	7.19E-03
Compression	7	5.69E-02	1.80E-01	3.81E-02	9.67E-03
Wellhead	8	3.50E-02	5.45E-02	2.57E-02	3.76E-03
Wellhead	9	1.52E-02	4.60E-02	1.20E-02	2.76E-03
Wellhead	10	4.52E-02	1.11E-02	1.76E-02	1.25E-03

Table 4-22 Hole Size Frequency Distribution (Lewthwaite 2006)

In order to calculate the hydrocarbon discharge rate, it is critical to establish the hole size from which the leak arises. Hence, once it is known which section is leaking, the hole size needs to be determined. There are four possible hole size ranges: 0-3mm, 3-18mm, 18-50mm and >50mm. During the simulation, the range is selected according to the probability of occurrence shown in Table 4-23. Once the range is selected, the specific hole size from this range is randomly sampled from a uniform distribution.

Module	Section Number	Probability of Occurrence			
		0-3mm	3-18mm	18-50mm	>50mm
Separation	1	0.20	0.62	0.13	0.05
Separation	2	0.20	0.62	0.13	0.05
Compression	3	0.20	0.61	0.15	0.03
Compression	4	0.20	0.62	0.15	0.04
Compression	5	0.20	0.63	0.14	0.04
Compression	7	0.20	0.63	0.13	0.03
Wellhead	8	0.29	0.46	0.22	0.03
Wellhead	9	0.20	0.61	0.16	0.04
Wellhead	10	0.60	0.15	0.23	0.02

Table 4-23 Hole Size Probability Distribution

The type of leak (oil, gas or condensate) is dependent on the section that is leaking, the inventory it contains and the location of the hole on the vessel. For example, consider the event where a leak develops in atmospheric separator – section 1. The vessel contains both oil and gas, however, it is unlikely that both would leak at the same time. The initial release is dependent on the location of the hole on the vessel. The height of the oil in the vessel, H_o, is determined as the proportion of the total vessel height, H_v, as shown in Figure 4-28, below.

In this research, H_v and H_O are assumed to be 15 and 8m, respectively. If the hole was to occur above H_O, the release is purely gas. However, if the hole was to occur below H_O, the discharge is initially oil until H_O is reduced to the level of the hole, after which the leak will consist of gas and condensate. The location of the hole is generated by randomly sampling from a uniform distribution.

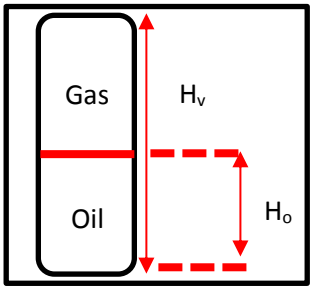


Figure 4-28 Separator Vessel

4.5.1.2 Calculating the Initial Hydrocarbon Discharge Rate

To model the hydrocarbon release, the following assumptions have been made:

1. Before the leak can be detected and isolated, the initial hydrocarbon discharge rate is calculated assuming that the inventory available is infinite and the driving pressure in the leaking section will remain constant.
2. There is no heat input to the system therefore the system temperature changes throughout the duration of the leak.
3. Gas and condensate leak in the same proportions as they exist within the vessel.
4. Gas discharge rate can be calculated by the laws of gas dynamics while the condensate discharge rate can be calculated by assuming that we have a reservoir of ideal incompressible fluid. This means that the gas and condensate have different discharge speeds, however, this gives the correct interpolation as the gas or condensate fractions approach zero.
5. The condensate vaporises immediately on release.
6. The gas and air mix perfectly and instantaneously on release, hence, resulting in uniform concentration.
7. The leak is considered to occur into a fixed specified volume.

4.5.1.2.1 Calculating Discharge Rate of Gas

The mass flow rate of gas, W_g, through a hole of cross-sectional area, A_h, is given as (Lewthwaite *et al.* 2006):

$$\boldsymbol{W_g = \rho_g A_h v_g} \tag{67}$$

where, ρ_g and v_g is the density and discharge speed of gas, respectively.

Using the laws of gas dynamics, the gas discharge rate can then be calculated. By assuming that the gas is a perfect gas, the constant K which is dependent on whether the release is choked or unchoked is calculated by:

$$\boldsymbol{K = \frac{P}{\rho_g{}^{\Upsilon}}} \tag{68}$$

where, P is the upstream pressure and Υ is the ratio of specific heats, C_p/C_v, where C_p is the specific heat capacity at constant pressure (J/Kg K) and C_v is the specific heat capacity at constant volume (J/Kg K).

The discharge speed of the gas is calculated as follows:

$$\boldsymbol{v_g{}^2 = 2\left(\frac{\Upsilon}{\Upsilon - 1}\right)\frac{P}{\rho_g}\left[1 - \frac{P_a}{P}\right]^{\frac{\Upsilon-1}{\Upsilon}}} \tag{69}$$

where, P_a is the ambient pressure (Pa) and the gas discharge rate when the flow is **unchoked** can be calculated as follows:

$$\boldsymbol{W_g = \left(2A_h{}^2\left(\frac{\Upsilon}{\Upsilon - 1}\right)K^{\frac{-1}{\Upsilon}}P_a{}^{\frac{1+\Upsilon}{\Upsilon}}\left[\left(\frac{P_a}{P}\right)^{\frac{1-\Upsilon}{\Upsilon}} - 1\right]\right)^{\frac{1}{2}}} \tag{70}$$

However, if the discharge speed of gas is equal or larger than the speed of sound, the flow becomes choked. The critical pressure ratio can be used as a criterion to declare if the flow is choked or unchoked. For **unchoked** flow, the critical pressure ratio is as follows:

$$\boldsymbol{\frac{P}{P_a} < \left(\frac{\Upsilon + 1}{2}\right)^{\frac{\Upsilon}{\Upsilon-1}}} \tag{71}$$

If the flow is choked, the critical pressure ratio has a maximum value of:

$$\boldsymbol{\left(\frac{2}{1 + \Upsilon}\right)^{\frac{\Upsilon}{\Upsilon-1}}} \tag{72}$$

Hence, the discharge speed of the gas for choked flow is as follows:

$$\boldsymbol{v_{gmax}} = \left(\frac{\mathbf{2}\gamma \boldsymbol{P}}{(\mathbf{1}+\gamma)\boldsymbol{\rho_g}}\right)^{\frac{\mathbf{1}}{\mathbf{2}}} \quad \textbf{(73)}$$

and the gas discharge rate when the flow is **choked** can be calculated as:

$$\boldsymbol{W_g} = \mathbf{A_h}\left(\boldsymbol{P\rho_g}\gamma\left(\frac{\mathbf{2}}{(\mathbf{1}+\gamma)}\right)^{\frac{\mathbf{1}+\gamma}{\gamma-\mathbf{1}}}\right)^{\frac{\mathbf{1}}{\mathbf{2}}} \quad \textbf{(74)}$$

Moreover, the gas discharge rate when the flow is choked is dependent on the gas density, which is assumed to vary during the leak. Hence, the gas discharge rate is re-expressed to remove dependencies on gas density by introducing α:

$$\boldsymbol{W_g} = \frac{\boldsymbol{dM}}{\boldsymbol{dt}} = \boldsymbol{V_g}\ \frac{\boldsymbol{d\rho_g}}{\boldsymbol{dt}} = \mathbf{A_h}\left(\boldsymbol{P\rho_g}\right)^{\frac{\mathbf{1}}{\mathbf{2}}}\boldsymbol{\alpha} \quad \textbf{(75)}$$

where, $\alpha = \left(\gamma\left(\frac{2}{1+\gamma}\right)^{\frac{\gamma+1}{\gamma-1}}\right)^{\frac{1}{2}}$

The change in density with time:

$$\frac{\boldsymbol{d\rho_g}}{\boldsymbol{dt}} = \frac{\mathbf{A_h}\left(\boldsymbol{P\rho_g}\right)^{\frac{\mathbf{1}}{\mathbf{2}}}\boldsymbol{\alpha}}{\boldsymbol{V_g}} = \frac{\mathbf{A_h}\left(\mathbf{K\rho_g}^{\gamma}\boldsymbol{\rho_g}\right)^{\frac{\mathbf{1}}{\mathbf{2}}}\boldsymbol{\alpha}}{\boldsymbol{V_g}} = \frac{\mathbf{A_h}\boldsymbol{K}^{\frac{\mathbf{1}}{\mathbf{2}}}\mathbf{\rho_g}^{\frac{\mathbf{1}+\gamma}{\mathbf{2}}}\boldsymbol{\alpha}}{\boldsymbol{V_g}} \quad \textbf{(76)}$$

where, $\mathrm{P} = \mathrm{K}\rho_g^{\gamma}$. Equation (76) is integrated to obtain the gas density which is then substituted into the gas discharge rate equation. This gives the equation for the gas discharge rate independent of the change in gas density:

$$\boldsymbol{W_g} = \mathbf{A_h}\boldsymbol{K}^{\frac{\mathbf{1}}{\mathbf{2}}}\boldsymbol{\alpha}\left(\frac{\mathbf{1}-\gamma}{\mathbf{2}}\left(\frac{\mathbf{A_h}\boldsymbol{K}^{\frac{\mathbf{1}}{\mathbf{2}}}\boldsymbol{\alpha}\mathrm{t}}{\boldsymbol{V_g}}\right)+\boldsymbol{\rho_g}^{\frac{\mathbf{1}-\gamma}{\mathbf{2}}}\right)^{\frac{\mathbf{1}+\gamma}{\mathbf{1}-\gamma}} \quad \textbf{(77)}$$

4.5.1.2.2 Calculating Discharge Rate of Gas-Condensate Mixture

The average density of the gas-condensate mixture is calculated using the following equation:

$$\boldsymbol{\rho} = \boldsymbol{\beta_g\rho_g} + (\mathbf{1.0}-\boldsymbol{\beta_g})\boldsymbol{\rho_c} \quad \textbf{(78)}$$

where, β_g is the volume concentration of gas in the upstream reservoir and ρ_g and ρ_c are the densities of the gas and condensate, respectively. The mass of the gas-condensate mixture is as follows:

$$\boldsymbol{M = \rho V} \tag{79}$$

The rate of mass discharge is as follows:

$$\frac{\boldsymbol{dM}}{\boldsymbol{dt}} = \boldsymbol{V}\frac{\boldsymbol{d\rho}}{\boldsymbol{dt}} \tag{80}$$

where, V is the volume that is constant as there is no contraction or expansion of the vessel walls.

Hence, the total mass flow rate, W, of the leaking mixture, is calculated as follows:

$$\mathbf{W} = \boldsymbol{\beta_g W_g} + (\mathbf{1.0} - \boldsymbol{\beta_g})\boldsymbol{W_c} \tag{81}$$

where, W_g and W_c is the mass flow rate of gas and condensate, respectively, obtained from the continuity equation:

$$\boldsymbol{W_g = \rho_g A_h v_g} \tag{82}$$

$$\boldsymbol{W_c = \rho_c A_h v_c} \tag{83}$$

where, v_c and v_g are the discharge speeds of gas and condensate, respectively.

Using Bernoulli's equation for an ideal incompressible fluid, the discharge speed of the condensate,v_c, can be calculated. Isentropic flow is calculated using the following equation:

$$\frac{\boldsymbol{P}}{\boldsymbol{\rho_c}} + \frac{\boldsymbol{v_c^2}}{\mathbf{2}} = \boldsymbol{constant} \tag{84}$$

At the point of release, the discharge speed is zero and the pressure is P. Hence, giving the constant term for the previous equation as:

$$\frac{\boldsymbol{P_a}}{\boldsymbol{\rho_c}} + \frac{\boldsymbol{v_c^2}}{\mathbf{2}} = \frac{\boldsymbol{P}}{\boldsymbol{\rho_c}} \tag{85}$$

Thus,

$$\boldsymbol{v_c} = \sqrt{\mathbf{2}\left(\frac{\boldsymbol{P - P_a}}{\boldsymbol{\rho_c}}\right)} \tag{86}$$

and the mass flow rate of the condensate can be calculated as:

$$W_c = \mathbf{A_h}\sqrt{\mathbf{2}\,(\boldsymbol{P - P_a})\boldsymbol{\rho_c}} \tag{87}$$

As the condensate is assumed to evaporate immediately on release to the atmosphere, it is not considered any further. The gas discharge rates for choked and unchoked flows can be calculated using equation (74) and (70), respectively.

However, as it is assumed that there is no input of heat to the system, the system temperature reduces over the duration of the leak. Reduction in system temperature, also results in the reduction of system pressure. During the leak, the ratio of condensate to gas changes due to the evaporation of the condensate as pressure reduces. Due to the change in heat entropy between the two phases, the gas does not behave adiabatically. The total entropy per unit mass is constant. The entropy per unit mass when the two phases are in equilibrium is given as follows:

$$\mathbf{s}_g - \mathbf{s}_c = \frac{\boldsymbol{\lambda}}{\mathbf{T}} \tag{88}$$

where, λ is the latent heat and T is the temperature. The total entropy in the system, s, is give as:

$$\mathbf{m}_g\mathbf{s}_g - \mathbf{m}_c\mathbf{s}_c = \mathbf{Ms} \tag{89}$$

where, m_g and m_c are the masses of gas and condensate, respectively and $M = m_g + m_c$. By manipulating Equations (88) and (89), the following equation is obtained:

$$\mathbf{s}_g = \frac{\boldsymbol{\lambda}}{\mathbf{T}}\left(\frac{\boldsymbol{\rho}_c}{\boldsymbol{\rho}_g}(1 - \boldsymbol{\rho}_g)\right) + \mathbf{s}_c \tag{90}$$

The gas is assumed to be satisfy the equation of a perfect gas:

$$\mathbf{P} = \boldsymbol{\rho}_g\mathbf{RT} \tag{91}$$

or

$$\mathbf{P} = \boldsymbol{\rho}_g{}^{\gamma}\mathbf{e}^{\frac{\mathbf{s}_g - \mathbf{s}_o}{\mathbf{c_v}}} \tag{92}$$

where, R and s_o are constants. The Clausius-Clapyron equation for a two-phase mixture is given as:

$$\frac{\mathbf{dP}}{\mathbf{dT}} = \frac{\boldsymbol{\lambda}}{\mathbf{T}}\left(\frac{1}{\boldsymbol{\rho}_g} - \frac{1}{\boldsymbol{\rho}_c}\right)^{-1} \tag{93}$$

By differentiating equation (91), the change in pressure with respect to time can be calculated as follows:

$$\frac{\mathbf{dP}}{\mathbf{dt}} = \frac{\mathbf{d}\boldsymbol{\rho}_g}{\mathbf{dt}}\mathbf{RT} + \mathbf{R}\boldsymbol{\rho}_g\frac{\mathbf{dT}}{\mathbf{dt}} \tag{94}$$

By substituting equation (94) into (93), the temperature term can be eliminated which leads to the following equation for average density change:

$$\frac{\mathbf{dP}}{\mathbf{dt}} = \frac{\frac{\mathbf{P}}{\rho_g}\frac{\mathbf{d}\rho_g}{\mathbf{dt}}}{\left(\mathbf{1} - \frac{\mathbf{P}}{\boldsymbol{\lambda}}\left(\frac{\mathbf{1}}{\rho_g} - \frac{\mathbf{1}}{\rho_c}\right)\right)} \quad \textbf{(95)}$$

Assuming that ds=0, as the change of entropy was negligible due to no heat transfer, the entropy term is eliminated to obtain a relationship between changes of gas density and mixture density. Differentiating equation (92) leads to:

$$\frac{\mathbf{dP}}{\mathbf{dt}} = \frac{\boldsymbol{\gamma}\mathbf{P}}{\boldsymbol{\rho}_\mathbf{g}}\frac{\mathbf{d}\boldsymbol{\rho}_\mathbf{g}}{\mathbf{dt}} - \frac{\mathbf{P}\boldsymbol{\lambda}\boldsymbol{\rho}_\mathbf{C}}{\mathbf{c_v T}\boldsymbol{\rho}}\frac{\mathbf{d}\boldsymbol{\beta}}{\mathbf{dt}} - \frac{\boldsymbol{\rho}_\mathbf{C}\mathbf{P}\boldsymbol{\lambda}}{\mathbf{c_v T}\boldsymbol{\rho}^\mathbf{2}}(\mathbf{1}-\boldsymbol{\beta})\frac{\mathbf{d}\boldsymbol{\rho}}{\mathbf{dt}} - \frac{\boldsymbol{\rho}_\mathbf{C}\mathbf{P}\boldsymbol{\lambda}}{\mathbf{c_v T}^\mathbf{2}\boldsymbol{\rho}}(\mathbf{1}-\boldsymbol{\beta})\frac{\mathbf{dT}}{\mathbf{dt}} \quad \textbf{(96)}$$

Using thermodynamics, entropy is defined as follows:

$$\mathbf{Tds} = \mathbf{dh} - \frac{\mathbf{dP}}{\boldsymbol{\rho}} \quad \textbf{(97)}$$

where, h is the enthalpy. By substituting ds=0 and $dh=c_pdT$, gives the following equation:

$$\mathbf{c_v}\boldsymbol{\gamma}\boldsymbol{\rho} = \frac{\mathbf{dP}}{\mathbf{dT}} \quad \textbf{(98)}$$

Manipulating the governing equations leads to:

$$\frac{\mathbf{dP}}{\mathbf{dt}}\frac{\boldsymbol{\lambda}}{\mathbf{T}\boldsymbol{\rho}}\left(\frac{1}{\rho_g} - \frac{1}{\rho_c}\right)^{-1} = \frac{\mathbf{d}\boldsymbol{\rho}_\mathbf{g}}{\mathbf{dt}}\left[\frac{\mathbf{P}}{\boldsymbol{\rho}_\mathbf{g}}\left(\mathbf{1} - \frac{\mathbf{P}}{\boldsymbol{\lambda}}\left(\frac{1}{\rho_g} - \frac{1}{\rho_c}\right)\right)^{-1}\left(\frac{\rho c_V}{P} + \frac{\rho_c}{T}(1-\beta_g)\left[\frac{1}{\rho_g} - \frac{1}{\rho_c}\right]\right) - \frac{\mathbf{c_v}\boldsymbol{\gamma}\boldsymbol{\rho}}{\boldsymbol{\rho}_g} - \frac{\boldsymbol{\lambda}\boldsymbol{\beta}_\mathbf{g}\boldsymbol{\rho}_c}{\mathbf{T}(\boldsymbol{\rho}_g - \boldsymbol{\rho}_c)}\right] \quad \textbf{(99)}$$

These equations are then solved numerically using Monte Carlo simulation to provide new proportions and discharge rates at incremented time steps. Iterations stop when the pressure of the leaking section becomes equal to the atmospheric pressure. A time stepping process is critical to calculate the change in gas concentration in the module.

4.5.1.2.3 Calculating Discharge Rate of Oil

An oil leak can occur via two ways: pre and post separation. If the leak occurs pre separation, it is assumed that water will be present in the leaking fluid. The oil discharge rate is then calculated using the following equation:

$$W_0 = \mathbf{A}_h\sqrt{\mathbf{2}\,(\boldsymbol{P} - \boldsymbol{P_a})\boldsymbol{\rho_o}} \quad \textbf{(100)}$$

where, ρ_o is the density of oil. The discharge rate of water can be calculated by substituting the density of water into Equation (100). However, once released, the water is not considered any further.

If the leak occurs post separation, the discharge rate is dependent of the location of the hole on the vessel. As explained earlier, if the hole was located above the height of the oil, H_O, the

release is purely gas. However, if the hole is located below H_O, the discharge is initially oil until H_O is reduced to the level of the hole. Hence, the oil discharge rate equation includes additional pressure due to the oil above the hole:

$$W_0 = \mathbf{A_h}\sqrt{\mathbf{2}\,(\boldsymbol{P} - \boldsymbol{P_a} + \boldsymbol{g\rho_o H_{HEAD}})\boldsymbol{\rho_o}} \quad \textbf{(101)}$$

where, g is the gravitational acceleration and $H_{HEAD} = H_O - H_H$, where H_H is the height of the hole. If the discharge continues after the $H_o < H_H$, then the leak will consist of gas and condensate.

4.5.1.3 Modelling the Activation of Safety Systems

The Fire and Gas Detection system is designed to be activated at gas concentrations in excess of 20% of the LEL of the gas. If the detection system was to become unavailable, it is assumed that the leak would be detected manually in 15 minutes. Once the leak has been detected, the isolation and blowdown valves should activate. Depending on the condition of the isolation and blowdown valves, the valves would activate after a delay time of 10, 20 or 30s.

Following the isolation of a process section, it is assumed that the inventory is no longer infinite. While the equations listed in Section 4.5.1.2 are still used to calculate the hydrocarbon discharge rates, the amount of inventory available will now decrease over time. The subsequent decrease in pressure, density and head of oil would also result in the decrease of discharge rates.

However, if the isolation valves on the leaking section are unavailable, it is assumed that the inventory from the adjacent sections would also contribute to the leak. If the sections are at a higher pressure, it is assumed that the inventory from the higher pressure section contributes to the leak until the pressure is equal to the section with a lower pressure. The two section inventories would then combine, this being a conservative approach to the modelling. The hydrocarbon discharge rate is then recalculated, taking into consideration the increase in inventory. The isolation valves connections are shown in Table 4-2 while the inventory of the connecting sections is outlined in Table 4-1.

Moreover, it is expected that the blowdown valves would also open to depressurise the process section and send some of the unwanted gas to flare. The rate at which the gas is

released when the valve is opened is calculated using equations (67)-(77). However, the area of the leak hole, A_h, in equations (67)-(77), is replaced with the area of the restriction orifice of the blowdown valve, A_{RO}. Table 4-24 outlines the restriction orifice diameters of the blowdown system valves. Failure of the blowdown valves would mean that the process section does not undergo depressurisation and hence the hydrocarbon discharge rate remains unaffected.

Section	Blowdown Valve	Restriction Orifice Diameter (mm)
2	BDV-1	49.3
3	BDV-2/BDV-3	27
4	BDV-4/BDV-5	10.9
5	BDV-6/BDV-7	9.9
6	BDV-8	29
7	BDV-9/BDV-10	11.1
11	BDV-11	16.5
12	BDV-12	17.9

Table 4-24 Restriction orifice diameter of blowdown system valves

Upon detection of a gas release, the deluge system is also activated. However, to develop a fully activated spray system, it is assumed that there is a time delay that is dependent on the following factors: (1) the volume of the dry pipework; (2) the pump system throughput and run up time and; (3) the time taken to open the valves on the deluge skid. In this research, the time delay is assumed to be 30 seconds. Once active and fully functional, there is a possibility that the deluge system could fail. Thus, the characteristics of offshore fires and explosions are influenced by whether ignition occurs during the active deluge period or after a failure (see Sections 4.5.1.7 and 4.5.2.2).

The status of these safety systems and its changes over the simulated time period are extracted from the result files that were produced by the Offshore Safety System Degradation and Maintenance Model. Hence, during the simulation of the Fire and Explosion Model, when a leak occurs, the code reads these results files and extracts the status of the safety system at any required time.

4.5.1.4 Module Ventilation Rate

As mentioned earlier, the modules are assumed to be enclosed, hence, ventilation is provided by a forced, controllable ventilation system. The ventilation rate is measured in air changes per hour (ACPH) and is defined as the number of times per hour a volume of air equal to the volume of the module is replaced. In this model, the ventilation rate is assumed as 50 ACPH. Following detection of the hydrocarbon leak, the ventilation system within the module would shutdown automatically and the natural ventilation would provide a minimal 1 ACPH.

4.5.1.5 Modelling Gas Cloud Build-up, Atmospheric Dispersion and Variation of Gas Concentration

Gas released into the module would form a gas cloud that will vary in size and concentration. A conservative approach is implemented to model the growth of the gas cloud. A worst case scenario is assumed, where the gas does not mix perfectly with the air and the gas cloud grows at uniform stoichiometric concentration, which expands until it fills up the module. If an ignition was to occur under these conditions, the highest overpressure would be generated. However, for an explosion to occur, the gas concentration must be between the lower and upper explosive limits. In addition to this, as the modules are modelled as enclosed, there is no upper limit on the gas concentration within the module. As the amount of ventilation available is limited, it is assumed that when the module volume is filled, the gas concentration can increase above the upper explosive limit and become incombustible. Following detection and isolation, the gas discharge rate, W_g, decreases. If the ventilation rate, V_R, is greater than W_g, the gas cloud concentration is assumed to uniformly decrease until it reaches zero while the volume remains equal to the module volume.

The volume outflow of gas at atmospheric pressure, q_g, is calculated as follows:

$$\boldsymbol{q_g = \frac{W_g}{\rho_a}} \qquad \textbf{(102)}$$

where, ρ_a is the atmospheric density. By taking into consideration, the change in gas volume in the module, V_{gm}, the volume concentration of gas within the module, c_g, can be calculated as follows:

$$\boldsymbol{\frac{dV_{gm}}{dt} = q_g - c_g(q_g + V_r)} \qquad \textbf{(103)}$$

Dividing Equation (103) by the total volume of the module, V_m, gives the following:

$$\frac{dc_g}{dt} + c_g\left(\frac{q_g + V_r}{V_m}\right) = \frac{q_g}{V_m} \quad (104)$$

Once, q_g and V_r are known, c_g can be calculated as a function of time.

The concentration profiles can take three forms:

1. **No Explosive Gas Concentration** – Figure 4-29 demonstrates the scenario where the gas concentration rises to a peak below the explosive region and therefore no explosion occurs.

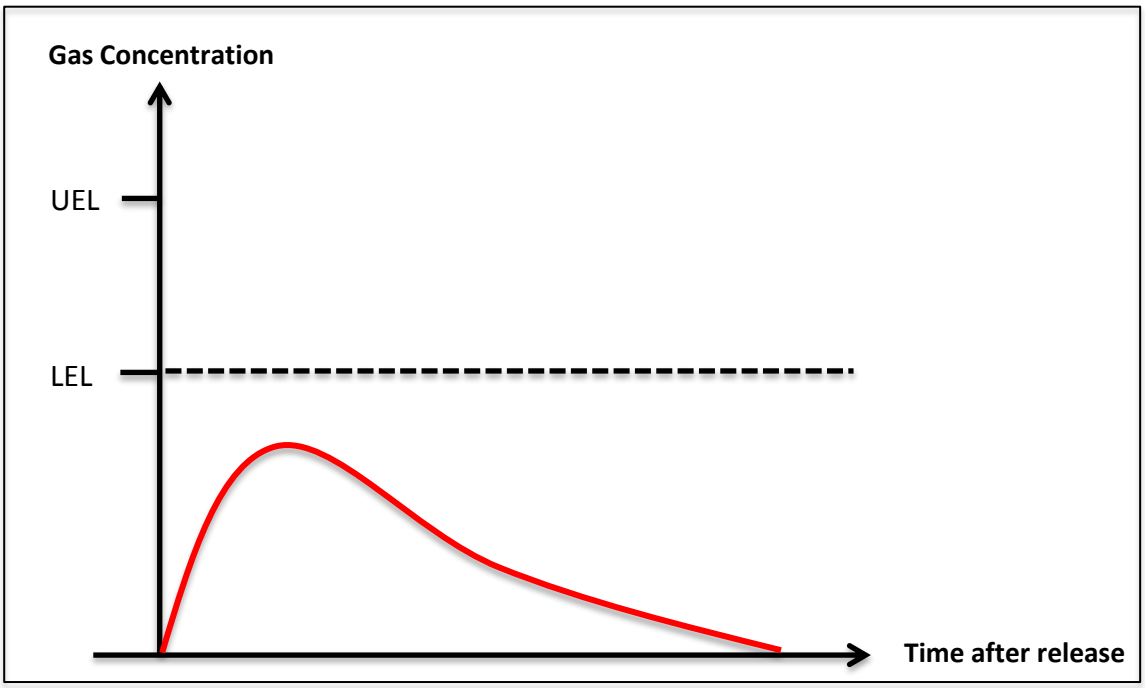


Figure 4-29 No Explosive Gas Concentration

2. **Gas Concentration exceeds the LEL but is below the upper explosive limit (UEL)** – Figure 4-30 demonstrates the scenario when the gas leak occurs at t=0. The gas concentration increases until at t = t_d, the gas concentration reaches the limit, CD, at which the gas detectors are set. At t=t_1, the gas concentration reaches the LEL. When the gas release is exhausted, the module concentration begins to decrease and passes the LEL for the second time at t=t_2. There's the potential for an explosion between t_1 and t_2 when the concentration is between the explosive limits.

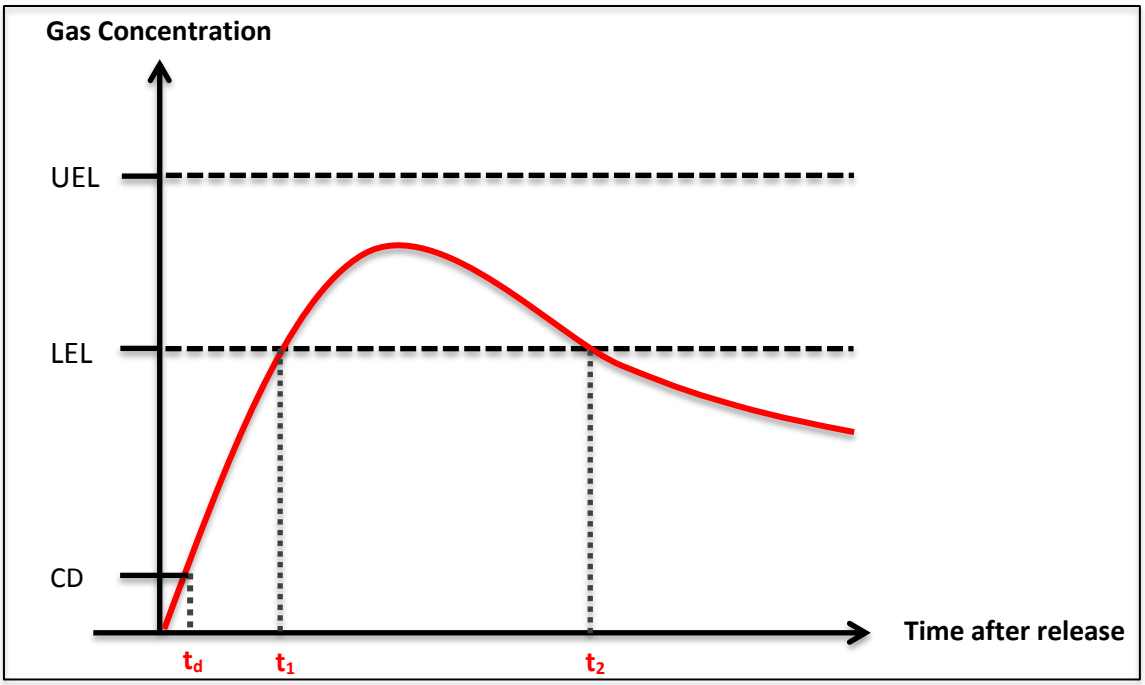


Figure 4-30 Gas Concentration exceeds the LFL but is below the UFL

3. **Gas Concentration exceeds the UEL –** Figure 4-31 demonstrates the scenario when the gas concentration reaches LEL at $t=t_1$ and continues to increase in concentration, hence passing through UEL at $t=t_2$. Following the full release, the concentration decreases and passes through UEL and LEL for the second time at $t=t_3$ and t_4, respectively. Hence, this scenario results in two time periods where the potential for an explosion exists: between t_1 and t_2 and between t_3 and t_4.

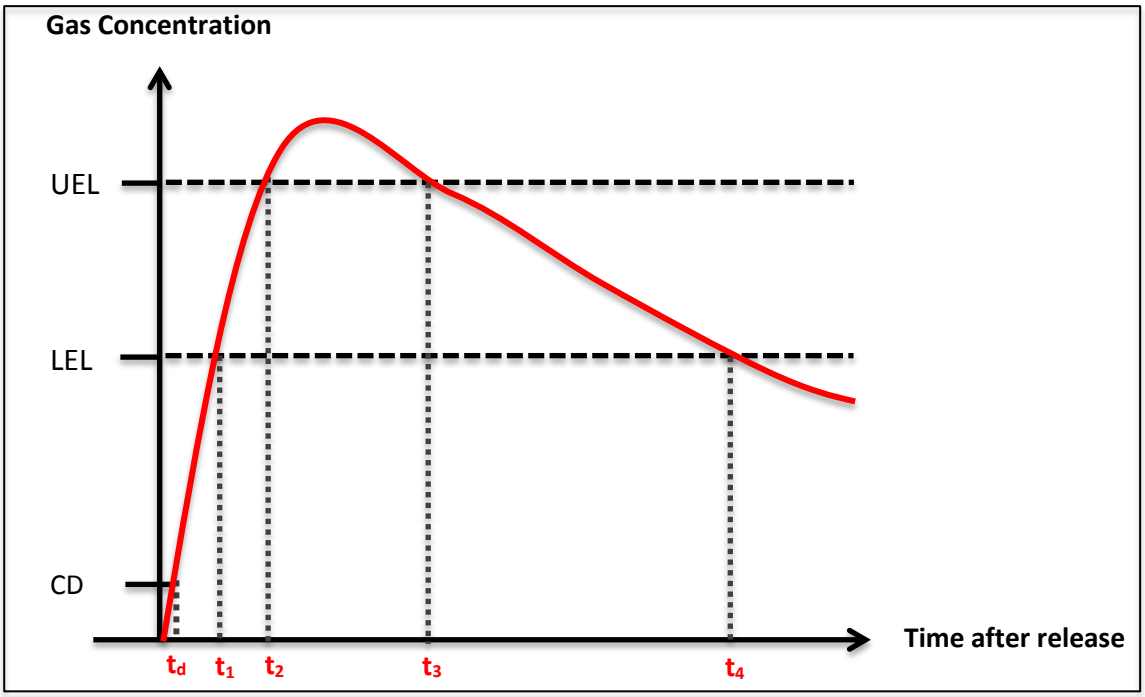


Figure 4-31 Gas Concentration exceeds the UFL

The above scenarios are implemented in the Fire and Explosion Model via conditional loop constructs. For instance, to check whether the gas concentration is between the stated threshold levels, 'else if' statements are used. The times at which the gas concentration reaches CD, LEL and UEL are then saved to an output file.

4.5.1.6 Modelling Oil Pool Build-up and Reduction

If the release is oil, it is assumed to form a pool which expands at a uniform depth of 5cm until the pool area equals to the floor area. The growth of the oil pool is directly proportional to its discharge rate. The area of the oil pool, A_p, is calculated as follows:

$$A_P(t) = \frac{\int_0^{t_{oil}} W_o(t)\,\mathrm{dt}}{\rho_o d_P} \qquad (105)$$

where, d_p is the depth of the oil pool and t_{oil} is the time for the discharge of oil.

Following ignition, the area of the oil pool is considered to increase only if the discharge rate is greater than the mass burn rate of the oil; otherwise the oil pool area will decrease until all oil has been burned. The following equation is used to calculate the decrease in pool area when m' is the mass burn rate per unit area of the oil and t_{burn} is the burn time of the pool fire:

$$\frac{m' \int_0^{t_{burn}} A_P(t)\, dt}{\rho_o d_P} \quad (106)$$

where, m' is the mass burn rate of the oil.

4.5.1.7 Modelling Ignition

Two types of ignition scenarios are modelled; immediate ignition and delayed ignition. Immediate ignition of a gas leak would result in a jet fire while the immediate ignition of an oil pool would result in a pool fire. Delayed ignition of a gas leak would result in an explosion. Moreover, a delayed ignition could occur pre- or post-isolation. Hence, the time of ignition is randomly sampled from an exponential distribution with a mean of 0.07, 0.28 and 0.0028 for immediate ignition, delayed ignition pre-isolation and delayed ignition post-isolation, respectively.

4.5.2 Outputs of the Fire and Explosion Model

4.5.2.1 Frequency of Fires and Explosions

Once, the leak characteristics, gas concentration within the module and the rate of occurrence of an ignition source are established, the frequencies of fires (jet and pool) and explosions can be generated for the same number of simulations as the Offshore Safety System Degradation and Maintenance Model and written to an output file.

4.5.2.2 Frequency of Mitigated and Unmitigated Explosions

Explosions can be further divided into mitigated and unmitigated explosions. This is because explosion characteristics are influenced by whether ignition occurs during the active deluge period or after its failure. Hence, mitigated explosions occur when the deluge system is fully functional, however, one of the following situations may arise:

1. The deluge system is fully functional, however, it fails prior to the gas concentration decreasing below LEL.
2. The deluge system is fully functional throughout the potentially explosive period.

Unmitigated explosions, on the other hand, may occur when the following situations arise:

1. The deluge system fails to activate when a high gas concentration is detected and the gas ignites.

2. The deluge system is activated but the gas ignites during the time taken to get the water spray to a fully functional state.
3. The deluge system is activated and fully functional, however, it fails to maintain the water spray for the duration of the explosive gas concentration and the gas ignites.

Once again, the above scenarios are modelled in the Fire and Explosion Model using conditional loop constructs such as 'if else' statements. The availability of the deluge system is obtained from analysing the .mat files generated from simulating the Offshore Safety System Degradation and Maintenance Model.

4.5.2.3 Distribution of Explosions Overpressures

The magnitude of the explosion is measured in terms of the overpressures generated. Blast Overpressures can be calculated using the following equation:

$$\boldsymbol{Opr = Opr_{MAX} e^{\left(A\left(\frac{c_g}{c_S}-2B+1\right)\left(\frac{c_g}{c_S}-1\right)\right)F_C}} \quad \textbf{(107)}$$

where, Opr_{MAX} is the maximum value the overpressure can be, c_g is gas concentration, c_s is the stoichiometric gas concentration, A and B are constants and F_c is the fraction of the module occupied by the gas cloud. These parameters are dependent on the availability of the deluge system and ignition location. However, in an enclosed module, the maximum overpressure generated is considered to be independent of the ignition location. Hence, enclosed modules only require one maximum overpressure, which is assumed to be 8 bar. The overpressure data assumed in this research is outlined in Table 4-25.

Overpressure Data		Units
Stoichiometric Gas Concentration	8.88	%
A – Deluge Inactive	-19.6930	
B – Deluge Inactive	1.0563	
Maximum Overpressure when Deluge Inactive	8.0	bar
A – Deluge Active	-18.2150	
B – Deluge Active	1.0070	
Maximum Overpressure when Deluge Active	0.32	bar

Table 4-25 Overpressure Data

When calculating the overpressure distribution resulting from an explosion, the explosive range between the flammable limits was split into bands: 5-6%, 6-7%, 7-8%, 8-9%, 9-10%, 10-11%, 11-12%, 12-13%, 13-14% and 14-15%. If ignition occurs when the gas concentration is

between any particular band, the proportion of the times that an explosion occurs is written to a text file.

4.5.2.4 Distribution of Flame Length of Jet Fires and Pool Fires

The magnitude of a jet fire is measured in terms of the flame length generated. In this research, the shape of a jet flame is assumed to be conical, hence, the length of the flame, L_{JET}, is calculated using the equation proposed by Considine & Grint (1985):

$$L_{JET} = 9.1 W_g{}^{0.5} \quad \textbf{(108)}$$

If the initial flame length is below 2m, it is assumed that the fire has not established and is omitted. The severity of the jet fire is characterised by the duration for which the flame length exceeds 2m. After isolation, the flame length of the jet fire is expected to decrease due to a decreasing gas discharge rate or due to the mitigating effects of the deluge system.

Similarly, the magnitude of the pool fire is measured in terms of the flame length generated. In this research, the shape of the pool flame is assumed to be cylindrical. The length of the flame, L_{POOL}, is calculated using the equation proposed by Pritchard & Binding (1993):

$$\frac{L_{POOL}}{D_P} = 55 u^{-0.03} \left[\frac{m'}{\rho_{air} \sqrt{g D_P}} \right]^{0.305} \quad \textbf{(109)}$$

If the initial flame length is below 2m, it is assumed that the fire has not established and is omitted. The severity of the pool fire is characterised by the duration for which the flame length exceeds 2m.

4.6 Summary

This chapter outlines the Platform Safety Model that has been developed to predict the costs, risks and service reliability of any given asset management policy for an offshore oil and gas installation. The model is implemented using standard PNs with high level extensions. High level extensions increase the ability of standard PNs to model complex component/system behaviour as well as a variety of different maintenance options that may be applied to offshore oil and gas assets. The Platform Safety Model is further divided into two sub models that work in conjunction with one another: (1) Offshore Safety System Degradation and Maintenance Model and (2) Offshore Fire and Explosion Model.

The Offshore Safety System Degradation and Maintenance Model models degradation, failure, inspection, and maintenance experienced by the different components of the offshore safety systems, i.e. fire and gas detection system, process isolation, process blowdown and deluge. In order to study the degradation and failure process of components in the safety systems, the condition states in which these components reside in throughout their lifecycle are defined using ISO standards or engineering judgement in the event that data is unavailable. The component life cycle generally begins in new/normal working condition. Over time, due to degradation mechanisms such as wear and corrosion, the component degrades and the level of degradation is revealed via an inspection. If the component is revealed to be in a degraded state, maintenance is performed to restore the component back to new/normal working condition. If the component is revealed to be in a functional failure state, the component is replaced and restored back to new/normal working condition. The degradation process of a component is assumed to be independent, i.e. it is not affected by the state of other components. Spurious failures have also been considered within the Offshore Safety System Degradation and Maintenance Model.

Each component subnet records statistics such as the amount of time the component resides in different condition states, the number of times the component has been subjected to minor or major repair, the total number of replacements, and the cost of preventive or corrective maintenance. The Offshore Safety System Degradation and Maintenance model also takes into consideration the effect of opportunistic maintenance, such that when

maintenance is being performed on one component, the other components that are part of the same system are maintained at the same time.

The Safety System Degradation and Maintenance PN model is implemented using a C++ code which is then solved using a Monte-Carlo simulation method. A number of simulations are performed and information such as the number of times a place of interest is marked with a token and the duration that the token resides in this particular place are extracted. After each simulation run, the data is saved to a results file. Once the data is considered to have converged, the result files are analysed using MATLAB software to produce statistics such as the probability of the system being in any of the condition states, the total number of component replacements over the system lifetime, the total number of maintenance interventions carried out on each component and the system availability. By assigning unit costs for the different types of maintenance activities, the costs of performing inspection and maintenance on offshore safety systems can also be estimated.

The Offshore Fire and Explosion Model is then used to model the occurrence of a hydrocarbon leak from a process vessel located within the three main modules; wellhead, separation and compression, of an offshore installation. The model utilises fluid flow modelling to calculate parameters such as the hydrocarbon discharge rate, gas cloud build-up and dispersion, oil-pool build-up and reduction. These parameters can then be used to predict the intensity of the fires and explosions in terms of the flame length produced in the event of a fire and the overpressures generated in the event of an explosion. Once the frequencies of fires and explosions are determined for a given asset management strategy, the optimal asset management strategy for the offshore safety systems can be determined which reduce the risks to an acceptable risk level, as shown in Chapter 6.

Chapter 5 -Platform Safety Model Application

5.1 Simulation of Offshore Safety Systems Degradation and Maintenance Model

A Petri Net has been developed to model the change in condition states of the four offshore safety systems, i.e. fire and gas detection system, blowdown valves, isolation valves and deluge system, and their components. For many stochastic processes modelled in the net, the changes occur at random times. Simulation of the Petri Net model is performed to investigate the state changes in the system and their respective times are recorded. As an asset management tool, the model can be used for multiple purposes, since it calculates a range of statistics such as system availability and the operational costs associated with implementing different asset maintenance strategies. These statistics are beneficial to offshore asset operations managers as they can be used to predict the amount of work necessary to ensure the required availability of the safety systems and hence the expected costs, so that they can allocate resources and budget accordingly. Consequently, the asset management system supports companies to make decisions with regards to choosing the optimal inspection, maintenance and repair strategy to achieve the desired balance of cost, risk and performance, as shown in Chapter 6.

5.1.1 Simulation Time

As mentioned in Chapter 1, offshore oil and gas installations have a service life of around 25 years. However, taking into consideration the recent changes in economic conditions, and an increase in oil and gas recovery possibilities, operators want to continue exploiting oil and gas reservoir fields and hence use these installations beyond their 25-year designed lifecycle instead of investing in a new one. As a result, these installations are expected to produce hydrocarbons 10 years beyond their original design life. Hence, to evaluate the performance of an offshore installation for extended life, it is necessary to simulate the model for a longer lifetime period. The model is simulated to predict the condition of offshore safety systems over a 35-year lifetime period. Moreover, as the lifetime of most offshore safety system components are typically between 4 to 5 years, this timeframe allows us to witness the entire lifecycle of the offshore safety systems on an offshore oil and gas installation.

5.1.2 Monte Carlo Sampling

Sampling from distributions is required for all stochastic transitions (Le and Andrews 2015b). For each simulation, the firing times of stochastically timed transitions are randomly sampled from the appropriate statistical distributions as described in Section 2.6.5.4, and the tokens are moved around the net accordingly until the prescribed lifetime of the system is reached. This entire process is repeated until the statistics that are collected converge.

5.1.3 Convergence Analysis

With Monte Carlo simulation, the accuracy of the results increases as the number of simulations performed increases. However, running a large number of simulations can significantly increase computational time. Convergence is achieved when running further simulations does not change the results significantly. Thus, by setting a threshold level of 1%, convergence is achieved by running fewer simulations than expected.

5.1.4 Output File

The results of each simulation is recorded to a .mat file. The results include the number of times a particular place is occupied or the amount of time a token resides in a particular place. The advantage of simulating Petri Nets over existing techniques is that a vast amount of performance statistics associated to the different components of the offshore safety systems can be generated. Three key component performance statistics that can be generated from the simulation of Petri Net model include:

1. **Condition Prediction:**
    - Mean time a component resides in any of the condition states
2. **Maintenance Prediction**
    - Number of Component Maintenance Interventions per lifetime
3. **Failure Prediction:**
    - Number of Component Failures per lifetime

These component statistics are then combined to generate performance statistics for their respective safety system. System performance statistics that can be obtained from the Petri Net model simulation include:

1. **System Prediction:**

- Mean time system resides in any of the condition states
- Subsystem Contribution to the Total System Downtime
- Component Contribution to the Total Subsystem Downtime
- System Availability

By generating the number of component interventions and failures, the following cost statistics can be calculated:

1. **Maintenance and Failure Cost Prediction:**
    - Cost of Preventive Maintenance
    - Cost of Corrective Maintenance
2. **Component Operational Cost Prediction**
3. **System Operational Cost Prediction**

Cost statistics are annualised to generate yearly summaries of the statistics for each component and their respective system. As a result, the change in values over the entire lifecycle of the offshore oil and gas installation can be analysed.

The Offshore Fire and Explosion model can then be used to generate the following statistics:

1. **Safety Prediction**
    - Frequency of the explosions, jet fires and pool fires in each module
    - Frequency of explosions, jet fires and pool fires from leaks in sections of each module
    - Distribution of explosion overpressures for each module
    - Distribution of flame lengths of jet fires and pool fires for each module
    - Duration of jet fires and pool fires for each module

This data can be used to reassess the offshore oil and gas installations' safety against fires and explosions. Changes to the safety regulatory regime can be implemented to reduce the risk level of the installation. Furthermore, the data can be used to rank the importance of the different safety systems. For instance, varying the degradation and failure rates of a system would reveal whether the system has an important effect on risks. If it does, better inspection and maintenance can be implemented to improve the reliability of the system and hence reduce the risks of fires and explosions.

5.2 Application of the Offshore Safety System Degradation and Maintenance Model

In the following sections, results obtained from simulating the Petri Net model have been presented. The input parameters of the model are the same as outlined in Chapter 4 – Section 4.4.

5.2.1 Component Analysis

5.2.1.1 Component Condition Prediction

The duration a component spends in each condition state is recorded for each simulation run. As the simulations progress, a mean time of residing in each condition is estimated. Figure 5-1 shows the convergence of the mean time of the submerged lift pump being in the new condition state over the 35-year prediction period, when a strategy of repair as soon as component is revealed to be in a state where repair is required, i.e. **Strategy 1,** is adopted.

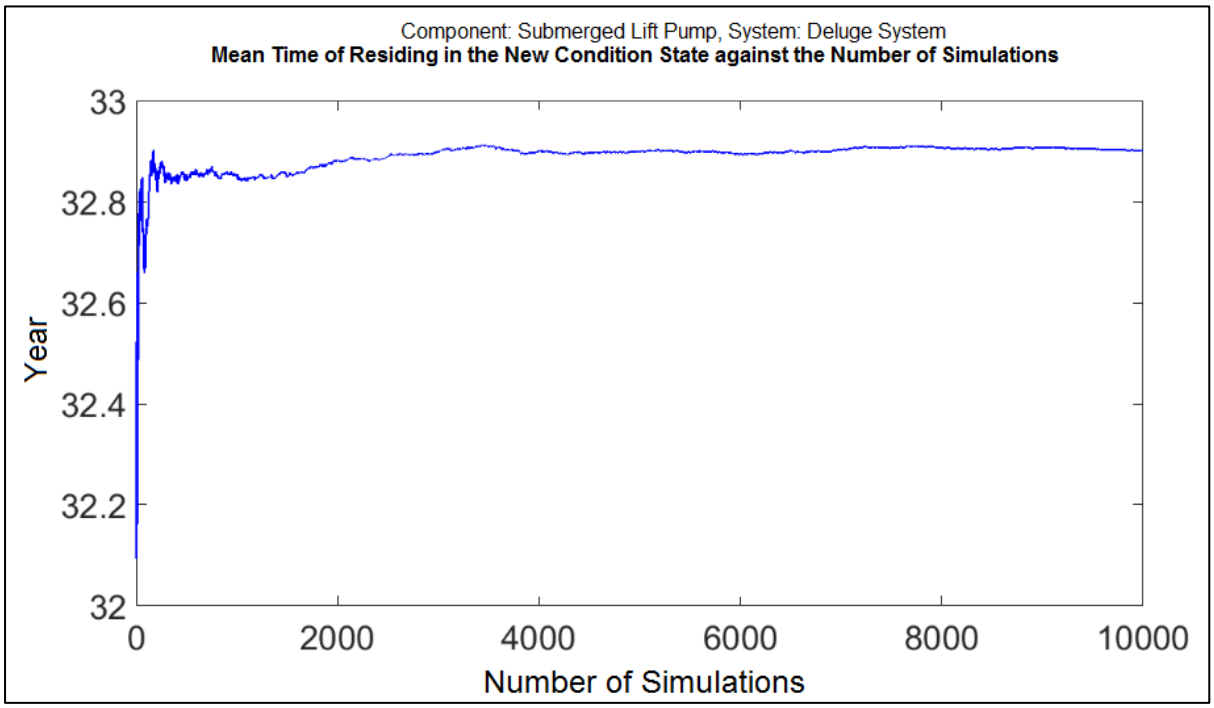


Figure 5-1 Convergence of Mean Time of Residing in the New Condition State for the Submerged Lift Pump

For **Strategy 1**, the results show that the mean time of the submerged lift pump residing in the 'New Working' state (P_1) is expected to be around 32.9 years over the 35 year simulation period. The component spends the remaining 1.23 years in the 'Degraded' state (P_2), 0.03 years in the 'Severely Degraded' state (P_3) and 0.84 years in the 'Functional Failure' state (P_4).

For 10,000 simulations carried out, it can be seen that, for the component, the convergence was achieved around 7000 simulations.

Figure 5-2 shows the probability of being in each condition state over the 35-year prediction period for 10,000 simulations when a strategy of repair as soon as component is revealed to be in a state where repair is required, i.e. **Strategy 1**, is adopted.

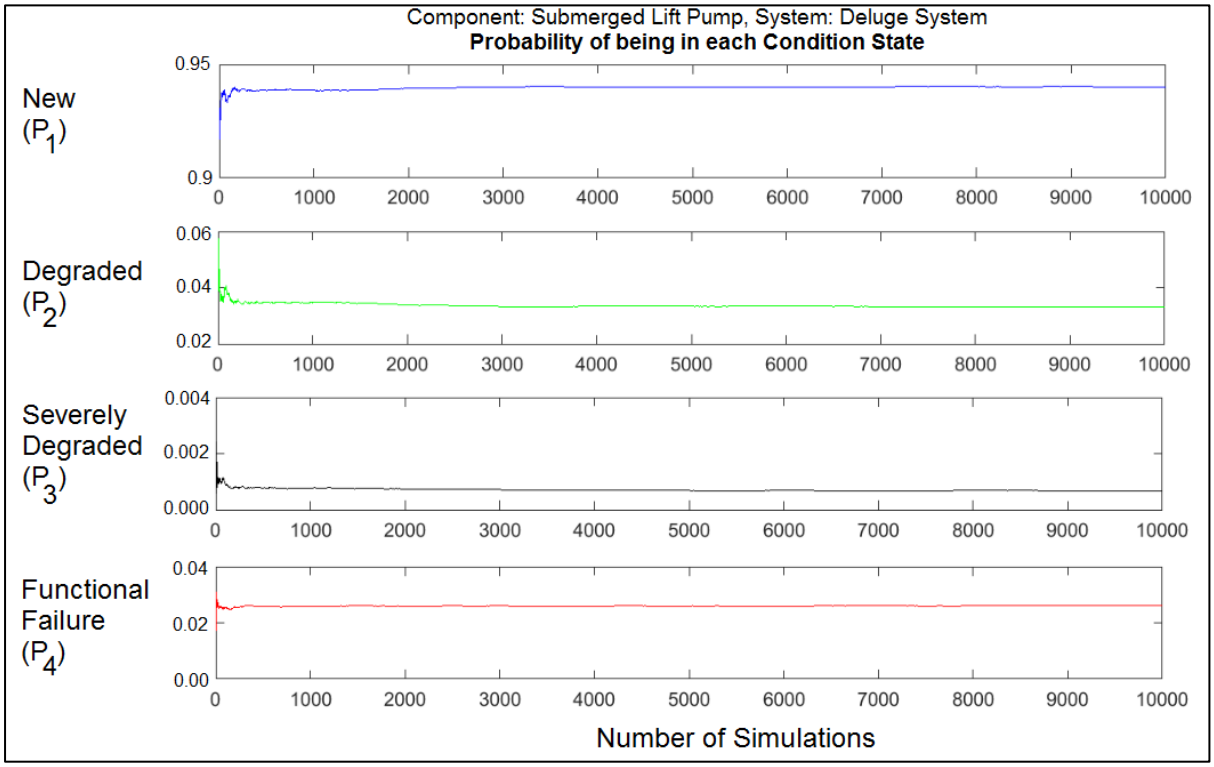


Figure 5-2 Convergence of Probability of being in each condition state over 35 years

The probability of being in any condition state is directly proportional to the time the component spends in that condition state. For **Strategy 1**, the probability of the Submerged Lift Pump being in 'New Working' state (P1) is around 94%, 3.51% in the 'Degraded' state (P_2), 0.09% in the 'Severely Degraded' state (P_3) and 2.4% in the 'Functional Failure' state (P_4). On average, since the probability of residing in 'Severely Degraded' state is less than the probability of residing in 'Functional Failure' state, it suggests that once in 'Severely Degraded' state, the component degrades quickly to 'Functional Failure' state.

Moreover, the probability of a component being in each condition state during every year can be obtained. As a result, the change in submerged lift pump condition at the end of each year of the 35-year prediction period can be illustrated as shown in Figure 5-3.

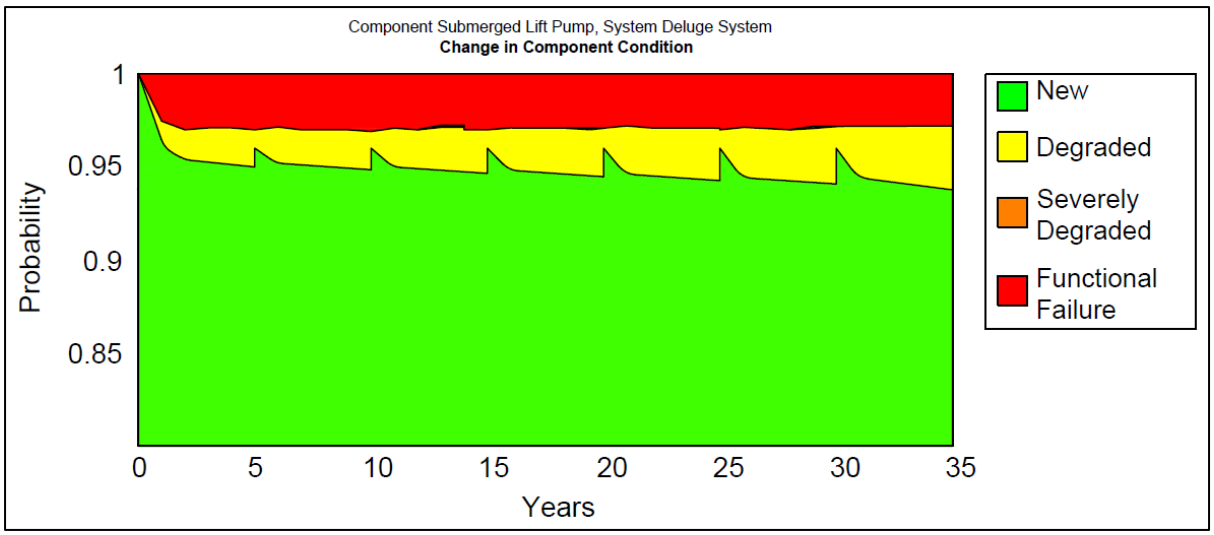


Figure 5-3 Condition distribution for the Submerged Lift Pump

At the start of each simulation, the submerged lift pump starts in 'New Working' state, hence, the probability of the submerged lift pump being in this condition is 1 at year 0. However, a spurious failure may occur almost instantly which explains why the submerged lift pump condition may change almost immediately from year 0 to year 1. During years 1 to 5, the pump ages and its condition degrades. Hence, the probability of it being in a 'Functional Failure' state increases. At the end of year 5, the safety systems undergo shutdown maintenance and the submerged lift pump is replaced regardless of its current condition. Hence, the probability of it being in 'New Working' state increases. A similar trend is experienced every 5 years as the system undergoes shutdown maintenance.

Component condition is revealed only when an inspection is carried out, which occurs every 3 months. Depending on the condition of the component, preventive or corrective maintenance work is carried out in order to restore it back to the 'new working' state as soon as possible. Hence, the probability of the component being in each condition state depends on the frequency of the inspection and mean time to allocate resources for repair.

Moreover, by collating the results of all 10,000 simulations, statistics describing the maximum, minimum, average and standard deviation of the time that the component spends in each condition state can be obtained. Statistics such as standard deviation allows us to measure the spread of the data around the mean value. A small standard deviation means that the dataset is quite close to the mean. Hence, the dataset can be considered reliable. Table 5-1 shows the

summary of the statistics obtained for all deluge system components for the 35-year prediction period. Note that in Table 5-1, the submerged lift pump, booster pump, air release valve, deluge valve, solenoid valve, deluge nozzle and fire and gas logic sensors have been abbreviated as SLP, BP, ARV, DV, SV, DN and FGS, respectively.

Condition States	Duration Spent in Condition State	SLP	BP	ARV	DV	SV	DN	FGS
New Working or Normal Opening Time	Minimum Years Achieved	24.827	22.571	20.704	20.939	20.959	30.861	31.811
	Maximum Years Achieved	34.697	34.759	34.613	34.414	34.442	33.525	34.908
	Average	32.901	32.950	30.925	30.600	30.617	32.695	33.587
	Standard deviation	0.976	1.009	1.585	1.746	1.697	0.365	0.469
Degraded or Degraded Opening Time	Minimum Years Achieved	0.000	0.000	0.226	0.435	0.321	N/A	N/A
	Maximum Years Achieved	9.892	11.636	13.476	13.460	13.513	N/A	N/A
	Average	1.162	1.216	3.466	3.701	3.680	N/A	N/A
	Standard deviation	0.973	1.008	1.506	1.650	1.605	N/A	N/A
Severely Degraded or Slow Opening Time	Minimum Years Achieved	0.000	0.000	0.000	0.000	0.000	N/A	N/A
	Maximum Years Achieved	0.537	0.608	1.090	1.349	1.364	N/A	N/A
	Average	0.024	0.026	0.294	0.393	0.395	N/A	N/A
	Standard deviation	0.056	0.058	0.155	0.182	0.183	N/A	N/A
Functional Failure	Minimum Years Achieved	0.017	0.017	0.017	0.017	0.018	1.475	0.092
	Maximum Years Achieved	2.522	2.493	4.242	4.659	4.438	4.139	3.189
	Average	0.913	0.808	0.315	0.307	0.308	2.305	1.413
	Standard deviation	0.379	0.355	0.212	0.212	0.213	0.365	0.469

Table 5-1 Duration (years) spent in each condition state by each of the deluge system components

Components such as the deluge nozzles and fire and gas logic sensors do not undergo degradation and are simply considered to be either in a “working” or “failed” state. Hence, only the duration spent in “new working” and “functional failure” states have been accounted for. An example pdf for the duration spent in each condition state by the SLP is shown in Figures 5-4 to 5-7, below.

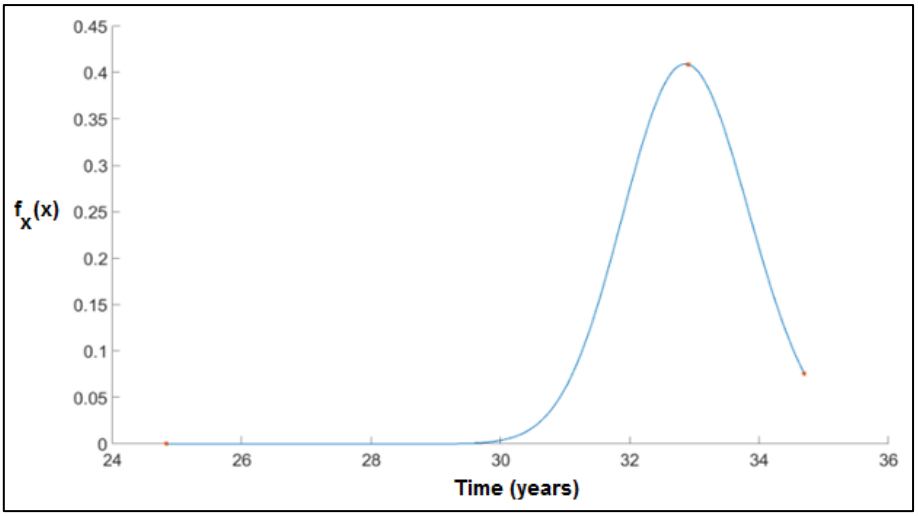


Figure 5-4 Negatively Skewed Lognormal Distribution for the duration spent in New Working State by the SLP

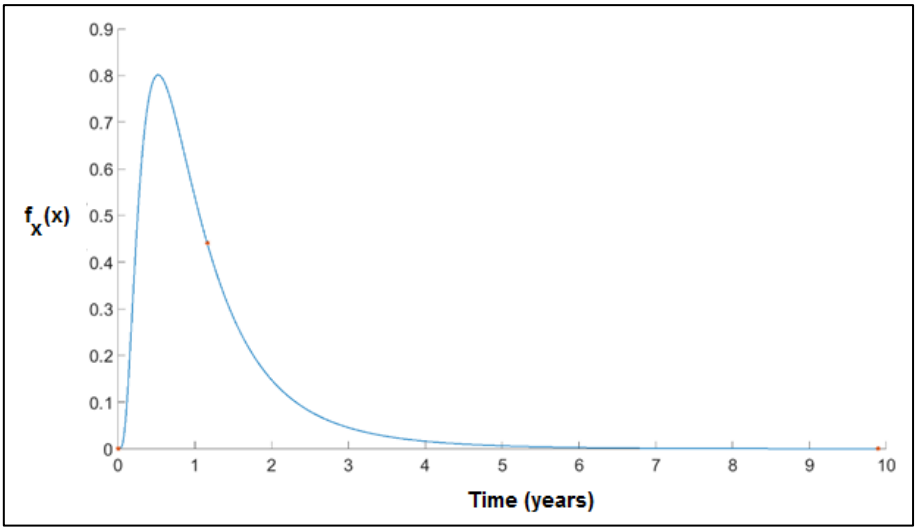


Figure 5-5 Positively Skewed Lognormal Distribution for the duration spent in Degraded State by the SLP

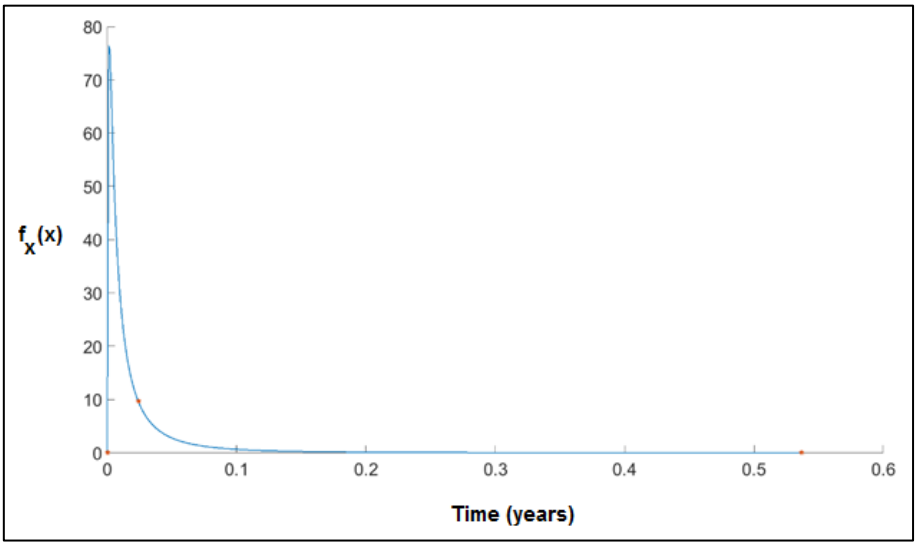


Figure 5-6 Positively Skewed Lognormal Distribution for the duration spent in Severely Degraded State by the SLP

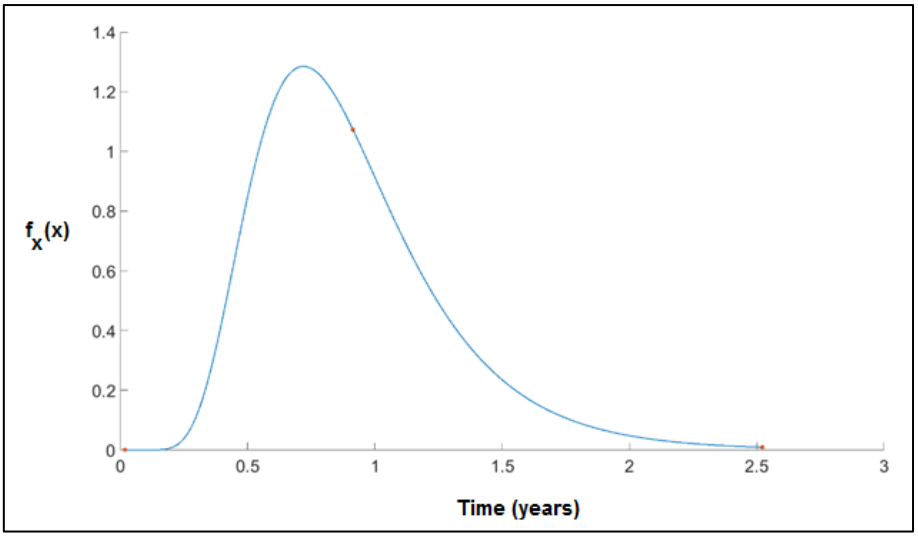


Figure 5-7 Positively Skewed Lognormal Distribution for the duration spent in Functional Failure State by the SLP

In summary, the predictions outlined in this section are useful to offshore asset operations managers as they allow them to evaluate the effectiveness of different inspection and maintenance strategies in terms of component performance.

5.2.1.2 Component Maintenance and Failure Prediction

Each component subnet contains a place that records the total number of interventions (minor PM, major PM and CM) it undergoes. Hence, the average number of interventions per year can also be examined as shown in Figure 5-8. For 10,000 simulations carried out, it can be seen that after the initial fluctuations convergence is achieved at around 6000 simulations. Figure 5-8 also shows that under **Strategy 1**, the submerged lift pump requires an average of 0.185 interventions per year.

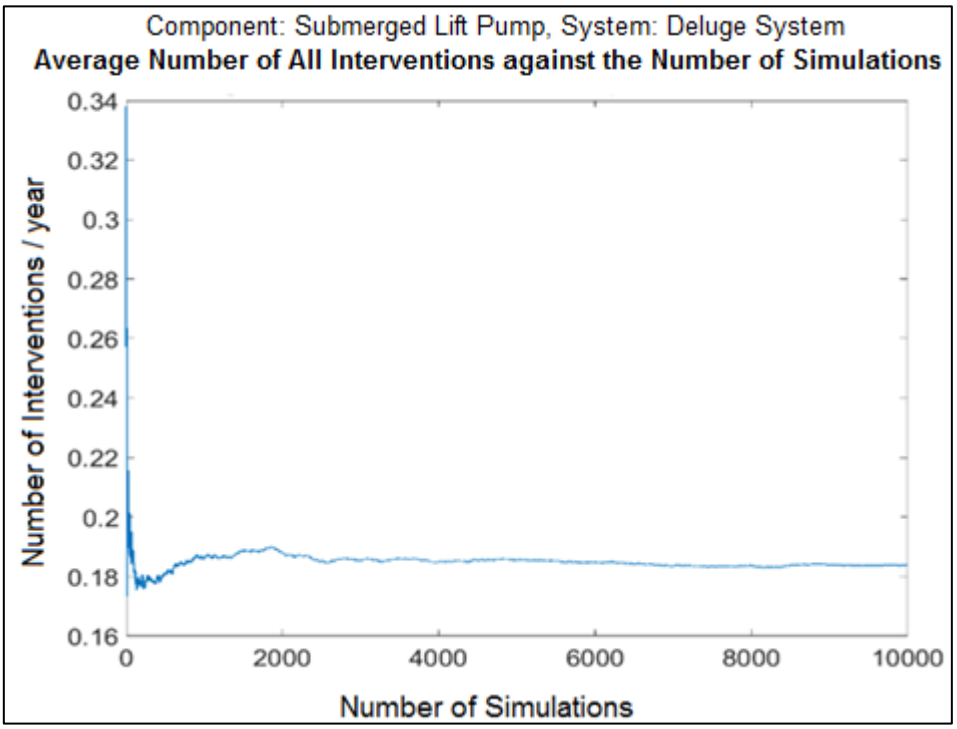


Figure 5-8 Convergence of Average Number of Interventions for the Submerged Lift Pump

Moreover, statistics that describe the expected number of interventions (minor PM, major PM and CM) that a component undergoes up to the end of the 35 year prediction period can also be recorded as shown in Table 5-2. The cost impact of managing asset ageing and extending the anticipated service life of assets is a business reality, requiring the allocation of sufficient resources to manage asset ageing and life extension related activities. The results presented in Table 5-2 can be used by offshore asset operations' managers to predict the expected maintenance costs under a given asset management strategy. Hence, it can be used to assist the decision making process in resource and budget allocation for the entire lifecycle of the platform, as well as its life extension period.

Intervention Type		SLP	BP	ARV	DV	SV	DN	FGS
Minor PM	Minimum Number Experienced	9	9	21	8	8	N/A	N/A
	Maximum Number Experienced	37	37	80	50	48	N/A	N/A
	Mean	22.48	22.45	49.46	25.68	25.77	N/A	N/A
	Standard Deviation	3.73	3.69	7.27	5.33	5.35	N/A	N/A
Major PM	Minimum Number Experienced	0	0	0	0	0	N/A	N/A
	Maximum Number Experienced	7	6	13	11	10	N/A	N/A
	Mean	0.71	0.78	3.90	2.67	2.67	N/A	N/A
	Standard Deviation	0.15	0.91	1.99	1.64	1.64	N/A	N/A
CM	Minimum Number Experienced	36	33	47	17	17	41	10
	Maximum Number Experienced	71	67	92	48	46	73	50
	Mean	51.22	48.19	66.56	30.44	30.60	55.23	27.51
	Standard Deviation	4.95	4.67	6.26	4.13	4.09	4.28	5.05

Table 5-2 Statistics on the expected number of maintenance interventions for each component of the Deluge System up to the end of Year 35

Components such as the deluge nozzle and fire and gas logic sensors do not undergo degradation and are simply considered to be either in a “working” or “failed” state. Hence, no PM has been accounted for these components. Meanwhile, all other components of the deluge system are regularly inspected for degradation. Minor or major PM is performed as soon as the ‘degraded’ or ‘severely degraded’ condition state is revealed. There are many benefits of PM. It increases the margin of safety by keeping the components in optimum condition with the aim of reducing or eliminating unplanned downtime. The lower the threshold value at which maintenance is performed, the lower the risk of component encountering a ‘functional failure’ state. Thus, avoiding unnecessary service disruption as well as preventing future unsafe events.

Based on Table 5-2, the air release valve undergoes the maximum number of minor PM work. The ARV opening time is likely to degrade over time due to exposure to sea water which is highly corrosive in nature. Hence, the ARV needs frequent intervention to restore its performance; measured in terms of opening time. Thus, minor PM work is required to repair any wear and restore it back to normal condition. Additionally, as a high number of minor PM work is performed on the ARV, the component is less likely to reach ‘severely degraded’ state,

hence, it does not require as much major PM work. However, once in the severely degraded state, due to the degradation rate and delay in inspection, the ARV is more likely to reach the 'functional failure' state. Hence, the component experiences a significant number of replacements compared to other components of the deluge system. Moreover, the component is also likely to experience a significant number of spurious failures.

On the other hand, the submerged lift pump and booster pump undergo the least amount of minor PM work compared to the other wear-out components, which includes; the air release valve, deluge valve and solenoid valve. This can be due to the degradation rate of the components which is quite low in comparison to the other wear-out components. Hence, they are less likely to reach a state that requires minor PM.

Figure 5-9 shows the cumulative number of maintenance interventions (minor PM, major PM and CM) for each component of the deluge system every 5 years.

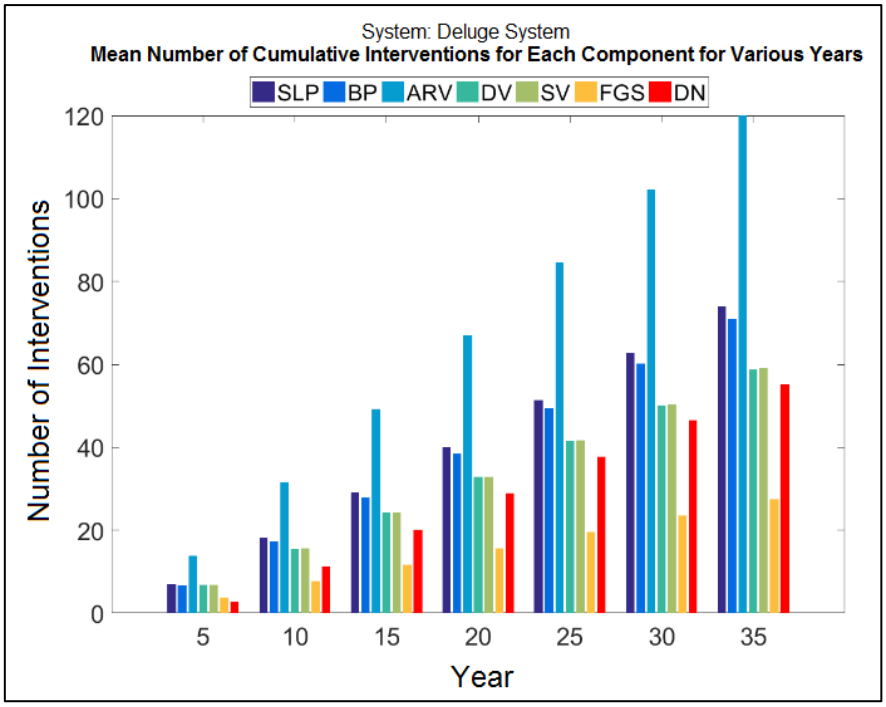


Figure 5-9 Cumulative Number of Interventions for each component of the Deluge System

Based on Figure 5-9, the air release valve is the component that undergoes the most amount of interventions while the fire and gas logic sensor undergoes the least amount of interventions. As explained earlier, the air release valve requires frequent intervention to restore its performance that may be affected as a result of corrosion. The fire and gas logic sensor, on the other hand, does not undergo minor or major PM work, hence the number of

interventions are mainly due to the number of replacements it undergoes. Thus, the number of interventions compared to the other components is relatively low.

Figure 5-10 shows the cumulative number of failures for each component of the deluge system for various years.

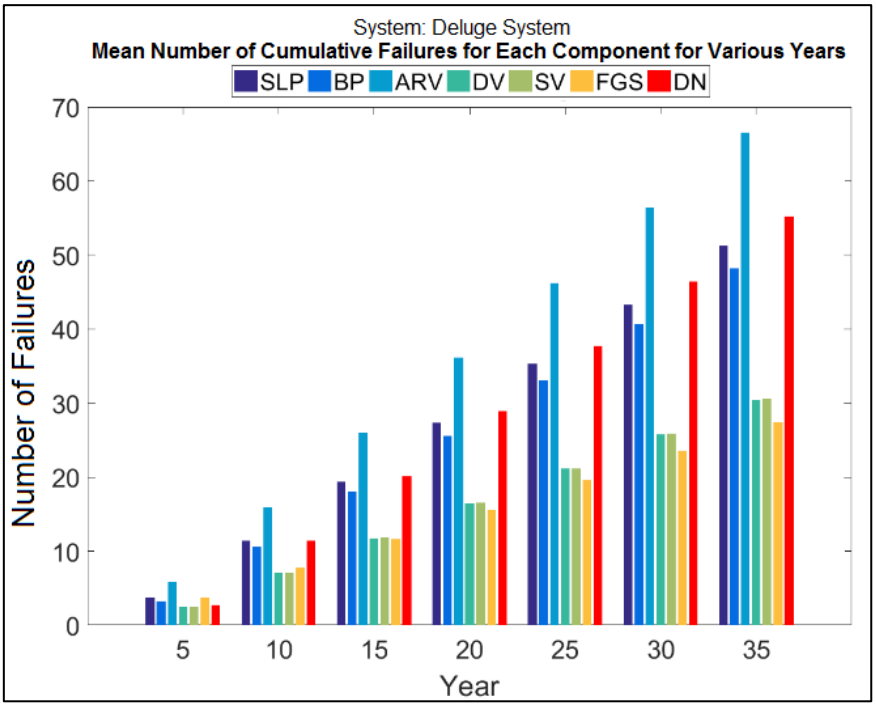


Figure 5-10 Cumulative Number of Failures for each component of the Deluge System

Figure 5-10 shows that the air release valve experiences the highest number of failures while the fire and gas logic sensor experiences the lowest number of failures. Although the air release valve is regularly monitored for degradation, once it reaches a state that requires maintenance, the component can go to functional failure state before inspection reveals the degraded state. Moreover, the high spurious failure rate explains the high number of failures the component experiences. This is due to exposure to sea water which is highly corrosive in nature. The deluge nozzle also experiences a high number of failures. This is as expected because marine fouling around the offshore oil and gas rig is likely to drift with the water flow to the upstream deluge system. These deposits can then flow through the pipes of the deluge system and block the nozzles. Moreover, the component is not regularly monitored for degradation. Using the above statistics, the expected cost of failure and maintenance over the 35-year prediction period can then be calculated by considering the costs associated with

the different maintenance interventions. Consequently, the cost of different asset maintenance strategies can then be evaluated. This is discussed in more detail in the next sub-section.

5.2.1.3 Component Maintenance and Failure Cost Prediction

Figure 5-11 shows the average yearly preventive maintenance cost for the submerged lift pump over the 35-year modelling period.

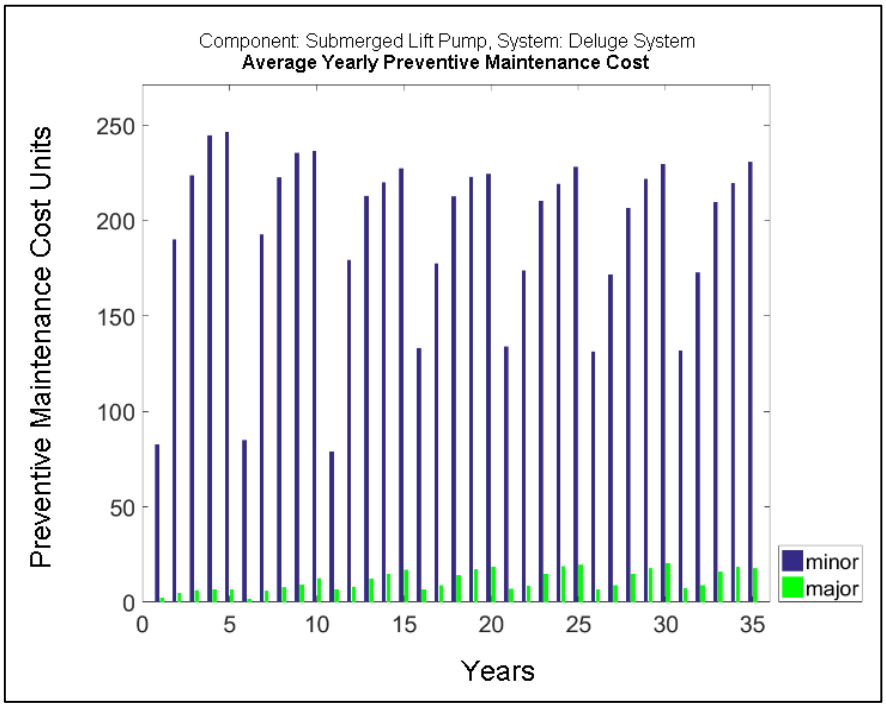


Figure 5-11 Average Yearly Preventive Maintenance Cost for the Submerged Lift Pump

The PM costs are divided into minor and major costs and the respective costs for each component have been outlined previously in Chapter 4 - Table 4-12. For each simulation, every time minor or major PM is performed on the component, a token is fired into P_{137} or P_{139} (see Chapter 4 - Figure 4-14), respectively, and the time at which this event occurs is recorded. The costs of performing minor or major PM is then evaluated for each year by multiplying the number of events by the cost of minor or major PM. Once all the simulation runs are completed annual statistics are evaluated. Therefore, the years where the average costs of minor or major PM are higher represent periods when the components are more likely to have degraded such that minor PM or major PM is required.

The above figure shows that the cost of performing minor PM is significantly higher than the cost of performing major PM on the submerged lift pump. This is as expected because although the unit cost assumed for minor PM is much lower than the unit cost of major PM (i.e. 300 units < 550 units), based on Table 5-2, the submerged lift pump undergoes a significantly higher number of minor PM than major PM. Hence, significantly high minor PM costs are incurred each year. Moreover, the figure also shows a cyclic pattern every 5 years. This is because, as previously outlined in Chapter 4, one of the maintenance policies considered in this research study is shutdown maintenance. Shutdown maintenance is assumed to occur every 5 years, when the components of the safety systems are replaced regardless of their condition. Therefore, the graph shows an increase in minor and major PM costs from year 1 to 5. After which the component is replaced and its lifecycle begins again. As the component is relatively new, less work is required to maintain its condition, hence the cost of performing minor and major PM decreases.

Figure 5-12 shows the average yearly corrective maintenance cost for the submerged lift pump over the 35-year modelling period.

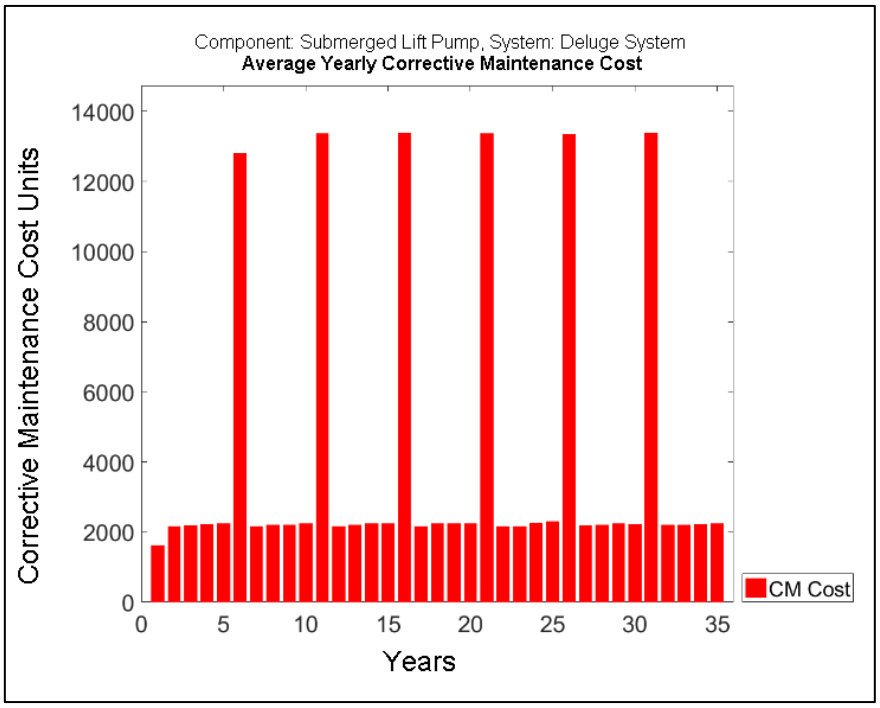


Figure 5-12 Average Yearly Corrective Maintenance Cost for the Submerged Lift Pump

For each simulation, every time CM is performed on the component, place P_{140} (see Chapter 4 – Figure 4-14) is marked and the time at which this event occurs is recorded. The costs of performing CM are then evaluated for each year by multiplying the number of tokens in P_{140} each year by the cost of CM. Once all the simulations are complete, the times at which place P_{140} was marked are grouped into individual years over the simulated time horizon (1-35).

The above figure shows that in year 1 the cost of CM is lower compared to the other years. This is because in year 1, the component undergoes only 3 inspections as the inspection interval is set to every 3 months. However, in year 2, the component is likely to experience inspection at the start of the year, hence undergoing 4 inspections in total. Thus, the cost of CM is lower in year 1.

The figure also shows a slight variation in CM costs over years 2 to 5. This is due to the stochastic nature of the Petri Net model. However, as the components of the safety system undergo shutdown maintenance every 5 years, the cost of CM increases significantly which explains the spike in year 6. A cyclic pattern is observed every 5 years.

By presenting the PM and CM costs as annualised summaries, offshore asset operations managers are able to better understand maintenance cycles, their associated costs and when these costs occur for different components of a system. The benefit of simulating the Petri Net model and obtaining these statistics is to assist offshore asset operations managers with the decision making process involved in budget allocation for maintenance of offshore safety systems. By observing the change in costs from year to year, one can evaluate the cost associated with implementing this particular maintenance strategy. As a result, the PN model can be used to test different maintenance strategies, assess the costs of using the different strategies and hence compare these strategies based on costs. This enables the improved use of condition and cost data in planning, maintenance and budgeting, hence, enables the development of asset management strategies that provide an appropriate level of service appropriate to specific budgets.

Moreover, unexpected component failures can result in unsafe situations as well as loss of production as it may be necessary to shutdown the platform before CM can be performed on

the component. For instance, if the deluge system were to become unavailable, production would be terminated until the component is replaced. Note, the level of shutdown would depend upon the criticality of the failure. For the purpose of this study, it is assumed that the entire platform is shutdown when the deluge system becomes unavailable due to component failure. Hence, in addition to the cost of replacing a component, a downtime cost is also incurred for every hour that the component is out of service. Figure 5-13 shows the average yearly failure costs which is split between CM costs and downtime costs for the submerged lift pump.

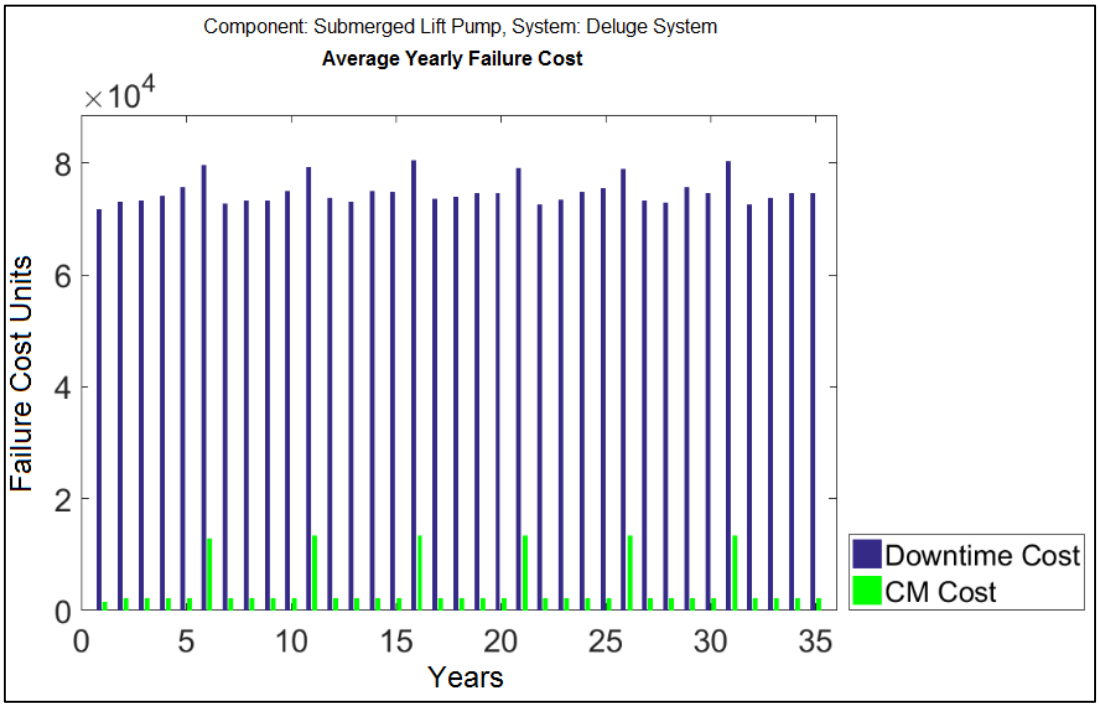


Figure 5-13 Average Yearly Failure Cost for the Submerged Lift Pump

In this study, the downtime cost is assumed to be 2000 units/hour for all components of the deluge system. For the submerged lift pump, the cost of performing CM is 2800 units per replacement. However, the submerged lift pump incurs a total downtime of 42 hours (Chapter 4 – Table 4-11) which explains the substantially high costs for downtime in comparison to the CM costs.

Figure 5-14 shows the cumulative PM costs for the wear-out components of the deluge system. As deluge nozzles and fire and gas logic sensors do not undergo PM, they are not

included in Figure 5-14. Based on Figure 5-9, the cumulative PM cost for the air release valve is one of the largest as it requires the largest number of minor PM work as explained earlier.

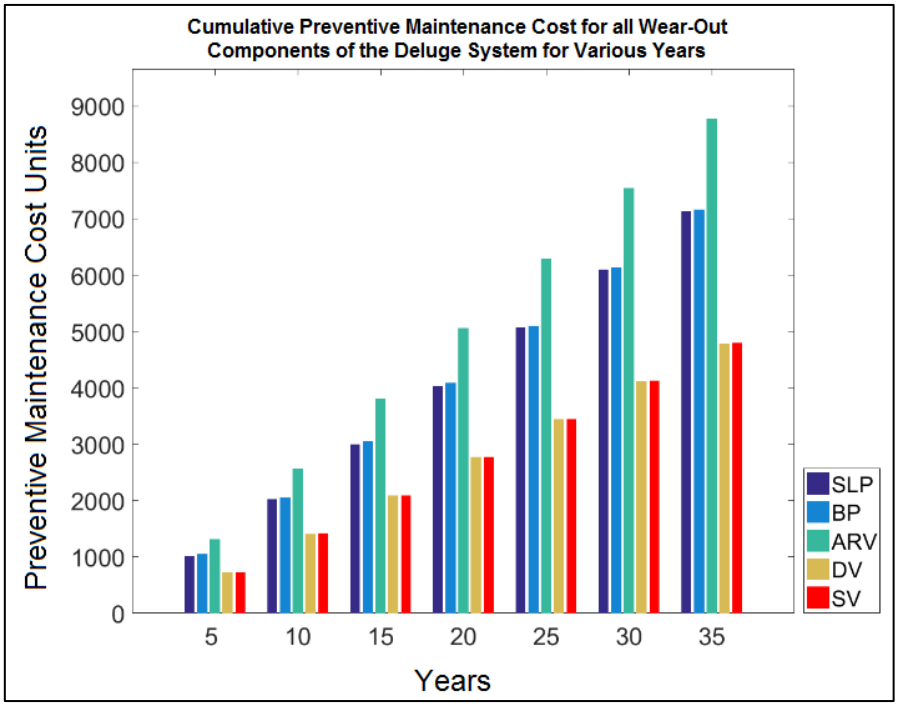


Figure 5-14 Cumulative Preventive Maintenance Cost for all Wear-Out Components of the Deluge System

Figure 5-15 shows the cumulative failure costs for all components of the deluge system.

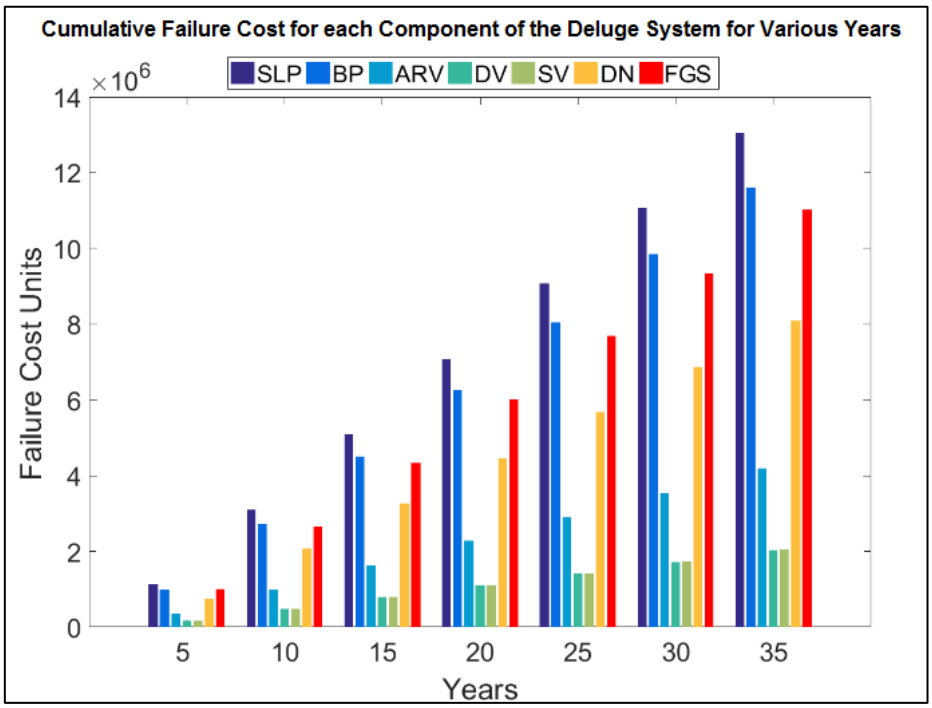


Figure 5-15 Cumulative Failure Cost for each component of the Deluge System

Based on Figure 5-15, the cumulative failure cost for the submerged lift pump is one of the largest. Although the air release valve is expected to undergo the maximum number of replacements, the cost of CM is only 500 units/replacement compared to 2500 units/replacement for the submerged lift pump. Moreover, the downtime costs for the submerged lift pump is much larger compared to the air release valve as the total downtime incurred every time the submerged lift pump is out of service is 42 hours compared to 6 hours incurred when the air release valve is out of service.

5.2.1.4 Component Operational Cost Prediction

Figure 5-16 shows the average yearly operational costs for the Submerged Lift Pump. The total operational cost of the component is evaluated by adding the cost of inspection, PM, CM and downtime.

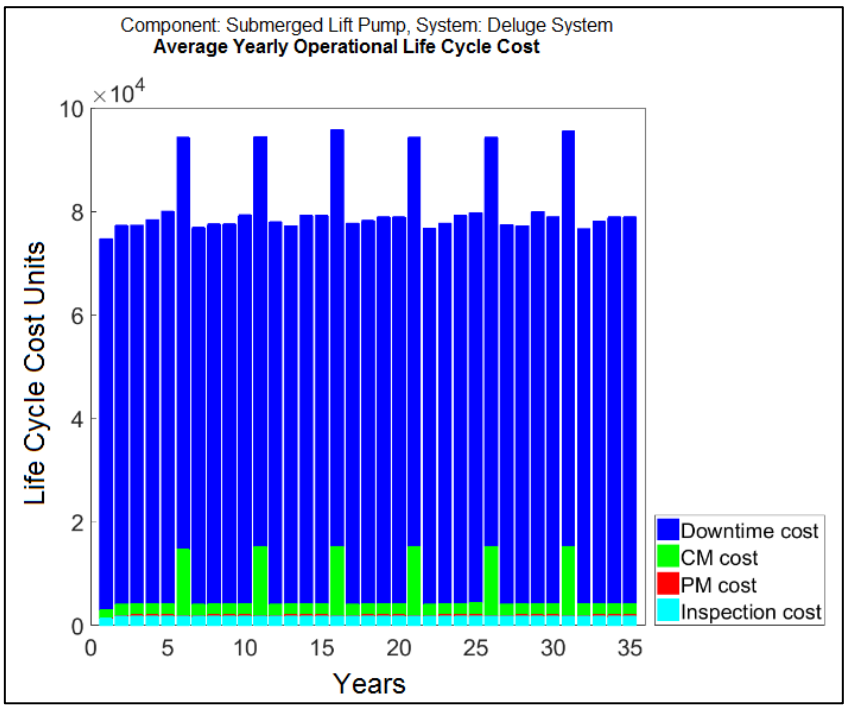


Figure 5-16 Average Yearly Life Cycle Cost for the Submerged Lift Pump

Based on Figure 5-16, the average yearly costs increase steadily from year 1 to year 5. This is because initially the submerged lift pump starts in 'new' working condition. However, as the component ages, it requires frequent maintenance (PM and CM) to restore its performance. Every 5 years, the component experiences shutdown maintenance where it is replaced. Hence, there is a significant increase in CM and downtime costs. As the component is

replaced, its age starts from 0 and hence the decrease in operational costs. A similar trend as that from year 1 to 6 is then followed hereafter. The results show that the majority of the operational costs for the submerged lift pump are due to downtime. Hence, a strategy that improves performance and reduces the number of failures would reduce the downtime costs, as proposed within this research.

5.2.2 System Analysis

5.2.2.1 System Condition Prediction

By combining the performance statistics of different components, the performance of the overall system can be predicted. Figure 5-17 shows the mean time of the Deluge System being in 'New Working' state.

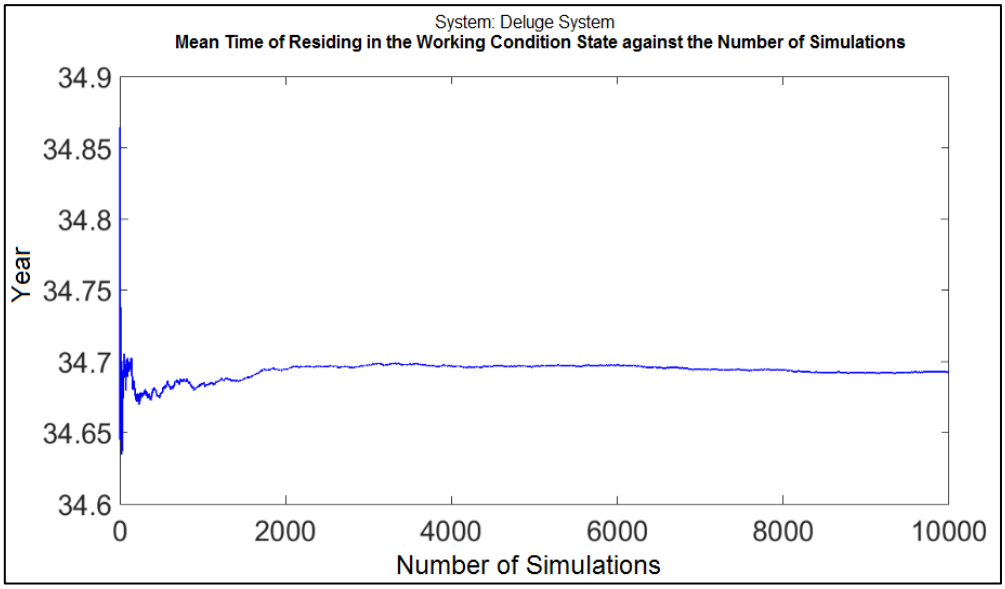


Figure 5-17 Mean Time of Residing in the Working Condition State against the number of simulations

For **Strategy 1** (i.e. repair as soon as component is revealed to be in a state where repair is required), the mean time the deluge system resides in the 'working' condition is roughly around 34.69 years over the 35 year prediction period. Based on this data, the deluge system has an availability of 99.11%.

Table 5-3 shows the summary of the statistics obtained for the deluge system for the 35 year prediction period.

Condition States		Duration (years)
Working	Minimum Number Achieved	32.926
	Maximum Number Achieved	34.983
	Average	34.693
	Standard deviation	0.222
Failed	Minimum Number Achieved	0.017
	Maximum Number Achieved	2.074
	Average	0.307
	Standard deviation	0.222

Table 5-3 Statistics on the duration (years) spent in each condition state by the Deluge System

5.2.2.2 Subsystem Failure Contribution to the Total Deluge System Downtime

By tracking the number of times a subsystem failure results in the failure of the overall safety system, the subsystem failure contribution to the total unavailability of the deluge system can be illustrated, as shown in Figure 5-18.

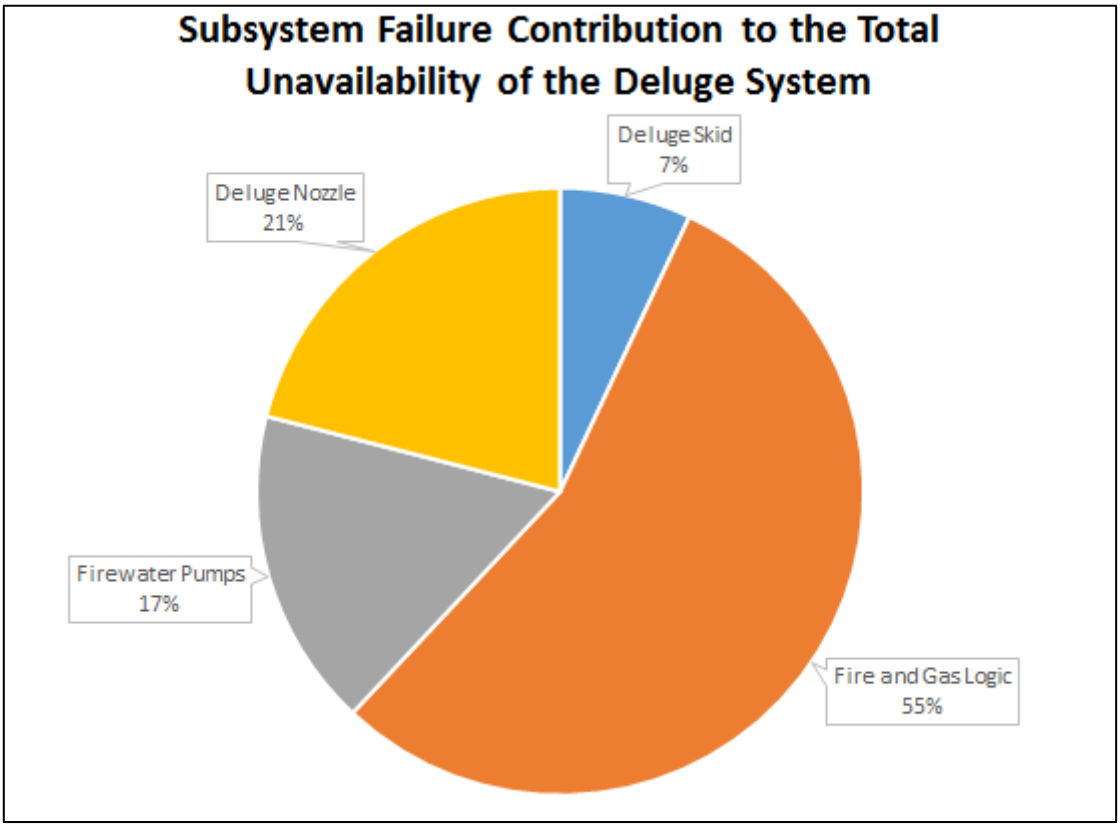


Figure 5-18 Subsystem Failure Contribution

It is evident from Figure 5-18, that the Fire and Gas Logic contributes to 55% of the total unavailability of the deluge system. Failure of the Fire and Gas Logic unit would mean that in the event of a fire, the firewater pump systems are not initiated Moreover, fire and gas

sensors are intended to protect people by generating an alarm earlier in the development of a fire. People need time to reach, and every second is critical during an actual fire event. The deluge nozzle contributes to 21% of the total unavailability while the firewater pumps contribute to 17% of the total unavailability. The deluge skid contributes the least amount of the total unavailability of the deluge system with 7%. The deluge skid comprises of the deluge valve and solenoid valves. These percentages are expected because compared to the deluge skid, the fire and gas logic unit is the most critical subsystem. Failure of the fire and gas logic unit to function on demand can escalate the consequences of a fire and explosion.

5.2.2.3 Whole System Operational Costs Prediction

The total cost of inspection, failure and maintenance for all components are added to give the total operational cost of the safety system. Figure 5-19 shows the average yearly operational cost for the deluge system. As components of the system age, the yearly operational cost of the deluge system increases with time. This is because the components are more likely to be in a state that requires frequent number of maintenance interventions to improve their condition. This is evidenced from year 1 to year 5. After year 5, all components are replaced during a shutdown maintenance. Hence, the cost incurred in year 6, 11, 16, 21, 26 and 31 are the highest.

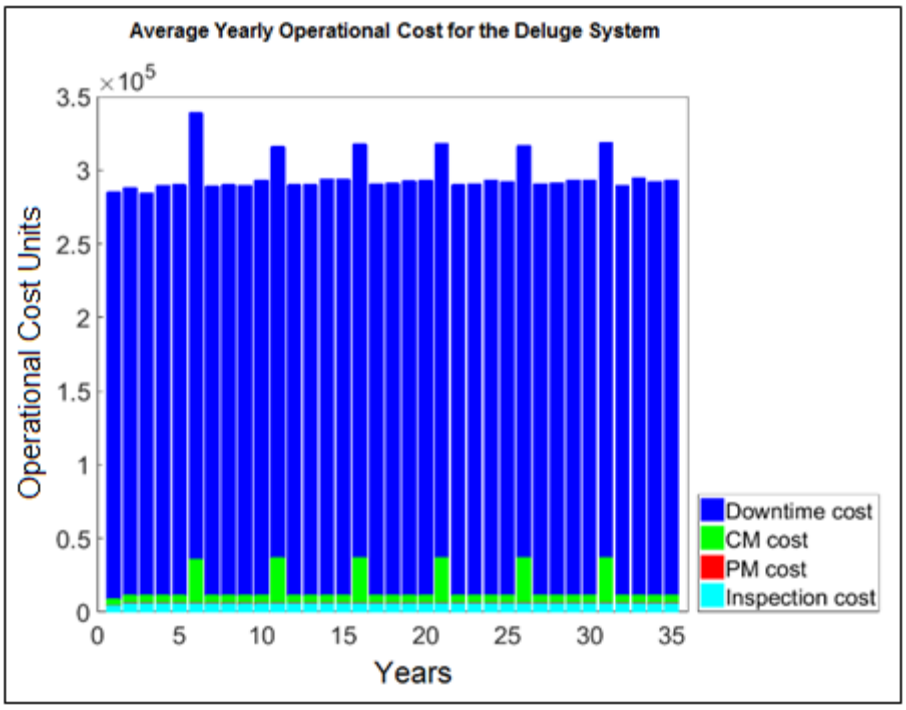


Figure 5-19 Average Yearly Operational Cost for the Deluge System

In conclusion, these statistics allow offshore asset operations managers to predict the total costs of any given asset management policy for the 35 year prediction period.

5.3 Sensitivity Analysis of Offshore Safety System Degradation and Maintenance Model

A sensitivity analysis is performed in which certain parameters of the Offshore Safety System Degradation and Maintenance model are varied and their effect on the unavailability and total operational costs is studied. The total operational cost for all safety systems is chosen because it is the main output used to evaluate asset management strategies while unavailability gives an insight into the performance of the four safety systems being considered. By conducting a sensitivity analysis, one can determine which parameters heavily influence the operational costs and unavailability of the safety systems. An analysis was carried out to determine the sensitivity of the following factors:

1. Asset Maintenance Strategy
2. Opportunistic Maintenance
3. Inspection Interval
4. Mean Time to Degradation

5.3.1 Effect of Varying Asset Maintenance Strategy

Four maintenance strategies that are investigated are shown in Table 5-4. The Petri Net model allows a specific maintenance strategy to be selected for the offshore safety systems individually. However, since it is not possible to demonstrate the effect of applying the four different maintenance strategies to the individual safety systems, each maintenance strategy is applied in turn to all four safety systems at once.

Strategy	Description
1	Repair as soon as component is revealed to be in a state where repair is required.
2	Minor Repair is disabled, only major repair and replacement is considered.
3	Major Repair is disabled, only minor repair and replacement is considered.
4	Both Minor and Major Repair are disabled, only replacement is considered.

Table 5-4 Four Maintenance Strategies possible for an Offshore Safety System

The effect of these maintenance strategies in terms of the safety system unavailability and total operational costs are shown in Table 5-5, below. Note that the following abbreviations

are used to represent the different safety systems: F&G – Fire and Gas Detection System, ISV – Isolation Valves, BDV – Blowdown Valves and DS – Deluge System.

Strategy	Safety System Unavailability				Total Operational Cost (unit cost)
	F&G	ISV	BDV	DS	
1	0.00008	0.01364	0.01548	0.00887	3.92579E+08
2	0.00016	0.02161	0.01891	0.00192	5.21735E+08
3	0.00012	0.01652	0.01822	0.00123	4.51387E+08
4	0.00016	0.02773	0.02466	0.00767	6.73948E+08

Table 5-5 Effect of Varying Asset Maintenance Strategies

Based on Table 5-5, with Strategies 1, 2 and 4 in place, the unavailability of the fire and gas detection system, process isolation and blowdown valves and deluge system increases as the number of maintenance interventions that can be performed on the different components of the system is reduced. As Strategy 3 executes minor repair and replacement compared to Strategy 4 which only executes replacement, the asset condition is maintained to a higher level with Strategy 3 in place as opposed to Strategy 4. Moreover, the unavailability of the fire and gas detection system, process isolation valves, process blowdown valves and deluge system for Strategy 3 is between Strategy 1 and 2. This is because with Strategy 2, the component is allowed to reach 'severely degraded' state before major repair is performed.

Moreover, it can be seen that Strategy 4 is the most expensive strategy. This is due to the fact that the cost of replacing a component is significantly higher than performing minor or major repairs on the component. Moreover, CM suffers a long downtime period. As Strategy 2 inhibits minor repairs and performs only major repairs and replacements it is the second most expensive strategy. This is because the cost of a major repair is higher than the cost of a minor repair. In summary, Strategy 1 and 3 which allow minor repair would result in lower operational costs.

In summary, the model can be used to study the effect of different maintenance options with the aim of decreasing unavailability and decreasing cost of offshore safety system maintenance.

5.3.2 Effect of Opportunistic Maintenance

The PN model allows the opportunistic maintenance to be enabled or disabled for the different offshore safety systems individually. The above four maintenance strategies can be implemented with opportunistic maintenance for the different offshore safety systems, as described previously in Chapter 4 – Section 4.4.4.5. The effect of enabling opportunistic maintenance in terms of the safety system unavailability and total operational cost is shown in Table 5-6, below.

Strategy	Safety System Unavailability				Total Operational Cost (unit cost)
	F&G	ISV	BDV	DS	
5	0.00011	0.01248	0.01316	0.00253	3.59132E+08
6	0.00009	0.01429	0.01515	0.00337	3.98818E+08
7	0.00011	0.01289	0.01539	0.00137	3.79014E+08
8	0.00014	0.02376	0.01974	0.00313	5.80204E+08

Table 5-6 Effect of Opportunistic Maintenance

Table 5-6 shows that by enabling opportunistic maintenance, both the unavailability of the fire and gas detection system, process isolation and blowdown valves and deluge system and the total operational costs decreases significantly. Strategy 1 is cheaper by 8.5% while Strategy 2 is cheaper by 23.6%, Strategy 3 is cheaper by 16.0% and Strategy 4 is cheaper by 13.9% with opportunistic maintenance.

5.3.3 Effect of Varying Inspection Interval

The Petri Net model allows the inspection frequency to be varied for the different offshore safety systems individually. The base case inspection intervals for the different systems are shown in Table 5-7 along with the additional inspection intervals that were investigated.

System	Base Case Inspection Interval (hours)	Inspection intervals (hours)
Fire and Gas Detection System	2190	168, 730, 1460 and 4380
Isolation Valves	1460	168, 730, 2190 and 4380
Blowdown Valves	1460	168, 730, 2190 and 4380
Deluge System	2190	168, 730, 1460 and 4380

Table 5-7 Five Inspection Intervals possible for an Offshore Safety System

The effect of varying the inspection interval on the unavailability and operational costs for the fire and gas detection system, isolation valves, blowdown valves and deluge system is shown in Tables 5-8, 5-9, 5-10 and 5-11, respectively. The blue colour represents the base case.

Inspection Interval (hours)	Safety System Unavailability	Total Operational Cost (unit cost)
168	0.00003	5.55364E+08
730	0.00042	5.79540E+08
1460	0.00201	5.91551E+08
2190	0.00424	6.10364E+08
4380	0.01415	6.63429E+08

Table 5-8 Effect of Varying Inspection Interval on the Fire and Gas Detection System

Inspection Interval (hours)	Safety System Unavailability	Total Operational Cost (unit cost)
168	0.00017	3.74014E+08
730	0.00424	4.48409E+08
1460	0.00484	5.35010E+08
2190	0.00823	6.17942E+08
4380	0.02520	8.62311E+08

Table 5-9 Effect of Varying Inspection Interval on the Isolation Valves

Inspection Interval (hours)	Safety System Unavailability	Total Operational Cost (unit cost)
168	0.01326	5.04401E+08
730	0.01336	5.44048E+08
1460	0.01408	6.14451E+08
2190	0.01597	6.85514E+08
4380	0.01620	9.03205E+08

Table 5-10 Effect of Varying Inspection Interval on the Blowdown Valves

Inspection Interval (hours)	Safety System Unavailability	Total Operational Cost (unit cost)
168	0.01499	4.78742E+08
730	0.01504	5.30468E+08
1460	0.01531	6.04537E+08
2190	0.01554	6.97360E+08
4380	0.01584	9.52774E+08

Table 5-11 Effect of Varying Inspection Interval on the Deluge System

Tables 5-8, 5-9, 5-10 and 5-11 show that as the inspection interval increases, the system unavailability increases. This is because components are more likely to reach 'Functional Failure' state before their condition is revealed by inspection.

5.3.4 Effect of Varying Degradation Rates

The mean time to reach different degradation states for each component is also varied. In the Petri Net model, this involved varying the characteristic life, i.e. the scale parameter (η) of the Weibull distribution by ±10% and ±20% while the shape parameter (β) was fixed. For instance, in the case of Submerged Lift Pump, the Weibull distribution parameters are β=1.5, η=35040 days. Decreasing the scale parameter, η, by 10%, results in updated set of Weibull distribution parameters, i.e. β=1.5 and η=29565 days. The effect of varying the degradation rates on the unavailability and total operational costs for the fire and gas detection system, isolation valves, blowdown valves and deluge system is shown in Table 5-12 below.

Change in η parameter values	System Unavailability				Total Operational Cost (unit cost)
	F&G	IS	BS	DS	
-20 %	0.00419	0.01475	0.01686	0.00993	6.32610E+08
-10 %	0.00407	0.01466	0.01586	0.00984	6.30527E+08
0	0.00405	0.01407	0.01571	0.00894	6.11319E+08
+10 %	0.00384	0.01386	0.01528	0.00860	6.11175E+08
+20 %	0.00350	0.01355	0.01539	0.00813	5.98569E+08

Table 5-12 Effect of Varying Mean Time to Degradation

Table 5-12 shows that by increasing the values of η parameter, the total operational cost decreases. This is as expected because increasing the values of η parameter means that the components would degrade at a slower rate, hence are less likely to require maintenance. Thus, by increasing the values of η parameter by 20%, the total operational costs are reduced by 2.09% in comparison to the base case. Moreover, as the components degrade slower they are less likely to be in a 'Functional Failure' state, and, thus, the number of failures experienced also reduces to a certain extent. Hence, by increasing the value of η parameter by 20%, the unavailability of the safety systems decreases. In reality, the component would be replaced by a component with a lower failure rate.

5.4 Simulation of Offshore Fire and Explosion Model

5.4.1 Simulation Time

The Fire and Explosion model simulates the same time horizon as the Offshore Safety System Degradation and Maintenance Model, i.e. over a 35-year lifetime period. This timeframe allows us to witness the behaviour of the offshore safety systems in the event a hydrocarbon leak occurs within the 35-year period in either of the three modules of the offshore oil and gas installation.

5.4.2 Convergence Analysis

As the accuracy of the results increases with increasing number of simulations, 10,000 simulation runs of the Offshore Fire and Explosion model were performed for an example oil and gas installation to estimate the frequencies of fires and explosions. Simulation convergence is achieved when running further simulations does not change the results significantly. Hence, the average number of explosions can be examined to check for convergence as shown in Figure 5-20. For 10,000 simulations carried out, it can be seen that, convergence is achieved around 7000 simulations. Under **Strategy 1**, the average number of explosions is 4 x 10^{-4} per year.

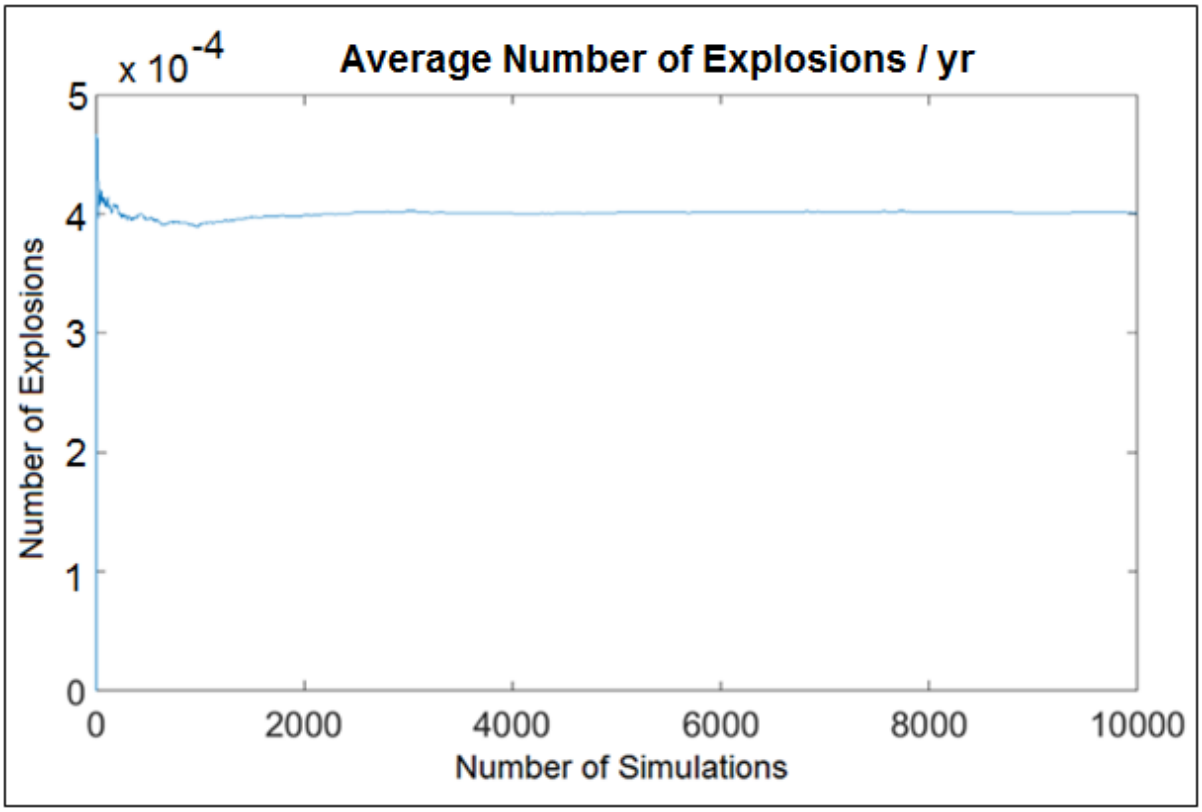


Figure 5-20 Average Number of Explosions per year against the Number of Simulations

5.4.3 Output File

The results for each simulation are recorded into a results file. The statistics that can be generated from the simulations of Fire and Explosion model include:

1. **Frequency of the explosions, jet fires and pool fires in each module**
2. **Frequency of explosions, jet fires and pool fires from leaks in sections of each module**
3. **Distribution of explosion overpressures for each module**
4. **Distribution of flame lengths of jet fires and pool fires for each module**
5. **Duration of jet fires and pool fires for each module**

5.5 Application of the Offshore Fire and Explosion Model

5.5.1 Offshore Oil and Gas Platform Results

The results from the separation, compression and wellhead module were combined to provide the overall predictions for the example offshore oil and gas installation. Table 5-13 shows the proportion of fires (jet and pool) and explosions occurring within each of the modules.

	Expected Proportion of Events occurring within each module (%)			
Module	**Explosion**	**Jet Fire**	**Pool Fire**	**Platform Total**
Separation	18	18	79	22
Compression	58	65	0	58
Wellhead	24	17	21	20

Table 5-13 Expected Proportion of Fires and Explosions occurring within each module

The separation module is made up of two sections, both of which are linked to each other and other sections located outside the module. Both sections contain oil and gas inventory. The separation module was estimated to generate approximately 22% of all the fires and explosions on the installation. Overall, the module generated 18% of explosions, 18% of jet fires and 80% of the pool fires.

The compression module is made up of four sections, all of which are linked to each other and sections located outside the module. All four sections contain gas inventory with three out of four containing condensate as well. The compression module was estimated to generate approximately 58% of all the fires and explosions on the installation. Overall, the

module generated 58% of explosions and 65% of jet fires. As none of the sections of the compression module contains any oil inventory, no pool fires were generated within this module.

The wellhead module is made up of three sections, all of which are linked to each other and sections located outside the module. All three sections contain gas inventory with one out of the three containing oil as well. The wellhead module was estimated to generate approximately 20% of all the fires and explosions on the installation. Overall, the module generated 24% of explosions, 17% of jet fires and 21% of pool fires.

In summary, the compression module generated the maximum number of explosions and jet fires due to its large gas inventory compared to the other modules. The separation module generated the maximum number of pool fires due to its large oil inventory compared to the other modules. Further statistics for each of three oil and gas processing modules have been outlined in the Sections 5.5.2, 5.5.3 and 5.5.4, respectively.

5.5.2 Separation Module

5.5.2.1 Explosions

The frequency of occurrence of explosions estimated to occur in the separation module is 4.222 x 10^{-2} per year, accounting for 18% of all ignitions within the module. Table 5-14 shows the frequency of occurrence of explosions originating from each section of the separation module as well as the proportion each section contributes to the total frequency of explosions within the separation module. The majority of explosions are predicted to occur from leaks in Section 1 which accounted for approximately 70% of the total explosions within the module. Analysis of these results show that although Section 2 contained gas at a higher pressure than Section 1, it did not generate the maximum number of explosions. This is justified by the fact that a section at higher pressure would release gas at a higher rate and therefore the concentration of the gas cloud quickly exceeds the upper explosive limit.

Section	Frequency (per year)	Proportion of total explosions (%)
1 – Atmospheric Separator	2.961E-02	70.128
2 – Inlet Separator	1.261E-02	29.872

Table 5-14 Explosion Frequency (per year) from leaks in sections of the separation module

The frequencies of explosions in terms of the overpressures generated are shown in Table 5-15. Over 99.6% of all explosions predicted to occur within the separation module generate an overpressure between 0 and 1 bar. This can be credited to the fact that the safety systems within the module function on demand majority of the times and hence the amount of gas released into the module is minimised sufficiently to limit the overpressures generated to less than 1 bar. The frequency of explosions occurring with sufficient overpressure to fail the internal safety wall of the module, 0.6 bar, is 2.90 x 10^{-2} per year, while the frequency of explosions occurring with sufficient overpressure to fail the platform, i.e. 1.6 bar, is 1.14 x 10^{-5} per year.

Overpressure (bar)		Frequency (per year)	Proportion (%)
from	to		
0	1	4.20E-02	99.573
1	2	1.34E-04	0.318
2	3	2.29E-05	0.054
3	4	5.71E-06	0.014
4	5	5.71E-06	0.014

5	6	5.71E-06	0.014
6	7	2.86E-06	0.007
7	8	2.86E-06	0.007
8	+	0.00E+00	0.000

Table 5-15 Explosion Frequency (per year) for the different overpressures for the separation module

The explosion frequencies can also be further categorised with respect to the overpressures generated and the leaking section as shown in Table 5-16. It is evident from Table 5-16 that the largest proportion of explosions were generated by Section 1 with an overpressure between 0 and 1 bar, 2.950 x 10^{-2} per year. Moreover, due to the effective nature of the gas detection system and deluge system, only a small number of explosions generated an overpressure greater than 1 bar on both sections.

Overpressure (bar)		Frequency (per year)	
from	**to**	**Section 1**	**Section 2**
0	1	2.950E-02	1.250E-02
1	2	4.290E-05	9.140E-05
2	3	1.430E-05	8.570E-06
3	4	0.000E+00	5.710E-06
4	5	0.000E+00	5.710E-06
5	6	5.710E-06	0.000E+00
6	7	0.000E+00	2.860E-06
7	8	0.000E+00	2.860E-06
8	+	0.000E+00	0.000E+00

Table 5-16 Explosion Frequency (per year) for the different sections of the separation module

Moreover, the model was refined to generate explosion frequencies for different gas concentration ranges as shown in Table 5-17. To obtain these explosion frequencies, the lower explosive limit (LEL) and the upper explosive limit (UEL) were adjusted to the upper bounds and lower bounds of the required ranges. It is evident from Table 5-17 that increasing the gas concentration range from 5-6% to 9-10%, increases the explosion frequencies. However, further increase of the gas concentration range results in a decrease of explosion frequencies. It is apparent that a marked difference exists in the concentrations of gas that react in an air atmosphere. As stated earlier in Chapter 3, the explosive range for methane-air mixtures is 5 to 15%. Expressing these concentrations in terms of the stoichiometric concentration, the lower and upper limits of the explosive range are 0.52 and 1.52 times the

stoichiometric ratio, and the optimum concentration is 1.05 times the stoichiometric ratio. Hence, the largest proportion of explosions occur between 9 and 10% which is the optimum explosive mixture of methane and air.

Concentration Range	Explosion Frequencies (per year)
5-6	2.712E-03
6-7	3.220E-03
7-8	3.463E-03
8-9	3.526E-03
9-10	3.580E-03
10-11	3.403E-03
11-12	2.932E-03
12-13	2.709E-03
13-14	2.564E-03
14-15	1.597E-03

Table 5-17 Explosion Frequencies for each concentration range for the Separation Module

Furthermore, the explosions are categorised depending on whether the explosions are mitigated or unmitigated. Table 5-18 shows the frequencies of mitigated and unmitigated explosions occurring for each concentration range for the separation module.

Concentration Range	Explosion Frequencies (per year)	
	Mitigated	Unmitigated
5-6	6.090E-04	2.103E-03
6-7	6.890E-04	2.531E-03
7-8	6.430E-04	2.820E-03
8-9	7.770E-04	2.749E-03
9-10	7.930E-04	2.787E-03
10-11	7.170E-04	2.686E-03
11-12	6.230E-04	2.309E-03
12-13	5.460E-04	2.163E-03
13-14	4.440E-04	2.120E-03
14-15	4.670E-04	1.130E-03
Total	**6.308E-03**	**2.340E-02**

Table 5-18 Mitigated and Unmitigated Explosion Frequencies for the Separation Module

Based on Table 5-18, unmitigated explosions occurred more frequently than mitigated explosions, accounting for 2.340×10^{-2} explosions per year. This can be due to the occurrence of any of the following scenarios:

1. The deluge system fails to activate when a high gas concentration is detected and the gas ignites.
2. The deluge system is activated but the gas ignites during the time taken to get the water spray to a fully functional state.
3. The deluge system is activated and fully functional, however, it fails to maintain the water spray for the duration of the explosive gas concentration and the gas ignites.

Further analysis reveals that most of the unmitigated explosions occurred due to Scenario 2, i.e. the deluge system is activated but the gas ignites during the time taken to get the water spray to a fully functional state, accounting for 2.326 x 10^{-2} explosions per year. The relative contribution of each scenario of the unmitigated explosion is shown in Table 5-19, below.

Scenario	Description	Explosion Frequencies (per year)
1	Deluge Fails to Activate	7.900E-05
2	Prior to Deluge being in Fully Functional state	2.326E-02
3	Water Spray not Maintained	4.700E-05

Table 5-19 Unmitigated Explosion Frequencies for the different unmitigated explosion scenarios for the Separation Module

5.5.2.2 Jet Fires

The frequency of occurrence of jet fires following immediate ignition of a leak in the separation module is 2.172 x 10^{-2} per year. Table 5-20 shows the frequency of occurrence of immediate jet fires originating from each section of the separation module as well as the proportion each section contributes to the total frequency of immediate jet fires within the separation module. The majority of jet fires are predicted to occur from leaks in Section 1 which accounted for approximately 58% of the total jet fires within the module. Analysis of these results show that although Section 2 contained more gas inventory at higher pressure than Section 1, it did not generate the maximum number of jet fires. This is can be due to the volume of gas released; bigger releases experience a higher likelihood of ignition. Section 1 connects to 5 other sections (i.e. Section 2, 3, 4, 5 and 11) while Section 2 connects to 2 other sections (i.e. Section 4 and 8) via isolation valves. If the isolation valve between these sections were to fail, the leak inventory would include the contents of the section adjacent to the valve. The possible inventory combinations connected with Section 1 have a high proportion of gas compared to the possible inventory combinations connected with Section 2. Hence, it

is more likely that Section 1 would release more gas than Section 3, thus, increasing its likelihood of ignition.

Section	Frequency (per year)	Proportion of Jet Fires (%)
1 – Atmospheric Separator	1.253E-02	57.715
2 – Inlet Separator	9.183E-03	42.285

Table 5-20 Jet Fire Frequency (per year) following immediate ignition of a leak in sections of the Separation Module

The frequency of occurrence of jet fires following an explosion or a pool fire in the module is 2.430×10^{-2} per year. Table 5-21 shows the frequency of occurrence of delayed jet fires originating from each section of the separation module as well as the proportion each section contributes to the total frequency of delayed jet fires within the separation module.

Section	Frequency (per year)	Proportion of Jet Fires (%)
1 – Atmospheric Separator	1.449E-02	59.638
2 – Inlet Separator	9.806E-03	40.362

Table 5-21 Jet Fire Frequency (per year) following delayed ignition of a leak in sections of the Separation Module

The frequency of delayed jet fires is greater than immediate jet fires which suggests that the majority of explosions and pool fires are followed by a jet fire. The majority 55% of jet fires that occurred in the separation module lasted between 0 and 3.6 minutes as shown in Table 5-22 below. The cut-off points shown in Table 5-22 have been adopted from Lewthwaite (2006). Only a small proportion of jet fires ≈ 1% lasted longer than 18 minutes. This can be due to the effective nature of the detection system in activating the isolation and blowdown valves, hence reducing the leak inventory. Moreover, the deluge system is also assumed to extinguish jet fires.

Fire Duration (mins)		Frequency (per year)	Proportion (%)
from	to		
0	3.6	2.541E-02	55.208
3.6	18	2.044E-02	44.410
18	36	3.400E-05	0.074
36	54	3.000E-05	0.065
54	72	5.710E-06	0.012
72	+	1.060E-06	0.002

Table 5-22 Jet Fire Duration for the Separation Module

The frequency of jet fires occurring over a sufficient duration to cause failure of the vessel or pipework, which is equal to 15 minutes, is 1.47 x 10^{-2} per year while the frequency of jet fires occurring with sufficient duration to cause failure of the platform, i.e. 72 minutes, is 1.060 x 10^{-6} per year.

Majority 72% of jet fires that occurred in the separation module generated a flame length between 0 and 10 meters while 20% of jet fires generated a flame length between 10 and 20 meters as shown in Table 5-23, below. Fires within enclosed modules are oxygen limited, and are extinguished if the release rate of gas from the leaking section exceeds the rate at which the gas is combusted. Moreover, as mentioned previously, the deluge system is also assumed to extinguish jet fires. Hence, the overall contribution of these factors result in the reduction of both jet fire flame length and duration.

Flame Length (m)		Frequency (per year)	Proportion (%)
from	to		
0	10	3.237E-02	71.601
10	20	8.877E-03	19.635
20	30	2.226E-03	4.924
30	40	5.910E-04	1.307
40	50	3.490E-04	0.772
50	60	2.000E-04	0.442
60	70	2.370E-04	0.524
70	80	2.090E-04	0.462
80	90	6.300E-05	0.139
90	+	8.710E-05	0.193

Table 5-23 Flame Length of the Jet Fire for the Separation Module

5.5.2.3 Pool Fires

The frequency of occurrence of pool fires estimated to occur in the separation module is 2.274 x 10^{-2} per year, accounting for 80% of all ignitions within the module. Table 5-24 shows the frequency of occurrence of pool fires originating from each section of the separation module as well as the proportion each section contributes to the total frequency of pool fires within the separation module. The majority of pool fires are predicted to occur from leaks in Section 1 which accounted for approximately 57% of the total pool fires within the module. Analysis of these results show that although Section 2 contained more oil inventory than Section 1, it did not generate the maximum number of pool fires. This can be due to the

volume of oil released; bigger releases experience a higher likelihood of ignition. Section 1 connects to 5 other sections (i.e. Section 2, 3, 4, 5 and 11) while Section 2 connects to 2 other sections (i.e. Section 4 and 8) via isolation valves. If the isolation valve between these sections were to fail, the leak inventory would include the contents of the section adjacent to the valve. The possible inventory combinations connected with Section 1 have a high proportion of oil compared to the possible inventory combinations connected with Section 2. Hence, it is more likely that Section 1 would release more oil than Section 3, thus, increasing its likelihood of ignition.

Section	Frequency (per year)	Proportion of Pool Fires (%)
1 – Atmospheric Separator	1.299E-02	57.099
2 – Inlet Separator	9.757E-03	42.901

Table 5-24 Pool Fire Frequency (per year) for a leak in sections of the Separation Module

The majority 97% of pool fires that occurred in the separation module lasted between 0 and 3.6 minutes as shown in Table 5-25 below. Only a very small proportion of pool fires ≈3% lasted longer than 3.6 minutes. The least frequent pool fires were those which lasted between 72 and 90 minutes.

Fire Duration (mins)		Frequency (per year)	Proportion (%)
from	to		
0	3.6	2.212E-02	97.134
3.6	18	2.300E-04	1.010
18	36	3.100E-04	1.361
36	54	1.100E-05	0.048
54	72	1.100E-05	0.048
72	90	3.000E-06	0.013
90	108	1.400E-05	0.061
108	144	2.000E-05	0.088
144	180	6.000E-06	0.026
180	216	1.400E-05	0.061
216	252	9.000E-06	0.040
252	288	2.000E-05	0.088
288	+	4.630E-06	0.020

Table 5-25 Pool Fire Duration for the Separation Module

Moreover, the majority of pool fires that occurred in the separation module generated a flame length between 0 and 1 meters as shown in Table 5-26, below. No fires generated a flame length greater than 3 meters. Due to an assumption that a pool fire cannot occur if the deluge system is functioning, as it will be extinguished before it can be established, all the pool fires occurring within the separation module coincide with an unavailability of the deluge system.

Flame Length (m)		Frequency (per year)	Proportion (%)
from	to		
0	1	3.659E-02	96.085
1	2	1.420E-03	3.729
2	3	7.100E-05	0.186
3	4	0.000E+00	0.000
4	5	0.000E+00	0.000
5	6	0.000E+00	0.000
6	+	0.000E+00	0.000

Table 5-26 Flame Length of the Pool Fire for the Separation Module

5.5.3 Compression Module

5.5.3.1 Explosions

The frequency of occurrence of explosions estimated to occur in the compression module is 1.333 x 10^{-1} per year, accounting for 58% of all ignitions within the module. Table 5-27 shows the frequency of occurrence of explosions originating from each section of the compression module as well as the proportion each section contributes to the frequency of all explosions within the compression module. The majority of explosions are predicted to occur from leaks in Section 3, which accounted for approximately 34% of the total explosions within the module.

Section	Frequency (per year)	Proportion of total explosions (%)
3 - Low Pressure Scrubbers and Compressors	4.546E-02	34.111
4 – Medium Pressure Scrubbers, Coolers and Compressors – Stage 1	2.641E-02	19.818
5 - Medium Pressure Scrubbers, Coolers and Compressors – Stage 2	3.064E-02	22.991
7 – Injection Scrubbers, Coolers and Compressors	3.076E-02	23.079

Table 5-27 Explosion Frequency (per year) from leaks in sections of the compression module

The frequencies of explosions in terms of the overpressures generated are shown in Table 5-28. Over 98% of all explosions predicted to occur within the compression module generate an overpressure between 0 and 1 bar. The frequency of explosions occurring with sufficient overpressure to fail the internal safety wall of the module, 0.6 bar, is 1.190 x 10^{-1} per year, while the frequency of explosions occurring with sufficient overpressure to fail the platform, 1.6 bar, is 2.180 x 10^{-3} per year.

Overpressure (bar)		Frequency (per year)	Proportion (%)
from	to		
0	1	1.294E-01	98.115
1	2	2.269E-03	1.720
2	3	1.060E-04	0.080
3	4	4.900E-05	0.037
4	5	1.400E-05	0.011

5	6	1.400E-05	0.011
6	7	1.100E-05	0.008
7	8	1.700E-05	0.013
8	+	6.000E-06	0.005

Table 5-28 Explosion Frequency (per year) for the different overpressures for the compression module

The explosion frequencies can also be further categorised with respect to the overpressures generated and the leaking section as shown in Table 5-29. It is evident from Table 5-29 that the largest proportion of explosions were generated by Section 3 with an overpressure between 0 and 1 bar, 4.530 x 10^{-2} per year. Moreover, due to the effective nature of the gas detection system and deluge system, only a small number of explosions generated an overpressure greater than 1 bar on all four sections of the compression module. None of the sections generated an overpressure greater than 8 bar.

Overpressure (bar)		Frequency (per year)			
from	to	Section 3	Section 4	Section 5	Section 7
0	1	4.510E-02	2.620E-02	2.980E-02	2.930E-02
1	2	1.200E-04	1.910E-04	8.000E-04	1.300E-03
2	3	0.000E+00	1.430E-05	1.140E-05	8.860E-05
3	4	8.570E-06	8.570E-06	8.570E-06	2.290E-05
4	5	0.000E+00	5.710E-06	0.000E+00	2.860E-05
5	6	2.860E-06	0.000E+00	1.140E-05	8.570E-06
6	7	2.860E-06	0.000E+00	8.570E-06	8.570E-06
7	8	2.860E-06	2.860E-06	5.710E-06	5.710E-06
8	+	0.000E+00	0.000E+00	0.000E+00	0.000E+00

Table 5-29 Explosion Frequency (per year) for the different sections of the compression module

The explosion frequencies for different gas concentration ranges are shown in Table 5-30. It is evident from Table 5-30 that increasing the gas concentration range from 5-6% to 9-10%, increases the explosion frequencies. However, further increase of the gas concentration range results in a decrease of explosion frequencies. The largest proportion of explosions occur between 9 and 10% which is the optimum explosive mixture of methane and air.

Concentration Range	Explosion Frequencies (per year)
5-6	8.708E-03
6-7	9.680E-03
7-8	1.056E-02
8-9	1.081E-02

9-10	1.097E-02
10-11	1.049E-02
11-12	9.691E-03
12-13	8.489E-03
13-14	5.850E-03
14-15	7.586E-03

Table 5-30 Explosion Frequencies for each concentration range for the Compression Module

The frequencies of mitigated and unmitigated explosions for each concentration range for the compression module is shown in Table 5-31.

Concentration Range	Explosion Frequencies (per year)	
	Mitigated	Unmitigated
5-6	1.170E-04	8.591E-03
6-7	1.260E-04	9.554E-03
7-8	1.230E-04	1.043E-02
8-9	1.570E-04	1.065E-02
9-10	1.540E-04	1.082E-02
10-11	1.200E-04	1.037E-02
11-12	9.100E-05	9.600E-03
12-13	1.090E-04	8.380E-03
13-14	1.110E-04	2.157E-03
14-15	1.800E-05	1.110E-02
Total	**1.126E-03**	**9.165E-02**

Table 5-31 Mitigated and Unmitigated Explosion Frequencies for the Compression Module

Based on Table 5-31, unmitigated explosions occurred more frequently than mitigated explosions, accounting for 9.165×10^{-2} explosions per year. Further analysis reveals that most of the unmitigated explosions occurred due to Scenario 2, i.e. the deluge system is activated but the gas ignites during the time taken to get the water spray to a fully functional state, accounting for 2.326×10^{-2} explosions per year. The relative contribution of each scenario of the unmitigated explosion is shown in Table 5-32, below. The results also show that none of the unmitigated explosions that occurred were a result of Scenario 3, i.e. the deluge system is activated and fully functional, however, it fails to maintain the water spray for the duration of the explosive gas concentration and the gas ignites.

Scenario	Description	Explosion Frequencies (per year)
1	Deluge Fails to Activate	1.500E-05

2	Prior to Deluge being in Fully Functional state	9.164E-02
3	Water Spray not Maintained	0.000E+00

Table 5-32 Unmitigated Explosion Frequencies for the different unmitigated explosion scenarios for the Compression Module

5.5.3.2 Jet Fires

The frequency of occurrence of jet fires following immediate ignition of a leak in the compression module is 5.346 x 10^{-2} per year. Table 5-33 shows the frequency of occurrence of immediate jet fires originating from each section of the compression module as well as the proportion each section contributes to the total frequency of immediate jet fires within the compression module.

Section	Frequency (per year)	Proportion of Jet Fires (%)
3 - Low Pressure Scrubbers and Compressors	1.167E-02	21.823
4 – Medium Pressure Scrubbers, Coolers and Compressors – Stage 1	8.746E-03	16.361
5 - Medium Pressure Scrubbers, Coolers and Compressors – Stage 2	1.319E-02	24.672
7 – Injection Scrubbers, Coolers and Compressors	1.986E-02	37.145

Table 5-33 Jet Fire Frequency (per year) following immediate ignition of a leak in sections of the compression module

The majority of jet fires are predicted to occur from leaks in Section 7 which accounted for approximately 37% of the total jet fires within the module. Analysis of these results show that although Section 5 contained more gas inventory than Section 7, it did not generate the maximum number of jet fires. Referring to Table 4-1 outlined in Chapter 4 of this thesis, we can see that Section 7 is assumed to be at a higher pressure than the other sections of the compression module. Previous experimental studies have shown that pressure can have a profound effect on the flammability limits of a methane/air mixture and the auto-ignition temperature of methane. Figure 5-21, below, shows the effect of pressure on the flammability range of methane in air (Mehta *et al.* 1998).

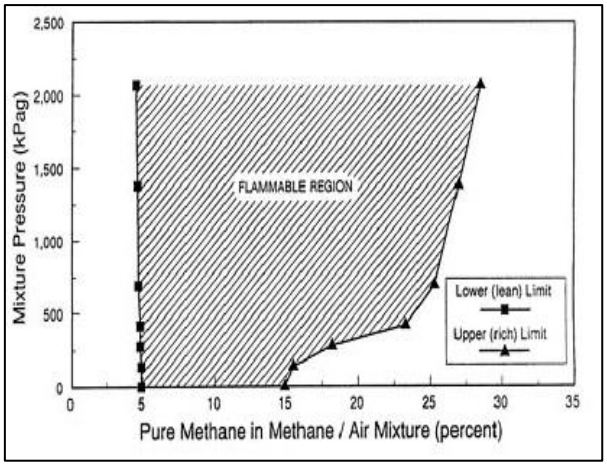


Figure 5-21 Effect of Pressure on the Flammability Limits of a Methane/Air Mixture (Mehta *et al.* 1998)

The figure shows that as the pressure increases, the lower flammability limit decreases slightly. However, the upper flammability limit can increase substantially as pressure increases. Hence, ignition of methane gas released at high pressure is more likely to sustain combustion as the pressure affects the flammability range.

Moreover, a fuel-air mixture can ignite without the introduction of an ignition source. The minimum auto-ignition temperature is the lowest temperature at which the gas vapours spontaneously ignite. Hydrocarbons that have been heated can ignite if they are exposed to air. Methane has the highest auto-ignition temperature as it contains only one carbon atom. Furthermore, the initial pressure that the gas is released can have an effect on its auto-ignition temperature. Caron *et al.* (1999) performed a series of experiments to determine the effect of methane/air mixtures at elevated pressures on the auto-ignition temperature. Figure 5-22 shows the effect of initial pressure on the auto-ignition temperature of methane in air.

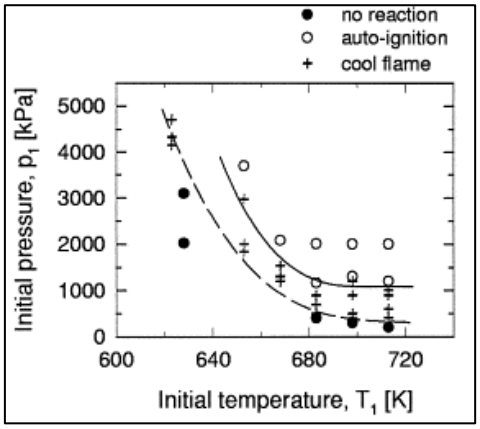


Figure 5-22 Effect of Initial Pressure on the Auto-Ignition Temperature of a Methane/Air Mixture (Caron *et al.* 1999)

The solid line in Figure 5-22 represents the pressures above which auto-ignition occurs for a methane concentration of 60 vol. %. It is evident from the figure that the higher the initial pressure of the methane/air mixture, the lower the auto-ignition temperature. Hence, a leak in Section 7 would release gas at very high pressures which can lower its auto-ignition temperature causing it to ignite without the presence of an ignition source. Thus, generating greater number of jet fires.

The frequency of occurrence of jet fires following an explosion or a pool fire is 1.082×10^{-1} per year. Table 5-34 shows the frequency of occurrence of delayed jet fires originating from each section of the compression module as well as the proportion each section contributes to the total frequency of delayed jet fires within the compression module. Similar proportion of delayed jet fires were produced by each section of the compression module.

Section	Frequency (per year)	Proportion (%)
3 - Low Pressure Scrubbers and Compressors	3.189E-02	29.483
4 – Medium Pressure Scrubbers, Coolers and Compressors – Stage 1	2.185E-02	20.195
5 - Medium Pressure Scrubbers, Coolers and Compressors – Stage 2	2.671E-02	24.687
7 – Injection Scrubbers, Coolers and Compressors	2.773E-02	25.635

Table 5-34 Jet Fire Frequency (per year) following delayed ignition of a leak in sections of the compression module

The frequency of delayed jet fires is greater than immediate jet fires which suggests that the majority of explosions and pool fires are followed by a jet fire.

The majority 57% of jet fires that occurred in the compression module lasted between 3.6 and 18 minutes as shown in Table 5-35 below. Only a small proportion of jet fires ≈ 0.1% lasted longer than 18 minutes. This can be due to the effective nature of the detection system in activating the isolation and blowdown valves, hence reducing the leak inventory. Moreover, no fires lasted longer than 54 minutes. This suggests that the deluge system was successful in extinguishing the jet fires without causing significant damage to the offshore oil and gas installation.

Fire Duration (mins)		Frequency (per year)	Proportion (%)
from	to		
0	3.6	6.818E-02	42.182
3.6	18	9.328E-02	57.711
18	36	1.710E-04	0.106
36	54	3.000E-06	0.002
54	72	0.000E+00	0.000
72	+	0.000E+00	0.000

Table 5-35 Jet Fire Duration for the Compression Module

Moreover, the majority 60% of jet fires that occurred in the compression module generated a flame length between 0 and 10 meters as shown in Table 5-36, below. Fires within enclosed modules are oxygen limited, and are extinguished if the release rate of gas from the leaking section exceeds the rate at which the gas is combusted. Moreover, as mentioned previously, the deluge system is also assumed to extinguish jet fires. Hence, the overall contribution of these factors result in the reduction of both jet fire flame length and duration.

Flame Length (m)		Frequency (per year)	Proportion (%)
from	to		
0	10	9.616E-02	60.059
10	20	4.374E-02	27.319
20	30	1.274E-02	7.957
30	40	3.686E-03	2.302
40	50	1.106E-03	0.691
50	60	1.117E-03	0.698
60	70	7.170E-04	0.448
70	80	3.630E-04	0.227
80	90	3.110E-04	0.194
90	+	1.697E-04	0.106

Table 5-36 Flame Length of the Jet Fire for the Compression Module

5.5.3.3 Pool Fires

No pool fires occurred within the compression module.

5.5.4 Wellhead Module

5.5.4.1 Explosions

The total frequency of occurrence of explosions estimated to occur in the wellhead module is 5.518 x 10^{-2} per year, accounting for 24% of all ignitions within the module. Table 5-37 shows the frequency of occurrence of explosions originating from each section of the wellhead module. As all sections of the wellhead module contain gas inventory, they are therefore capable of producing an explosion. The majority of explosions are predicted to occur from leaks in Section 10, which contains gas at high pressure.

Section	Frequency (per year)	Proportion of total explosions (%)
8 – Wellhead and Production Header Lines	1.147E-02	20.780
9 – Gas Injection Line	1.215E-02	22.027
10 – Gas Lift Line	3.156E-02	57.192

Table 5-37 Explosion Frequency (per year) from leaks in sections of the wellhead module

The frequencies of explosions in terms of the overpressures generated are shown in Table 5-38. Over 93% of all explosions predicted to occur within the wellhead module generate an overpressure of less than 1 bar. The frequency of explosions occurring with sufficient overpressure to fail the internal safety wall of the module, 0.6 bar, is 4.910 x 10^{-2} per year, while the frequency of explosions occurring with sufficient overpressure to fail the platform, 1.6 bar, is 2.310 x 10^{-3} per year.

Overpressure (bar)		Frequency (per year)	Proportion (%)
from	to		
0	1	5.114E-02	92.678
1	2	2.920E-03	5.292
2	3	9.430E-04	1.709
3	4	9.100E-05	0.165
4	5	2.600E-05	0.047
5	6	2.300E-05	0.042
6	7	2.600E-05	0.047
7	8	1.100E-05	0.020
8	+	0.000E+00	0.000

Table 5-38 Explosion Frequency (per year) for the different overpressures for the wellhead module

The explosion frequencies can also be further categorised with respect to the overpressures generated and the leaking section as shown in Table 5-39. It is evident from Table 5-39 that the largest proportion of explosions were generated by Section 9 with an overpressure between 0 and 1 bar, 1.010 x 10^{-2} per year. Moreover, due to the effective nature of the gas detection system and deluge system, only a small number of explosions generated an overpressure greater than 1 bar on all three sections of the wellhead module.

Overpressure (bar)		Frequency (per year)		
from	to	Section 8	Section 9	Section 10
0	1	1.020E-02	1.010E-02	3.080E-02
1	2	1.020E-03	1.370E-03	5.340E-04
2	3	2.060E-04	5.430E-04	1.940E-04
3	4	2.860E-06	5.430E-05	3.430E-05
4	5	0.000E+00	1.430E-05	1.140E-05
5	6	2.860E-06	1.710E-05	2.860E-06
6	7	2.860E-06	2.290E-05	0.000E+00
7	8	0.000E+00	8.570E-06	2.860E-06
8	+	0.000E+00	0.000E+00	0.000E+00

Table 5-39 Explosion Frequency (per year) for the different sections of the Wellhead Module

The explosion frequencies for different gas concentration ranges are shown in Table 5-40. It is evident from Table 5-40 that increasing the gas concentration range from 5-6% to 9-10%, increases the explosion frequencies. However, further increase of the gas concentration range results in a decrease of explosion frequencies. The largest proportion of explosions occur between 9 and 10% which is the optimum explosive mixture of methane and air.

Concentration Range	Explosion Frequencies (per year)
5-6	3.802E-03
6-7	4.331E-03
7-8	4.505E-03
8-9	4.520E-03
9-10	4.560E-03
10-11	4.311E-03
11-12	4.140E-03
12-13	2.000E-03
13-14	3.230E-03
14-15	3.802E-03

Table 5-40 Explosion Frequencies for each concentration range for the Wellhead Module

The frequencies of mitigated and unmitigated explosions for each concentration range for the wellhead module is shown in Table 5-41.

Concentration Range	Explosion Frequencies (per year)	
	Mitigated	Unmitigated
5-6	1.831E-03	1.971E-03
6-7	2.017E-03	2.314E-03
7-8	2.071E-03	2.434E-03
8-9	2.094E-03	2.426E-03
9-10	2.106E-03	2.454E-03
10-11	2.097E-03	2.214E-03
11-12	1.929E-03	2.211E-03
12-13	1.731E-03	2.690E-04
13-14	1.750E-03	1.480E-03
14-15	1.831E-03	1.971E-03
Total	**1.763E-02**	**1.777E-02**

Table 5-41 Mitigated and Unmitigated Explosion Frequencies for the wellhead module

Based on Table 5-41, unmitigated explosions occurred more frequently than mitigated explosions, accounting for 1.177×10^{-2} explosions per year. Further analysis reveals that most of the unmitigated explosions occurred due to Scenario 2, i.e. the deluge system is activated but the gas ignites during the time taken to get the water spray to a fully functional state, accounting for 2.039×10^{-2} explosions per year. The relative contribution of each scenario of the unmitigated explosion is shown in Table 5-42, below.

Scenario	Description	Explosion Frequencies (per year)
1	Deluge Fails to Activate	1.650E-04
2	Prior to Deluge being in Fully Functional state	2.039E-02
3	Water Spray not Maintained	1.120E-04

Table 5-42 Unmitigated Explosion Frequencies for the different unmitigated explosion scenarios for the Wellhead Module

5.5.4.2 Jet Fires

The frequency of occurrence of jet fires following immediate ignition of a leak in the wellhead module is 1.753×10^{-2} per year. Table 5-43 shows the frequency of occurrence of immediate jet fires originating from each section of the wellhead module as well as the proportion each section contributes to the total frequency of immediate jet fires within the wellhead module.

Similar proportion of immediate jet fires were produced by each section of the wellhead module.

Section	Frequency (per year)	Proportion of Jet Fires (%)
8 – Wellhead and Production Header Lines	6.649E-03	37.921
9 – Gas Injection Line	5.794E-03	33.044
10 – Gas Lift Line	5.091E-03	29.035

Table 5-43 Jet Fire Frequency (per year) following immediate ignition of a leak in sections of the wellhead module

The frequency of occurrence of jet fires following an explosion or a pool fire is 2.391 x 10^{-2} per year. Table 5-44 shows the frequency of occurrence of delayed jet fires originating from each section of the wellhead module as well as the proportion each section contributes to the total frequency of delayed jet fires within the compression module. The majority of jet fires are predicted to occur from leaks in Section 10 which accounted for approximately 42% of the total jet fires within the module. Section 10 contains more gas inventory than the other sections of the wellhead module which explains the high percentage of jet fires.

Section	Frequency (per year)	Proportion of Jet Fires (%)
8 – Wellhead and Production Header Lines	7.057E-03	29.512
9 – Gas Injection Line	6.889E-03	28.810
10 – Gas Lift Line	9.966E-03	41.678

Table 5-44 Jet Fire Frequency (per year) following delayed ignition of a leak in sections of the wellhead module

The frequency of delayed jet fires is greater than immediate jet fires which suggests that the majority of explosions and pool fires are followed by a jet fire.

The majority 99.8% of jet fires that occurred in the wellhead module lasted between 0 and 18 minutes as shown in Table 5-45 below. Only a small proportion of jet fires ≈ 0.2% lasted longer than 18 minutes. This can be due to the effective nature of the detection system in activating the isolation and blowdown valves, hence reducing the leak inventory.

Fire Duration (mins)		Frequency (per year)	Proportion (%)
from	to		
0	3.6	2.071E-02	50.159
3.6	18	2.050E-02	49.651
18	36	2.900E-05	0.070
36	54	1.700E-05	0.041
54	72	2.000E-05	0.048
72	+	1.230E-05	0.030

Table 5-45 Jet Fire Duration for the Wellhead Module

Moreover, the majority 56% of jet fires that occurred in the wellhead module generated a flame length between 0 and 10 meters as shown in Table 5-46, below. A small proportion of jet fires generated a flame length greater than 20 meters. This can be due to the effective nature of the deluge system which is assumed to have extinguished the jet fires. 1.4% of the jet fires generated a flame length greater than 90 meters. This would have been due to the failure of the deluge system to maintain the water spray for the duration of the fire.

Flame Length (m)		Frequency (per year)	Proportion (%)
from	to		
0	10	2.330E-02	56.219
10	20	8.011E-03	19.329
20	30	4.117E-03	9.934
30	40	2.306E-03	5.564
40	50	8.910E-04	2.150
50	60	8.260E-04	1.993
60	70	8.140E-04	1.964
70	80	3.690E-04	0.890
80	90	2.170E-04	0.524
90	+	5.940E-04	1.433

Table 5-46 Flame Length of the Jet Fire for the Wellhead Module

5.5.4.3 Pool Fires

The frequency of occurrence of pool fires estimated to occur in the wellhead module is 2.274 x 10^{-2} per year, accounting for 21% of all ignitions within the module. Table 5-47 shows the frequency of occurrence of pool fires originating from each section of the wellhead module as well as the proportion each section contributes to the total frequency of pool fires within the wellhead module. All pool fires are predicted to occur from leaks in Section 8. This is because Section 9 and 10 of the wellhead module contain no oil inventory.

Section	Frequency (per year)	Proportion (%)
8 – Wellhead and Production Header Lines	6.063E-03	100.0000
9 – Gas Injection Line	0.000E+00	0.0000
10 – Gas Lift Line	0.000E+00	0.0000

Table 5-47 Pool Fire Frequency (per year) for a leak in sections of the Wellhead Module

The majority 99% of pool fires that occurred in the wellhead module lasted between 0 and 3.6 minutes as shown in Table 5-48 below. No fires lasted longer than 216 minutes. This is a result of the deluge system functioning on demand and for the entire duration of the pool fire.

Fire Duration (mins)		Frequency (per year)	Proportion (%)
from	to		
0	3.6	5.966E-03	99.054
3.6	18	1.100E-05	0.183
18	36	6.000E-06	0.100
36	54	1.100E-05	0.183
54	72	3.000E-06	0.050
72	90	1.400E-05	0.232
90	108	0.000E+00	0.000
108	144	3.000E-06	0.050
144	180	6.000E-06	0.100
180	216	3.000E-06	0.050
216	252	0.000E+00	0.000
252	288	0.000E+00	0.000
288	+	4.000E-05	0.000

Table 5-48 Pool Fire Duration for the Wellhead Module

Moreover, the majority 99% of pool fires that occurred in the wellhead module generated a flame length between 0 and 1 meters as shown in Table 5-49, below. No fires generated a flame length greater than 2 meters.

Flame Length (m)		Frequency (per year)	Proportion (%)
from	to		
0	1	1.025E-02	98.520
1	2	1.540E-04	1.480
2	3	0.000E+00	0.000
3	4	0.000E+00	0.000
4	5	0.000E+00	0.000

5	6	0.000E+00	0.000
6	+	0.000E+00	0.000

Table 5-49 Flame Length of the Pool Fire for the Wellhead Module

5.6 Sensitivity Analysis of Offshore Fire and Explosion Model

Varying parameters such as ventilation rate, leak frequency and ignition probability would not have any significant effect on factors such as the operational costs and unavailability of the safety systems. Instead, parameters such as ignition probability would have only influenced the time at which ignition occurs, while the ventilation rate would have only affected the rate of increase of concentration of the gas cloud build-up within the module, and controls the rate of reduction of the volume of gas in the module when the ventilation rate exceeds the release rate. Hence, a sensitivity analysis of the Offshore Fire and Explosion model parameters was not considered as it only gives an indication on how to deal with operational issues rather than asset management issues.

5.7 Summary

The Platform Safety Model was demonstrated by application to the safety systems found on offshore oil and gas installations. The inputs of its Offshore Safety System Degradation and Maintenance sub-model are the distribution of times that a component degrades to a certain condition state, repair and inspection rates.

Simulation of this sub-model via Monte Carlo Simulation generates a variety of results that shows the future performance of the offshore safety systems and its components over a 35-year prediction period. In particular, the model can be used to predict future component conditions, expected number of maintenance interventions and failures and the costs of implementing different maintenance options. A system level analysis also permits the average downtime to be estimated as well as the contribution of the subsystem to the whole system downtime. These statistics are highly beneficial to offshore asset operations managers as they can be used to predict the amount of work necessary to ensure high availability of the safety systems and hence the expected costs, so that they can allocate resources and budget accordingly.

Moreover, a sensitivity analysis was carried out to study the effects of different input parameters on the unavailability and operational costs of the four safety systems under consideration. It is evident from the study that input parameters such as inspection interval and degradation rates have a significant effect on the system unavailability and operational costs. Hence, in order to improve the accuracy of the model, it is necessary to find accurate estimates of these parameters.

The Fire and Explosion model, on the other hand, works in conjunction with the Offshore Safety System Degradation and Maintenance Model. The model takes into consideration the operation of the offshore safety systems in the event a hydrocarbon leak occurs within the 35-year prediction period in either of the three main modules, i.e. the separation, compression and wellhead modules, of the offshore oil and gas installation. The inputs of the Offshore Fire and Explosion model include the hydrocarbon inventory data, section operating data and safety system availability data from the Offshore Safety System Degradation and Maintenance Model. Simulation of this model generates statistics such as frequencies of fires and explosions, flame lengths and overpressures generated under a specified asset management strategy of the safety systems. These statistics aim to provide guideline for risk analysis of offshore fire and explosion.

In summary, the Platform Safety Model developed in this research project supports offshore oil and gas companies to make improved decisions with regards to choosing the optimal inspection, maintenance and repair strategy that will minimise safety system failures and hence frequencies of fires and explosions. Unlike traditional models, the Petri Net based Platform Safety Model can be easily adapted to investigate degradation and failure of several offshore systems and are not limited to safety systems. The model can be easily used to gather information such as the effects of inspection and maintenance on offshore safety system performance and risks. Hence, it can be concluded that Petri Nets are an appropriate method for modelling asset management of offshore oil and gas installations.

Chapter 6 - Optimisation of the Platform Safety Model

6.1 Introduction

Accidental release of hydrocarbons on offshore oil and gas installations can lead to undesirable consequences with significant safety, environmental and commercial implications. For instance, immediate ignition of a high-pressure gas or oil release could result in a jet fire or pool fire with large flame lengths and could be long-lasting. Delayed ignition of a high-pressure gas cloud could result in an explosion which generates high overpressures. Offshore asset operations managers are under increasing pressure to minimise operational costs whilst maintaining reliability and availability targets, as well as operate within safety regulations. Therefore, the trade-off between conflicting objectives must be considered in a decision support process.

The Platform Safety Model is used to predict the frequency of a fire or explosion, the frequency of exceeding any level of overpressure and the frequency of unacceptable fires. These predictions are dependent on the reliability of the safety systems in place. Component inspection intervals and intervention strategies have a significant impact on the reliability of these systems, as well as the operational costs. Hence, an optimisation technique is required to find the optimal inspection, maintenance and repair strategy that will produce the lowest operational costs whilst minimising the frequencies of fires and explosions to an acceptable level.

The number of possible strategy combinations depends on numerous factors and because this number increases exponentially with the number of systems (N), the inspection interval (T), and the number of maintenance alternatives (M), selecting the optimum inspection, maintenance and repair strategy is a challenging task. The simplest way to find the optimum solution is by exhaustively evaluating all possible candidate solutions to find the best one. However, this can be computationally expensive and time consuming. Therefore, an appropriate optimisation technique is required to find the most suitable one. A brief overview of different optimisation techniques have been outlined in Section 6.2.

6.2 Overview of Optimisation Techniques

Optimisation can be defined as a task of finding the input of the process which yield the maximum or minimum output. The input consists of variables; the process is known as an objective function; and the output is a cost or fitness. Classically, the optimisation problem is defined using a single objective function, shown as follows:

$$\min \boldsymbol{Q}(\boldsymbol{x}) \tag{115}$$

$$\text{subject to} \quad \boldsymbol{g_i}(\boldsymbol{x}) \geq \mathbf{0}, \qquad \boldsymbol{i} = \mathbf{1}, \cdots, \boldsymbol{m} \tag{116}$$

$$\boldsymbol{h_i}(\boldsymbol{x}) = \mathbf{0}, \qquad \boldsymbol{j} = \mathbf{1}, \cdots, \boldsymbol{p} \tag{117}$$

where, the objective function, Q(x), must be minimised subject to the m inequality constraint functions, $g_i(x)$, and the n equality constraint functions, $h_i(x)$, using the design vector, x, to provide a solution vector x*.

There are many techniques which can be used to solve such a problem. Some of these candidate methods are discussed below:

6.2.1 Mathematical Programming

Two types of mathematical programming methods exist: (1) Direct and (2) Indirect methods. Direct methods move from a starting point through consistently improved values of the objective function to an optimum solution. Indirect methods, on the other hand, solve a set of algebraic equations and the solution obtained is the optimum of the objective function.

6.2.1.1 Indirect Methods

There are two types of indirect methods (Pike 1986): (1) Analytical methods and (2) Geometric Programming. Analytical methods also referred to as the classical theory of maxima and minima. It is concerned with identifying the extreme points of a function. Geometric programming is an extension of analytical methods. Both methods require a well-defined objective function. However, when a specific algebraic objective function does not exist, indirect methods can be dismissed. Hence, they are not considered any further.

6.2.1.2 Direct Methods

6.2.1.2.1 Linear Programming

A model is a linear program when the objective function and constraints contain linear expressions and the decision variables are continuous (Ho and Ji 2006). The linear programming problem may be expressed in standard form as follows:

$$\textbf{min} \sum_{i=1}^{n} c_i x_i \tag{118}$$

$$\textbf{subject to} \quad \sum_{i=1}^{n} a_{ij} x_i = b_j, \qquad j = 1, \cdots, m \tag{119}$$

$$\textbf{and} \quad x_i \geq 0, \qquad i = 1, \cdots, n \tag{120}$$

where, **x** is the column vector of n components that we wish to determine. Note that each element of **x** is constrained to be greater than 0. This is a common requirement in this type of optimisation because most practical optimisation problems will require nonnegative values for **x**. The given constants of the system are provided by an **m** component column vector **b**, an m x n matrix **a**, and an **n** component column vector **c**.

Although a general form has been presented, many other forms of this problem arise that are easily converted to the canonical form. For instance, the constraints may initially be inequalities and these can be converted to the equalities by introducing slack and surplus variables:

$$\textbf{slack} \qquad \sum_{i=1}^{n} a_{ij} x_i \leq b_j \quad \textbf{gives} \quad \sum_{i=1}^{n} a_{ij} x_i + y_j = b_j \tag{121}$$

$$\textbf{surplus} \qquad \sum_{i=1}^{n} a_{ij} x_i \geq b_j \quad \textbf{gives} \quad \sum_{i=1}^{n} a_{ij} x_i - y_j = b_j \tag{122}$$

where, $y_j \geq 0$. Variables which are not required to be nonnegative can be transformed via:

$$x_k = u_k - v_k \quad k = 1, \cdots, p \tag{123}$$

where, $u_k \geq 0$ and $v_k \geq 0$. Substituting this form retains the linear form of the problem and requires all variables to be nonnegative. This problem now has n+p variables and a degree of redundancy since the representation of x_k is not unique. To overcome this, x_k is eliminated by using a constraint equation and is written in terms of other nonnegative variables giving the standard linear form with n-p variables and m-p constraints.

Linear programming problems can be solved via many algorithms, e.g. the simplex algorithm (Dantzig 1951) and the interior point method (Karmarkar 1984). Ho and Ji (2006) defines algorithm as “a set of fixed computational rules for solving a particular class of problems. It

applies the rules repeatedly to the problem, each iteration moves the solution closer to the optimum solution".

The main advantage of linear programming is its simplicity. However, it is unable to deal with problems that consist of more than one objective function. Most real life problems often involve multiple and even conflicting objectives. Hence, in such cases, linear programming would be deemed inappropriate.

6.2.1.2.2 Nonlinear Programming and Multi-Variable Search Methods

Nonlinear programming is quite similar to linear programming as it contains an objective function, general constrains and variable bounds. However, nonlinear programming contains at least one nonlinear function. This could either be the objective function or some or all of the constraints. Multi-variable search methods incorporate the theory and algorithms of nonlinear programming. These methods start at a feasible starting point and move towards the optimum solution in steps of improved values.

Constrained nonlinear programming problems can be solved via many different algorithms, which include: generalised reduced gradient method (Frank and Wolfe 1956), sequential linear programming (Griffith and Stewart 1961), sequential quadratic programming (Wilson 1963), augmented Lagrangian method (Hestenes 1969), feasible direction methods (Zoutendijk 1970), penalty (Broyden and Attia 1988) and barrier methods (Fiacco and McCormick 1990).Unconstrained nonlinear programming problems can be solved via methods such as the Quasi-Newton method (Davidon 1991) and the conjugate-gradient method (Fletcher and Reeves 1964).

However, the convergence rate of nonlinear programming techniques is slow. Hence for applications in which repetitive solutions are required such as the reliability assessment of offshore oil and gas safety systems, nonlinear programming techniques can prove computationally expensive. In addition, for a specific type of engineering problem, the objective function can be non-differentiable. Hence, this could limit the use of nonlinear programming techniques in handling certain objective functions.

6.2.1.2.3 Integer Programming

Integer programming is an extension of linear programming. The only difference between integer programming problems and linear programming problems is that one or more of the decision variables must be integer, i.e. take discrete values. An all-integer programming problem is one where all decision variables are constrained to take only integer values. A mixed-integer programming problem is one where only some decision variables are constrained to take integer values, with the remainder being continuous. A zero-one programming problem is one where all design variables are constrained to take on values of either 0 or 1.

All integer programming problems have an associated linear programming problem which is identical except for allowing all the variables to take non integer values. These are known as discrete problems and their standard form is given as follows:

$$\boldsymbol{min\ Q(x)} \quad \textbf{(124)}$$

$$\textbf{subject to} \quad \boldsymbol{x \in R \quad x_i \in \mathbf{Z}^{+}\ \forall i \in I} \quad \textbf{(125)}$$

where, I is the set of integer values and R is the feasible region of the continuous problem.

However, unlike linear programming problems, integer programming problems are difficult to solve as no efficient general algorithm is known for their solution. Algorithms for integer programming problems rely on two basic concepts: (1) relaxations and (2) bounds. Hence, before an integer programming algorithm can be applied, the integer restriction on the problem should be relaxed first to form a linear programming model. Two main algorithms for solving integer programming problems include:

1. The Branch-and-Bound Algorithm

The branch-and-bound algorithm (Land and Doig 1960) consists of two strategies, alternately followed, till the desired solution is obtained. One strategy involves dividing the complete feasible solution space of the problem into two sub-problems, and the other strategy involves solving the two sub-problems to obtain the lower bound or upper bound of the objective function, if the original problem is to minimise or maximise the objective respectively. The advantage of exhaustive search techniques like branch-and-bound methods is that an optimal

solution can be found. However, most problems are complicated which means that the computational time is unacceptable for large instances of the problem.

2. The Cutting-Plane Algorithm

The cutting-plane algorithm (Dantzig 1959) involves the addition of extra constraints (i.e. cutting planes) to reduce the feasible region until the continuous problem is solved. The new solution to the further constrained mode may or may not be an integer (Ho and Ji 2006). Hence, the integer programming problem can be solved by continuing the process until an integer solution is found. One main disadvantage of the cutting-plane algorithm is that the size of the linear programming sub-problems increases with every iteration. This is because cutting plane constraints are always added to the existing set of constraints and are never deleted. Moreover, as an exponential number of iterations may be required to find the optimal solution, the computational time increases significantly.

6.2.1.2.4 Heuristic and Metaheuristic Algorithms

Although, algorithms are able to produce solutions for most programming problems, the computational effort required is an exponential function of the problem size (Ho and Ji 2006). For instance, consider a problem with 20 discrete variables which can each take on 30 values, the number of possible solutions is equal to 30^{20}. This means that 3×10^{29} combinations would need to be searched. Algorithms are only effective when used to solve small instances to optimality. For large problems, methods commonly struggle to generate an optimal solution within a reasonable amount of time. In this case, heuristics algorithms may offer better performance guarantees than any algorithm and are likely to lead to a solution that is approximately optimal or near-optimal.

There are different types of heuristics algorithms such as (1) Constructive Algorithm and (2) Local Search Algorithm. Constructive algorithms start from an empty solution and iteratively add new elements to an initial empty “partial” solution, until a complete solution is found. Local search algorithms, on the other hand, explore the neighbourhood of the current solution. If the neighbouring solution has a better objective value than the current solution, it becomes the new current solution. This process is iterated until there is no possibility of improvement in the neighbouring solution.

One of the main disadvantages of the local search algorithms is that it terminates at a point called local optimum, which may be far from any global optimum. To overcome this limitation, metaheuristic algorithms can be used to find near-optimal solutions. These include:

1. Simulated Annealing Algorithm

The simulated annealing algorithm (Kirkpatrick *et al.* 1983) is based on the analogy between the simulation of the annealing of solids and the problem of solving large combinatorial optimisation problems. Annealing is a physical process in which a solid in a heat bath is heated by increasing the temperature of the heat bath to a maximum value. This causes the solid to melt. The heat bath is then cooled slowly. As a result, all the particles arrange themselves in the low energy ground state of a corresponding lattice, as long as the maximum temperature is sufficiently high and the cooling is carried out sufficiently slowly. This concept of the natural process of finding a minimum energy state can be used to find the global optima of given nonlinear functions.

At each iteration, a new point is randomly generated. The distance between the new point and the current point is based on a probability distribution with a scale proportional to the temperature. The objective function of each point is evaluated. If the new point has a better function value than the current point, it is replaces the current point. The algorithm accepts all new points that lower the objective as well as with a certain probability, the new points that raise the objective. Acceptance of the points that raise the objective, allows the algorithm to avoid getting trapped in a local minima during early iterations and it is able to explore globally for better solutions.

Simulated annealing is capable of dealing with highly nonlinear programming problems with several constraints. The technique is robust and relatively easy to apply even for complex problems. Moreover, unlike local search algorithms, simulated annealing is not restricted to finding the local optima. The solutions obtained via these techniques are close to the global minimum with a polynomial upper bound for the computational time and are independent of initial conditions. However, it can be difficult to find a suitable acceptable criteria to decide the probabilities of moving from one solution to another. There is a clear trade-off between the quality of the approximate solutions and the time required to compute them.

2. Genetic Algorithm

Genetic algorithms (GA) (Holland 1975) are search algorithms based on the principles of natural selection and Darwin's theory of survival of the fittest (Goldberg 1989) to solve optimisation problems. Given a population of individuals, natural selection promotes survival of the fittest individuals from one generation to another. Figure 6-1 shows the main steps of the GA process.

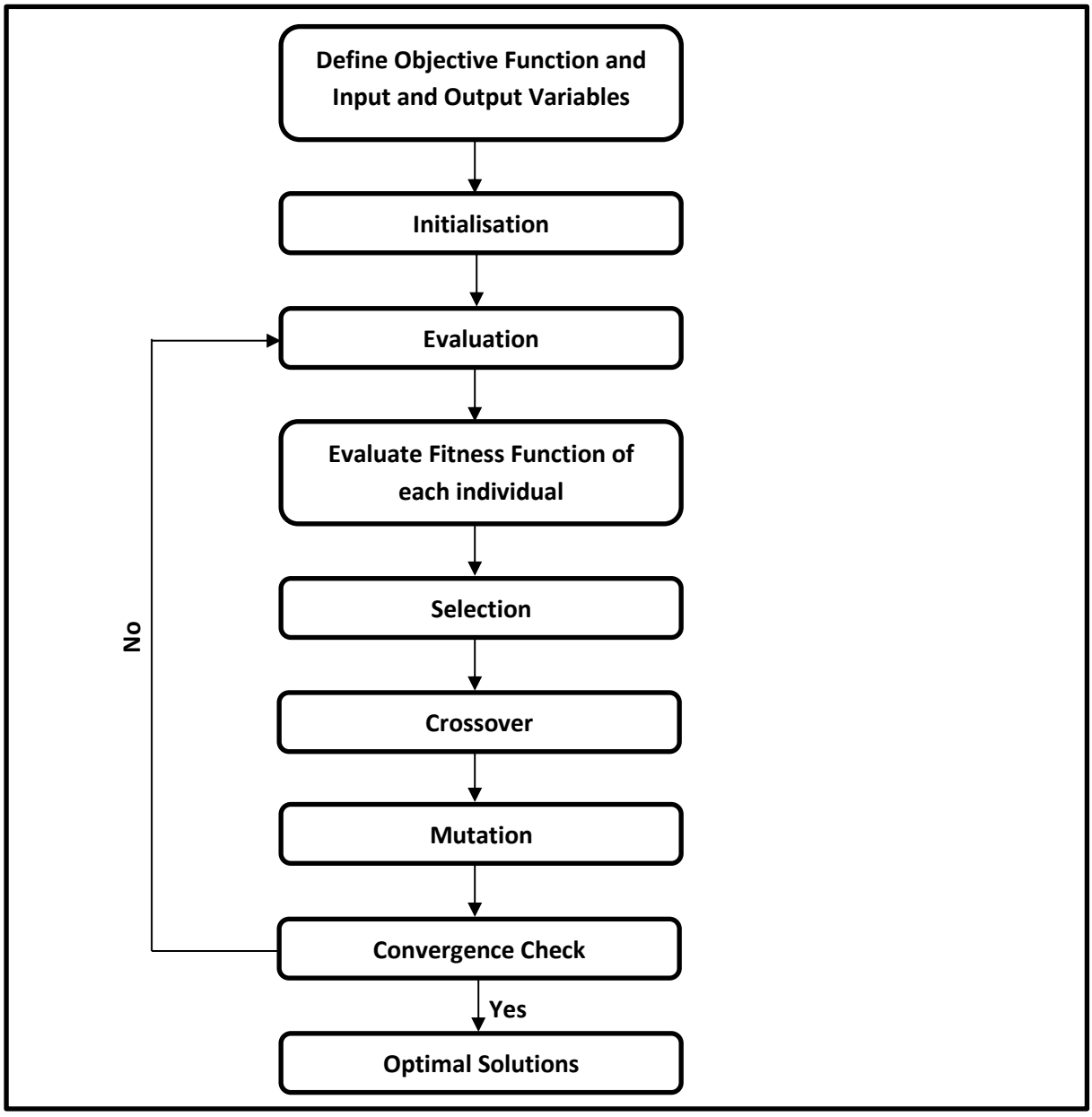


Figure 6-1 Flowchart showing the Genetic Algorithm Process

The first step of the GA process is to define the objective function and the variables to be optimised. The user must decide which variables of the problem are most important. Too many variables can obstruct the GA process.

The next step is initialisation which randomly generates a set of strings (chromosomes) referred to as a population of individuals. Each chromosome represents a potential solution to the optimisation problem. The chromosome can be constituted with an orderly alignment of binary or real coded variables of the system. Each of these variables are referred to as genes. A gene is characterised by its position in the chromosome and a set of possible values, also known as alleles. The choice of coding type; binary or real, is dependent on the number and type of variables (real or integer). Each gene is allowed a range of feasible values called search space.

Evaluation decodes binary strings and each chromosome of population of generation i is evaluated to give a measure of fitness. The fitness of a chromosome is measured via a function called the objective function or fitness function. Selection selects chromosomes from the current population according to the selection probability. Chromosomes with larger fitness value are retained in the next generation, while those with the lowest fitness value are discarded. The selected chromosomes act as parents to crossover and produce offspring. Crossover can either be of a: single-point or two-point. In a single-point crossover, the parent chromosomes are cut at some random position and their segments are swapped to form children chromosomes. In a two-point crossover, there will be two break points in the parent chromosomes that are randomly chosen. At the breakpoint, the segment of the two chromosomes are swapped to create children chromosomes. An example of the crossover process is shown in Figure 6-2 below.

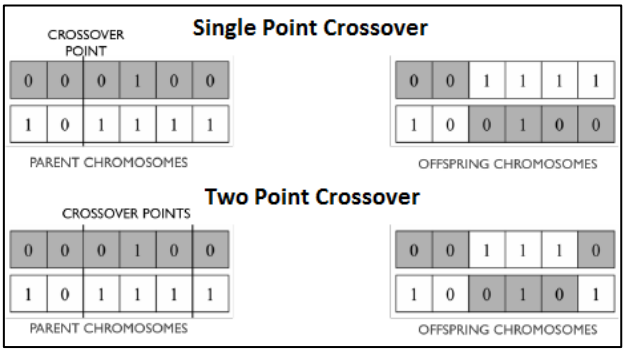


Figure 6-2 Example of the Crossover Process

Newly reproduced chromosomes are then transferred to a mutation pool. The mutation operator alters one or more gene values in a chromosome. Mutation maintains diversity within the population by increasing the search space and prevents premature convergence to a local optimal point. The new population will then go through the same process where each individual is decoded for the fitness value evaluation. Once the population has converged, i.e. produce similar fitness value, the algorithm terminates. The best chromosome in a population represents the optimal or near-optimal solutions to the problem.

GAs have been demonstrated to provide globally optimal solutions for a wide range of engineering problems (Goldberg, 1989). Unlike traditional methods, GA searches from a population of points rather than a single point. GAs ability to parallel process points reduces the risk of locating false peaks in multimodal search spaces and allows faster computation. GAs works with a coding of variables, i.e. with a discrete search space, rather than using the variables directly. Moreover, GA uses objective function information, instead of derivatives like gradient techniques in order to climb the current peak. To guide their search, GAs use probabilistic transition rules rather than fixed transition rules to move from one solution to another and an initial random population. GA is more robust than transitional methods due to its ability to handle a broad range of problem types.

6.3 Discussion

A range of optimisation algorithms are available to find the optimum solution to different optimisation problems. GA has been chosen to optimise problems solved by the Platform Safety Model developed in this research due to their flexibility to solve a wide range of optimisation problems as seen in previous research studies with a diversity of variables (continuous or discrete) and constraint types. Moreover, it is important to note that GA can provide a set of optimum solutions, not just one optimum solution like traditional methods. This feature is particularly useful when optimising multi-objective problems like the one considered in this research in which there is more than one objective. In multi-objective problems, the fitness of each individual is reported as multiple values. In this case, there is usually no single optimal solution instead a set of optimal solutions. Each solution represents a trade-off between the objectives and all of the optimal solutions have the same fitness rank known as Pareto-optimal set. The choice of the final solution is dependent on the user. Hence,

due to the various advantages outlined, multi-objective GA has been used to optimise the problem at hand. Application of multi-objective GA to the current optimisation problem is outlined in Section 6.4.

6.4 Offshore Risk Optimisation

6.4.1 Objective Function

The Platform Safety Model was implemented using standard Petri Nets with high level extensions as previously described in Chapter 4. The model is divided into two sub models: (1) Offshore Safety System Degradation and Maintenance Model and (2) Offshore Fire and Explosion Model. The Offshore Safety System Degradation and Maintenance Model simulates the life of all offshore safety system components and the effects of degradation, failure, inspection and maintenance on them. The main outputs of this model include unavailability and the operational cost over a chosen time period for each safety system. The Offshore Fire and Explosion Model, on the other hand, simulates the effect of a hydrocarbon leak from a process vessel located within the three main modules of an offshore oil and gas installation in the event that the safety system. The main outputs of this model include the frequencies of the fires and explosions generated and the magnitude of the fires in terms of the flame length generated, the duration of the fires and the magnitude of the explosions in terms of the overpressures generated.

Problems solved by both models can be optimised with respect to a variety of objectives that depend on specific requirements for the offshore oil and gas asset. For the modelling purposes of this research, it is of interest to optimise a number of objectives at the same time. The three objectives selected in this optimisation study are to find an asset management strategy that minimises the operational costs, frequencies of fires and explosions to an acceptable level.

A typical platform can be designed to withstand overpressures of up to around 3 bar and flame lengths of up to 10 meters and fire duration of up to around 15 minutes. Assuming that an offshore oil and gas installation has been designed and constructed to this threshold limit, our aim is to minimise the risk of events capable of generating overpressures exceeding 3 bar, flame lengths exceeding 10 meters and fire durations exceeding 15 minutes.

The objective functions used in the optimisation method in this study are defined as follows:

$$\boldsymbol{f_1 = min\ P(operational\ cost)} \quad \textbf{(126)}$$

where,

$$\textbf{Operational Cost} = \sum_{i=1}^{N}\left(\boldsymbol{n_1^i \times C_1^i + n_2^i \times C_2^i + n_3^i \times C_3^i}\right) + \boldsymbol{N_I C_I} \quad \textbf{(127)}$$

where, i ≥ 1, i ∈ N

N is the number of safety system components

n_1^i is the expected number of minor preventive repairs on component *i*

n_2^i is the expected number of major preventive repairs on component *i*

n_3^i is the expected number of corrective repairs on component *i*

C_1^i is the cost of minor preventive repair on component *i*

C_2^i is the cost of major preventive repair on component *i*

C_3^i is the cost of corrective repair and downtime on component *i*

N_I is the number of inspections

C_I is the cost of inspection

$$\boldsymbol{f_2 = min\ P(unacceptable\ fires\ with\ flame\ lengths\ above\ 10\ meters\ threshold\ and\ duration\ \ over\ 15\ minutes\ threshold}\ ) \quad \textbf{(128)}$$

$$\boldsymbol{f_3 = min\ P(explosion\ overpressure\ above\ 3\ bar\ threshold)} \quad \textbf{(129)}$$

6.4.2 Variables

The following input variables were considered:

1. Inspection Interval
2. Opportunistic Maintenance
3. Maximum Number of Minor Repairs
4. Maximum Number of Major Repairs

Table 6-1 summaries the possible values each of the above variables can take.

Variable Number	Input Variables	Binary Representation	Possible Values	Number of options for the selected variable	Number of bits required to represent variable selection
1	Inspection Interval	00 01 10 11	168 730 1460 2190	4	2
2	Opportunistic Maintenance	0 1	Disabled Enabled	2	1
3	Maximum Number of Minor Repairs	00 01 10 11	0 1 2 3	4	2
4	Maximum Number of Major Repairs	00 01 10 11	0 1 2 3	4	2

Table 6-1 Input Variables and their value range

6.4.3 Evaluation

Each variable is represented by a string of bits and a bit can take a value of 0 and 1, depending on the range of possible values that a particular input variable can take. For instance, variable 1 can take 4 values, so a 2 bit string is used to represent these $2^2 = 4$ options. Variable 2 can take 2 values, so 1 bit string is used to represent these $2^1 = 2$ options. Hence, a 14 bit long string is used to represent a safety system as shown below:

$$Safety\ System = \underbrace{\overbrace{01}^{2\ bits}}_{var\ 1}\ \underbrace{\overbrace{1}^{1\ bit}}_{var\ 2}\ \underbrace{\overbrace{00}^{2\ bits}}_{var\ 3}\ \underbrace{\overbrace{11}^{2\ bits}}_{var\ 4}$$

Figure 6-3 14 bit string is used to code the input variables for a single safety system

The binary strings provides a mapping of each possible value of any input variable. For instance, a 2 bit string is used to represent the input variable 1 (var 1 in Figure 6-2) - 'inspection interval'. When this binary string is decoded it gives these possible values: 00, 01, 10, and 11. However, the inspection interval takes the following values: 168, 730, 1460 and 2190. For example, the coding then maps value '01' (value for var 1 in Figure 6-2) to represent '730' hours inspection interval.

6.4.4 Initialisation

Each full set of variables with its specific values is known as an individual. To solve the problem, an initial population of individuals is randomly generated, with each individual representing a random possible solution to the problem. In the present application, a population size of 50 was chosen. The choice of population size can affect the run time of the GA by several orders of magnitude. De Jong (1975) carried out a study on GA parameters and found that a small population size improved initial performance, however, premature convergence can occur, i.e. the GA rapidly converges to a sub-optimal solution, as only a small part of search space is explored. A large population size, on the other hand, improved long-term performance, i.e. the GA converges to near-optimal solutions. However, an excessive number of iterations are required when solving problems with a substantial number of parameters which slows down the GA process (Jain and Jain 1997). Experiments conducted by De Jong (1975) indicated that the best population size was 50 – 100 individuals.

6.4.5 Evaluating the Fitness Function of Each Individual

The fitness function value is calculated for each individual of the population. For instance, if we were to optimise the operational costs, the objective function is used to evaluate the operational cost for each individual. A fitness function then determines the fittest individual by implementing a ranking system which ranks the operational cost produced by each individual. The individual which produces the lowest operational cost is considered as the fittest individual in the population.

6.4.6 Selection and Reproduction

6.4.6.1 Pareto Ranking

In a single objective optimisation problem, the fitness of each individual is relatively easy to rank as the individual with the best objective function value is the best solution for the problem. However, in a multi-objective optimisation, a criterion does not exist which concludes that one solution is better than another as no total order exists in a set of solutions. Thus, a particular ranking technique known as Pareto Ranking (Fonseca and Fleming 1995) is employed. The method ranks each individual according to a degree of dominance. Figure 6-4 demonstrates the objective ranking procedure.

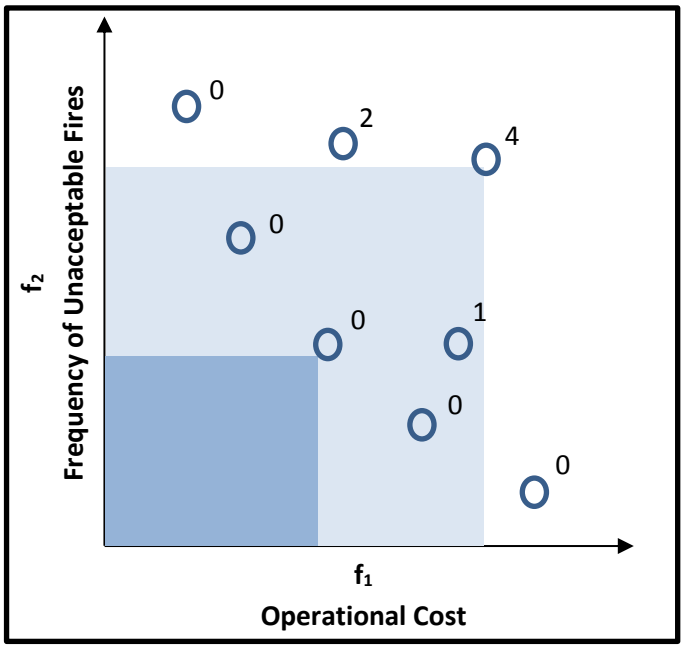


Figure 6-4 Pareto Ranking

The figure shows a trade-off between two objective values, f_1: operational costs and f_2: frequency of unacceptable fires. The fitness value for each individual in a population is evaluated and a population of candidate solutions is plotted as shown in Figure 6-4.

The candidate solution labelled '4' is dominated by four solutions within the rectangle of which it is a vertex. This means that the candidate solution is dominated by four other solutions that have better values of both objectives in this problem.

Nondominated or Pareto-optimal solutions are labelled as '0' as no other candidate solutions exist which improve on both of their criterion values. The boundary that these nondominated solutions form is called the Pareto-optimal Front.

In this research, a trade-off between three objective functions is considered, hence, the Pareto-optimal front is three-dimensional. However, the performance of the algorithm is difficult to evaluate from a three-dimensional Pareto surface. Therefore, the three projections of the Pareto surface onto the corresponding two-dimensional planes are provided instead.

6.4.6.2 Selection Rate

In order to maintain diversity in the current nondominated front, parameter known as selection rate is used. The selection rate limits the number of individuals on the Pareto front (elite members). It decides how many individuals are to be retained for the next generation. If only a few are selected, the number of genes available for the next generation is limited. However, selecting too many would allow a bad candidate solution the chance to contribute bad genes to the next generation. In this optimisation study, the selection fraction is set to 0.5 which means that if the Pareto-optimal front consist of 20 individuals, only 10 are retained for the next step giving 40 free spaces to be filled in the next step. The 10 individuals are also known as elite.

6.4.6.3 Ranking Selection

Individuals are mated to create offspring and this process is repeated until the remaining 40 places are occupied with new offspring. In this study, ranking selection (Bauer 1994) is the method chosen to pair the individuals. Ranking selection assigns probabilities to each individual. The biggest probability is allocated for the fittest individual to be chosen for recombination. The cumulative probabilities sum is then calculated. A random number between 0 and 1 is generated. The first individual with the cumulative sum greater than the random number is chosen. The process is repeated to identify the second individual to pair. However, in some cases, the individual might get selected twice. To avoid the individual pairing with itself, the process is repeated until a different individual is selected.

6.4.7 Crossover

The frequency in which crossover is applied also has an effect on the overall performance of the GA. Changing the crossover rate adjusts the chance in which solutions in the population will have the crossover operation applied to them (Jacobson and Kanber 2015). A high crossover rate allows for many new, potentially superior, solutions to be found during the crossover process. A low crossover rate allows the transfer of genetic information from fitter individuals to the next generation. Hence, the crossover rate should be set to a reasonably high rate as it allows us to search for new solutions while allowing a small percentage of population to retain genetic information from fitter individuals for the next generation. In this optimisation study, a single-point crossover is chosen and the crossover probability is set to

0.8. The crossover process is repeated for each pair of parent chromosomes that are selected. Once all the children chromosomes are generated, the next generation of the population will be the same size, i.e. it will consist of 50 individuals, where 10 are elite individuals from the previous generation and 40 are children.

6.4.8 Mutation

The mutation rate indicates what percentage of the total number of bits in a population will mutate. In this optimisation study, each individual is a 14 bit string in a population size of 50. This creates a population of 14 x 50 = 700 bits. A bitwise mutation rate of 0.01 is used, which means that a bit-string chromosome with 700 bits in it has, on average, 7 bit flip mutations per generation. There is no correct value for the mutation rate, however, some mutation rates provide better results than others. A higher mutation rate allows for more genetic diversity in the population and prevents premature convergence to a local optimum point. However, if the mutation rate is too high it can cause too much genetic variation between each generation causing it to lose good solutions it found in its previous population. Moreover, if the mutation rate is too low it can slow down the GA process significantly hindering its ability to find a satisfactory solution. Hence, the mutation rate is set to a value that allows for enough diversity to prevent the algorithm plateauing, however, not so much that it causes the algorithm to lose valuable genetic information from the previous population. Moreover, one limitation of mutation is that it also mutates the best solutions which can prevent the GA converging to the best solutions. To prevent this from occurring, an algorithm is developed to prevent mutation on the elite individuals from the previous generation.

6.4.9 Next Generation and Convergence

After mutation, the fitness of each individual is evaluated and the process of direct selection, crossover and mutation process is repeated for several generations. The algorithm is terminated when the generations converge, i.e. no progress in fitness value is observed in the population for several generations. In this study, the GA was set to 100 generations and algorithm is considered to have converged when all the individuals are in the top rank (rank 0 – the first Pareto Front).

6.5 Results and Discussion

6.5.1.1 Optimum Policies

Figure 6-5 shows the fitness of the population at Generation 1. The optimisation initiates with a population of 50 randomly generated inspection, maintenance and repair strategies. The fitness of each individual is evaluated and plotted as shown below.

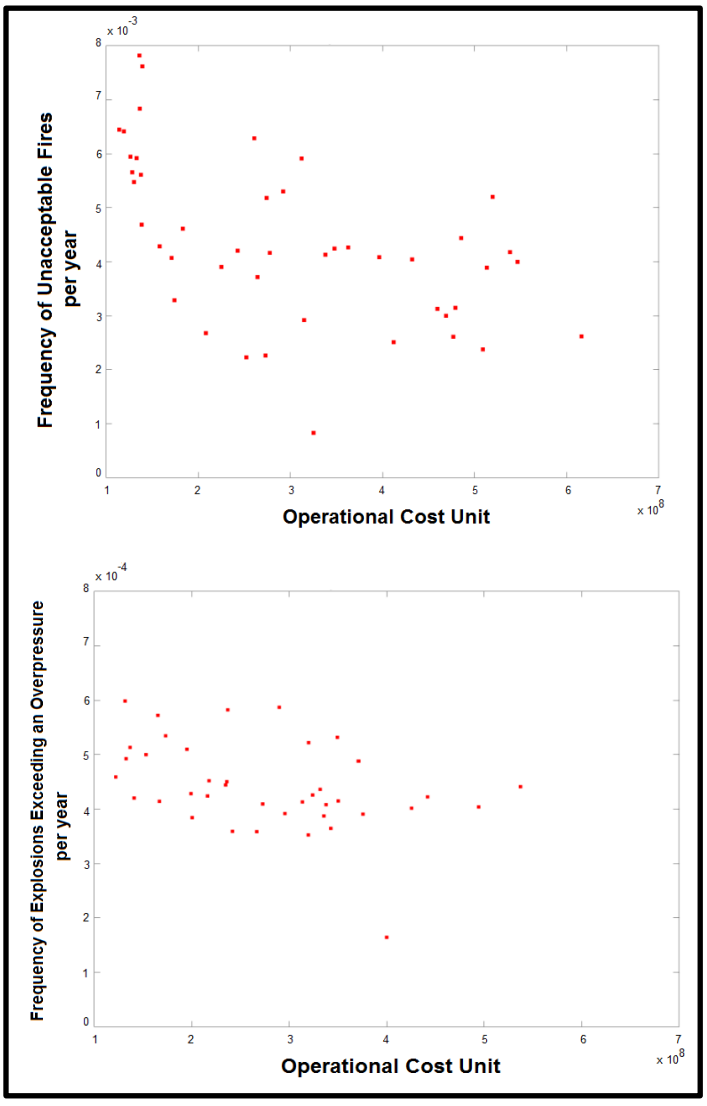


Figure 6-5 Fitness of the Population: Generation 1

As the number of generations' increases, the fitness of the population gradually improves as shown in Figures 6-6, 6-7 and 6-8 for generations 10, 20 and 30, respectively.

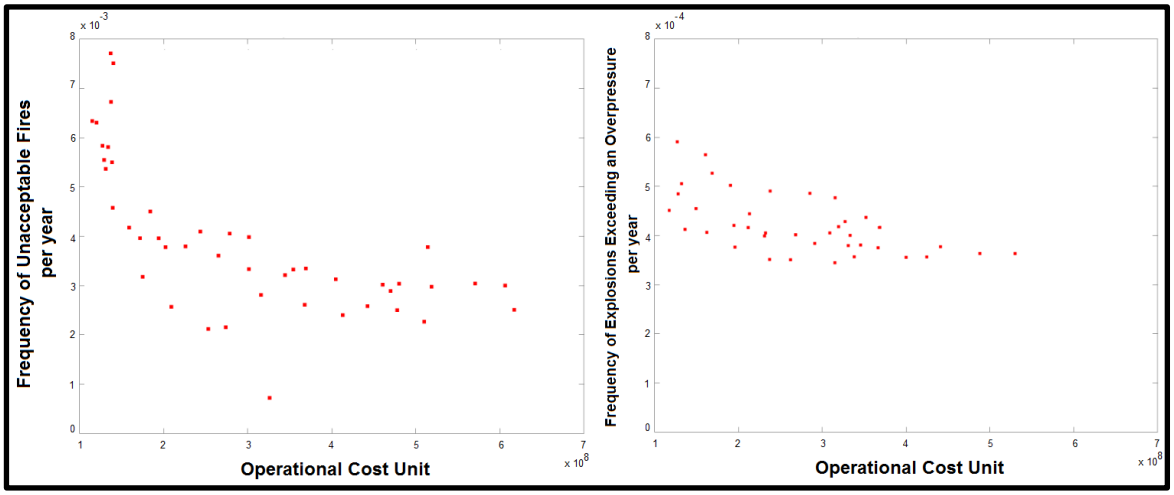
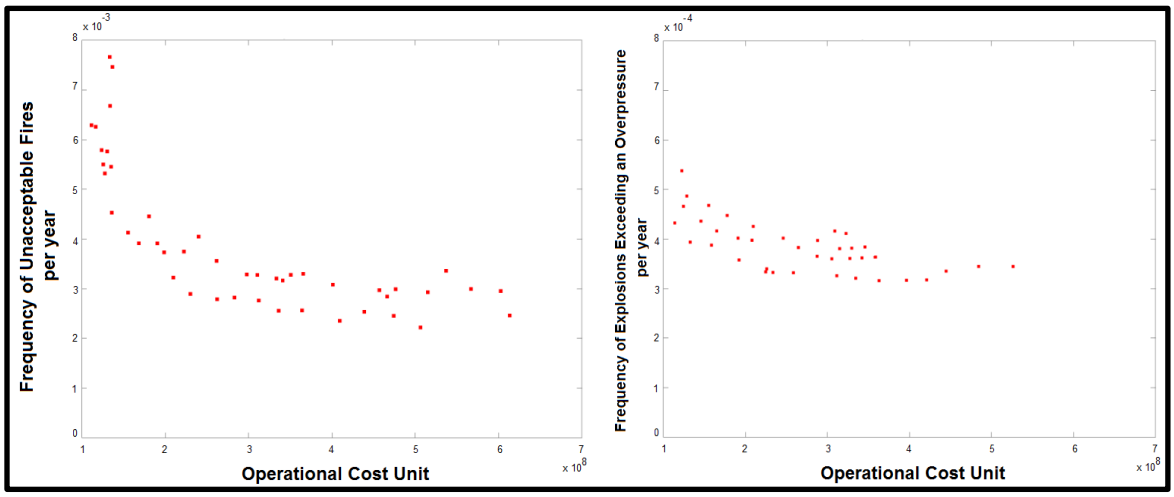


Figure 6-6 Fitness of the Population: Generation 10



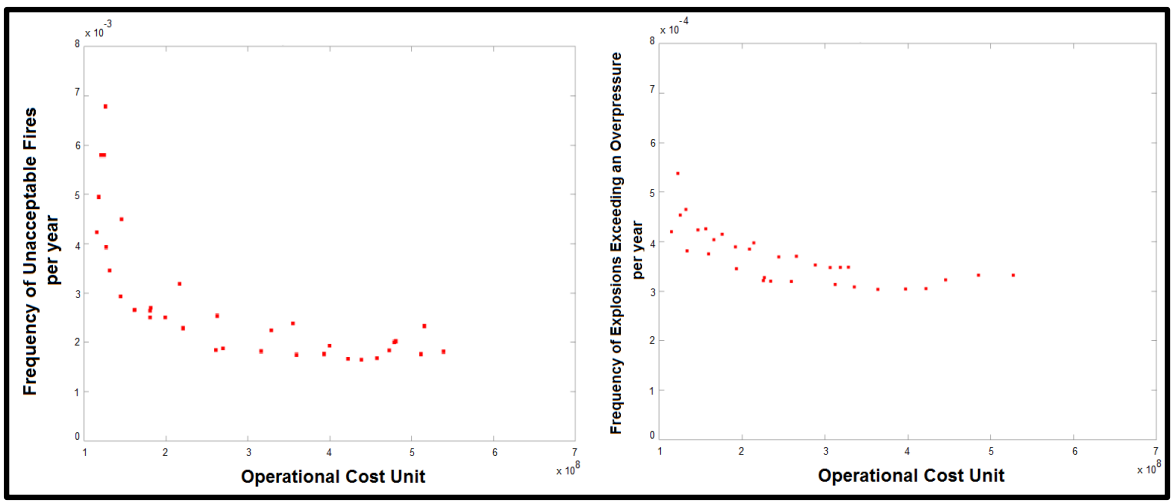


Figure 6-8 Fitness of the Population: Generation 30

The GA process continues until convergence is achieved by Generation 40 as a well-defined Pareto-optimal front is achieved as shown in Figure 6-9, below. There has been little change in the fitness of the individuals that exist in the population for several generations.

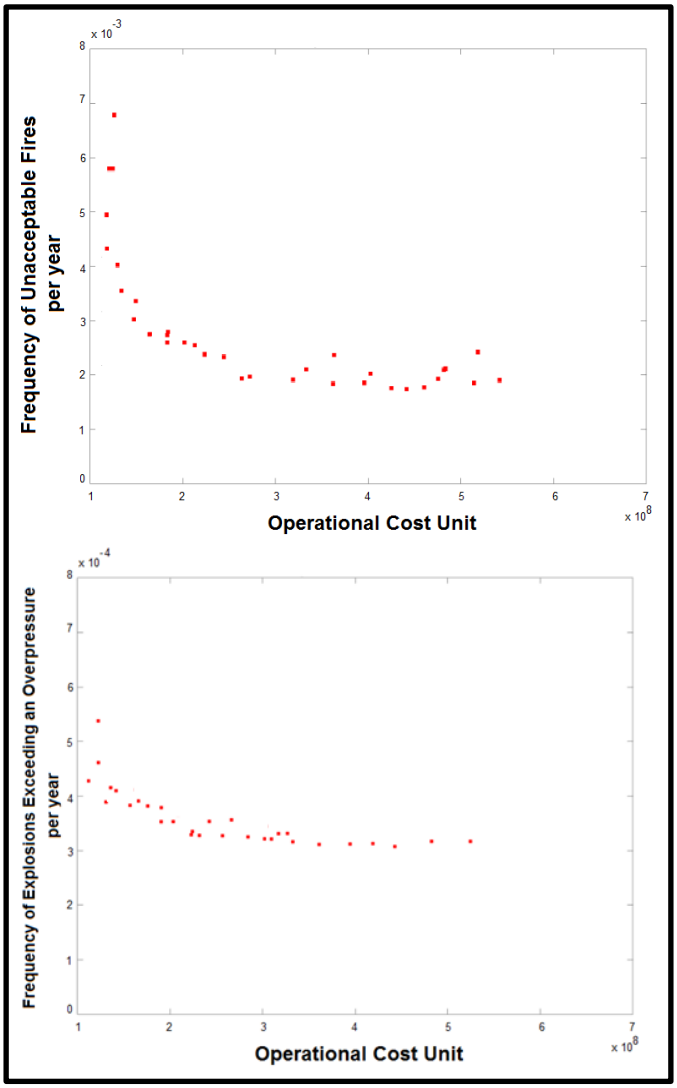


Figure 6-9 Fitness of the Population: Generation 40

The final generation comprises of a set of 13 optimum inspection, maintenance and repair strategies as shown in Figure 6-10, below. Majority of the population members are Pareto optimal, where they are not dominated by any other solution in the population.

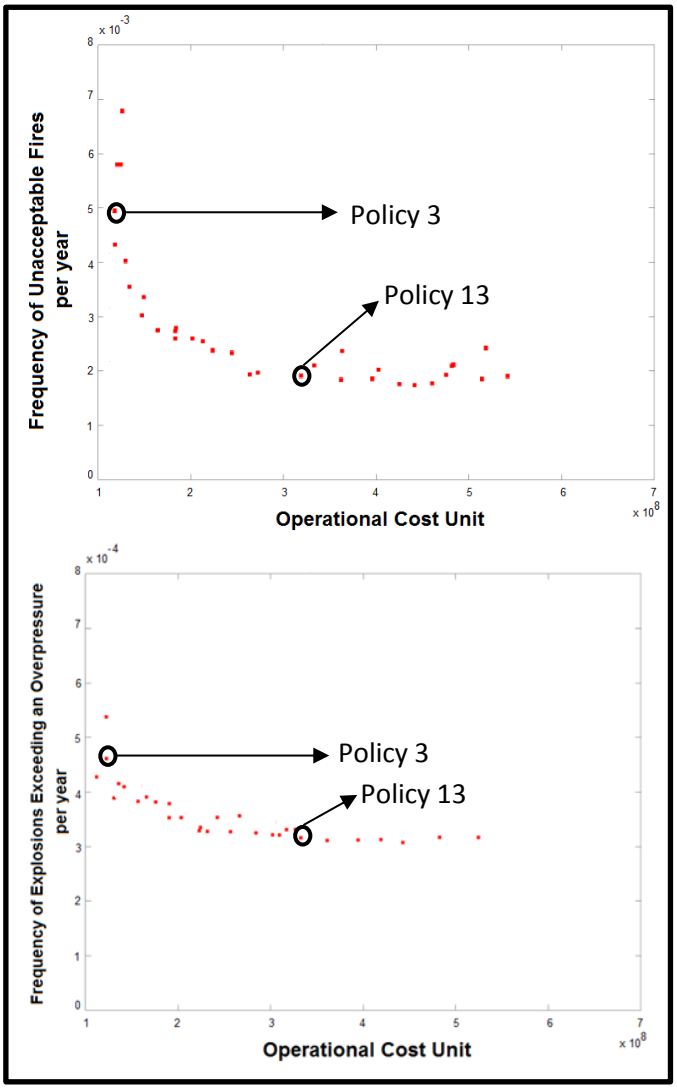


Figure 6-10 Fitness of the Population: Generation 50

The overall Pareto-optimal front shows that as the operational cost increases the frequencies of unacceptable fires and explosions exceeding an overpressure of 3 bar decreases. This is as expected because operational costs increases when inspection is carried out more frequently (every week as opposed to every three months). Moreover, by increasing the frequency of inspection, the component is more likely to undergo maintenance as soon as it is revealed to be in a state where repair is required, hence, the number of component failures is significantly reduced and so are the resultant fires and explosions. Table 6-2 outlines the details of the 13 optimal inspection, maintenance and repair strategies obtained.

Policy ID	Opportunistic Maintenance	Deluge System Inspection Interval	Isolation Valve Inspection Interval	Blowdown Valve Inspection Interval	Fire and Gas Detection System Inspection Interval	Deluge System Max Number of Minor Repair	Isolation Valve Max Number of Minor Repair	Blowdown Valve Max Number of Minor Repair	Deluge System Max Number of Major Repair	Isolation Valve Max Number of Major Repair	Blowdown Valve Max Number of Major Repair	Operational Cost Unit	Frequency of Unacceptable fires/yr	Frequency of Explosions Exceeding an Overpressure/yr
1	0	168	168	168	168	1	3	3	3	2	2	1.98E+08	2.67E-03	3.67E-04
2	1	168	168	168	168	2	0	2	1	0	2	1.51E+08	3.00E-03	3.98E-04
3	1	720	2160	1440	168	3	1	1	3	3	0	1.47E+08	5.00E-03	4.56E-04
4	1	168	168	168	1440	3	1	1	3	3	0	2.25E+08	2.58E-03	3.33E-04
5	1	168	168	168	2160	2	3	1	1	0	2	2.52E+08	2.42E-03	3.25E-04
6	0	168	168	1440	168	1	3	3	3	3	2	2.62E+08	2.33E-03	3.25E-04
7	1	168	168	168	168	1	3	3	3	3	2	2.88E+08	1.98E-03	3.22E-04
8	0	2160	1440	168	2160	1	3	1	1	0	2	5.37E+08	1.96E-03	3.20E-04
9	0	168	1440	168	2160	1	3	1	3	3	2	4.48E+08	1.97E-03	3.15E-04
10	1	168	168	168	168	2	3	1	3	2	0	4.25E+08	1.97E-03	3.20E-04
11	0	168	1440	1440	168	2	3	1	3	2	0	4.80E+08	1.97E-03	3.33E-04
12	1	168	2160	720	168	2	3	3	3	2	0	3.48E+08	1.99E-03	3.45E-04
13	1	168	168	168	168	3	1	3	3	0	0	3.98E+08	1.98E-03	3.43E-04

Table 6-2 13 optimum inspection, maintenance and repair strategies

Unit – Inspection Interval: hours and Opportunistic Maintenance: 0 – disabled, 1 – enabled

6.5.1.2 Chosen Solution

Two optimal asset management strategies have been chosen; Policy 3 and 13. Policy 3 was chosen as low operational costs were obtained in comparison to the other candidate solutions. This is because the components of the different safety systems are inspected less frequently. However, with Policy 3, the frequencies of unacceptable fires and explosions exceeding an overpressure limit of 3 bar is higher than the other candidate solutions. This is because component degradation is not revealed sooner than expected, due to the low inspection frequency, therefore the safety system components are more likely to reach a functional failure state. Failure of either one of the safety systems in the event of an accidental hydrocarbon leak could significantly increase the frequencies of fires and explosions generated.

Policy 13, on the other hand, performs inspection more frequently which explains the high operational costs in comparison to Policy 3. Moreover, as component degradation is revealed sooner than expected; the safety systems are less likely to reach a functional failure state and the resultant frequency of unacceptable fires and explosions exceeding an overpressure is significantly lower.

However, the choice is entirely dependent on the offshore oil and gas company and their requirements. If the main priority of the company is to maintain high standards of safety, Policy 13, is the recommended strategy. On the other hand, if the main priority of the company is to reduce operational costs as much as possible in order to survive the oil price turndown, Policy 3 is the recommended strategy.

6.5.1.3 Computational Time for Each Model

The Petri Net based Offshore Safety System Degradation and Maintenance Model takes approximately 5 minutes to run 10,000 simulations for a system of 60 components over a 35-year prediction period. The Petri Net contains a total of 1267 places and 1047 transitions of which 523 are normal transitions, 258 are place conditional transitions, 225 are reset transitions and 41 are probabilistic transitions. A total of 4844 arcs were used.

The Offshore Fire and Explosion Model, on the other hand, takes approximately 30 minutes to run 10,000 simulations for a 35-year prediction period. However, in the event of an oil leak from either of the three modules, due to the complexity of the leak and the additional parameters that are considered, the model takes approximately 2 hours to run 10,000 simulations for a 35-year prediction period.

The total time taken to optimise the Platform Safety Model was approximately 72 hours, i.e. each generation takes approximately 1 hour.

6.6 Summary

An optimisation framework using Multi-Objective Genetic Algorithm has been developed to assist offshore asset operations managers to select the best inspection, maintenance and repair strategy. The optimisation tool looks for asset management policies that will produce the lowest expected operational cost whilst minimising the frequencies of unacceptable fires and frequencies of explosions exceeding an overpressure.

The chapter presents a detailed review of a range of techniques that can be used to solve different optimisation problems. In this research, Genetic Algorithm has been chosen due to its flexibility to solve the optimisation problem at hand. A thorough explanation of the technique and the steps involved in finding the optimum solutions have been presented. The optimisation decisions are based on changes to controllable inputs such as inspection interval, opportunistic maintenance and maximum number of minor and major repairs. As a result of the optimisation, 13 optimum asset management policies have been found. Two solutions were selected; Policy 3 and 13. Policy 3 provides the lowest operational costs whilst Policy 13 provides the lowest frequencies of unacceptable fires and explosions exceeding an overpressure limit of 3 bar.

Both optimal asset management policies represent a wide variety of inspection, maintenance and repair strategies for the asset. These optimum asset management policies assist the decision making process of offshore asset operations managers by providing a range of optimal solutions with the choice being dependent on the needs of the offshore company.

Chapter 7 - Conclusion

7.1 Summary

Oil and gas production meets around 50% of the total primary energy needs of the UK, and in the UK, this is carried out offshore in the mature basin of the North Sea. There are currently over 383 producing fields with a supporting infrastructure of 14,000 km of pipelines, connecting installations to onshore terminals. As a mature basin, where development first began in 1967, and coupled with some of the harshest offshore weather conditions in the world, much of the existing infrastructures in the North Sea are ageing and require expensive retrofitting or replacement to be able to continue to operate safely. In 2014, it was estimated that approximately 50% of offshore installations are operating beyond their original design life, often specified as 25 years.

Ageing is characterised by degradation which is caused mainly by corrosion and fatigue. The performance of ageing installations can be highly irregular as degradation rates can vary throughout the lifecycle of the component and are dependent on factors such as the number of maintenance interventions. As equipment on these installations age, asset operations managers are often faced with an increasing challenge to keep equipment in an acceptable condition accounting for budgetary constraints and the need to avoid service disruptions and hazardous situations such as fires and explosions due to accidental release of hydrocarbon inventory.

To address these challenges, the aim of this research is to develop a practical and systematic tool to predict the risks, costs and service reliability of any given asset management policy for an offshore oil and gas installation. This requires an in depth understanding of the degradation and failure process of key systems and their components, and the effect of different inspection, maintenance and repair strategies on the condition of these systems. The offshore industry can use this information to improve their current knowledge, practises and assessment procedures. The data and statistics generated have the potential to significantly improve decision making capabilities for offshore assets in terms of investment and risk reduction.

In this thesis, the key systems studied were four safety systems found on most offshore oil and gas installations;

- Fire and gas detection system
- Process isolation system
- Blowdown system
- Deluge system.

Effective maintenance management of these safety systems is critical for ensuring that the risks to the installation remain at an acceptable level. Unavailability of these safety systems can risk having an impact on critical layers of protection used against the effects of fires and explosions in the event of an accidental release. This can, therefore, increase the consequence of such effects, potentially causing significant damage to the structural integrity of the offshore installation as well as risking the lives of its crew members. Hence, significant effort in both design and operation of offshore installations should be expended in reducing the risks associated with fires and explosions.

Chapter 2 highlighted the importance of a risk-based approach towards offshore asset management. A range of techniques that can be employed for identifying hazards and quantifying these hazards have been reviewed. However, several shortcomings associated with these techniques have been identified. For instance, the inability of HAZOP and FMEA to quantify hazards in a process and incapability of FTA and ETA to model non-constant degradation rates, dependencies between the components of a system and the main processes involved in the asset management of offshore oil and gas installations such as inspection and maintenance of offshore systems. On the other hand, Markov models have been shown to be effective at modelling the dynamic behaviour and dependencies among components. However, when applied to large engineering systems, Markov models can grow to be excessively large, making it difficult to construct and solve analytically. This then requires a numerical solution that requires large amounts of computational power and time to resolve. A further disadvantage of Markov models, is that like FTA and ETA, Markov models are also limited to constant failure rates for each component.

Petri Nets can overcome the limitations of the aforementioned techniques. They provide a modelling formalism that is a combination of tree-based techniques and Markov modelling.

They are capable of providing a graphical representation of the system, and statistical dependencies among components which are represented via states and transitions between these states. However, unlike Markov models, Petri nets are not limited to constant failure and repair rates for each component. In addition to exponential distributions for generating event firing times, Weibull distributions can also be used. Hence, Petri Net models are considered to be more efficient for modelling the risks and reliability of large engineering systems such as the safety systems considered in this study. Moreover, they have never been applied to offshore safety systems and their components.

Additionally, in order to effectively model the risks of fires and explosions on an offshore installation, it is necessary to model the occurrence of an accidental release from the key processing modules that are found offshore; the wellhead, separation and compression modules. Chapter 3 outlined a range of predictive techniques that can be employed for modelling the release, build-up and dispersion of gas, and, if ignited, the resulting fire and explosion consequences. A gaseous release will form a vapour cloud of a certain size and gas concentration. According to literature, the most effective method of modelling gas cloud dispersion in an enclosed module without any wind effects as the one modelled in this research is by using simple diffusion equations.

Immediate ignition of a gas or oil release would result in an explosion or pool fire, respectively, while delayed ignition of a gas release would result in a jet fire. In this research, the models developed by Considine and Grint (1985) and Pritchard and Binding (1993) were used to predict the magnitude of jet and pool fires, respectively, in terms of the flame lengths generated. While a variety of models have been developed to predict explosion overpressures; literature suggests that advanced CFD models are the most effective method of modelling gas cloud build-up. However, combining complex geometries with the number of possible leak scenarios would make this method impractical. As only an estimate of the overpressure generated is required for our purposes, phenomenological models are deemed appropriate.

Chapter 4 describes the development of the Platform Safety Model. The Platform Safety model is divided into sub models;

- the Offshore Safety System Degradation and Maintenance Model,
- the Offshore Fire and Explosion Model.

The Platform Safety Model is implemented using standard Petri Net with high level extensions to increase the standard Petri Nets ability to model complex component/system behaviour as well as a variety of different maintenance options.

The Offshore Safety System Degradation and Maintenance Model models dynamic processes such as degradation, failure, inspection and maintenance experienced by the components of the offshore safety systems. In order to study the degradation and failure process of components in the safety systems, the condition states in which these components reside in throughout their lifecycle are defined using ISO standards or engineering judgement. The Petri Net model contains places which represent the different condition states of a component (e.g. new, degraded, severely degraded or functional failure). Over time, due to degradation mechanisms such as wear and corrosion, the component degrades affecting its reliability and performance. The level of degradation is revealed via an inspection. If the component is revealed to be in a degraded state, Preventive Maintenance is performed to restore the component back to new/normal working condition. If the component is revealed to be in a functional failure state, Corrective Maintenance is performed and the component is restored back to new/normal working condition. Hence, maintenance is scheduled according to the criticality of the component. Moreover, every 5 years, the platform is shutdown to carry out corrective maintenance on all safety systems. The model also takes into consideration the effect of opportunistic maintenance; this is when maintenance of several components that fall under the same system can be executed together to minimise equipment downtime. Spurious failures have also been considered within the Offshore Safety System Degradation and Maintenance Model.

The Offshore Safety System Degradation and Maintenance model is implemented using a C++ code which is then solved using Monte-Carlo simulation. The model was simulated to predict the condition of offshore safety systems over a 35-year lifetime period. A variety of statistics was analysed from the model data such as probability of the system being in any of the condition states, the total number of component replacements over the system lifetime, the total number of maintenance interventions carried out on each component and the system

availability. By assigning unit costs for the different types of maintenance activities, the costs of performing inspection and maintenance on offshore safety systems were also estimated.

The Offshore Fire and Explosion Model, on the other hand, models the occurrence of a hydrocarbon leak from a process vessel located within the three enclosed modules; wellhead, separation and compression. The model utilises fluid flow modelling techniques to calculate parameters such as the hydrocarbon discharge rate, gas cloud build-up and dispersion, oil-pool build-up and reduction. The model also assumes gas, condensate and oil release occurring with changing temperature, implying negligible entropy. The Offshore Fire and Explosion model is then used in conjunction with the Offshore Safety System Degradation and Maintenance Model to predict the frequencies of fires and explosions in the event that the safety systems fail to function on demand and a source of ignition is present. The frequencies of explosions are dependent not only on the occurrence of an ignition source but also on the time periods that the gas concentration is within the explosive range. The combined models are also capable of predicting the intensity of fires and explosions in terms of the flame length produced in the case of a fire and its duration, and the overpressures generated in the case of an explosion.

Chapter 5 demonstrates the capability of both the Offshore Safety System Degradation and Maintenance and the Offshore Fire and Explosion model. A sensitivity analysis was carried out on the input parameters of the Offshore Safety System Degradation and Maintenance model to study its effect on the unavailability and operational costs of the four safety systems under consideration. It is evident from this study that input parameters such as inspection intervals and degradation rates have a significant effect on the system availability and operational costs. The data and statistics generated via both models can be used to investigate the effects of different inspection and maintenance strategies, predict future asset condition, expected downtime due to component failure and frequency of fires and explosions in the event that an accidental release ignites and the safety systems are in a failed state.

Chapter 6 describes the development of an optimisation framework for identifying optimum inspection, maintenance and repair strategies that minimise the frequencies of unacceptable

fires and frequencies of explosions exceeding an overpressure limit of 3 bar. An optimisation study was carried out using Multi-Objective Genetic Algorithm due to its capability of solving a wide range of optimisation problems with two or more objective functions with a range of variables and constraint types. The output of this optimisation study provides information on the effect of a wide range of inspection, maintenance and repair strategies, from which an optimum asset maintenance strategy can be selected that balances costs versus risks.

7.2 Conclusions

The main aim of this research was to develop a practical and systematic tool that is able to predict the risks, costs and service reliability of any given asset management policy for an offshore oil and gas installation. To meet this aim, the following objectives have been achieved:

- **To model the degradation and failure of offshore safety systems such as fire and gas detection system, process isolation, process blowdown and deluge.**

  The research demonstrates the development of an Offshore Safety System Degradation and Maintenance Model using standard Petri Nets with high level extensions. It demonstrates the suitability of Petri Nets for modelling dynamic processes such as degradation, failure, inspection and maintenance experienced by the components of the offshore safety systems. The model is solved using the Monte Carlo simulation method to generate a variety of statistics, such as the expected number of failures and maintenance interventions over a chosen prediction period, and find its correlation with associated costs of implementing different asset management strategies. A sensitivity analysis on the input parameters, such as the inspection interval, maintenance strategy and degradation rates, was carried out to determine their effect on the operational costs and unavailability of offshore safety systems.

- **To model the occurrence of a hydrocarbon leak from three enclosed modules, i.e. wellhead, separation and compression module on an offshore installation; generate the discharge rate, allowing for variation of the gas concentration in the module to be calculated over time.**

  The research demonstrates the development of an Offshore Fire and Explosion model. This model is capable of modelling the occurrence of a hydrocarbon leak from the three main enclosed processing modules, i.e. wellhead, separation and compression module,

on an offshore installation. The model utilises fluid flow modelling equations to model the following parameters: hydrocarbon release, gas cloud build-up and dispersion and oil pool build-up and reduction.

- **To estimate the frequencies of jet fires, pool fires and explosions in the event of safety system unavailability and hence predict the overpressures generated as a result of an explosion and the length and duration of the flame generated as a result of a jet or pool fire.**

  The research demonstrates the integration of fluid flow modelling with the Petri Net modelling technique to model an accidental hydrocarbon release, and in the event when the offshore safety systems, modelled within the Petri Net framework, fail to function on demand, the consequent fires and explosions on offshore oil and gas installations are modelled. Statistics, such as frequencies of fires and explosions, are generated. The model is also capable of predicting the overpressures generated from a gas explosion and the flame lengths generated from a fire and its duration.

- **To derive a set of maintenance and inspection strategies that can be applied to the ageing assets to produce an acceptable risk level.**

  The research demonstrates the suitability of Petri Nets for integrating fire and explosions modelling with the asset management framework which is first of its kind.

- **To develop an optimisation technique to find the optimum asset management strategies that minimise the operational costs whilst providing an acceptable risk level.**

  The research demonstrates the application of the Multi-Objective Genetic Algorithm to a typical Platform Safety Model to find the optimum asset maintenance strategies that minimise the operational costs whilst providing an acceptable risk level.

In conclusion, the proposed model delivers a practical tool for offshore asset operations managers to assess the degradation and failure process of offshore safety systems and their components, and enables the investigation of the effects of different inspection, maintenance and repair strategies on the offshore assets. The model can be employed to model the risks of fires and explosions for any given asset management policy as well as to determine the optimal maintenance strategy provided the risks to the offshore installation are at an acceptable level.

7.3 Key Findings of the Research

Key findings of this research include the following:

- **Improved understanding of a risk-based approach towards asset management of offshore oil and gas installations:** The research has provided a detailed review of offshore hazards that can significantly affect the structural integrity of offshore oil and gas installations and their workforce, particularly fires and explosions, not attempted in previous work. Investigation of past incidents such as the Piper Alpha Disaster in 1988 and the Deepwater Horizon Explosion and Oil Spill in 2010 revealed the need for a comprehensive examination of risks inherent to offshore oil and gas production and thus, a reassessment of the current maintenance policies that are in place for managing ageing offshore oil and gas installations. The research appraises a variety of techniques that can be employed to model risks and reliability of offshore oil and gas installation. However, several shortcomings in the current modelling techniques were revealed and the need for a new modelling technique.
- **Improved understanding of modelling fires and explosions on offshore oil and gas installations**: The research critically appraises a range of techniques used for modelling hydrocarbon release, gas cloud build-up and dispersion, oil pool build-up and reduction, ignition of hydrocarbon release and the consequent fires and explosions which has not been attempted in previous work. A great deal of information is available on modelling these parameters, the physics of which are not fully understood, hence most of the models that are applicable to offshore situations are generally crude approximations.
- **Improved understanding of the degradation and failure process of offshore safety systems and their components:** The study provides a detailed description of the degradation and failure process of the key safety systems which includes the fire and gas detection system, process isolation and blowdown, and deluge system. Compared to previous work, the current research provides a far more detailed overview of the key safety systems found on offshore oil and gas installations.
- **Improved understanding of Offshore Safety System Inspection and Maintenance:** The study provides a detailed overview of inspection and maintenance process that is implemented on offshore oil and gas installations to manage its assets.

- **Application of Petri Net modelling technique to model Asset Management of Offshore Oil and Gas Installations:** The research shows the development of the Offshore Safety System Degradation and Maintenance Model using standard Petri Nets with high level extensions. The research shows the suitability of Petri Nets to stochastically model the degradation, failure, inspection and maintenance of the offshore safety systems and their components. The effects of different types of maintenance interventions such as condition-based PM, CM and shutdown maintenance were successfully captured via the model. Moreover, dependencies among different components of a system were modelled via opportunistic maintenance. This model can therefore be considered to contain far more detail than other models presented in literature. The model is easily applicable to large engineering systems such as the ones considered in the study. Moreover, it can be used to predict the costs, risks and service reliability of any given asset management policy for other sectors such as the aviation, chemical and nuclear industry.
- **Integration of Fluid Flow modelling with Petri Net modelling to model accidental hydrocarbon release and the consequent fires and explosions on offshore oil and gas installations:** The research shows the development of the Offshore Fire and Explosion Model using fluid flow modelling equations. Parameters such as hydrocarbon release, gas cloud build-up and dispersion, oil pool build-up and reduction and ignition of the release can all be modelled via the Offshore Fire and Explosion Model. Moreover, the model can be used in conjunction with the Petri Net model which is first of its kind. The model can be used to predict the frequencies of fires and explosions in the event that the safety systems modelled in the Offshore Safety System Degradation and Maintenance Model fail to function on demand and an ignition source is present. The model can also be used to predict the risks to the offshore installation in terms of the flame length generated in the event of a fire and overpressures generated in the event of an explosion.
- **Offshore Safety System Long term Operational and Maintenance Knowledge:** The model calculates outputs such as safety system availability and operational costs for any given asset management policy for a defined prediction period. Moreover, statistics such as frequencies of fires and explosions can also be obtained for any given asset management policy. Hence, the model can successfully be used to predict the costs, risks and service reliability for an offshore oil and gas installation which is more comprehensive and

detailed than other models presented in literature. These statistics are highly beneficial to offshore asset operations managers as they can assist with the following decisions:

- **Inspection and Maintenance decisions** are based on how a component is degrading and the impact inspection and maintenance has on the asset.
- **Optimisation decisions** are based on the changes in asset condition as a result of small changes to controllable inputs such as inspection interval, opportunistic maintenance and maximum number of minor and major repairs.

- **Application of Multi-Objective Genetic Algorithm to optimise the Platform Safety Model:** The research shows how Multi-Objective Genetic algorithm can be applied to the Platform Safety Model to find the optimal inspection, maintenance and repair strategies in order to reduce the frequencies of unacceptable fires and frequencies of explosions exceeding an overpressure of 3 bar which is first of its kind.

7.4 Future Work and Recommendations

The following future work has been recommended to further enhance the modelling capability of the Platform Safety Model:

- **Use of historical degradation and failure data**

In this research, due to the unavailability of historical data, distributions used to describe degradation and failure rates were estimated based on engineering judgement. This can have an effect on the accuracy of the model and the statistics obtained. Hence, to increase the accuracy of the model, detailed analysis of historical data sourced from offshore oil and gas companies should be carried out to derive the distributions for the time taken to reach degraded and functional failure state utilised within the Offshore Safety System Degradation and Maintenance Model.

- **Improve the Petri Net code**

Future work should be focused on improving the efficiency of the Petri Net code to reduce computational time. Currently, it takes approximately 5 minutes to run 10,000 simulations for a 35 year prediction period. However, when the Petri Net is used in conjunction with the Offshore Fire and Explosion Model, the simulation time increases significantly from 5 minutes to 2 hours, mainly in the event of an oil leak from either of three modules on the offshore

installation. Hence, the model efficiency should be further explored to increase its capability to handle more complex problems without significantly increasing the computational time.

- **Development of Petri Net models for other offshore assets**

The work should also focus on the development of Petri Net models for other assets found on offshore oil and gas installations such as the main oil and gas processing systems. This allows offshore asset operations managers to make informed investment decisions not only with regards to the safety systems but also the main processing units that need to be frequently inspected and maintained to reduce the risks of accidental hydrocarbon release.

- **Model Other Offshore Hazards**

This research focuses mainly on the effects of fires and explosions to offshore oil and gas installations. However, several other hazards can affect the integrity of offshore oil and gas installations, such as ship collisions, structural failure and well blowout. Thus, future work should be focused on modelling the effects of these hazards and minimising their effects.

- **Fatality Modelling**

Future work should focus on modelling the number of fatalities in the event of a fire and/or explosion and minimise the risks to personnel to an acceptable yet practical level.

- **Use of Hybrid Optimisation**

While the research shows successful application of multi-objective GA to the Platform Safety Model, the capability of newer techniques such as hybrid heuristic techniques should be explored to improve the search ability and computational effort.

References

Acton, M.R., Sutton, P., and Wickens, M.J., 1990. An investigation of the mitigation of gas cloud explosions by water sprays. *Gas engineering and management*, 31 (7–8), 166–172.

Andrews, J., 2012. A modelling approach to railway track asset management. *Proceedings of the Institution of Mechanical Engineers, Part F: Journal of Rail and Rapid Transit*, 227 (1), 56–73.

Andrews, J. and Fecarotti, C., 2014. Asset Management of Aging Process Plant. *Proceedings of the 3rd International Workshop & Congress on eMaintenance*, 77–83.

Andrews, J., Smith, R., and Gregory, J., 2005. Procedure to calculate the explosion frequency for a

module on an offshore platform. *Institution of Chemical Engineers*, 69–82.

Andrews, J.D. and Dunnett, S.J., 2000. Event-tree analysis using binary decision diagrams. *IEEE Transactions on Reliability*, 49 (2), 230–238.

Andrews, J.D. and Moss, T.R., 2002. *Reliability and Risk Assessment*. Second. London: Professional Engineering Publishing.

Arnold, K. and Stewart, M., 2008. *Surface production operations: Design of oil handling systems and facilities*. Third. Elsevier.

Arntzen, B.Y., 1998. Modelling of Turbulence and Combustion for simulation of gas explosions in complex geometries. The Norwegian University.

Back III, G.G., Beyler, C.L., and Hansen, R., 2000. Quasi-steady-state model for predicting fire suppression in spaces protected by water mist systems. *Fire Safety Journal*, 35 (4), 327–362.

Bagster, D.F. and Schubacht, S.A., 1996. The prediction of jet-fire dimensions. *Journal of Loss Prevention in the Process Industries*, 9 (3), 241–245.

Bain, B., Huser, A., Falck, A., Bolsover, A., and Spitzenberger, C., 2014. Modelling of Accidental Hydrocarbon Releases in QRAs : Hole Size Versus Initial Release Rate Basis. *IChemE Symposium Series*, 24 (159), 1–12.

Baker, Q.A., Tang, M.J., Scheiir, E.A., and Sihra, G.J., 1996. Vapor Cloud Explosion Analysis. *Process Safety Progress*, 15 (2).

Balasubramanian, N., Chang, C.-T., and Wang, Y.-F., 2002. Petri-Net Models for Risk Analysis of Hazardous Liquid Loading Operations. *Industrial & Engineering Chemistry Research*, 41 (19), 4823–4836.

Bauer, R.J., 1994. *Genetic Algorithms and Investment Strategies*. Wiley.

Baukal, C.E., 2001. *The John Zink Combustion Handbook*. CRC Press.

Begain, K., Bolch, G., and Herold, H., 2012. *Practical Performance Modeling: Application of the MOSEL Language*. Springer US.

Van den Berg, A.C., 1985. The multi-energy method: A framework for vapour cloud explosion blast prediction. *Journal of Hazardous Materials*, 12 (1), 1–10.

Van den Berg, A.C., Opschoor, G., and Zeeuwen, J.P., 1984. Blast effects from vapour cloud explosion. *In 9th International Symposium on the Prevention of Occupational Accidents and Diseases in the Chemical Industry*.

Bill, R.G., Hansen, R.L., and Richards, K., 1997. Fine-spray (water mist) protection of shipboard engine rooms. *Fire Safety Journal*, 29 (4), 317–336.

Bjerketvedt, D., Bakke, J.R., and van Wingerden, K., 1997. Gas explosion handbook. *Journal of Hazardous Materials*, 52 (1), 1–150.

Brasie, W.C. and Simpson, D.W., 1968. Guidelines for estimating damage explosion. *Symposium on Loss Prevention in the Process Industries*.

Briš, R., 2013. Evaluation of the production availability of an offshore installation by stochastic Petri nets modeling. *The International Conference on Digital Technologies*.

British Petroleum, 2005. North West Hutton Decommissioning Programme.

Britter, R.E. and McQuaid, J., 1988. Workbook on the dispersion of dense gases. *Journal of Occupational Accidents*, 11 (2), 149.

Broyden, C.G. and Attia, N.F., 1988. Penalty functions, Newton's method, and quadratic programming. *Journal of Optimization Theory and Applications*, 58 (3), 377–385.

BS 3811, 1984. Glossary of Maintenance Management Terms used in Terotechnology.

Burgess, D., Strasser, A., and Grumer, J., 1961. Diffusive burning of liquid fuels in open trays. *Symposium of the American Chemical Society*, 3 (3), 91–106.

Caron, M., Goethals, M., De Smedt, G., Berghmans, J., Vliegen, S., Van't Oost, E., and van den Aarssen, A., 1999. Pressure dependence of the auto-ignition temperature of methane/air mixtures. *Journal of Hazardous Materials*, 65 (3), 233–244.

Cates, A. and Samuels, B., 1991. A simple assessment methodology for vented explosions. *Journal of Loss Prevention in the Process Industries*.

Catlin, C.A., 1990. CLICHE - a generally applicable and practicable offshore explosion model. *IChemE Symposium Series*, 68B (122), 245–253.

CCPS, 1996. Guidelines for Use of Vapor Cloud Dispersion Models. American Institute of Chemical Engineers.

Cepin, M. and Mavko, B., 2002. A dynamic fault tree. *Reliability Engineering and System Safety*, 75 (1), 83–91.

Chamberlain, G.A., 1987. Developments in Design Methods for Predicting Thermal Radiation From Flares. *Chemical Engineering Research and Design*, 65 (July 1987), 299–309.

Chandrasekaran, S., 2016. Offshore Structural Engineering: Reliability and Risk Assessment.

Chew, S., 2010. Systems reliability modelling for phased missions with maintenance-free operating periods. Loughborough University.

Chippett, S., 1984. Modeling of vented deflagrations. *Combustion and Flame*, 55 (2), 127–140.

Considine, M. and Grint, G.C., 1985. Rapid assessment of the consequences of LPG releases. *Proceedings of the Gastech 84 LNG/LPG Conference*.

Cowing, M.M., Paté-Cornell, M.E., and Glynn, P.W., 2004. Dynamic modeling of the tradeoff between productivity and safety in critical engineering systems. *Reliability Engineering and System Safety*, 86 (3), 269–284.

Craven, A., 1972. Thermal radiation hazards from the ignition of emergency vents. *IChemE Symposium Series*, 33, 7–11.

Crowl, D.A. and Louvar, J.F., 1990. Chemical Process Safety: Fundamentals with Applications. *Prentice Hall PTR*.

Cullen, W.D., 1990. The Public Inquiry Into the Piper Alpha Disaster, 1.

Dantzig, G.B., 1951. Maximisation of a Linear Function of Variables Subject to Linear Inequalities. *Activity Analysis of Production and Allocation*, 339–347.

Dantzig, G.B., 1959. Note on Solving Linear Programs in Integers. *Naval Research Logistics Quarterly*, 6 (1), 75–76.

Davidon, W.C., 1991. Variable Metric Method for Minimization. *SIAM Journal on Optimization*, 1 (1), 1–17.

Dawkins, J. and Hale, J., 2004. A systematic approach to multi-stage network attack analysis. *Proceedings of the Second IEEE International Information Assurance Workshop*, 48–56.

Dejean, J., Averbuch, D., Maurel, P., Gainville, M., S, G., and Johnsen, O., 2007. Risk-based design of offshore oil and gas production system-management of uncertainties by integrating flow assurance and reliability aspects into a stochastic Petri nets model. *Proceedings of the European safety and reliability conference*, 3, 2443–50.

DNV, 2010. Risk Based Inspection of Offshore Topsides Static Mechanical Equipment, (October), 74.

Fairweather, M. and Vasey, M.W., 1982. A mathematical model for the prediction of overpressures generated in totally confined and vented explosions. *Symposium (International) on Combustion*, 19 (1), 645–653.

Fiacco, A. V and McCormick, G.P., 1990. *Nonlinear Programming: Sequential Unconstrained Minimization Techniques*. Society for Industrial and Applied Mathematics.

Fisher, H.G., Forrest, H.S., and Grossel, S.S., 1992. *Emergency relief system design using DIERS technology : the Design Institute for Emergency Relief Systems (DIERS) project manual*. New York: DIERS.

Fleming, K.N., 2004. Markov models for evaluating risk-informed in-service inspection strategies for nuclear power plant piping systems. *Reliability Engineering and System Safety*, 83 (1), 27–45.

Fletcher, R. and Reeves, C.M., 1964. Function minimization by conjugate gradients. *The Computer Journal*.

Fonseca, C.M. and Fleming, P.J., 1995. An Overview of Evolutionary Algorithms in Multiobjective Optimization. *Evolutionary Computation*, 3 (1), 1–16.

Frank, M. and Wolfe, P., 1956. An algorithm for quadratic programming. *Naval Research Logistics Quarterly*, 3 (1–2), 95–110.

Fthenakis, V.M., 1993. *Prevention and Control of Accidental Releases of Hazardous Gases*. Wiley.

Gifford, F.A., 1961. Uses of routine meteorological observations for estimating atmospheric dispersion. *Nuclear Safety*, (2), 47–51.

Goldberg, D.E., 1989. *Genetic algorithms in search, optimization, and machine learning*. Addison-Wesley Longman Publishing Co., Inc.

Grannes, S.G., Ackerson, M.A., Green, G.R., and of Mines, U.S.B., 1990. *Preventing automatic fire suppression system failures on underground mining belt conveyors*. U.S. Deptment of Interior, Bureau of Mines.

Griffith, R.E. and Stewart, R.A., 1961. A Nonlinear Programming Technique for the Optimization of Continuous Processing Systems. *Management Science*, 7 (4), 379–392.

Health & Safety Executive, 1988. Tolerability of risk from nuclear power stations. *Fire Safety Journal*, 13 (2–3), 227–229.

Health & Safety Executive, 2001. Reducing risks, protecting people, HSE's decision-making process, Technical Report. *HMSO, London*, 30.

Health & Safety Executive, 2006a. Plant ageing: Management of equipment containing hazardous fluids or pressure. *Health and Safety Executive*.

Health & Safety Executive, 2006b. Assessment Principles for Offshore Safety Cases (APOSC). *Health and Safety Executive*, 10–60.

Health & Safety Executive, 2010. Plant Ageing Study, 34–67.

Health & Safety Executive, 2014. HID Inspection Guide Offshore, 1–40.

Hestenes, M.R., 1969. Multiplier and gradient methods. *Journal of Optimization Theory and Applications*, 4 (5), 303–320.

Ho, W. and Ji, P., 2006. *Optimal Production Planning for PCB Assembly*. Springer Science & Business Media.

Høiset, S., Hjertager, B.H., Solberg, T., and Malo, K.A., 2000. Flixborough revisited - An explosion simulation approach. *Journal of Hazardous Materials*.

Hokstad, P. and Johnsen, R., 2010. Ageing and life extension for offshore facilities in general and for specific systems. *SINTEF Report*, (March).

Holland, J.H., 1975. *Adaptation in Natural and Artificial Systems*. The University of Michigan Press.

Hope, S. and Bjordal, E.N., 1984. Methodologies for Hazard Analysis and Risk Assessment in the Petroleum Refining and Storage Industry, 20 (4), 43–56.

Horrocks, P., Mansfield, D., Parker, K., Thomson, J., Atkinson, T., and Worsley, J., 2010. Managing Ageing Plant. *Health and Safety Executive*.

Hottel, H.C. and Hawthorne, W.R., 1949. Diffusion in laminar flame jets. *Symposium on Combustion*

and Flame, and Explosion Phenomena, 3 (1), 254–266.

ISO 10816, 1998. Mechanical vibration - Evaluation of machine vibration by measurements on non-rotating parts, 3.

ISO 17776, 2000. Petroleum and Natural Gas Industries: Offshore Production Installations Guidelines on Tools and Techniques for Hazard Identification and Risk Assessment.

Jacobson, L. and Kanber, B., 2015. *Genetic Algorithms in Java Basics*. Apress.

Jain, L.C. and Jain, R.K., 1997. *Hybrid Intelligent Engineering Systems*. World Scientific.

Jensen, K. and Kristensen, L.M., 2009. Coloured Petri Nets: Modelling and Validation of Concurrent Systems. *Science*.

De Jong, K.A., 1975. An analysis of the behavior of a class of genetic adaptive systems.

Kalghatgi, G.T., 1983. The visible shape and size of a turbulent hydrocarbon jet diffusion flame in a cross-wind. *Combustion and Flame*, 52, 91–106.

Karmarkar, N., 1984. A new polynomial-time algorithm for linear programming. *Combinatorica*, 4 (4), 373–395.

Kawauchi, Y. and Rausand, M., 2002. A new approach to production regularity assessment in the oil and chemical industries. *Reliability Engineering and System Safety*, 75 (3), 379–388.

Keane, K., 2013. Piper Alpha: Aberdeen Offshore Conference Teaching Disaster Lessons. *BBC News*.

Kirkpatrick, S., Gelatt, C.D., and Vecchi, M.P., 1983. Optimisation by Simulated Annealing. *Science*, 220, 671–680.

Kletz, T. a., 1997. Hazop—past and future. *Reliability Engineering & System Safety*, 55 (3), 263–266.

Land, A.H. and Doig, A.G., 1960. An Automatic Method of Solving Discrete Programming Problems. *Econometrica*, 28 (3), 497–520.

Le, B., 2014. Modelling railway bridge asset management. The University of Nottingham.

Le, B. and Andrews, J., 2012. Modelling railway bridge asset management. *Proceedings of the Institution of Mechanical Engineers, Part F: Journal of Rail and Rapid Transit*, 227 (6), 644–656.

Le, B. and Andrews, J., 2015a. Modelling wind turbine degradation and maintenance. *Wind Energy*, 19 (4), 571–591.

Le, B. and Andrews, J., 2015b. Petri net modelling of bridge asset management using maintenance-related state conditions. *Structure and Infrastructure Engineering*, 12 (6), 730–751.

Lea, C.J. and Ledin, H.S., 2002. A review of the state-of-the-art in gas explosion modelling. *Health and Safety Laboratory Report HSL*.

Lees, F.P., 1996a. Loss Prevention in the Process Industries (2nd Edition).

Lees, F.P., 1996b. *Loss Prevention in the Process Industries: Hazard Identification, Assessment, and Control*. Butterworth-Heinemann.

Lewthwaite, J.L., 2006. Design modelling to minimise the risk for offshore platforms. Loughborough University.

Lewthwaite, J.L., Andrews, J.D., Dunnett, S.J., Gregory, C.A.J., and Smith, R., 2006. Risk modelling of fires and explosions in open-sided offshore platform modules. *Proceedings of the Institution of Mechanical Engineers, Part O: Journal of Risk and Reliability*, 220 (2), 123–135.

Li, Y.F., Zio, E., Lin, Y.H., and Kumar, M., 2012. Petri-Net Simulation Model of a Nuclear Component Degradation Process. *Esrel*, 10.

Liang, T., Liu, M., Liu, Z., Zhong, W., Xiao, X., and Lo, S., 2015. A study of the probability distribution of pool fire extinguishing times using water mist. *Process Safety and Environmental Protection*, 93 (June), 240–248.

Mannan, S., 2013. *Lees' process safety essentials : hazard identification, assessment and control*.

Mannan, S. and Lees, F.P., 2005. *Lees' loss prevention in the process industries : hazard identification, assessment, and control.* Elsevier Butterworth-Heinemann.

Martin, J.W., 2011. Unexpected Consequences: Why The Things We Trust Fail.

Mehta, S.A., Moore, R.G., Laureshen, C.J., Samuel, P., Teichrob, R.R., and Bennion, D.B., 1998. Safety Considerations For Underbalanced Drilling of Horizontal Wells Using Air Or Oxygen-containing Gas. *Journal of Canadian Petroleum Technology*, 37 (9).

Melnick, E.L. and Everitt, B.S., 2008. Encyclopedia of Quantitative Risk Analysis and Assessment.

Mobile North Sea Limited, 2003. *Beryl Alpha Safety Case*.

Mohammed, M.J. and Ali, A.A., 2015. Fuzzy Petri Net Controller for Quadrotor System using Particle Swam Optimization, 11 (1).

Nivolianitou, Z.S., Leopoulos, V.N., and Konstantinidou, M., 2004. Comparison of techniques for accident scenario analysis in hazardous systems. *Journal of Loss Prevention in the Process Industries*, 17 (6), 467–475.

Palacios, A., Muñoz, M., and Casal, J., 2009. Jet fires: An experimental study of the main geometrical features of the flame in subsonic and sonic regimes. *AIChE Journal*, 55 (1), 256–263.

Pasquill, F., 1961. The estimation of the dispersion of windborne material. *The Meteorological Magazine*, 90 (1063).

Pecht, M., 1995. *Product Reliability, Maintainability, and Supportability Handbook*. Second. Taylor & Francis.

Perry, R.H., Green, D.W., and Maloney, J.O., 1997. *Perry's Chemical Engineers' Handbook*. McGraw-Hill.

Petri, C.A., 1962. Kommunikation mit Automaten. Technische Hochschule Darmstadt.

Petrofac, 2010. Section 13 - Shutdown Systems and ESDV Testing.

Pike, R.W., 1986. *Optimization for engineering systems*. Van Nostrand Reinhold.

Prasad, K., Patnaik, G., and Kailasanath, K., 2002. A numerical study of water-mist suppression of large scale compartment fires. *Fire Safety Journal*, 37 (6), 569–589.

Prescott, D. and Andrews, J., 2013. Investigating railway track asset management using a Markov analysis. *Proceedings of the Institution of Mechanical Engineers Part F-Journal of Rail and Rapid Transit*, 229 (4), 402–416.

Pritchard, M. and Binding, T., 1993. FIRE 2: a new approach for predicting thermal radiation levels from hydrocarbon pool fires. *Symposium on Major Hazards Onshore and Offshore*, 130, 491–505.

Puttock, J.S., 1995. Fuel gas explosion guidelines - the congestion assessment method. *IChemE Symposium Series*, (139).

Ramsay, C.G., Bolsover, A.J., Jones, R.H., and Medland, W.G., 1994. Quantitative risk assessment applied to offshore process installations. Challenges after the piper alpha disaster. *Journal of Loss Prevention in the Process Industries*, 7 (4), 295–304.

Rausand, M. and Hoyland, A., 2004. *System Reliability Theory: Models, Statistical Methods, and Applications (2nd Edition)*. John Wiley & Sons.

Reisig, W. and Rozenberg, G., eds., 1998. Lectures on Petri Nets I: Basic Models, Advances in Petri Nets, the Volumes Are Based on the Advanced Course on Petri Nets. London, UK, UK: Springer-Verlag.

Roberts, O.F.T., 1923. The Theoretical Scattering of Smoke in a Turbulent Atmosphere. *Proceedings of the Royal Society of London A: Mathematical, Physical and Engineering Sciences*, 104 (728), 640–654.

De Rozieres, F., Prescott, D., and Andrews, J., 2014. A stochastic model for railway track asset management. *Reliability Engineering and System Safety*, 76–84.

Simpson, B., 1997. *Containment Structures: Risk, Safety and Reliability: Proceedings of the IABSE Henderson Colloquium*. Taylor & Francis.

Skelton, B., 1997. *Process Safety Analysis: An Introduction*. Institution of Chemical Engineers.

Sonju, O.K. and Hustad, J., 1984. An experimental study of turbulent jet diffusion flames, (Norwegian Maritime Res.).

Stacey, A., Birkinshaw, M., and Sharp, J., 2008. Life Extension Issues for Ageing Offshore Installations. *International Conference on Offshore Mechanics and Arctic Engineering*, (June), 1–17.

Stapelberg, R.F., 2009. *Handbook of Reliability, Availability, Maintainability and Safety in Engineering Design*. Springer Science & Business Media.

Stern, A.C., 2014. *Air Pollution: Supplement to Measurements, Monitoring, Surveillance, and*

Engineering Control. Elsevier Science.

Sutton, I., 2014. Offshore Safety Management. *Offshore Safety Management*.

Sutton, O.G., 1953. *Micrometeorology*. New York: McGraw-Hill.

Swaminathan, S., 1999. Dynamic probabilistic risk assessment using event sequence diagrams, 63, 224.

Thangamani, G., 2011. Availability analysis of a Lube oil system using Generalized Stochastic Petri Net. *2011 IEEE International Conference on Quality and Reliability*, 186–190.

Thangamani, G., 2012. Generalized Stochastic Petri Nets for Reliability Analysis of Lube Oil System with Common-Cause Failures. *American Journal of Computational and Applied Mathematics*, 2 (4), 152–158.

The Guardian, 2010. Owner of Deepwater Horizon drilling rig agrees to $211m damages settlement.

Thomas, P.H., 1963. The size of flames from natural fires. *Symposium (International) on Combustion*, 9 (1), 844–859.

Tijms, H., 2012. Understanding Probability.

Tweeddale, M., 2003. *Managing Risk and Reliability of Process*. Gulf Professional Publishing.

U.S. Nuclear Regulatory Commission, 1975. Reactor safety study: An assessment of accident risks in U. S. commercial nuclear power plants., 1400 (October), 10.

United States Code of Federal Regulations, 2011. Title 30 - Mineral Resources.

United States International Trade Commission, 1986. Offshore platform jackets and piles from the Republic of Korea and Japan.

Vesely, W.E., 1969. *Analysis of Fault Trees by Kinetic Tree Theory*. Idaho Nuclear Corporation. Idaho.

Volovoi, V., 2004. Modeling of system reliability Petri nets with aging tokens. *Reliability Engineering and System Safety*, 84 (2), 149–161.

Wilson, R.B., 1963. A Simplical Algorithm for Concave Programming.

Zabetakis, M.G. and Burgess, D.S., 1961. *Research on the hazards associated with the production and handling of liquid hydrogen*. U.S. Dept. of the Interior, Bureau of Mines.

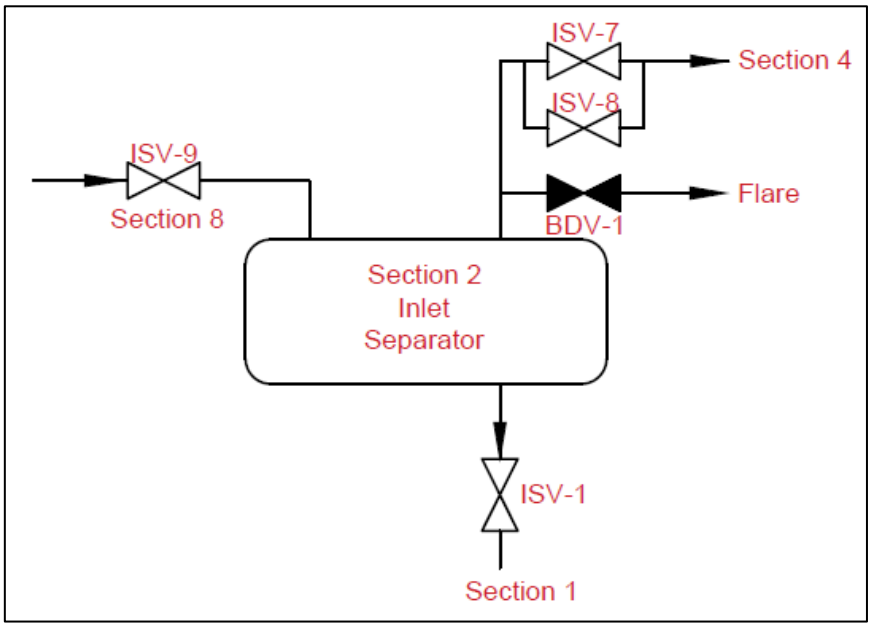
Zio, E., 2012. Prognostics and Health Management of Industrial Equipment. *Diagnostics and Prognostics of Engineering Systems: Methods and Techniques*, 4018, 333–356.

Zoutendijk, G., 1970. *Methods of Feasible Directions: A Study in Linear and Non-linear Programming*. Elsevier.

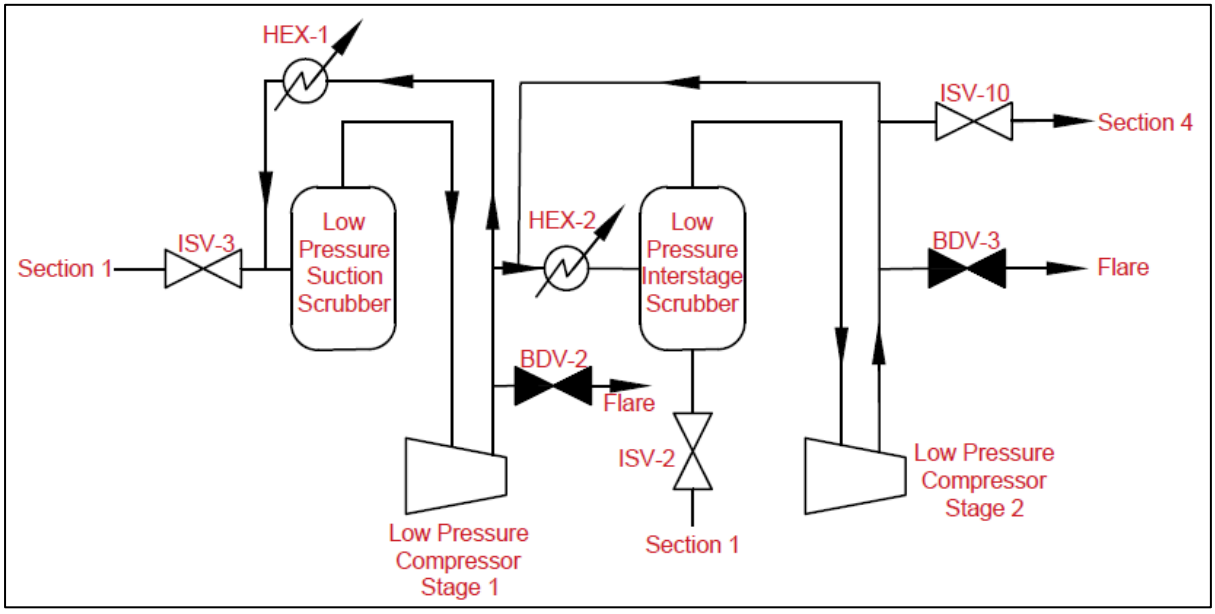
Appendix A

Schematic Diagrams of the Sections on the Platform

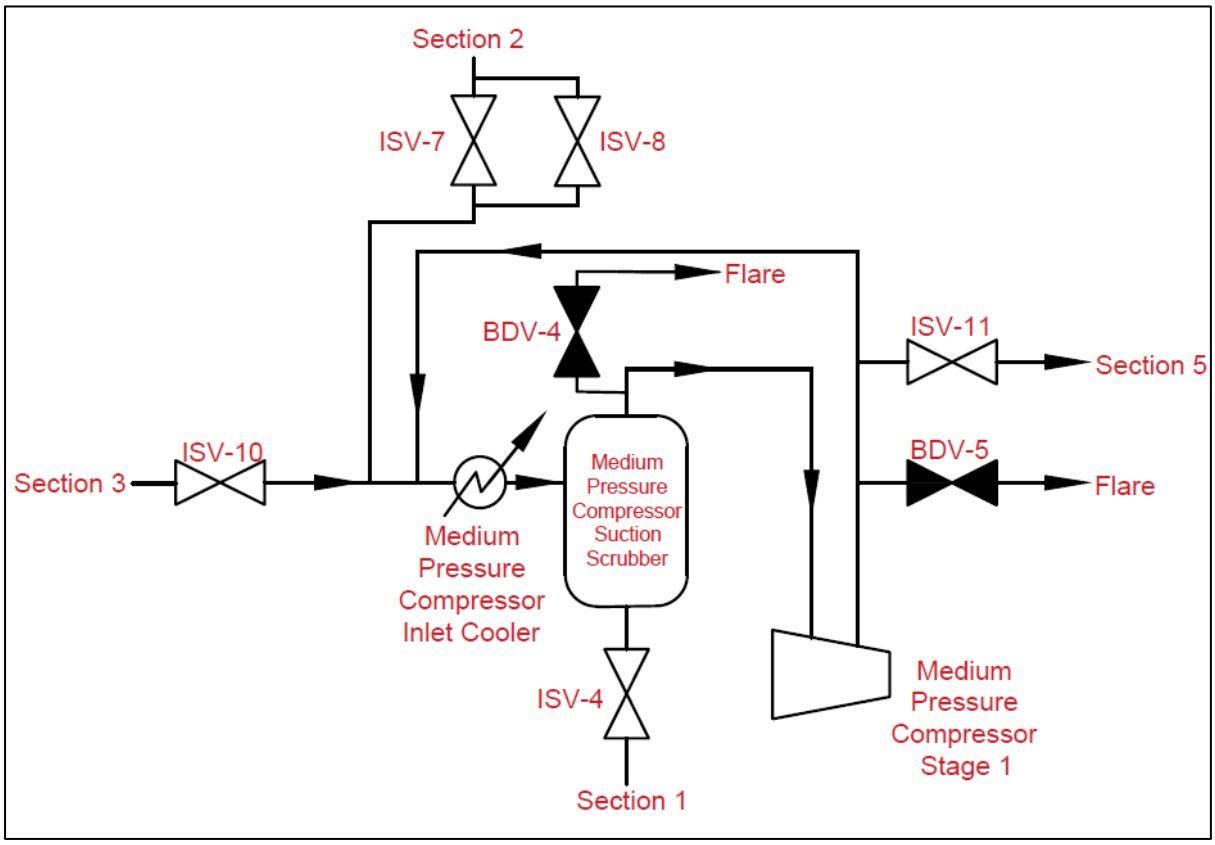
Section 2 – The Inlet Separator



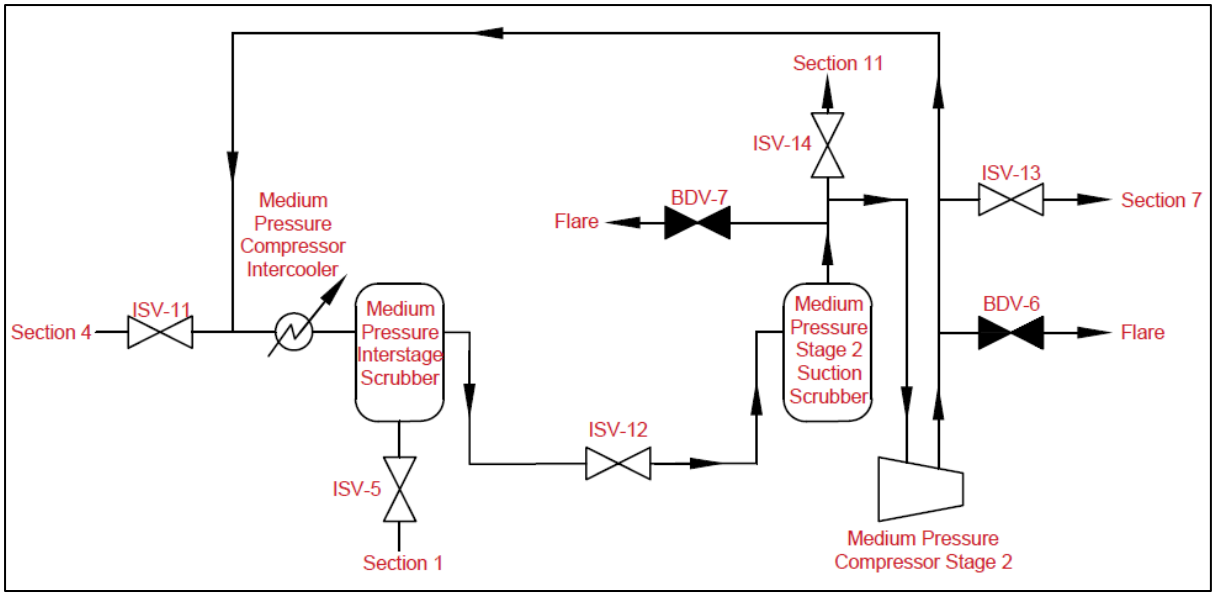
Section 3 – The Low Pressure Scrubbers and Compressors



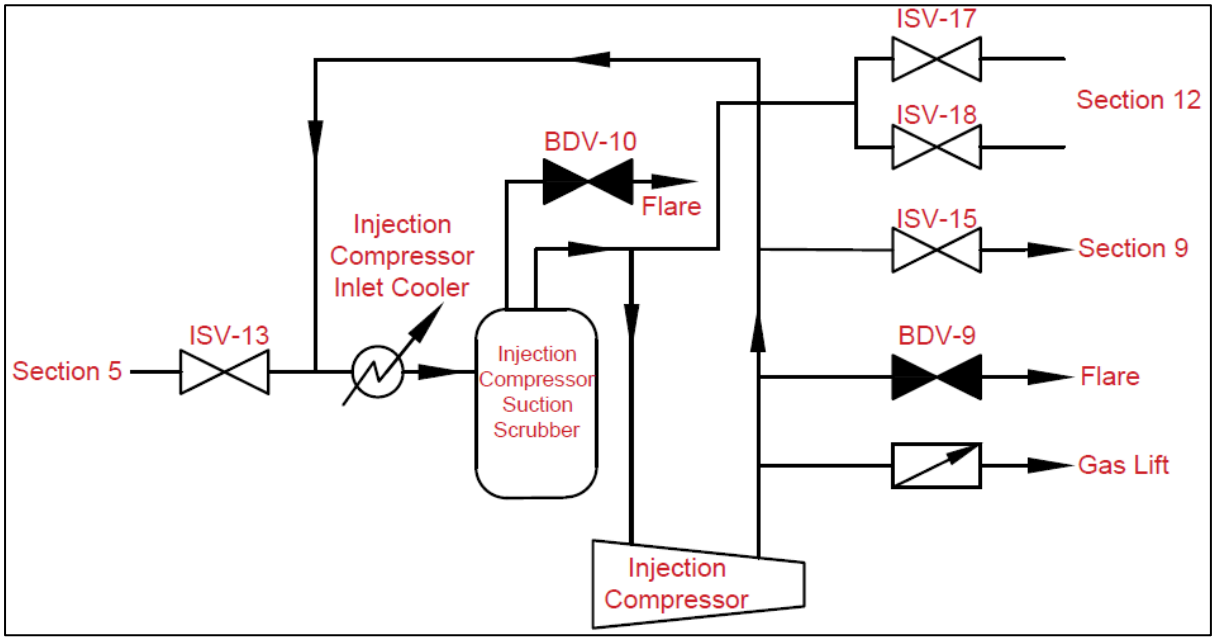
Section 4 – The Medium Pressure Scrubbers and Compressors (Stage 1)



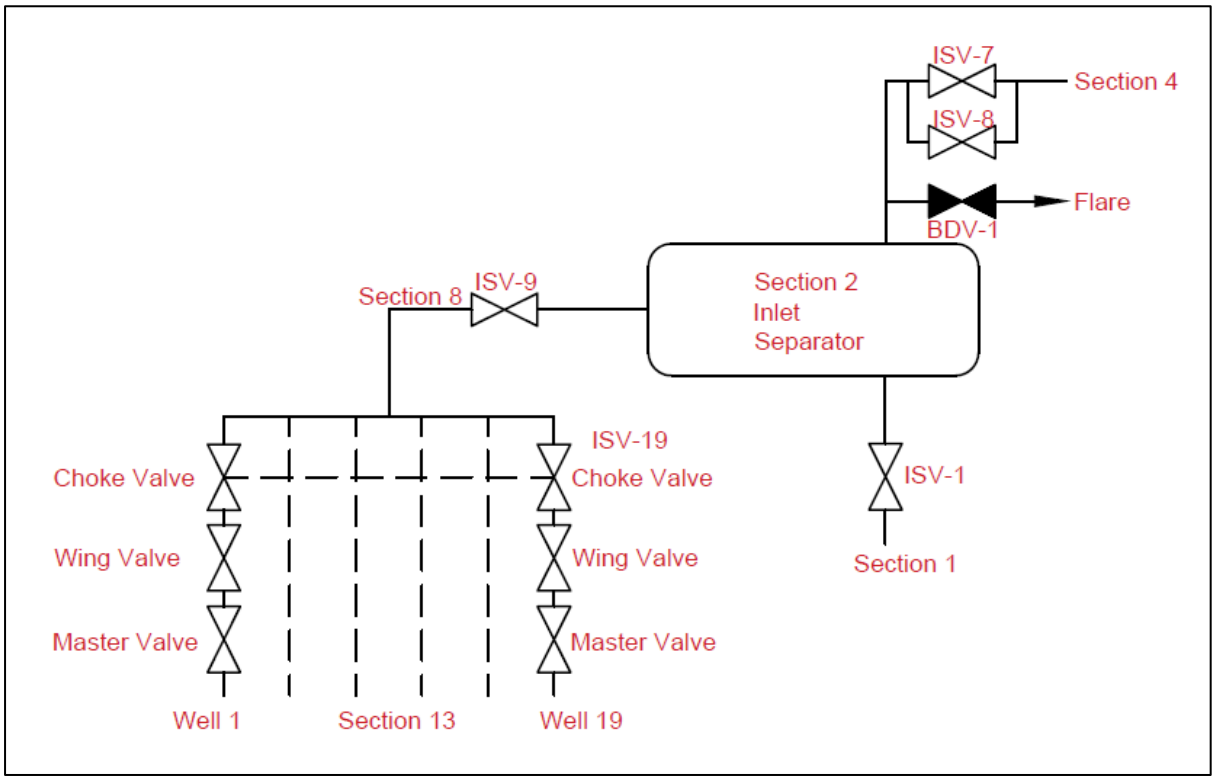
Section 5 – The Medium Pressure Scrubbers and Compressors (Stage 2)



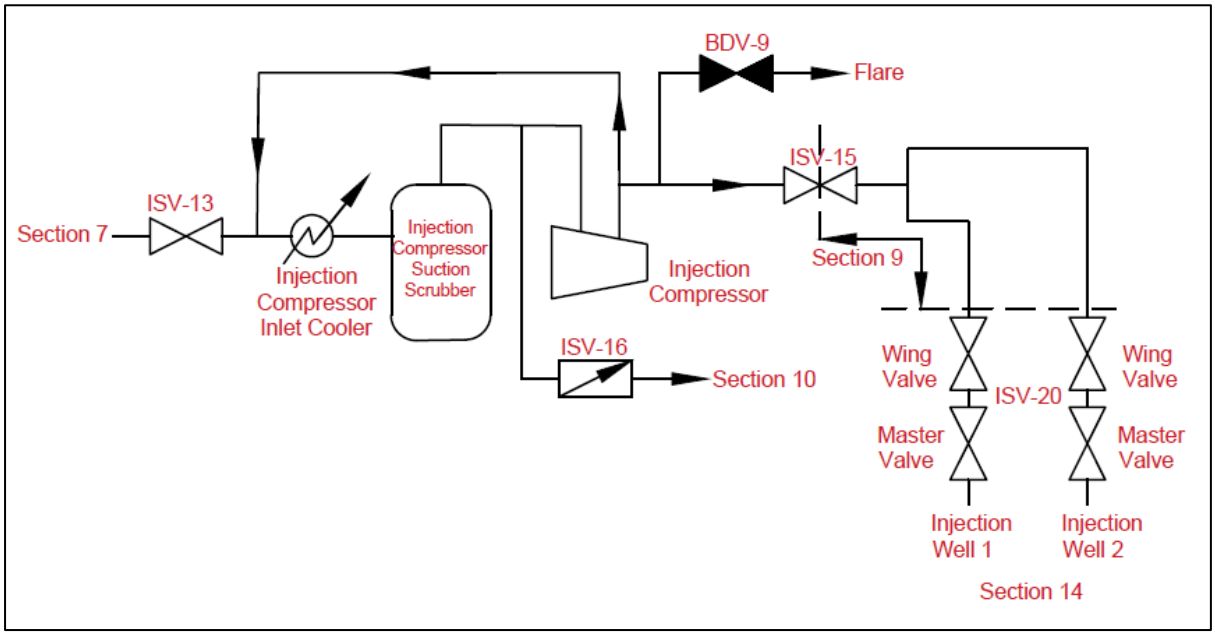
Section 6 – The Injection Compressors



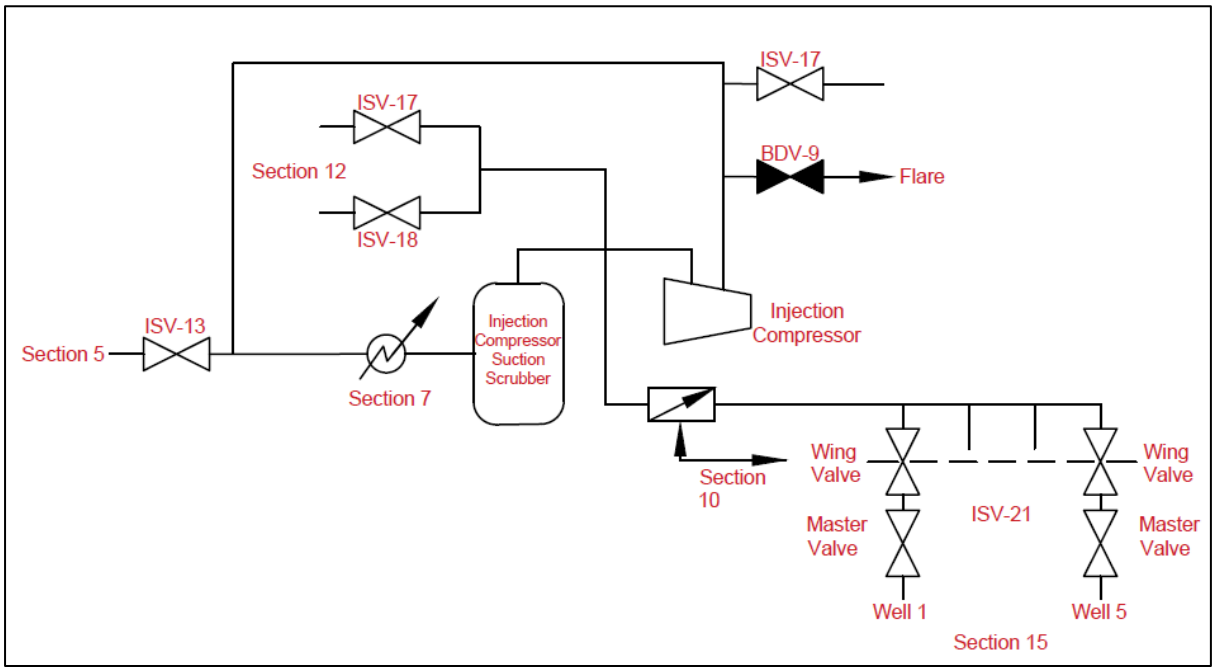
Section 8 – The Wellhead and Production Header Lines



Section 9 – The Gas Injection Line



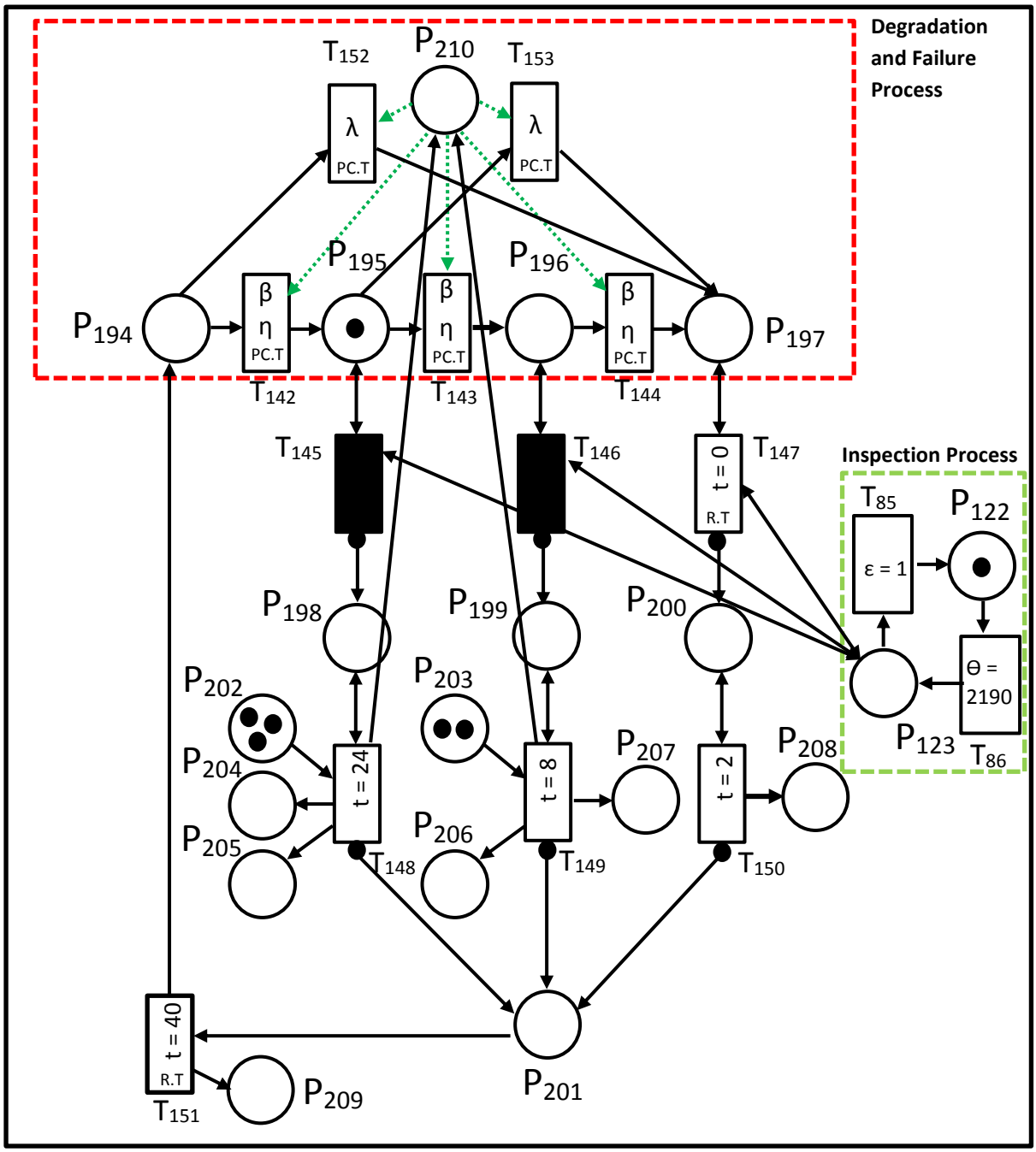
Section 10 – The Gas Lift Line



Appendix B

Petri Nets for Other Components of the Deluge System

Component: Booster Pump, System: Deluge System



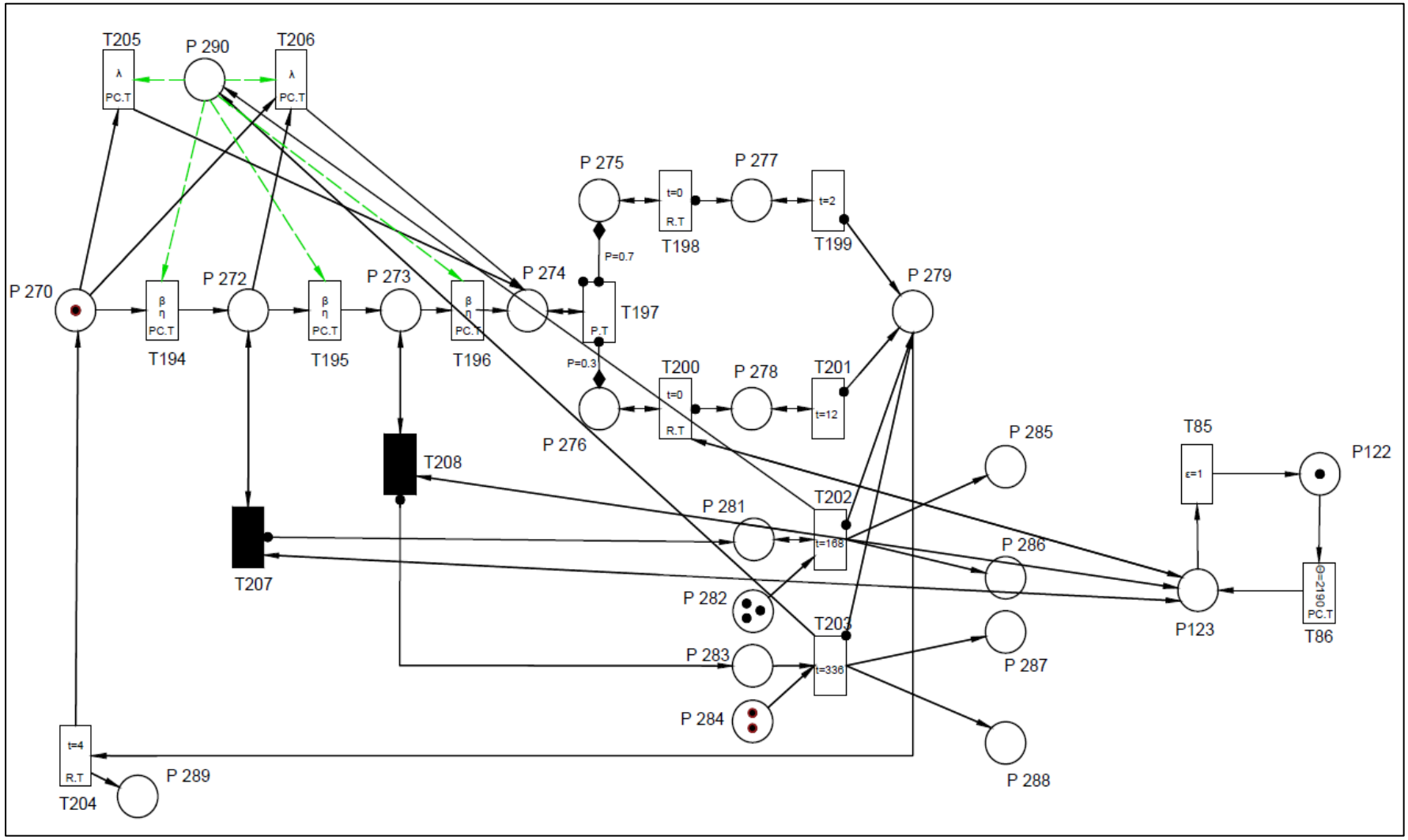
Petri Net Model showing the inspection and maintenance process for a Booster Pump

Place	Description
P122	No Periodic Inspection
P123	Periodic Inspection Underway
P194	New State
P195	Degraded State
P196	Severely Degraded State
P197	Functional Failure State

P198	Degraded State Revealed needing minor PM
P199	Severely Degraded State Revealed needing major PM
P200	Functional Failure State Revealed needing CM
P201	Maintenance Scheduled
P202	Maximum Number of Minor Repairs
P203	Maximum Number of Major Repairs
P204	Current Number of Minor Repairs
P205	Records statistics associated with the number of minor repairs and the corresponding costs incurred.
P206	Current Number of Major Repairs
P207	Records statistics associated with the number of major repairs and the corresponding costs incurred.
P208	Records statistics associated with the number of failures and the corresponding costs incurred.
P209	Total Number of Interventions
P210	Total Number of Repairs performed on the component

Description of the Places in the Booster Pump Model

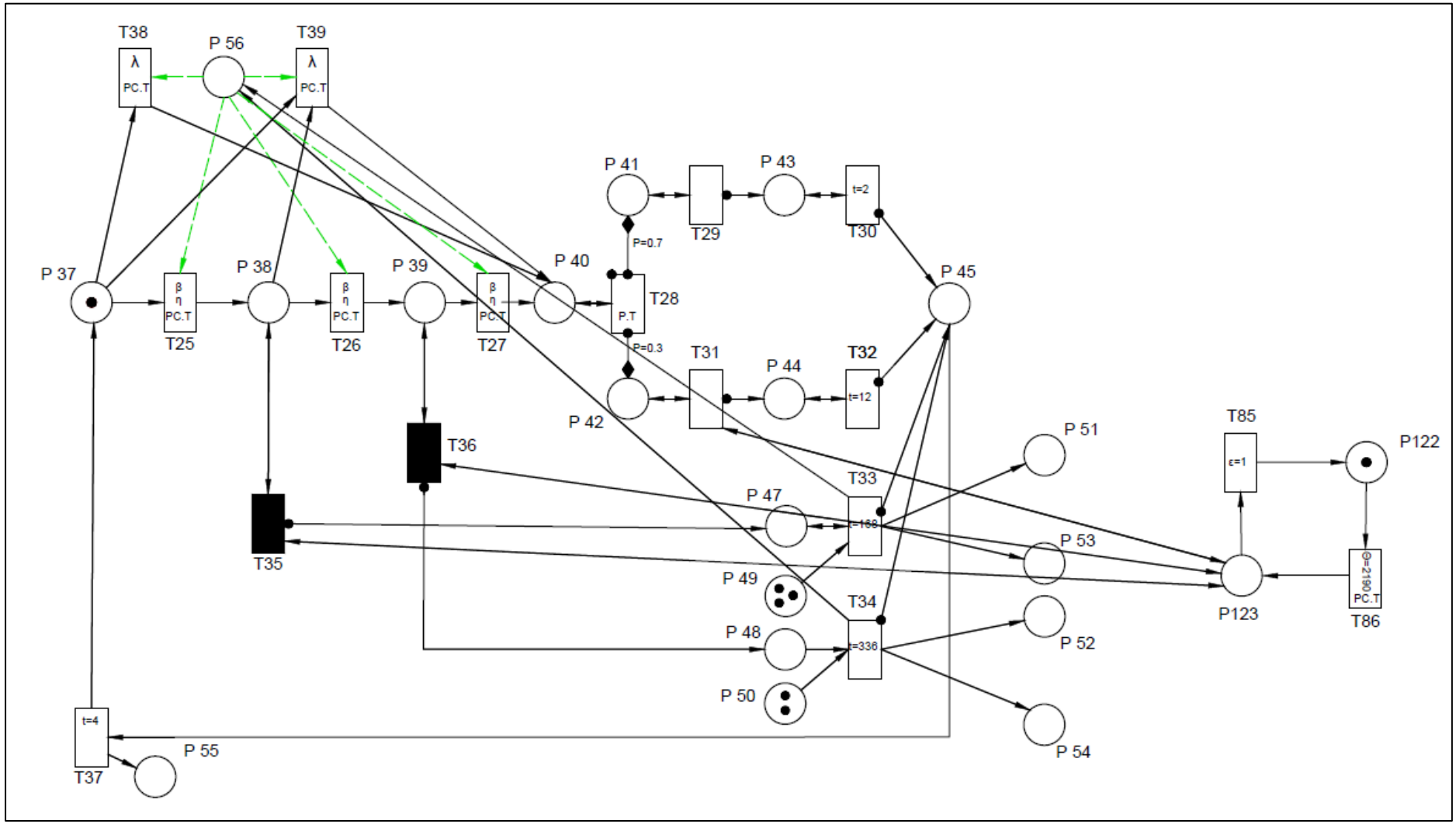
Component: Air Release Valve, System: Deluge System



Place	Description
P122	No Periodic Inspection
P123	Periodic Inspection Underway
P270	Normal Opening Time
P272	Degraded Opening Time
P273	Slow Opening Time
P274	Functional Failure State
P275	Fails Closed
P276	Fails to Open
P277	Revealed Failure
P278	Unrevealed Failure
P281	Degraded Opening Time Revealed needing minor PM
P283	Slow Opening Time Revealed needing major PM
P279	Maintenance Scheduled
P282	Maximum Number of Minor Repairs
P284	Maximum Number of Major Repairs
P286	Current Number of Minor Repairs
P285	Records statistics associated with the number of minor repairs and the corresponding costs incurred.
P288	Current Number of Major Repairs
P287	Records statistics associated with the number of major repairs and the corresponding costs incurred.
P289	Total Number of Interventions
P290	Total Number of Repairs performed on the component

Description of the Places in the Air Release Valve Model

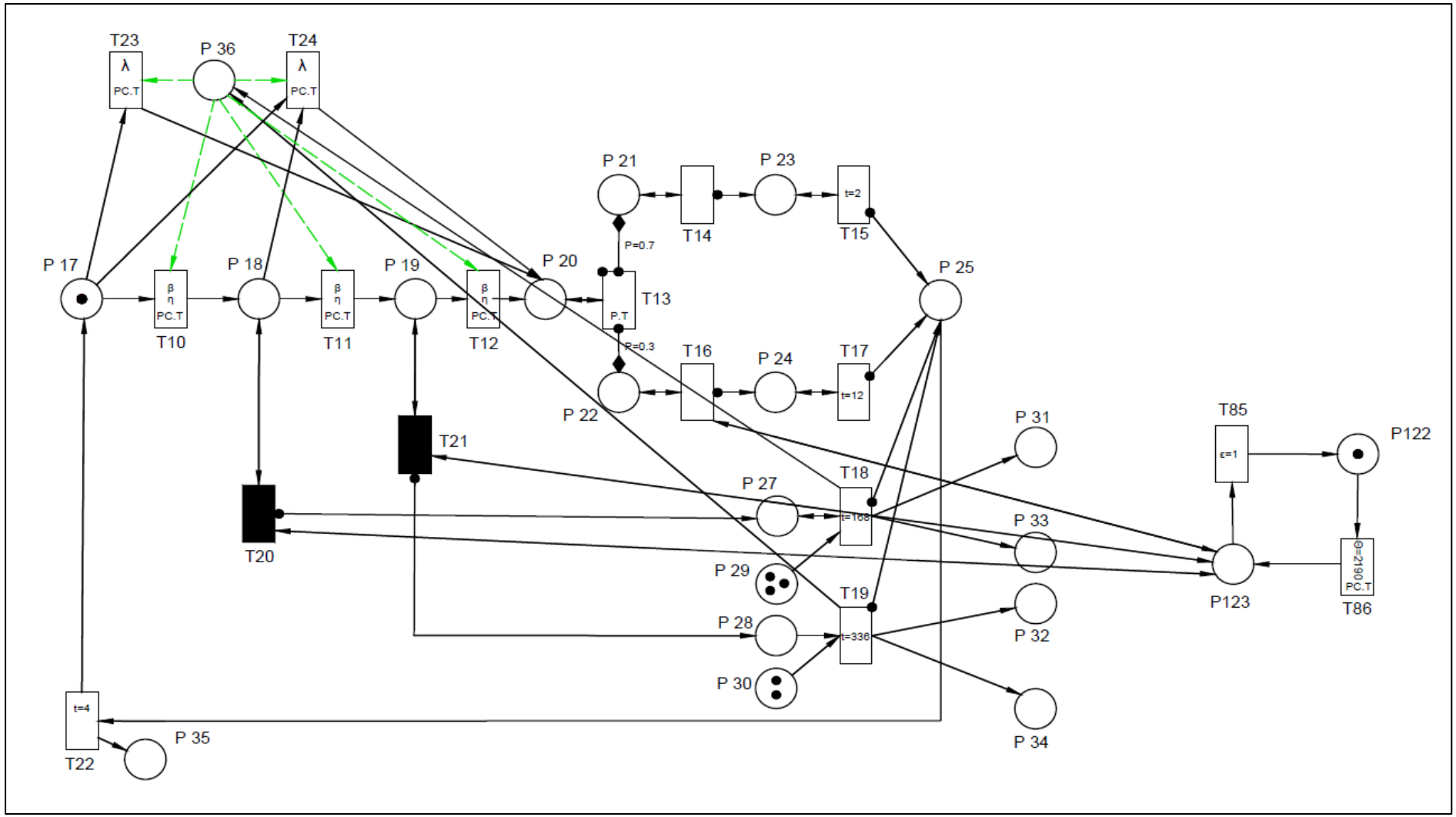
Component: Solenoid Valve, System: Deluge System



Place	Description
P122	No Periodic Inspection
P123	Periodic Inspection Underway
P37	Normal Opening Time
P38	Degraded Opening Time
P39	Slow Opening Time
P40	Functional Failure State
P41	Fails Closed
P42	Fails to Open
P43	Revealed Failure
P44	Unrevealed Failure
P47	Degraded Opening Time Revealed needing minor PM
P48	Slow Opening Time Revealed needing major PM
P45	Maintenance Scheduled
P49	Maximum Number of Minor Repairs
P50	Maximum Number of Major Repairs
P53	Current Number of Minor Repairs
P51	Records statistics associated with the number of minor repairs and the corresponding costs incurred.
P54	Current Number of Major Repairs
P52	Records statistics associated with the number of major repairs and the corresponding costs incurred.
P55	Total Number of Interventions
P56	Total Number of Repairs performed on the component

Description of the Places in the Solenoid Valve Model

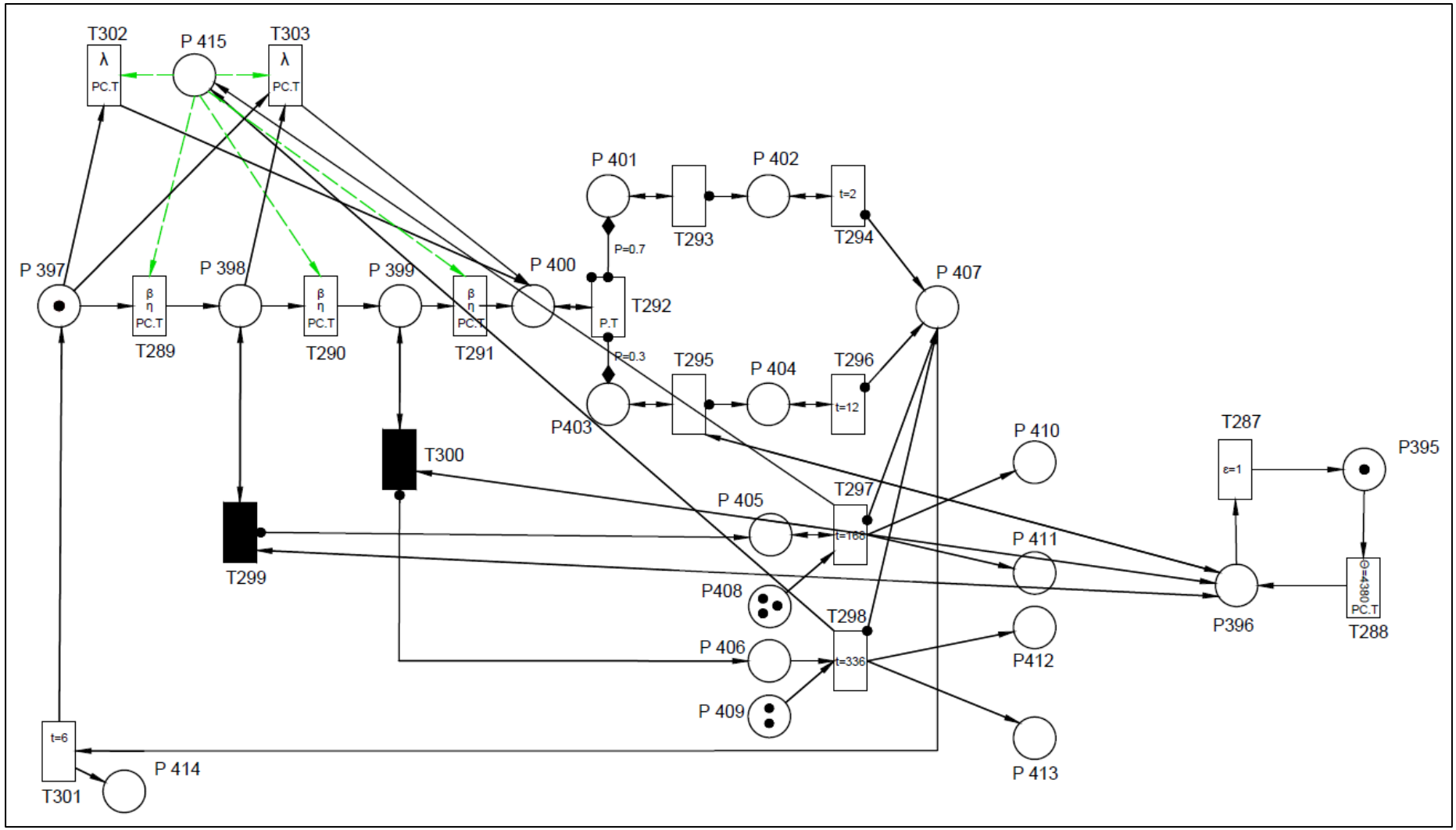
Component: Deluge Valve, System: Deluge System



Place	Description
P122	No Periodic Inspection
P123	Periodic Inspection Underway
P17	Normal Opening Time
P18	Degraded Opening Time
P19	Slow Opening Time
P20	Functional Failure State
P21	Fails Closed
P22	Fails to Open
P23	Revealed Failure
P24	Unrevealed Failure
P27	Degraded Opening Time Revealed needing minor PM
P28	Slow Opening Time Revealed needing major PM
P25	Maintenance Scheduled
P29	Maximum Number of Minor Repairs
P30	Maximum Number of Major Repairs
P33	Current Number of Minor Repairs
P31	Records statistics associated with the number of minor repairs and the corresponding costs incurred.
P34	Current Number of Major Repairs
P32	Records statistics associated with the number of major repairs and the corresponding costs incurred.
P35	Total Number of Interventions
P36	Total Number of Repairs performed on the component

Description of the Places in the Solenoid Valve Model

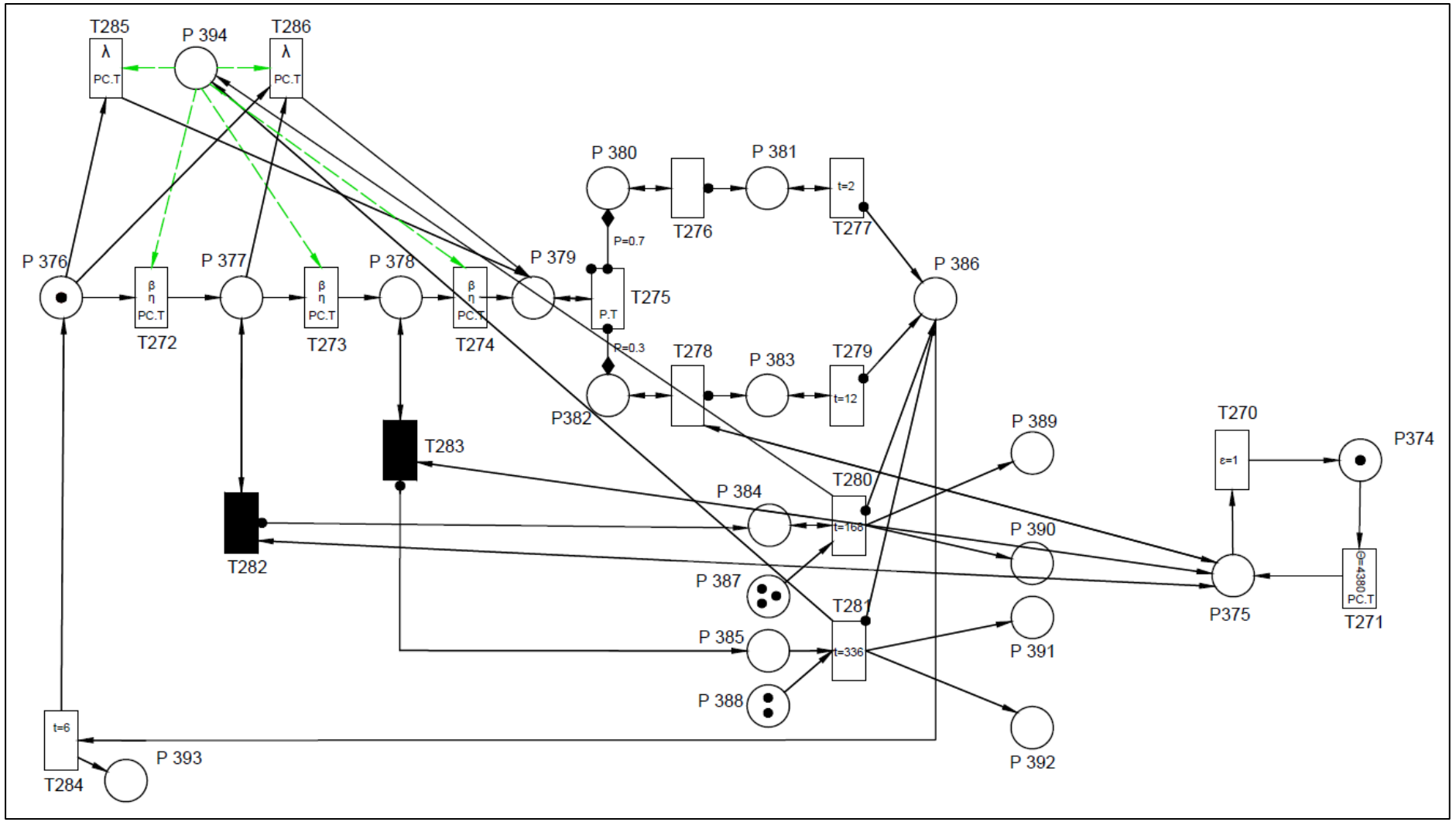
Component: ISV-1, System: Isolation Valves



Place	Description
P395	No Periodic Inspection
P396	Periodic Inspection Underway
P397	Normal Closing Time
P398	Degraded Closing Time
P399	Slow Closing Time
P400	Functional Failure State
P401	Fails Open
P403	Fails to Close
P402	Revealed Failure
P404	Unrevealed Failure
P405	Degraded Closing Time Revealed needing minor PM
P406	Slow Closing Time Revealed needing major PM
P407	Maintenance Scheduled
P408	Maximum Number of Minor Repairs
P409	Maximum Number of Major Repairs
P410	Current Number of Minor Repairs
P411	Records statistics associated with the number of minor repairs and the corresponding costs incurred.
P412	Current Number of Major Repairs
P413	Records statistics associated with the number of major repairs and the corresponding costs incurred.
P414	Total Number of Interventions
P415	Total Number of Repairs performed on the component

Description of the Places in the Isolation Valve Model

Component: BDV-1, System: Blowdown Valves



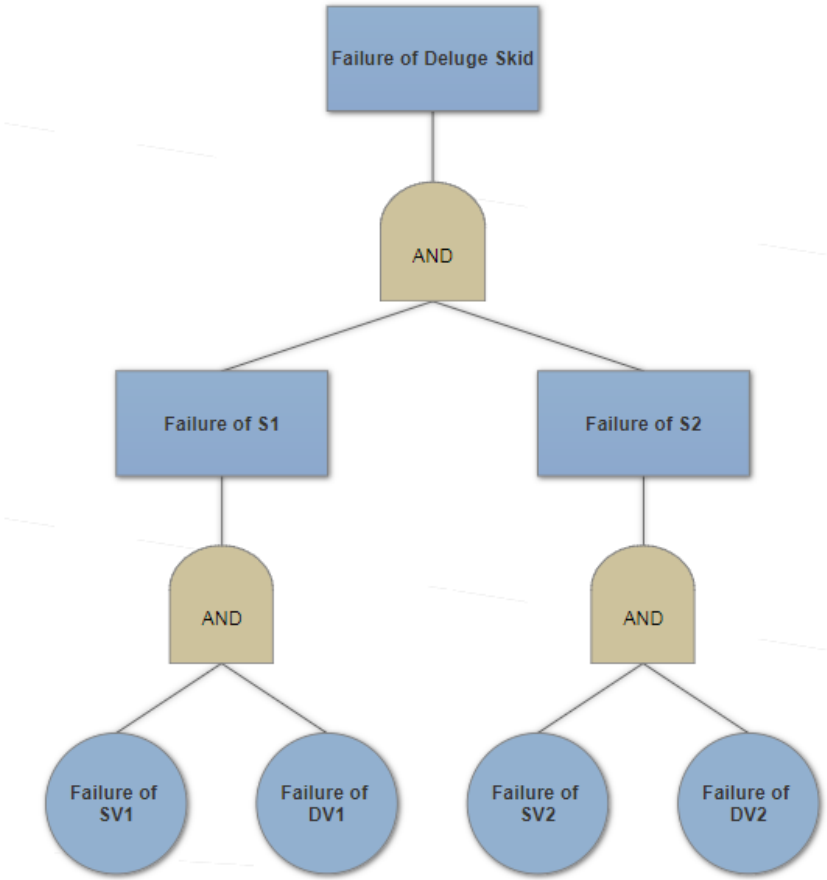
Place	Description
P374	No Periodic Inspection
P375	Periodic Inspection Underway
P376	Normal Opening Time
P377	Degraded Opening Time
P378	Slow Opening Time
P379	Functional Failure State
P380	Fails Closed
P382	Fails to Open
P381	Revealed Failure
P383	Unrevealed Failure
P384	Degraded Opening Time Revealed needing minor PM
P385	Slow Opening Time Revealed needing major PM
P386	Maintenance Scheduled
P387	Maximum Number of Minor Repairs
P388	Maximum Number of Major Repairs
P389	Current Number of Minor Repairs
P390	Records statistics associated with the number of minor repairs and the corresponding costs incurred.
P391	Current Number of Major Repairs
P392	Records statistics associated with the number of major repairs and the corresponding costs incurred.
P393	Total Number of Interventions
P394	Total Number of Repairs performed on the component

Description of the Places in the Blowdown Valve Model

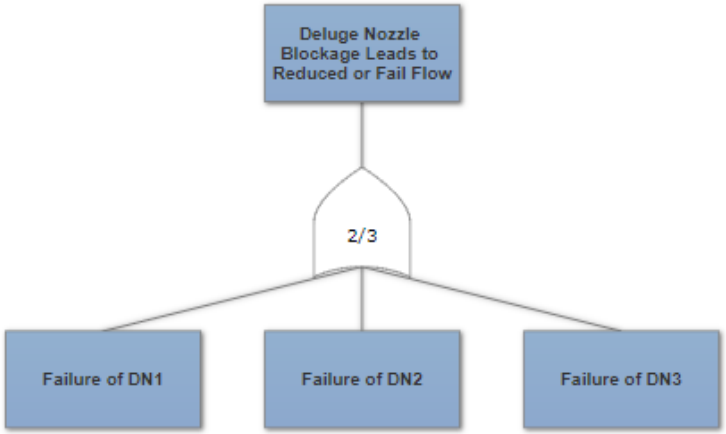
Appendix C

Fault Tree Diagrams for the Different Subsystems

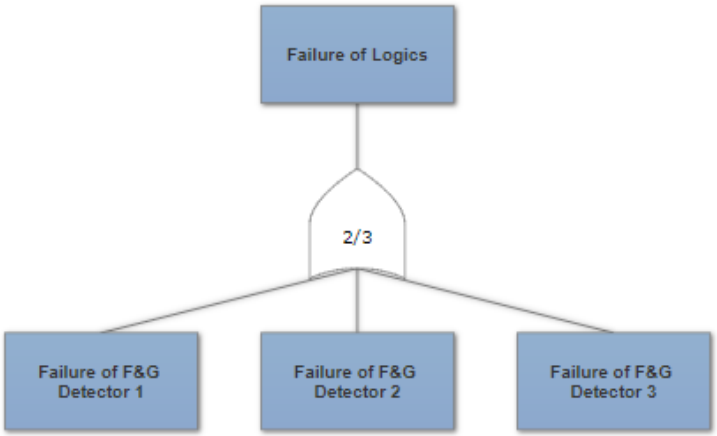
Fault Tree Diagram for Deluge Skid



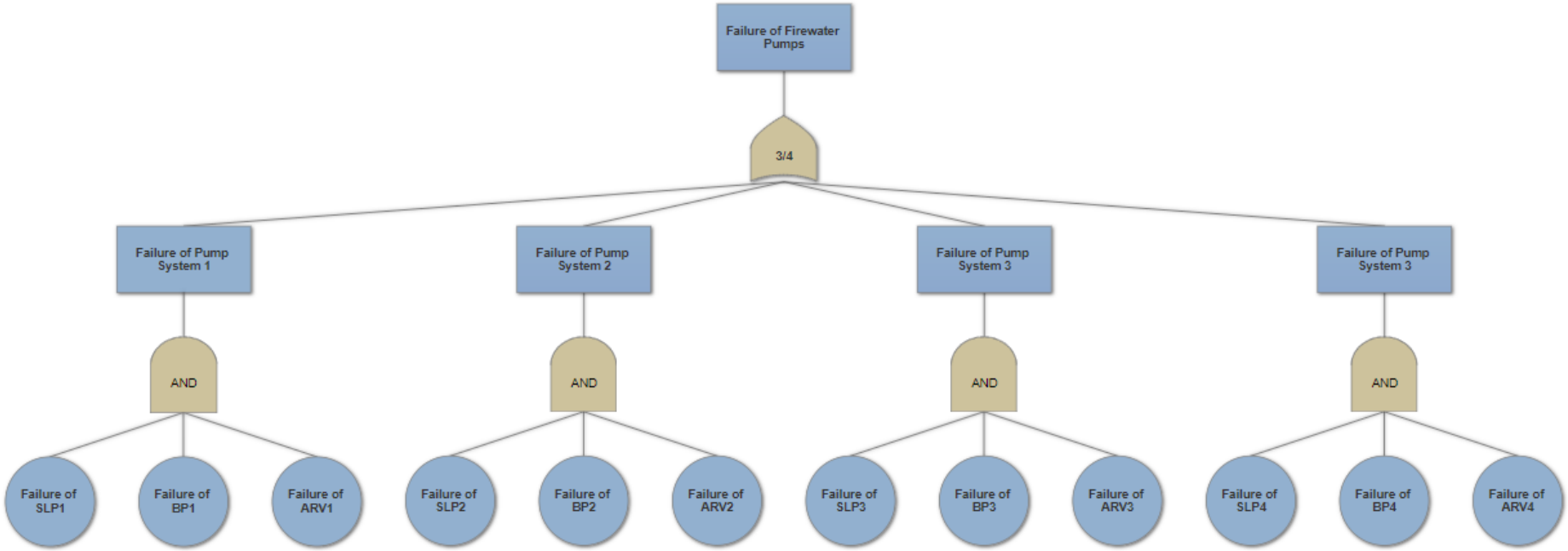
Fault Tree Diagram for Deluge Nozzle



Fault Tree Diagram for the Fire and Gas Logics



Fault Tree for the Firewater Pumps



Appendix D

Enhancements made to De Rozieres Code

D.1 Addition of Probabilistic Transition (C++ Source File):

```
//  Generated by StarUML(tm) C++ Add-In
#include "Probabilistic_Transition.h"
#include "Arc.h"
#include <QtGlobal>
#include <string>
#include "Generic_Tools/Exception_Pool.h"

#include "Generic_Tools/Tools.h"
#include "Generic_Tools/My_Exception.h"

using namespace PN_Models;

///*************************    enable()    *************************///
/*void Probabilistic_Transition::enable()
{
  //This case doesn't make any sense in the perspective of a PN model but, the code has to
be protected against it.
  if(m_inputArcs.empty())
    {
      m_state = DISABLED;
      m_initialDelay = 0.0;
      m_currentRemainingDelay = 0.0;
      return;
    }

  for (unsigned int i=0;i < m_inputInhibitorArcs.size();i++)
    {
      if(m_inputInhibitorArcs.at(i)->getPlace()-
>getCurrentNumberOfTokens()>=m_inputInhibitorArcs.at(i)->getMultiplicity())
        {
          m_state = DISABLED;
          m_initialDelay = 0.0;
          m_currentRemainingDelay = 0.0;
          return;
        }
    }

  for (unsigned int i=0;i < m_inputArcs.size();i++)
    if(m_inputArcs.at(i)->getPlace()->getCurrentNumberOfTokens()<m_inputArcs.at(i)-
>getMultiplicity())
```

```
    {
      m_state = DISABLED;
      m_initialDelay = 0.0;
      m_currentRemainingDelay = 0.0;
      return;
    }

  //If we are here, it means that the transition should be ENABLED
  if(m_state == DISABLED)
    {
      double newDelay = 0;
      m_state = ENABLED;
      bool isTheCase = false;

      if(!isTheCase)//If there is not cases true to change the delay parameters, the normal
(default) delay parameters is used
        newDelay = m_delayParameters->generateDelay();

      m_initialDelay = newDelay;
      m_currentRemainingDelay = newDelay;
    }
}*/
///*************************    fire()    *************************///
void Probabilistic_Transition::fire()
{
   unsigned int i=0;
   for (i=0;i < m_inputArcs.size();i++)
      m_inputArcs.at(i)->getPlace()->subtractTokens(m_inputArcs.at(i)->getMultiplicity());
   for (i=0;i < m_outputArcs.size();i++)
      m_outputArcs.at(i)->getPlace()->addTokens(m_outputArcs.at(i)->getMultiplicity());
   double tmp_prob = qrand()/(double)RAND_MAX;
   for (i=0;i<m_outputProbabilisticArcs.size();i++)
      m_outputProbabilisticArcs.at(i)->setFiring(false);
   for (i = 1; i<m_prob_intervals.size();i++)
      if(tmp_prob> m_prob_intervals.at(i-1) && tmp_prob <=m_prob_intervals.at(i))
      {
         for (unsigned int k = 0; k<m_outputProbabilisticArcs.size(); k++)
         {
            if( (m_probabilisticPlaces.at(i-1)->m_ID.m_id == m_outputProbabilisticArcs.at(k)-
>getPlaceID()) && (m_probabilisticPlaces.at(i-1)->m_ID.m_subModel ==
m_outputProbabilisticArcs.at(k)->getPlaceSubmodelID()))
            {
               m_probabilisticPlaces.at(i-1)->addTokens(m_outputProbabilisticArcs.at(k)-
>getMultiplicity());
               m_outputProbabilisticArcs.at(k)->setFiring(true);
               break;
            }
```

```
        }
        break;
      }
}
///*************************    generateIntervals()
*************************///
void Probabilistic_Transition::generateIntervals()
{
   unsigned int i;
   double tmp_sum = 0.0;
   for (i = 0; i <m_probabilities.size();i++)
      tmp_sum+=m_probabilities.at(i);
   if (tmp_sum != 1.0)
   {
      for (i = 0; i <m_probabilities.size();i++)
         m_probabilities.at(i) = m_probabilities.at(i)/tmp_sum;
   }
   std::vector<double> interval_upper;
   interval_upper.push_back(0.00); // so that 0 goes to 1st interval
   for(i = 0; i <m_probabilities.size()-1;i++)
      interval_upper.push_back(interval_upper.at(i)+m_probabilities.at(i));
   interval_upper.push_back(1.00);
   m_prob_intervals = interval_upper;
}
///*************************    newClone()    *************************///
PN_Models::Transition* Probabilistic_Transition::Probabilistic_Transition::newClone() const
{
   return new Probabilistic_Transition(*this);
}

///*************************    addProbability(...)    *************************///
void Probabilistic_Transition::addProbability(const double &prob)
{
   m_probabilities.push_back(prob);
}
///*************************    addProbabilisticPlace(...)
*************************///
void Probabilistic_Transition::addProbabilisticPlace(PN_Models::Place & p)
{
   m_probabilisticPlaces.push_back(&p);
}

///*************************    Probabilistic_Transition(...)
*************************///
Probabilistic_Transition::Probabilistic_Transition(PN_Models::Identification const& ID,const
Delay_Parameters &dp, std::vector<Place*> const& pplaces)
   :Transition(ID,dp), m_probabilisticPlaces(pplaces)
```

```
{}
///*************************    Probabilistic_Transition(...)
*************************///
Probabilistic_Transition::Probabilistic_Transition(PN_Models::Identification const& ID,const
Delay_Parameters &dp)
   :Transition(ID,dp)
{}

///*************************    ~Probabilistic_Transition()
*************************///
Probabilistic_Transition::~Probabilistic_Transition()
{
}
///*************************    Probabilistic_Transition(...)
*************************///
Probabilistic_Transition::Probabilistic_Transition(const Probabilistic_Transition & toCopy)

:Transition(toCopy),m_probabilities(toCopy.m_probabilities),m_prob_intervals(toCopy.m_p
rob_intervals), m_probabilisticPlaces(toCopy.m_probabilisticPlaces)
{
}
///*************************    operator= ()    *************************///
Probabilistic_Transition& Probabilistic_Transition::operator= (Probabilistic_Transition
const& toCopy)
{
   if(this != &toCopy)
   {
      Transition::operator=(toCopy);
      m_probabilities = toCopy.m_probabilities;
      m_prob_intervals = toCopy.m_prob_intervals;
      m_probabilisticPlaces = toCopy.m_probabilisticPlaces;
   }
   return *this;
}

///*************************    getProbabilisticPlaces()
*************************///
const std::vector<Place*> &Probabilistic_Transition::getProbabilisticPlaces()
{
   return m_probabilisticPlaces;
}
///*************************    clearAllProbabilisticPlaces()
*************************///
void Probabilistic_Transition::clearAllProbabilisticPlaces()
{
   m_probabilisticPlaces.clear();
}
```

```
///*************************    toString()    *************************///
std::string Probabilistic_Transition::toString() const
{
   std::string r = std::string("\nPlace Conditionnal Transition >> Intial Delay ");
   r+= Generic_Tools::toString(m_initialDelay);
   r+=" Remaining Delay ";
   r += Generic_Tools::toString(m_currentRemainingDelay);

   r+= m_delayParameters->toString();
   r += " State ";
   switch(m_state)
   {
   case DISABLED:
      r += "DISABLED\n";
      break;
   case ENABLED:
      r += "ENABLED\n";
      break;
   }

   if(!m_inputArcs.empty())
   {
      for (unsigned int i=0;i < m_inputArcs.size();i++)
      {
         r+="Input Arcs :";
         r+=m_inputArcs.at(i)->toString()+"\n";
      }
   }
   if(!m_outputArcs.empty())
   {
      for (unsigned int i=0;i < m_outputArcs.size();i++)
      {
         r+="Output Arc :";
         r+=m_outputArcs.at(i)->toString()+"\n";
      }
   }
   if(!m_inputInhibitorArcs.empty())
   {
      for (unsigned int i=0;i < m_inputInhibitorArcs.size();i++)
      {
         r+="Input Inhibitor Arcs :";
         r+=m_inputInhibitorArcs.at(i)->toString()+"\n";
      }
   }
   if(m_inputInhibitorArcs.empty()&&m_outputArcs.empty()&&m_inputArcs.empty())
      r+="\n";
```

```
   return Node::toString()+r+".";
}
```

D.2 Addition of Probabilistic Transition (Header File):

```
#ifndef PROBABILISTIC_TRANSITION
#define PROBABILISTIC_TRANSITION

#include <string>
#include "Transition.h"
#include "Delay_Parameters.h"
#include "Place.h"

namespace PN_Models
{
 class Probabilistic_Transition : public Transition {
 private:
    std::vector<double> m_probabilities;
    std::vector<double> m_prob_intervals;
    std::vector<Place*> m_probabilisticPlaces;


 public:
   Probabilistic_Transition(PN_Models::Identification const& ID,const Delay_Parameters
&dp);
   Probabilistic_Transition(PN_Models::Identification const& ID,const Delay_Parameters
&dp, std::vector<Place*> const& pplaces);

   ~Probabilistic_Transition();
   Probabilistic_Transition(const PN_Models::Probabilistic_Transition & toCopy);
   Probabilistic_Transition& operator= (PN_Models::Probabilistic_Transition const& toCopy);
   PN_Models::Transition* newClone() const;
   const std::vector<double> &getProbabilities();
   void generateIntervals();
   void addProbability(const double &prob);
   void addProbabilisticPlace(PN_Models::Place &p);
   const std::vector<Place*> &getProbabilisticPlaces();
   void clearAllProbabilisticPlaces();
   std::string toString() const;
   bool normed();
   void norm_probabilities();
 //   void enable();
    void fire();
 };
}
#endif // PROBABILISTIC_TRANSITION
```

D.3 Addition of Uniform Distribution (C++ Source File):

```
#include "Uniform2.h"

#include <QtGlobal>//For qrand() and thread safety !

#include "string"
#include <math.h>
#include <stdlib.h>

#include "Generic_Tools/My_Exception.h"
#include "Generic_Tools/Tools.h"

using namespace PN_Models;

///************************    Uniform2(...)    ************************///
Uniform2::Uniform2(double min_val, double max_val)
{
 setMinVal(min_val);
 setMaxVal(max_val);
}
///************************    generateDelay()    ************************///
double Uniform2::generateDelay(const double &truncation, const bool &fired) const
{
 if (fired)
    return qMax((qrand()/(double)RAND_MAX)*(m_max_val-m_min_val)+m_min_val, 0.0);
     else
   return qMax((qrand()/(double)RAND_MAX)*(m_max_val-m_min_val)+m_min_val -
truncation, 0.0);
}
///************************    newClone()    ************************///
Delay_Parameters *Uniform2::newClone() const
{
 return new Uniform2(*this);
}
///************************    getMinVal()    ************************///
double Uniform2::getMinVal()
{
 return m_min_val;
}
///************************    getMaxVal()    ************************///
double Uniform2::getMaxVal()
{
 return m_max_val;
}
///************************    setMinVal(...)    ************************///
void Uniform2::setMinVal(double minval)
```

```
{
 /* if (minval >= m_max_val)
   throw Generic_Tools::My_Exception("Trying to set a wrong min value for
uniform",__FILE__,__LINE__);
*/
 m_min_val = minval;
}
///************************    setMaxVal(...)    ************************///
void Uniform2::setMaxVal(double maxval)
{
 /*if (maxval <= m_min_val)
   throw Generic_Tools::My_Exception("Trying to set a wrong max value for
uniform",__FILE__,__LINE__);
*/
 m_max_val = maxval;
}
///************************    toString()    ************************///
std::string Uniform2::toString() const
{
 std::string r = std::string(" Min of uniform Delay =");
 r += Generic_Tools::toString(m_min_val);
 return r;
}
```

D.4 Addition of Uniform Distribution (Header File):

```
#ifndef UNIFORM2_H
#define UNIFORM2_H

#include "Delay_Parameters.h"

namespace PN_Models
{
 class Uniform2 : public Delay_Parameters
    {
    private:
     //The cumulative distribution function for the exponential distribution is:
     // F(t) = 1-exp(-rate*t);
     //With F(t) between 0 & 1.
     double m_min_val, m_max_val;//Inverse scale parameter
    public:
     Uniform2(double min_val, double max_val);
     double generateDelay(const double &truncation, const bool &fired) const;
     PN_Models::Delay_Parameters* newClone() const;
     double getMinVal();
     double getMaxVal();
      void setMinVal(double minval);
```

```
        void setMaxVal(double maxval);
       std::string toString() const;//Common method for self-description
     };
}
#endif // UNIFORM2_H
```

D.5 Addition of Save and Open Option (C++ Source Code):

```
#include "Save_Open_Class.h"

#include <QFile>
#include <QtWidgets/QScrollBar>
#include <QtCore/QTextStream>
#include <QMessageBox>

using namespace Save_Open;

///*************************    Save_Open_Class()
*************************///
Save_Open_Class::Save_Open_Class()
{
}
///*************************    saveProject(...)    *************************///
bool Save_Open_Class::saveProject(QList<QMdiSubWindow *> views, View::Diagram_Scene
*scene, View::Shadow_Scene * shadowScene)
{
  QFile file(scene->getSceneName());
  if(!file.open(QIODevice::WriteOnly))
    return false;
  QDataStream out(&file);   // we will serialize the data into the file
  out.setVersion(QDataStream::Qt_4_8);

  //Magic Number and save version
  //Identify this kind of file, thus we might be able to know wether the file loaded comes
from this application or not
  out << QString("This an unique application developed by F.De Rozieres!");
  double version = 1.0;
  bool saveShadows = false;
  if (shadowScene->isUsed())
  {
     QMessageBox msgBox;
     msgBox.setText("The net contains \"status\" settings.");
     msgBox.setInformativeText("Do you want to keep it?\n(You will be able to open saved
file only with this version of software)");
     msgBox.setStandardButtons(QMessageBox::Save | QMessageBox::Discard);
     msgBox.setIcon(QMessageBox::Question);
     msgBox.setDefaultButton(QMessageBox::Save);
```

```
    int ret = msgBox.exec();

    if (ret == QMessageBox::Save)
    {
      version = 1.1;
      saveShadows = true;
    }
}

 out << version;//The version of this file

 //Create this list of Diagram_Items and Arrows to save them.
 QList<View::Diagram_Item *> diagList;
 QList<View::Arrow *> arrowsList;
 foreach (QGraphicsItem *item, scene->items())
  {
```

D.6 Addition of Sensitivity analysis

Sensitivity Analysis (SA) is aimed to obtain and compare results of simulations performed with different parameters. The changeable parameters are:

- Inspection interval, one value for all systems (controlled in MCS_Handling::setSystemParameters)

- Mean time to degradation of components for each system (controlled in the lately added special function MCS_Handling::setSystemParametersT).

SA can be performed for any subset of these parameters or for all of them in one time. Each parameter loops through 5 values, including the reference value, which is set by default when SA for this parameter is not enabled. Hence, all parameters except current have their reference values.

SA can also be performed for some predefined sets of parameters known as strategies. In this case, multiple parameters are changed simultaneously according to the table of strategies. The parameters are:

- Maximum number of minor and major component maintenances for the Deluge system, with allowed zero value.
- Enable opportunistic maintenance.

All of the above parameters are managed by MCS_Handling::setSystemParameters

To run SA, launch the PetriNet application, open the desired network and press the right of two Simulate buttons. This brings up the dialog, where one can choose variables for SA, including Strategies. If nothing is chosen, only reference case will be computed. After the desired set of variables is confirmed by the OK button, the standard simulation dialog is shown. Here one may set general simulation parameters, such as number of simulations, finish time, etc. and run simulations.

The given number of simulations will be performed for the reference case and for each non-reference value of each of the chosen variable and/or for each strategy. Results of each case will be saved to separate subfolder, located in the output folder, like the following: <looping_variable_name><value>, or 'reference' for the reference case.

After simulations are completed, one may run the MATLAB script - LeakagesFldSAOpt.m Matlab to read and analyse further results.

D.7 Addition of Automated Launch mode

The automated launch mode allows MATLAB scripts to run Petri net simulations with needed parameters. This mode becomes enabled when application is launched with more than 1 command line parameter. In this case application shows its windows, but makes no requests to user and does not need any GUI action. It receives from command line path to .pn file, path to output folder, and path to .ini file with parameters to be used in simulation. Then application performs number of simulations on the specified .pn network, according to settings listed in .ini. It then writes results to the specified folder. Unlike SA mode, in Automated Launch mode application produces only one set of results.

The example of command line:
PetriNet_Software.exe
C:\Users\user\qt_petri_net_software\Restored_Model\Restored_1t_tmp.pn ..\..\DebugTmpOutput ..\..\debugInput.ini

The .ini file has to be similar to the following:

```
// EXAMPLE OF .INI
-----------------------------------------
numberOfSimulationToDo = 2000
simulationTime = 302400
simulationStep = 1

defaultNoMinor = false
defaultNoMajor = false
defaultNoOpportunistic = true
defaultNumberOfMinor = 3
defaultNumberOfMajor = 2
defaultNumberOfMinorIsol = 3
defaultNumberOfMajorIsol = 2
defaultNumberOfMinorBd = 3
defaultNumberOfMajorBd = 2

defaultDelugeInspection = 730
defaultFnGInspection = 336
defaultIsolationInspection = 1460
defaultBlowdownInspection = 1460
```

fRateFactor = 1;
---

where,
defaultNoMinor, defaultNoMajor, defaultNumberOfMinor and defaultNumberOfMajor are parameters related to Deluge system only (although this is not reflected in their names)
fRateFactor is all component failure rate value.

Most of parameters listed in .ini file are also used in SA and, as mentioned above, are controlled by MCS_Handling::setSystemParameters and MCS_Handling::setSystemParametersT. But here are 4 new parameters (defaultNumberOfMinorIsol, defaultNumberOfMajorIsol, defaultNumberOfMinorBd, defaultNumberOfMajorBd), which are controlled within the newly added function MCS_Handling::setSystemParameters2.

Such a file is normally written by runPN.m Matlab script before each launch of application during multi-objective GA task. Since runPN.m is a part of GA fitness function implementation, the .ini file is being overwritten on each iteration of the Matlab GA solver.

D.8 C++ implementation of SA and Automated Launch mode

The IDs of places and transitions are directly listed in c++ code. The internal representation of Petri network is accessed and changed in methods MCS_Handling::setSystemParameters, MCS_Handling::setSystemParametersT, and MCS_Handling::setSystemParameters2 (via std::vector<PN_Models::Place*> m_places propety of PN_Models::PN_Model* m_model MSC_Handling's private property). The functions are called from the Main_Window::on_actionRun_SensitivitySimulation_triggered(). Here the SA loop and Automated Launch actions are implemented.

The MCS_Handling::setSystemParameters function deals with all Deluge system parameters and, additionally, with the NoOpportunistic flag. It contains lists of place IDs, which represent maximum number of minor and major maintenances in the lifecycle of each component of the Deluge system.

Also it contains IDs of 4 transitions, where inspection intervals are defined, and IDs of places for NoMajor, NoMinor and NoOpportunistic flags. The function finds listed in its code network objects and sets to them values received as parameters.

The MCS_Handling::setSystemParametersT function changes the Weibull distribution η parameter in certain transitions. Unlike above, it receives the list of transition IDs as an argument. The single list ever passed to the function, contains Weibull-distributed transitions between component states for all components. It is defined in Main_Window::on_actionRun_SensitivitySimulation_triggered().The function accesses all Weibull distributions in the transition, reads η values, multiplies them by a coefficient received as parameter, and sets back.

The MCS_Handling::setSystemParameters2 function is very similar to a part of setSystemParameters , where numbers of repairs for Deluge system are set up, and it does the same work with Isolation and Blowdown systems. It is added for usage in Automated Launch mode in order to let MATLAB solver to change the parameters of all systems, and do it separately. The function contains lists of places, where numbers of repairs of Isolation and Blowdown systems are defined (MSC_Handling.cpp). Thus, Deluge system repair parameters are still controlled in setSystemParameters.

These 3 functions overwrite related parameters of network objects with the values received as their arguments. However, this does not suit the repetitive nature of the SA. Hence, in order to roll to the original values back, the Petri network has to be re-read to the newly created PN_Model object, and the property PN_Models::PN_Model* m_model has to be updated. The is implemented in the Interface::sceneToPNmodel(Diagram_Scene* scene) method of the class Interface (Interface.cpp), and invoked in Main_Window.cpp,. The method reads the Diagram_Scene object, creates the new PN_Model and deletes the old scene known as Interface.

Addition of Dependencies

The following dependencies were added to the existing Petri Net Software:

- Qt 5.7.1 with MinGW 5.3.0 and Qt Creator 4.2.0
- MATLAB R2015b 32-bit

Changes made to the existing Source Code to build the program

In View/Diagram_Item.cpp MouseEvent->posF() were changed to MouseEvent->pos(). (MouseEvent does not have posF method).

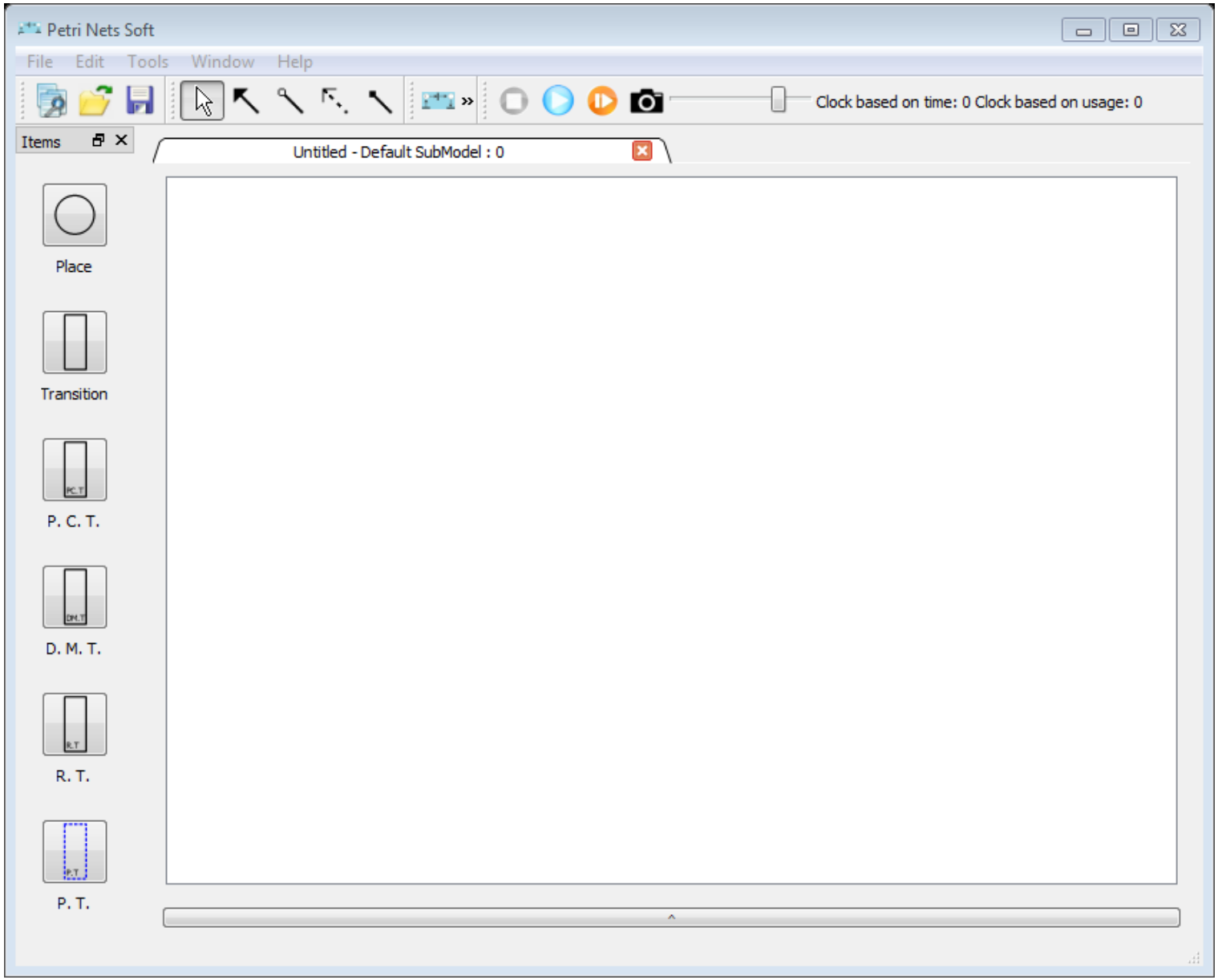
In View/Diagram_Item.h corresponding variables (m_draggingCentrePoint and m_mousePosition) were changed from QPointF to QPoint.

In PN_Models/All_PN_Models_Headers.h all #include “*.hpp” were changed to “*.h”.

In View/Diagram_Item.cpp constructor call QGraphicsRectItem(parent, scene) was changed to QGraphicsRectItem(parent). (QGraphicsRectItem does not have constructor that accepts QGraphicsItem and QGraphicsItem).

Appendix E

Screenshot of the Modelling Tool


Petri Nets Soft
File
Edit
Tools
Window
Help
Clock based on time: 0 Clock based on usage: 0
Items
Untitled - Default SubModel : 0
Place
Transition
P. C. T.
D. M. T.
R. T.
P. T.